Past and current distribution of heather (*Erica sp.*) on the Sanetti Plateau, Bale Mountains, Ethiopia

Kumulative Dissertation

zur Erlangung des akademischen

Doktorgrades der Naturwissenschaften (Dr. rer. nat.)

der

Naturwissenschaftlichen Fakultät III

Agrar- und Ernährungswissenschaften,

Geowissenschaften und Informatik

der

Martin-Luther-Universität Halle-Wittenberg

vorgelegt von

M.Sc. Frau Betelhem Mekonnen Muluneh

Halle (Saale), 20 Nov 2023

Vollständiger Abdruck der von der Fakultät für Agrar- und Ernährungswissenschaften, Geowissenschaften und Informatik der Martin-Luther-Universität Halle-Wittenberg genehmigten Dissertation zur Erlangung des Grades eines Doktors der Naturwissenschaftlichen (Dr. rer. nat.).

Die Arbeiten zur vorliegenden Dissertation wurden im Zeitraum von August 2017 bis Nov 2023 an der Abteilungen für Bodenbiogeochemie (unter Leitung von Prof. Dr. Bruno Glaser) der Martin-Luther-Universität Halle-Wittenberg und an der Abteilung für Bodenkunde (unter Betreuung von em. Prof. Dr. Wolfgang Zech) der Universität Bayreuth durchgeführt.

Dissertation eingereicht am: 13 Apr 2023

Tag der Verteidigung: 20 Nov 2023

Erstgutachter: Prof. Dr. Bruno Glaser

Zweitgutachter: Prof. Dr. Eva Lehndorff (Gutachter)

Drittegutachter: em. Prof. Dr. Wolfgang Zech

Prüfungsausschuss: Prof. Dr. Robert Mikutta (Vorsitz)

Prof. Dr. Bruno Glaser (Gutachter)

Prof. Dr. Eva Lehndorff (Gutachter)

em. Prof. Dr. Wolfgang Zech (Gutachter)

Prof. Dr. Edgar Peiter

Prof. Dr. Hans-Jörg Vogel

Dedicated to my mentor, Wolfgang Zech, who encouraged my enthusiasm to pursue higher education and persistently supported me in achieving my goals,

and

to the memory of my parents, Mekonnen Muluneh and Fekadenesh Bedada, who always believed in my ability to be successful in the academic arena. You are gone, but your belief in me has made this journey possible.

Table of Contents

Abbreviations

AHP	**A**frican **H**umid **P**eriod
AFLPs	**A**mplified **F**ragment **L**ength **P**olymorphisms
A/C	**A**rtemisia/**C**henopodiaceae
Ah	Topsoil mineral horizon
AMS	**A**ccelerated **M**ass **S**pectrometry
AP	**A**rborea **P**ollen
B horizons	Subsoil mineral horizons
BC	**B**lack **C**arbon
BPCAs	**B**enzene **P**olycarboxylic **A**cids
BSTFA	**Bi**s (trimethylsilyl)**tri**fluor**a**cetamide
C horizons	Parent material mineral horizons
CPA	**C**hemical **P**roxy of **A**lteration
DCM	**Di**chloro**m**ethane
EC	**E**lectrical **C**onductivity
EA-IRMS	**E**lemental **A**nalyzer coupled with an **I**sotope **R**atio **M**ass **S**pectrometer
FID	**F**lame **I**onization **D**etector
F/(A+X)	**F**ucose/(**A**rabinose+**X**ylose)
GC	**G**as **C**hromatography
H1	**H**einrich Event **1**
HI	**H**ydrogen **I**ndex
ITCZ	**I**ntertropical **C**onvergence **Z**one
LGM	**L**ast **G**lacial **M**aximum
LPZ	**L**ocal **P**ollen **Z**ones
masl	**m**eter **a**bove **s**ea **l**evel

(G+M)/(A+X)	(**G**alactose+**M**annose)/(**A**rabinose+**X**ylose)
NCP	**N**on-**C**ellulosic **P**olysaccharides
NMP	**N**-**M**ethyl-2-**P**yrrolidone
NPA	**N**on-**A**rboreal **P**ollen
O layers	**O**rganic soil horizons
TOC	**T**otal **O**rganic **C**arbon
TN	**T**otal **N**itrogen
TFA	**T**ri**f**luoroacetic **A**cid
XRF	**X**-**R**ay **F**luorescence
YD	**Y**ounger **D**ryas

List of Figures

List of papers

This cumulative dissertation is based on the following peer-reviewed scientific articles:

I.   **Mekonnen, B.,** Glaser, B., Lemma, B., Bromm, T., Zech, M., Nemomissa, S., Bekele, T., Zech, W. (2019) Chemotaxonomic patterns of vegetation and soils along altitudinal transects of the Bale Mountains, Ethiopia and implications for paleovegetation reconstructions Part I: Stable isotopes and sugar biomarkers. *E&G Quaternary Science Journal*. 68, 177–188, https://doi.org/10.5194/egqsj-68-177-2019

II. Lemma, B., **Mekonnen, B.,** Glaser, B., Zech, W., Nemomissa, S., Bekele, T., Bittner, L., Zech, M. (2019) Chemotaxonomic patterns of vegetation and soils along altitudinal transects of the Bale Mountains, Ethiopia and implications for paleovegetation reconstructions Part II: Lignin–derived phenols and leaf wax–derived *n*–alkanes. *E&G Quaternary Science Journal,* 68, 189–200, https://doi.org/10.5194/egqsj-68-189-2019

III. **Mekonnen, B**., Glaser, B., Zech, W., Bittner, L., Bromm, T., Lemma, B., Nemmomisa, S., Bekele, T., Zech, M. (2022) Terrestrial versus aquatic source identification of sedimentary *n*-alkane and sugar biomarkers – a case study from the Bale Mountains, Ethiopia. *Journal of Paleolimnology,* 70, 347–360, https://doi.org/10.1007/s10933-023-00298-5

IV. **Mekonnen, B.,** Glaser, B., Zech, R., Zech, M., Schlutz, F., Bussert, R., Addis, A., Gil-Romera, G., Nemomissa, S., Bekele, T., Bittner, L., Solomon, D., Manhart, A., Zech, W. (2022) Climate, vegetation and fire history during the past 18,000 years, recorded in high altitude lacustrine sediments on the Sanetti Plateau, Bale Mountains (Ethiopia). *Prog Earth Planet Sci* 9, 14, https://doi.org/10.1186/s40645-022-00472-9

V.   **Mekonnen, B.,** Glaser, B., Zech, M., Bromm, T., Nemmomisa, S., Bekele, T., Zech, W. (2022) Factors determining the distribution of *Erica* on the Sanetti Plateau, Bale Mountains National Park, Ethiopia. *Alpine Botany*, 133, 135–147, https://doi.org/10.1007/s00035-023-00295-4

Summary

The ongoing rise in global temperature is one of the most important factors that will affect vegetation composition and tree line displacement. East African high-altitude mountains are susceptible to climate change and human activities and offer crucial insight into the spatial and temporal dynamics of the region's ecosystems. However, little is known on the past environment of these high-altitude mountain ecosystems. This is mostly challenged by a lack of suitable sediment archives, reliable radiocarbon dating, and unambiguous proxy interpretation. In East Africa, the Ericaceous belt characterizes the higher tree line ecotone. It extends from 3200 to 3800 m asl in the Bale Mountains. However, discrete heather (*Erica sp.*) patches, primarily restricted to boulder-rich sites, are found above 3800 m asl, while Afroalpine species such as *Helichrysum*, *Alchemilla,* and grass mainly cover the vast area of the Sanetti Plateau. Previous paleoenvironmental studies suggest that Ericaceous vegetation extended to the higher altitudes of the Sanetti Plateau during the beginning of the Holocene, correlating with warmer and wetter climatic conditions, and the *Erica* patches are supposed as relics of this expansion. By contrast, other studies suggest human-induced fire as a cause factor for the decline of the *Erica* tree line. However, it is still unclear why these *Erica* patches are mainly restricted to the big boulders.

In this thesis, the potential of stable isotopes ($\delta^{13}C$ and $\delta^{15}N$), sugar biomarkers, lignin, and *n*-alkanes is assessed to distinguish *Erica* from other dominant plants and their implication for paleovegetation reconstruction. Moreover, the sources of *n*-alkanes and sugar biomarkers in two sediment archives of the Bale Mountains (Garba Guracha and B4 depression on the Sanetti Plateau) are investigated. By examining the sediments of a depression located above the upper tree line of *Erica* at 3950 m asl, the climate, fire, and vegetation history of the Sanetti Plateau is reconstructed using a multi-proxy approach. Besides, the environmental features and soil properties of *Erica* patches and nearby *Erica*-free sites covered by Afroalpine vegetation are investigated in order to uncover determining factors for the current patchy distribution of *Erica* on the Sanetti Plateau.

All dominant plants along the northeast and southwest transects of the Bale Mountains are characterized as C3 vegetation. *Erica* spp. could not be differentiated from other dominant plants by their stable isotope signatures. Moreover, due to degradation and mineralization, $\delta^{13}C$ and $\delta^{15}N$ become more positive in the soils below the dominant vegetation. *Erica* is characterized by low sugar content and high (G+M)/(A+X) ratios. However, a similar pattern cannot be retained in the soils. Instead, the ratios generally increase due to preferential degradation of arabinose and xylose and microbial input of galactose and mannose. *Erica* spp. was characterized by cinnamyl percentages of > 40% and a high ratio of C/(V+S+C). However, the ratio decreases in the soils below *Erica* due to selective degradation and increases below *Festuca,* likely due to lignin input by roots. A low C_{31}/C_{29} ratio further characterizes *Erica* leaves. However, this ratio is also affected by degradation. Therefore, the use of these proxies alone will not result in unambiguous palaeovegetation reconstruction in the Bale Mountains. The relative abundances of long-chain *n*-

alkanes C_{29}, C_{31}, and C_{33} in sediments are similar to the modern samples, indicating that they are derived from terrestrial sources. By contrast, the relative contribution of C_{27} and mid-chain n-alkanes C_{23} and C_{25} is significantly higher in sediments of Garba Guracha and B4 and lower in modern samples. This finding proves that aquatic macrophytes are the likely source of mid-chain n-alkanes in sediments. The relatively high abundances of galactose and mannose in the Garba Guracha sediments might be attributed to contributions by both soil and aquatic microorganisms. The relative abundances of fucose and rhamnose are significantly higher in the Garba Guracha sediments than in the modern samples. Moreover, sediment samples are characterized by higher ratios of (fuc + rham) / (ara + xyl) than modern samples. Therefore, this ratio can be used as a proxy for organic matter source identification in the Bale Mountains. Nevertheless, since using a single proxy often leads to ambiguity, a muti-proxy approach is implemented to reconstruct the paleoenvironmental condition of the Sanetti Plateau.

The results of this thesis provide a new deglaciation age for the Sanetti plateau at 18.2 cal kyr BP. After deglaciation at about 18 cal kyr BP, a steppe-like herb-rich grassland with maximum Chenopodiaceae/Amaranthaceae and Plantago existed. Dry climatic conditions were recorded between 16.6 and 15.7 cal kyr BP with a desiccation layer at 16.3 cal kyr BP, documenting a temporary phase of maximum aridity on the plateau correlating with Heinrich Event 1. At 15.7 cal kyr BP, an abrupt onset of the African Humid Period, almost 1000 years before the onset of the Bølling–Allerød warming in the North-Atlantic region and about 300 years earlier than in the Lake Tana region, is recorded. *Erica* pollen increased significantly between 14.4 and 13.6 cal kyr BP in agreement with periodically wet and regionally warm conditions. Similarly, fire events, documented by increased black carbon contents, correlate with wet and warm environmental conditions that promote the growth of *Erica* shrubs. This allows to conclude that biomass and, thus, fuel availability is one important factor controlling fire events in the Bale Mountains.

Erica and control plots without *Erica* have comparable topography and soil texture except for the higher amounts of boulders covering the *Erica* plots. However, soils covered by *Erica* patches generally have higher total organic carbon and black carbon contents and a higher carbon-to-nitrogen ratio indicating fresh organic matter input and availability of combustible fuel. Moreover, it implies that *Erica* did not fully cover control plots in the former time because the soil horizons would have similar properties to the corresponding horizons of the *Erica* plots. In addition, soils of the *Erica* plots showed more positive $\delta^{13}C$ values than the control soils, possibly attributed to water stress. In general, the structure of the landscape and soil conditions of control plots might support the growth of *Erica*. However, *Erica* growing between boulders at the upper timberline seems to benefit strongly from the favorable microclimate created by dark basalt boulders and the physical protection against grazing and fire.

Zusammenfassung

Der anhaltende globale Temperaturanstieg ist einer der wichtigsten Faktoren, der die Zusammensetzung der Vegetation und die Verschiebung der Baumgrenze beeinflussen wird. Die ostafrikanischen Hochgebirge sind anfällig für den Klimawandel und menschliche Aktivitäten und bieten entscheidende Einblicke in die räumliche und zeitliche Dynamik der Ökosysteme dieser Region. Allerdings ist nur wenig über die frühere Umwelt dieser hochgelegenen Bergökosysteme bekannt. Dies wird vor allem dadurch erschwert, dass es an geeigneten Sedimentarchiven, zuverlässigen Radiokohlenstoffdatierungen und eindeutigen Proxy-Interpretationen mangelt. In Ostafrika charakterisiert der *Erica*-Gürtel den Ökoton der höheren Baumgrenze. Der *Erica*-Gürtel erstreckt sich von 3200 bis 3800 m asl in den Bale-Bergen. Oberhalb von 3800 m asl finden sich jedoch vereinzelte Heidekrautflächen (*Erica* sp.), die hauptsächlich auf felsenreiche Standorte beschränkt sind, während Afroalpine Arten wie *Helichrysum*, *Alchemilla* und Gräser hauptsächlich die weite Fläche des Sanetti-Plateaus bedecken. Frühere paläoökologische Studien deuten darauf hin, dass sich die *Erica*-Vegetation zu Beginn des Holozäns in die höheren Lagen des Sanetti-Plateaus ausbreitete, vermutlich im Zusammenhang mit wärmeren und feuchteren Klimabedingungen korreliert; die heute noch vorkommenden *Erica*-Flecken werden als Relikte dieser Ausbreitung interpretiert. Im Gegensatz dazu deuten andere Studien auf vom Menschen verursachte Brände als Ursache für den Rückgang der *Erica*-Baumgrenze hin. Es ist jedoch noch unklar, warum diese *Erica*-Flecken hauptsächlich auf blockreichen Standorten beschränkt sind.

In dieser Arbeit wird zunächst geprüft ob sich *Erica* von anderen Pflanzen in Bezug auf Gehalte an stabilen Isotopen (δ^{13}C und δ^{15}N), Zucker-Biomarkern, Lignin und *n*-Alkanen unterscheiden und sich damit zur Rekonstruktion der Paläovegetation eignen. Darüber hinaus werden die Quellen von *n*-Alkanen und Zucker-Biomarkern in zwei Sedimentarchiven des Bale-Gebirges (Garba Guracha und B4-Senke auf dem Sanetti-Plateau) untersucht. Anhand der Analyse von Sedimenten oberhalb der oberen Baumgrenze von *Erica* auf 3950 m asl befindet, wird die Klima-, Feuer- und Vegetationsgeschichte des Sanetti-Plateaus mit Hilfe eines Multiproxy-Ansatzes rekonstruiert. Außerdem werden die Umweltmerkmale und Bodeneigenschaften von *Erica*-Flecken und nahegelegenen *Erica*-freien Standorten mit Afroalpiner Vegetation untersucht, um die Faktoren zu ermitteln, die für die derzeitige lückenhafte Verbreitung von *Erica* auf dem Sanetti-Plateau ausschlaggebend sind.

Alle dominanten Pflanzen entlang der nordöstlichen und südwestlichen Transekte der Bale Berge von 2550 bis 4377 m asl sind C3-Pflanzen charakterisiert. *Erica spp*. konnten anhand ihrer stabilen Isotopensignaturen nicht von anderen dominanten Pflanzen unterschieden werden. Darüber hinaus werden δ^{13}C und δ^{15}N in den Böden unterhalb der dominanten Vegetation aufgrund von Degradation und Mineralisierung positiver. *Erica* ist durch einen niedrigen Zuckergehalt und ein hohes (G+M)/(A+X)-Verhältnis gekennzeichnet. Ein ähnliches Muster lässt sich jedoch in den Böden nicht nachweisen. Stattdessen steigen die Verhältnisse im Allgemeinen aufgrund des bevorzugten Abbaus von Arabinose und Xylose und des mikrobiellen Eintrags von

Galaktose und Mannose. *Erica* spp. zeichnete sich durch Cinnamyl-Anteile von > 40 % und ein hohes Verhältnis von C/(V+S+C) aus. Das Verhältnis sinkt jedoch in den Böden unterhalb von *Erica* aufgrund selektiven Abbaus von Cinnamyl-Einheiten und steigt unter *Festuca*, wahrscheinlich aufgrund des Lignineintrags durch die Wurzeln. Ein niedriges C_{31}/C_{29}-Verhältnis von *n*-Alkanen kennzeichnet die Blätter von *Erica*. Allerdings wird auch dieses Verhältnis durch den Abbau beeinflusst. Daher eignen sich diese Proxies alleine nicht für eine eindeutige Rekonstruktion der Paläovegetation in den Bale Mountains. Die relativen Häufigkeiten der langkettigen *n*-Alkane C_{29}, C_{31} und C_{33} in älteren Sedimenten sind ähnlich wie in rezenten Oberboden Proben, was darauf hindeutet, dass sie aus terrestrischen Quellen stammen. Im Gegensatz dazu ist der relative Beitrag von C_{27} und mittelkettigen *n*-Alkanen C_{23} und C_{25} in den Sedimenten von Garba Guracha und B4 signifikant höher als in rezenten Proben. Dieses Ergebnis beweist, dass aquatische Makrophyten die wahrscheinliche Quelle für mittelkettige *n*-Alkane in Sedimenten sind. Die relativ hohen Gehalte an Galaktose und Mannose in den Sedimenten von Garba Guracha könnten auf Beiträge sowohl von Boden-als auch von aquatischen Mikroorganismen zurückgeführt werden. Der relative Anteil von Fucose und Rhamnose ist in den Garba-Guracha-Sedimenten deutlich höher als in den rezenten Proben. Außerdem weisen die Sedimentproben ein höheres Verhältnis von (fuc + rham)/ (ara + xyl) auf als die modernen Proben. Daher kann dieses Verhältnis als Näherungswert für die Identifizierung der organischen Materie im Bale-Gebirge verwendet werden. Da die Verwendung einer einzigen Proxy-Probe jedoch oft zu Unklarheiten führt, wird ein Multi-Proxy-Ansatz verwendet, um die paläoökologischen Bedingungen auf dem Sanetti-Plateau zu rekonstruieren.

Nach dem Abschmelzen der Gletscher auf dem Sanetti-Plateau um 18 cal kyr BP existierte ein steppenartiges, kräuterreiches Grasland mit einem Maximum an Chenopodiaceae/Amaranthaceae und Plantago. Trockene Bedingungen zwischen 16,6 und 15,7 cal kyr BP führten zu einer völligen Austrocknung der Senke um 16,3 cal kyr BP. Diese Trockenheit auf dem Plateau korreliert mit dem Heinrich-Ereignis 1. Um 15,7 cal kyr BP wurde ein abrupter Beginn der afrikanischen Feuchtperiode festgestellt, fast 1000 Jahre vor dem Beginn der Bølling-Allerød-Warmzeit in der nordatlantischen Region und etwa 300 Jahre früher als in der Tanasee-Region. *Erica*-Pollen nahmen zwischen 14,4 und 13,6 cal kyr BP in Übereinstimmung mit periodisch feuchten und regional warmen Bedingungen deutlich zu. Ebenso korrelieren intensive Feuerereignisse, belegt durch erhöhten Gehalte an Black Carbon, mit feuchten und warmen Umweltbedingungen, die das Wachstum von *Erica*-Sträuchern fördern. Dies lässt den Schluss zu, dass die Biomasse und damit die Verfügbarkeit von Brennmaterial ein wichtiger Faktor ist, der die Feuerereignisse in den Bale Mountains kontrolliert.

Probeflächen mit und ohne *Erica* (Kontrollflächen) haben eine vergleichbare Topografie und Bodentextur. Allerdings weisen die *Erica*-plots stets große Basaltblöcke auf und im allgemeinen höhere Gehalte an organischem kohlenstoff und Black Carbon sowie ein höheres Kohlenstoff-zu-Stickstoff-Verhältnis auf was auf den Eintrag von frischer organischer Substanz. Außerdem deutet dies darauf hin, dass die Kontrollflächen früher nicht vollständig mit *Erica* bestockt waren, denn

sollten zumindest die bodenhorizon wie die entsprechenden Horizonte der *Erica*-Flächen aufweisen. Darüber hinaus wiesen die Böden der *Erica*-Parzellen positivere δ^{13}C-Werte auf als die Kontrollböden, was möglicherweise auf Wasserstress zurückzuführen ist. Topographie und Bodenbedingungen der Kontrollflächen oberhalb 3800 m asl würden das Wachstum von *Erica*. Die dunklen Basalt-Blöcken oberhalb der oberen Waldgrenze scheinen jedoch das Mikroklima zu verbessern und vor Beweidung und Feuer zu schützenund so das Überleben von *Erica* zu ermöglichen.

Acknowledgments

The dissertation is the outcome of all-rounded support from many individuals.

First and foremost, I would like to express my deepest gratitude to my supervisor Prof. em. Dr. Wolfgang Zech, for his excellent guidance, inspiration, encouragement, and caring mentorship. He put the seeds of knowledge on the subject since my master's program and provided me with sufficient resources, academic support, insightful feedback throughout the process. It would not have been possible to finish this thesis without his unwavering backing in every way.

I am also extremely grateful to my co-supervisor Prof. Dr. Bruno Glaser, for welcoming me to his working group, establishing a pleasant working atmosphere, and granting me access to the laboratory. His constant scientific assistance, insightful comments, encouragement, patience, understanding, care, and vital life time advises at crucial times have also been invaluable to me.

I would like to express my sincere appreciation to Prof. Dr. Michael Zech for his guidance, reading my drafts, and for providing valuable feedback and insights. I am very thankful for the fruitful discussions, follow-ups, and encouraging words.

I would like to express my gratitude to Prof. Dr. Sileshi Nemomissa and Prof. Dr. Tamrat Bekele for their helpful feedback and suggestions during the writing process, as well as for their kind words of encouragement.

Special thanks to Tobias Bromm for his unwavering support in the laboratory and for always being there for me on personal matters.

I would like to thank everyone I got to know and work with at Martin-Luther-University, Halle-Wittenberg, in the Department of Soil Biogeochemistry. In particular, I would like to express my gratitude to Marianne Zech for the stable isotope measurements, her warm hospitality, thoughtful care, and the wonderful experiences we shared on our travels together. I would like to express my great appreciation to Heike Maennicke for all the help she provided me with the laboratory work and for freely sharing her knowledge and experience with me in terms of methodology. I am also thankful to my colleagues Dr. Lucas Bittner and Dr. Bruk Lemma for their help and support. I would like to greatly acknowledge Gudrun Nemson-von Koch and her family, as well as Christine Krenkewitz, for all the love, support, and encouragement they have given me over the years.

I would also like to extend my sincere gratitude to the Department of Plant Biology and Biodiversity Management, Addis Ababa University, for its scientific collaboration. I also thank Ethiopian Wildlife Authority and Ethiopian Biodiversity Institute for allowing us to access the Bale Mountains National Park.

Above all, all praise goes to God for giving me the stamina and strength to complete this work!!

I. Extended Summary

1. Introduction

1.1. Background

Global climate change is significantly influencing vegetation composition and tree line displacement (Kidane et al., 2022; Körner, 2007; Körner, 2012). This is especially severe in tropical rainforest zones, where temperatures rise at a mean rate of 0.26 ± 0.05 °C every decade due to increased anthropogenic greenhouse effects (Malhi and Wright, 2004). Due to their vulnerability to climate change and human impacts, East African high-altitudes provide vital information on past and present vegetation dynamics. Furthermore, they produce essential natural resources, such as wood and non-wood products, and serve as a hygro-buffer, benefitting the water balance of the mountain ecosystem and the agricultural areas in the adjacent lowlands (Miehe & Miehe, 1994). Moreover, a diverse range of indigenous flora and fauna can be found in the high-altitude African mountains. Therefore, a better understanding of the ecological status of these sites and what causes tree line dynamics helps biodiversity practitioners to develop an effective biodiversity plan and understand how climate change and human activity affect biodiversity.

Various global and regional climatic events have occurred in the East African Mountains (Costa et al., 2014; Lamb et al., 2018; Thompson et al., 2002). For instance, during the Last Glacial Maximum (LGM; 23–18 cal kyr BP), East African mountains such as Kilimanjaro, Mount Kenya, Mount Bada, Rwenzori, Mount Elgon, and Ethiopian highlands were covered by ice (Groos et al., 2021; Lamb et al., 2018; Mark and Osmaston, 2008; Osmaston et al., 2005; Thompson et al., 2002). In addition, a brief dry event related to Heinrich Event 1 (H1) was recorded in northern and southern Africa around 16–17 cal kyr BP (Lamb et al., 2007; Marshall et al., 2009; Mohtadi et al., 2014; Stager et al., 2011; Tierney et al., 2008). Furthermore, studies from northern Africa provide evidence for the occurrence of the African Humid Period (AHP) between about 15.5 and 5 cal kyr BP (Costa et al., 2014; Kuzmicheva et al., 2014; Lamb et al., 2007; Tierney et al., 2013, 2011; Tierney and DeMenocal, 2013). This climatic variability triggers the responsiveness of the altitudinal tree limit as environmental conditions constrain tree growth with increasing altitude. As a result, during the dry and cold LGM and warm and wet Holocene periods, tree lines were lowered and rose in tropical Africa (Groos et al., 2021; Umer et al., 2007; Wu et al., 2007).

Erica, also known as heathers or heath, is one of the most widely spread plant genera in the family of Ericaceae (Kron et al., 2002; Oliver, 1989). Its geographical range includes Europe, the Middle East, and Africa (Mcguire and Kron, 2011; Quézel, 1978). The Ericaceous belt forms the upper tree line ecotone in East Africa. Similar to other African mountains, the ericaceous vegetation is highly distributed in northern (Siemen Mountains and Tigray) and southern Ethiopia (Bale Mountains, Bada, and Arsi highlands) (Friis et al., 2010). In the Bale Mountains, the Ericaceous belt covers an area of 90,000 ha and ranges in altitude from about 3200 to 3800 m asl (Hailemariam et al., 2016; Miehe and Miehe, 1994). It is mainly dominated by *Erica trimera* (Engl.) and *Erica arborea* L. (*Erica* hereafter) (Hedberg, 1951; Miehe and Miehe, 1994). Studies

2

from the surroundings of the Bale Mountains indicate the presence of Ericaceous vegetation since 2.5 myr (Bonnefille, 1983). Moreover, similar studies suggest that the Ericaceous belt in Mount Bada was formed between 8000 and 3500 cal kyr BP (Bonnefille and Hamilton, 2015).

The Bale Mountains were one of the highly glaciated mountains during the LGM (Groos et al., 2021; Osmaston et al., 2005; Tiercelin et al., 2008). Due to the temperature decrease, the Afroalpine vegetation belt shifted downward by 700 m (Groos et al., 2021). A pollen study from the glacial lake Garba Guracha shows that Ericaceous vegetation started to expand to the higher altitudes of the Sanetti Plateau with the beginning of the Holocene correlating with the warmer and wetter environmental conditions (Umer et al., 2007). This study is also supported by Kuzmicheva et al. (2013), which reported the expansion of the ericoid family on the Sanetti Plateau at around 10 cal kyr BP. However, Umer et al. (2007) and Bittner et al. (2020) further described a dry event around 4.5 cal kyr BP, which resulted in the decrease of the *Erica* vegetation in altitude and area, while Afroalpine species such as *Alchemilla* and *Helichrysum* expanded on the Sanetti Plateau. Currently, the vast area of the Sanetti Plateau, above ca. 3800 m asl, is mainly covered by Afroalpine species. By contrast, discrete *Erica* patches are primarily restricted to boulder-rich sites. These *Erica* patches are supposed to be relics of the former expansion of *Erica* during the warmer early Holocene (Miehe and Miehe, 1994). However, it is still unclear why these *Erica* patches are mainly restricted to the big boulders.

While climatic fluctuations are being considered to play a significant role in determining vegetation changes in the Bale Mountains (Miehe and Miehe, 1994; Umer et al. 2007), other scholars argue that human-induced fire is the most likely explanation for the decrease of the *Erica* tree line (Kidane et al., 2012; Miehe and Miehe, 1994; Wesche et al., 2000). Fire has been recorded in the Bale Mountains for hundreds to thousands of years (Gil-Romera et al., 2019). However, whether previous fires were linked to human impacts or natural lightning is unclear. According to Ossendorf et al. (2019), human settlement began around 47 cal kyr BP. Currently, fires in the Bale Mountains are primarily caused by pastoralists who have settled in the national park, believing that removing *Erica* shrubs improves pasture quality and eliminates predators and insects that attack their livestock. However, the impact of human-induced fire on vegetation composition change and biodiversity conservation is debatable (Johansson et al., 2018).

The main objectives of this thesis are:

(i)   To assess the utility of stable isotopes, hemicellulose sugars, *n*-alkanes, and lignin biomarkers for the chemotaxonomic characterization of modern plants and soils in the Bale Mountains, as well as their applicability for paleoenvironmental reconstruction

(ii)   To identify terrestrial versus aquatic sedimentary *n*-alkanes and sugar biomarkers

(iii)   To reconstruct the paleoenvironmental history of the Sanetti Plateau using a multi proxy-approach as deduced from a sedimentary archive

(iv)   To identify the factors responsible for the current distribution of the *Erica* patches on the Plateau.

1.2.   Stable isotopes, hemicellulose sugars, *n*-alkanes, and lignin biomarkers

Many ecological processes and vegetation changes caused by climate change and anthropogenic factors are traced using stable carbon ($\delta^{13}C$) and nitrogen ($\delta^{15}N$) isotopes (Dawson et al., 2002; Marshall et al., 2007). $\delta^{13}C$ analyses of leaves and soils determine historical alterations in C3 woodland and C4 grassland boundaries (Eshetu, 2002). This is because C3 and C4 plants have different photosynthetic processes. For instance, savannah grasses that use the C4 metabolic pathways are enriched in $\delta^{13}C$ (~ -14‰), while trees and grasses that use C3 cycles are depleted in $\delta^{13}C$ (~ -27‰) (Eshetu and Högberg, 2000; Marshall et al., 2007; Tiunov, 2007). Besides, $\delta^{13}C$ is a prominent proxy for determining plant water status (Fischer, 2011). Water stress leads to less negative $\delta^{13}C$ values in dry tissue due to stomatal constraints on gas diffusion during periods of biomass production (Körner, 1999). Furthermore, $\delta^{13}C$ is a valuable indicator of the source of organic matter in marine environments (Meyers, 1994). Despite its widespread use, $\delta^{13}C$ interpretation is often limited by factors such as soil organic matter degradation and methanogenesis, which question the credibility of reconstructed paleovegetation using bulk isotope analyses (Farquhar et al., 1982; Zech et al., 2007).

Sugar monomers, *n*-alkanes, and lignin are used for the chemotaxonomic characterization of vascular plants (Schädel et al., 2010). For example, pentose sugars such as arabinose and xylose are abundant in plants, while hexose sugars like galactose and mannose are the main components of bacterial cell walls (Gunina and Kuzyakov, 2015; Oades, 1984). Therefore, a ratio between these sugar biomarkers (galactose + mannose)/(arabinose + xylose) is used to distinguish between microbial and terrestrial-derived organic matter in modern soils (Jia et al., 2008; Oades, 1984).

n-Alkanes are essential constituents of epicuticular plant leaf waxes (Kolattukudy, 1970), which protect the plants against excessive evaporation and fungal and insect attacks (Eglinton and Hamilton, 1967; Koch et al., 2009). Due to their recalcitrant nature, *n*-alkanes are well preserved in sedimentary archives. As a result, they received increasing scientific attention during the last decades as molecular markers to trace the origin of organic matter and as proxies for paleoclimate studies (Eglinton and Eglinton, 2008; Glaser and Zech, 2005) The potential of *n*-alkanes for chemotaxonomic studies has been suggested based on the finding that the homologues C_{27} and C_{29} are predominately derived from trees and shrubs, whereas homologues C_{31} and C_{33} are predominately derived from grasses and herbs (Schäfer et al., 2016; Zech et al., 2009).

Lignin-derived phenols of the vanillyl (V), syringyl (S), and cinnamyl (C) types are used to differentiate sources of organic matter in soils and provide information about the state of degradation of vascular plant materials in the terrestrial and aquatic sediments (Hedges et al., 1988; Tareq et al., 2006, 2004; Ziegler et al., 1986). For instance, low ratios of S/V ~ 0 were considered a proxy of gymnosperms, and high values of S/V ratios were found to indicate the presence of

angiosperms (Tareq et al., 2004). Likewise, the C/V ratios are proposed to indicate the abundance of woody (C/V < 0.1) and non-woody (C/V > 0.1) vegetation in soils and sediments (Tareq et al., 2011). Moreover, the ratios of acid to aldehyde forms of vanillyl $(Ac/Al)_v$ and syringyl units $(Ac/Al)_v$ were suggested as proxies for quantifying the degree of lignin degradation (Amelung et al., 2002; Hedges et al., 1985).

1.3. Paleoenvironmental reconstruction

Paleoecological studies enable a better understanding of the factors responsible for spatial and temporal vegetation changes. However, paleoenvironmental reconstruction is often challenged by a lack of suitable sediment archives, reliable dating, and unambiguous proxy interpretation. For instance, our knowledge of the paleoenvironmental history of the Bale Mountains is mainly from pollen-based studies done in Garba Guracha (Umer et al., 2007). Pollen is a powerful proxy that provides a broad understanding of changes in climate and vegetation (Brewer et al., 2013). However, its reliability is often challenged by the difference in pollen production and dispersion among different taxa (Hevly, 1981). In addition, distinguishing between terrestrial and aquatic sedimentary organic matter is a prerequisite in paleoenvironmental investigations. $\delta^{13}C$ measurements of bulk sediments and TOC/N ratios are widely used in paleoenvironmental reconstruction. However, since the organic matter in the sedimentary archives is derived from different sources, it is often difficult to unambiguously identify between terrestrial and aquatic sources by using only a single proxy (Andersson et al., 2012; Meyers and Ishiwatari, 1993). Lipid biomarkers such as n-alkane ratios complement organic matter source identification in paleoenvironmental reconstruction (Zech et al., 2012, 2009). The ratio between long-chain and mid-chain n-alkanes, is frequently used for organic matter source identification. This is because long-chain n-alkanes are abundant in terrestrial plants, while mid-chain n-alkanes characterize aquatic macrophytes (Ficken et al., 2000). Likewise, in paleolimnological studies, Hepp et al. (2016) used the sugar ratios fucose/(arabinose + xylose) and (fucose + xylose)/arabinose as proxies to distinguish between terrestrial and aquatic sedimentary organic matter. The Hydrogen index (HI) is also used as an indicator of lake level fluctuation and weathering intensity (Talbot and Livingstone, 1989). Moreover, due to their geochemical stability, lithogenic elements such as Zr, Hf, Nb, and Ti are often used in paleoenvironmental studies to indicate detrital and allochthones input (Davies et al., 2015).

Black carbon (BC) is used to reconstruct fire history due to its polycyclic aromatic structure, which highly resists chemical and biological degradation (Glaser et al., 1998; Kuzyakov et al., 2014; Preston and Schmidt, 2006). Furthermore, the ratios between individual benzene polycarboxylic acids (BPCA) can be used as indicators of fuel sources and the degree of combustion (Wolf et al., 2013). In the Bale Mountains, fire history is so far reconstructed using charcoal counts (Gil-Romera et al., 2019). While charcoal is usually detected visually using a microscope, BC is detected using BPCA as a molecular marker, which enables quantifying the

complex signature of pyrogenic carbon more precisely, especially when charcoal is not visible anymore.

Therefore, in this dissertation, the origin of sedimentary *n*-alkanes and sugar biomarkers in sedimentary archives of the Bale Mountains were studied. Moreover, all the above-mentioned biomarkers and proxies are combined to reconstruct the paleoenvironmental history of the Bale Mountains by investigating a depression located on the Sanetti Plateau.

1.4. Environmental factors determining the occurrence of *Erica* on the Sanetti Plateau

Climate and anthropogenic factors such as fire and grazing are postulated as determining factors for the displacement of the upper tree line of the ericaceous vegetation in the Bale Mountains (Fagúndez, 2013; Jacob et al., 2015; Johansson et al., 2018; Kidane et al., 2022; Miehe and Miehe, 1994; Wesche et al., 2000). However, the impact of soil properties and topography is not well known. For example, on the Sanetti Plateau, *Erica* patches occur above its upper tree limit, often growing on boulder-rich sites between the boulders, while areas located a few meters away without boulders are covered by Afroalpine vegetation. The big boulders are assumed to protect against fire and grazing (Miehe and Miehe, 1994). Moreover, dark basalt boulders may have created a microclimate suitable for the survival of *Erica* patches. To better understand the situation, this thesis evaluates whether boulder-rich *Erica* plots differ in soil properties and topographic features compared to nearby locations without *Erica* (control plots).

1.5. Research questions

This Ph.D. dissertation is part of the DFG research unit 2358 entitled "The Mountain Exile Hypothesis – How humans benefited from and re-shaped African high altitude ecosystems during the Quaternary climate change" within Sub-Project 2 "Human impact on fire history and destruction of *Erica* vegetation at the Sanetti Plateau, Ethiopia, as assessed by biogeochemical proxies of Anthrosols and depression sediments" which aims to reconstruct the chronology and intensity of the human occupation of the Bale Mountains and possible impacts on the deforestation of the Sanetti Plateau. The main focus of this Ph.D. dissertation is to contribute to a better understanding of the past and present status of the Ericaceous vegetation and possible drivers of its spatial and temporal dynamics in the Bale Mountains by answering the following questions.

(i) Do stable isotopes, sugar biomarkers, *n*-alkanes, and lignin phenols allow to chemotaxonomically differentiate between *Erica* and other dominant plants and their respective soils in the Bale Mountains?

(ii) Are *n*-alkanes and sugar biomarkers potential biomarkers for organic matter source identification of sedimentary archives in the Bale Mountains?

(iii) Did the high altitudes of the Sanetti Plateau experience similar climatic fluctuations in timing as the lower regions in northern and eastern Africa during the Late Glacial?

(iv) When and to what degree did *Erica* occupy the high altitudes of the Sanetti Plateau, where only patches are found at present?

(v) Are these patches of *Erica* relics documenting climate deterioration or human-induced fire?

(vi) Are topography and the soil properties of *Erica* plots different from nearby control plots occupied by Afroalpine plants?

(vii) Is there any evidence that *Erica* has occupied the non-*Erica* sites during former times?

2. Study area

2.1. Geographical setting

The Bale Mountains National Park is situated on the eastern side of the rift valley in the National Regional State of Oromia, 400 kilometers southeast of Addis Ababa. It lies between 6º 40' and 7º 10' N and 39º 30' and 39º 58' E (Hillman, 1988). The National Park was established in 1971 to preserve the diverse and unique flora and fauna (Hillman, 1986). The Bale massif, a component of the Eastern Afromontane hotspot, is one of Conservation International's Key Biodiversity Areas (Brooks et al., 2004)
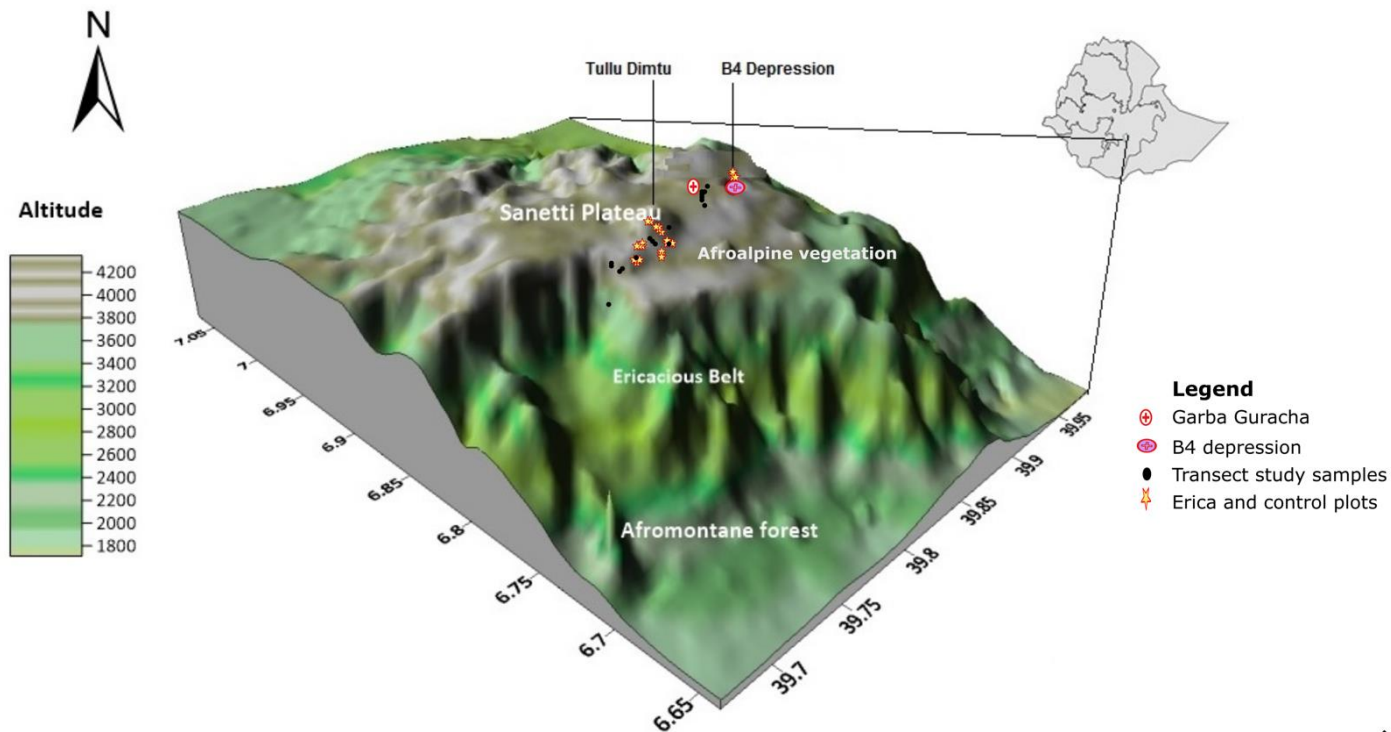
Fig. 1 Digital elevation map showing the geographical location of the Bale Mountains and the sample locations

2.2. Geomorphology and geology

The Bale Mountains were created by volcanic eruptions 40 million years ago, during the Miocene and Oligocene epochs (Billi, 2015a). The mountains cover 2200 km^2, divided into three geographic regions: the northern slopes (3000–3800 m asl), the southern escarpment (1400–3800 m asl), and the central Plateau (3800–4377 m asl) (Hillman, 1988). The Sanetti Plateau is the most extensive continuous high-altitude Plateau on the continent above 3000 m asl. While the majority of the Plateau is flat, covered with Afroalpine flora, it is flanked by three mountains: Batu (4307 m asl), Konteh (4132 m asl), and Tullu Dimtu (4377 m asl) (Hedberg, 1964; Hillman, 1988, 1986; Miehe

and Miehe, 1994). The Bale Mountains were glaciated during Marine Isotope Stages 3 and 2 (Osmaston et al., 2005). According to Gross et al. (2021), an ice cap of up to 265 km^2 covered the mountains between 42 and 27 cal kyr BP. This is clearly shown by moraines, boulders, glacial lakes, and depressions punctuating the Plateau. Previous studies have reported that the mountains deglaciated around 16 cal kyr BP (Bittner et al., 2020; Groos et al., 2021; Umer et al., 2007).

The soils in the Bale Mountains are derived from the Miocene basalt and trachyte lavas that lie over Mesozoic sediments. They are characterized as shallow, gravelly, silty-loamy, reddish or dark brown, and black (Abbate et al., 2015; Billi, 2015b; Kidane et al., 2012; Miehe and Miehe, 1994). According to the World Reference Base soil classification system, most soils in the Bale Mountains can be classified as Leptosols, Cambisols, or Andosols (Zech et al., 2022).

2.3.   Climate

The climate of the Bale Mountains, like that of the rest of the Ethiopian highlands, is influenced by topography and the seasonal movement of the Intertropical Convergence Zone (ITCZ) and the Congo air barrier (CAB). While the ITCZ separates dry northeasterly and wet southeasterly trade winds, the CAB depicts the convergence of Atlantic and Indian Ocean air masses (Costa et al., 2014; Levin et al., 2009; Tierney et al., 2011). The Bale Mountains have a brief dry season and a bimodal rainy season (Kidane et al., 2012; Miehe and Miehe, 1994). The dry season lasts from November to February, whereas the first wet seasons last from March to June followed by the second wet season from July to October. During the dry season, the ITCZ is positioned south of the equator and forms high-pressure cells across the Sahara and West Asia, which results in the dominance of the northeasterly winds. As the ITCZ moves north towards the Tropic of Cancer, the prevailing wind direction changes from northeast to southeast. The rain-bearing air masses drive from the Indian Ocean and the Atlantic Ocean through the Congo Basin (Lemma et al., 2020; Tierney et al., 2011; Van Campo and Gasse, 1993). The mean maximum temperature at Dinsho (3170 m asl) is 11.8 °C, while the mean minimum temperature ranges from 0.6 °C to 10 °C, with frost frequently occurring in the high mountain elevations from November to January (Hillman, 1986; Tiercelin et al., 2008). The southern section of the mountains receives the most precipitation and humidity, with 1000-1500 mm per year, while the northern part receives between 800 and 1000 mm per year (Miehe and Miehe 1994; Umer et al. 2007). The Sanetti Plateau is distinguished by significant diurnal temperature changes ranging from -15 ºC to +26 ºC. For the entire year, the flora undergoes severe temperature differences within a day, experiencing "summer every day and winter every night" (Hedberg, 1964).

2.4.   Vegetation

Similar to other East African mountains, the vegetation of the Bale Mountains shows a distinct zonation due to variations in altitude and associated climatic conditions (Friis, 1986; Hedberg, 1951). Furthermore, human intervention impacts current vegetation formation (Belayneh et al., 2013). Accordingly, the vegetation of the Bale Mountains is divided into the Afromontane belt,

the Ericaceous belt, and the Afroalpine vegetation (Friis, 1986; Hedberg, 1951) (Fig. 1). The Afromontane forest is further divided into a southern declivity, or zonation of Harenna forest (1450 to 3200 m asl. to the southwest), and a northern declivity (drier montane forest, 2200 to 3750 m asl). While the southern declivity vegetation is dominated by *Warburgia ugandensis, Croton macrostachyus*, *Podocarpus falcatus*, *Syzygium guineense*, the northern declivity is characterized by *Juniperus procera, Hagenia abyssinica,* and *Hypericum revolutum* (Yineger et al., 2008). The Ericaceous belt spans between ca. 3200 and 3800 m asl across all aspects of the massif and is dominated by *Erica arborea* L. and *Erica trimera* (Engl.) (Hailemariam et al., 2016). While the lower boundary of the Ericaceous belt (3300–3500 m asl) is covered with *Erica*-dominated *Hagenia-Hypericum* forests, the central part is covered with monotonous *Erica trimera* stands that extend to the upper boundary (ca. 3800 m asl) (Friis et al., 2010). In the southern parts, the older *Erica* stands with a densely branched shrub canopy, and moss covering the ground is dominant. *Erica trimera* forms tall trees up to 15 m with abundant epiphytes (Miehe and Miehe, 1994). The Afroalpine vegetation above 3800 m asl is open and rich in tussock grasses, dominated by *Helichrysum splendidum-Alchemilla haumannii* dwarf-scrubs, *Kniphofia foliosa*, and Giant *Lobelia* (*L. rhynchopetalum*) (Hedberg, 1964), accompanied by patches of *Erica,* growing between big boulders (Miehe and Miehe, 1994; Friis et al., 2010). Frequent bushfires keep *Erica* in low (up to 3 m), shrubby regeneration phases (Johansson et al., 2012).

3. Sample collection and preparation

For chemotaxonomic characterization of the vegetation using stable isotopes, lignin, *n*-alkanes, and sugar biomarkers, leaves of the dominant plant species (n = 25: *Erica, Alchemilla haumannii, Helichrysum splendidum, Lobelia rhynchopetalu, Kniphofia foliosa*, and *Festuca abyssinica*) were collected along a northeast (3870 to 4134 m asl) and a southwest transect (2550 to 4377 m asl). In addition, organic and mineral topsoil layers (n = 37) below the standing vegetation were sampled. Besides, source identification of *n*-alkanes and sugar biomarkers in sedimentary archives of Garba Guracha, a glacial lake located at 3850 m asl, and B4 depression, located at 3970 m asl above the upper limit of *Erica* on the Sanetti Plateau, was done by comparing with modern data sets.

The paleoenvironmental reconstruction was undertaken by investigating sediments of a 2.55 m deep B4 depression. Sediment samples were taken (n = 105) at high resolution (2 cm) from the laminated bottom part of the profile between 55 and 255 cm and every 5 to 10 cm from the brownish upper part. In addition, ten sediment samples were collected from the profile for radiocarbon dating. Contemporary plants growing around the depression were also collected for comparison. Texture, pollen, *n*-alkanes, XRF, and black carbon content of the sediments were quantified.

To identify the factors responsible for the current distribution of *Erica* on the Sanetti Plateau, soil samples were taken from ten different soil profiles; five below *Erica* patches and five below nearby non-*Erica* (control) plots covered by Afroalpine vegetation. In addition, leaf samples of *Erica*, grass, and *Helichrysum* growing on the plots were collected. Total organic carbon and

nitrogen, stable isotopes, black carbon, pH, and EC of the soils were evaluated. Before laboratory analyses, all leaf and soil samples were air-dried and finely ground using a ball mill. Soil samples were sieved using 2 mm mesh prior to grinding. Similarly, aliquots of sediment samples were dried at 105 °C and finely ground for the biogeochemical analyses.

4. Methodology

The methods used for this doctoral thesis are presented here briefly. For further details, the reader is referred to the respective methodology sections of the included publications.

4.1. Elemental and stable isotopes analyses

Total organic carbon (TOC), total nitrogen (TN), and the natural abundance of $\delta^{13}C$ and $\delta^{15}N$ of the samples were measured using an elemental analyzer coupled to an isotope ratio mass spectrometer (EA-IRMS). The precision of $\delta^{13}C$ and $\delta^{15}N$ measurements was 0.2‰ and 0.3‰, respectively. Carbon and nitrogen stocks were calculated according to Batjes (1996)

$$\text{SOC}_{\text{stock}} = \sum_{i=1}^{k} SOC \times BD \times t \times \left(1 - \left(\frac{S}{100}\right)\right) \tag{1}$$

where $\text{SOC}_{\text{stock}}$ is the total amount of organic carbon (in kg m^{-2}), SOC is the proportion of organic carbon (kg Mg^{-1}) in layer i, BD is the bulk density (Mg m^{-3}) of layer i, t is the thickness of this layer (m), and S is the volume of the fraction of fragments >2 mm.

4.2. Non-cellulose sugar biomarkers

Sugar biomarkers in the plant, soil, and sediment samples were extracted by hydrolyzing the samples with 10 mL of 4M trifluoroacetic acid (TFA) (Zech and Glaser, 2009). After extraction, the filtrates were evaporated and passed through XAD and Dowex resin columns to remove humic substances and cations, respectively (Amelung et al., 1996). Subsequently, the samples were derivatized with N-methyl-2-pyrrolidone (NMP), and individual monosaccharide sugars (arabinose, fucose, galactose, glucose, mannose, rhamnose, ribose, and xylose) were quantified using gas chromatography equipped with a flame ionization detector (GC-FID).

4.3. *n*-alkanes

n-Alkanes were extracted by Soxhlet extraction using dichloromethane (DCM) and methanol (1:1) as solvents for 24 h (Zech and Glaser, 2008). After extraction, 50 µl of 5α androstane was added to the total lipid extract as an internal standard, and the excess solvent was removed by rotary evaporation. Subsequently, *n*-alkanes were eluted with 3 ml of hexane DCM/MeOH (1:1). Finally, *n*-alkanes were quantified using GC-FID.

4.4. Lignin

Lignin phenols were extracted using the cupric oxidation (CuO) method developed by Hedges and Ertel (1982) and modified later on by Goñi and Hedges (1992). After digesting the samples under high pressure at 170 °C for 2 h, they were purified by adsorption on C18 columns, desorbed by ethylacetate, and concentrated under a flow of nitrogen gas for 30 min. Finally, the samples were derivatized using 200 µL of N, O-bis(trimethylsilyl)trifluoroacetamide (BSTFA), and 100 µL of pyridine and quantified using GC-FID. The content of each lignin phenol (in mg g^{-1}) was calculated from the sum of the following CuO oxidation products.

$$\text{Vanillyl (V)} = \text{vanillin} + \text{acetovanillone} + \text{vanillic acid} \tag{2}$$

$$\text{Syringyl (S)} = \text{syringaldehyde} + \text{acetosyringone} + \text{syringic acid} \tag{3}$$

$$\text{Cinnamyl (C)} = \text{p-coumaric acid} + \text{ferulic acid} \tag{4}$$

4.5. Black carbon

Black carbon was analyzed using benzene polycarboxylic acids (BPCA) as molecular markers following Glaser et al. (1998) and modified by Brodowski et al. (2005). Samples were hydrolyzed with 10 ml 4 M TFA and rinsed several times with de-ionized water to remove polyvalent cations. Subsequently, the samples were digested with 65% nitric acid for 8 hours at 170 °C in a high-pressure digestion apparatus. The solution was passed through Dowex 50 W resin columns (200 to 400 meshes) to remove polyvalent cations. After derivatization with BSTFA, BPCA were measured using GC-FID.

4.6. Physical properties and inorganic geochemistry

Clay (<6.3 µm) and silt (6.3–63 µm) fractions were quantified using a Mastersizer S (Malvern Instruments) after treating the samples with H_2O_2 and HCl. The sand fraction (63–2000 µm) was determined by wet sieving. It should be, however, noted that the clay fraction used in this study does not quantitatively correspond to the clay fraction defined by the pipette method, as the fraction < 2 µm is underestimated by the Mastersizer. Electrical conductivity and pH were measured with a glass electrode.

4.7. Analyses in collaboration

The following analyses were carried out in collaboration and the results are used in this thesis.

4.7.1 Mineral and elemental composition

Major and minor elemental compositions were determined using a Philips 2404 X-Ray Fluorescence Spectrometer. Qualitative mineral identification was carried out on bulk samples using X-ray diffraction.

4.7.2 Radiocarbon dating

To establish a reliable chronology, radiocarbon dates were obtained by dating alkali-soluble organic matter extracted from carbonate-free bulk samples using accelerated mass spectrometry (AMS) in the Radiocarbon Laboratory of the University of Erlangen, Germany. A Bayesian age-depth model was made using the IntCal13 calibration curve in the package Bacon Blaauw and Christeny (2011) in R software (R Core Team, 2013).

4.7.3 Pollen

Palynological analyses were done by preparing 1 ml samples following standard procedures. Microscopic analyses took place under 400x magnification, backed by oil immersion (1250x). Pollen identification was done by using an existing reference collection of ~ 5000 slides (in Goettigen) and relevant literature (Gosling et al., 2013; Schüler and Hemp, 2016). The nomenclature of the common types follows Beug (2004). Detailed analyses were carried out on 38 samples from the lower part of B4 profile (251–69 cm) Pollen influx (grains cm^{-1} a^{-1}) was calculated using exotic *Lycopodium* spore markers. the A/C (*Artemisia*/Chenopodiaceae) ratio was calculated by dividing the number of Artemisia by that of Chenopodiaceae/Amaranthaceae. to estimate humidity conditions (Herzschuh, 2007; Li et al., 2010; Van Campo and Gasse, 1993).

5. Results and discussion

5.1. Potential of stable isotopes, sugars, lignin, and *n*-alkanes as biomarkers for the reconstruction of paleoenvironmental changes (manuscript 1 and 2)

Identification of unambiguous proxies and biomarkers is essential for robust paleoenvironmental reconstruction. Accordingly, the potential of stable isotopes, sugars, lignin, and *n*-alkanes to differentiate between *Erica* and other dominant vegetation in the Bale Mountains was evaluated. The δ^{13}C values of the investigated plants range between -27.5 (*Erica*) and -23.9‰ (*Kniphofia*), well within the range typical for C$_3$ plants (Eshetu and Högberg, 2000; Marshall et al., 2007; Tiunov, 2007). The δ^{13}C values of *Erica* are not significantly different from the other plants (Fig. 3). Moreover, the occurrence of C$_4$ plants cannot be confirmed due to the admittedly quite limited plant samples. Similarly, no significant difference was revealed between δ^{13}C values of soils below *Erica* and other dominant plants. However, increasing δ^{13}C values are recorded with increasing soil depth, attributing to the preferential enzymatically controlled loss of ^{12}C during soil organic matter degradation (Farquhar et al., 1982).

The δ^{15}N values of leaves show high variability, ranging from -4.8 (*Erica*) to 5.1‰ (*Alchemilla*) (Fig. 2). This variability can be explained by different nitrogen sources and different mechanisms of N uptake with the presence of mycorrhiza. Similar to the δ^{13}C results, the δ^{15}N values of *Erica* are not significantly different from other plants. δ^{15}N values of the investigated Ah-horizons are significantly higher than the leaf samples. This enrichment is mainly due to organic matter degradation and mineralization of preferably ^{14}N (Natelhoffer and Fry, 1988).
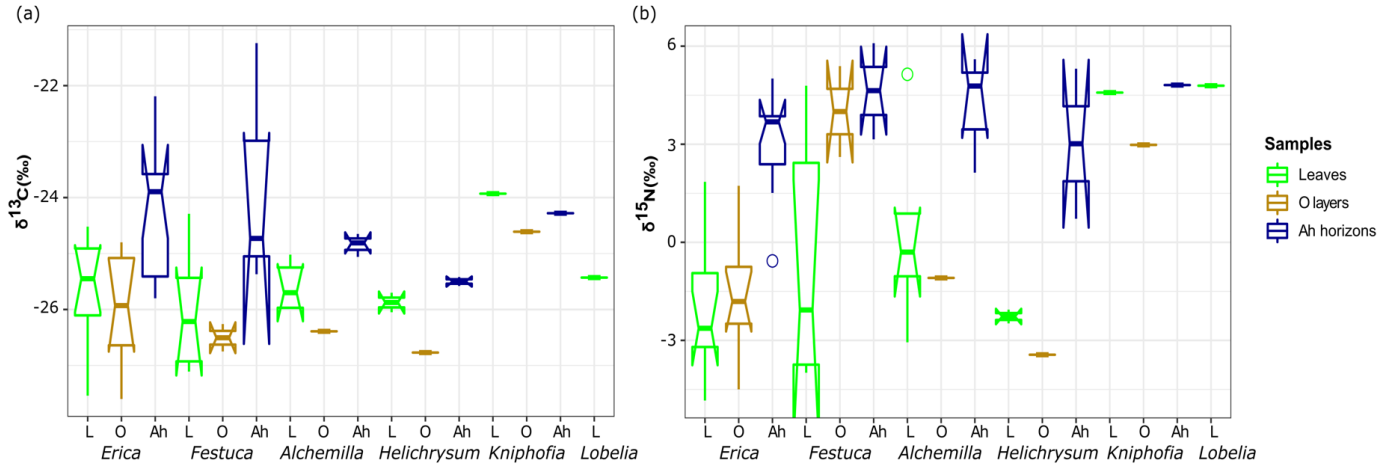
Fig. 2 *Boxplot diagrams showing $\delta^{13}C$ (a) and $\delta^{15}N$ (b) results for leaves (L), O-layers, and Ah-horizons of the investigated dominant vegetation types in the Bale Mountains. The upper and lower bold lines indicate the 75th and 25th quartiles, respectively, and the bold middle line shows the median. The lines extending outside the box (whiskers) show variability outside the quartiles, and notches indicate the 95% confidence interval of the median. Circles represent outliers. Note that short horizontal single lines are due to small sample sizes.*

Erica leaves are characterized by low total non-cellulosic sugar contents and significantly higher (G + M)/ (A + X) and (F / (A+X)) ratios than *Alchemilla*, *Festuca,* and *Helichrysum* (Fig. 3). However, the ratios generally increase in the respective O-layers and Ah-horizons, indicating that both arabinose and xylose are preferentially degraded, or that galactose and mannose are built-up by soil microorganisms. Apart from soil microorganisms, a considerable contribution of root-derived sugars, including root exudates, is also very likely (Gunina and Kuzyakov, 2015). As a result, soils under *Alchemilla* and *Festuca* yield (G+M)/(A+X) ratios similar to those of *Erica* leaves.
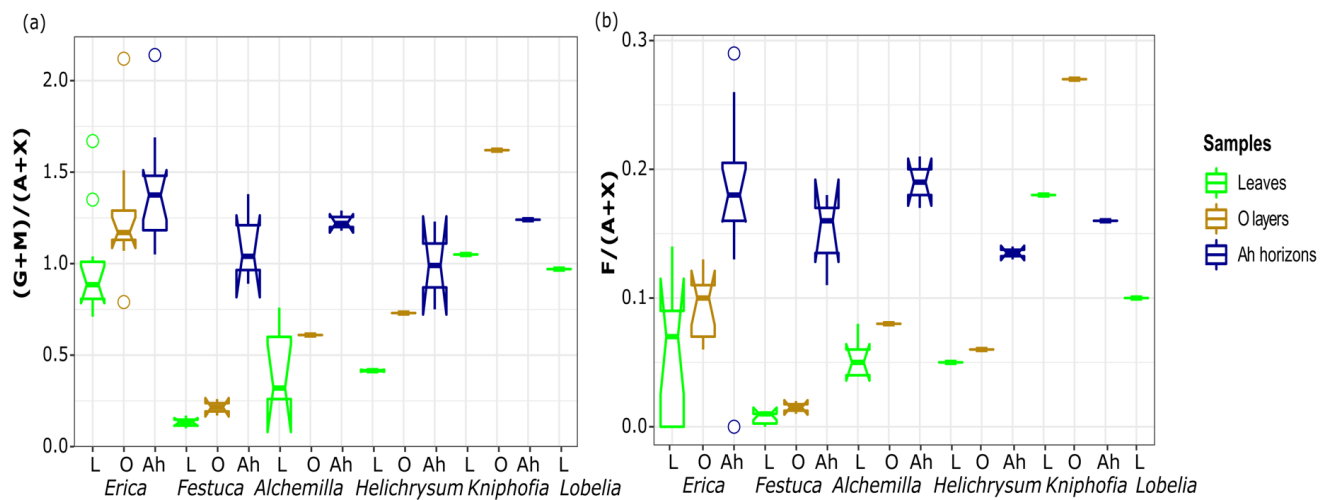
Fig. 3. *Boxplot diagram showing the (a) (G + M) / (A + X) and (b) F / (A + X) ratios of leaves (L), O-layers, and Ah-horizons, respectively, along the altitudinal transect across the Bale Mountains. The upper*

14

and lower bold lines indicate 75ᵗʰ and 25ᵗʰ quartiles, respectively, and the bold middle line shows the median. The lines extending outside the box (whiskers) show variability outside the quartiles, and notches indicate the 95 % confidence interval. White circles represent outliers. Note that short horizontal single lines are due to small sample sizes.

Lignin analysis results indicate that cinnamyl percentages of > 40% characterize *Erica spp.*, whereas all other plants are characterized by cinnamyl percentages of < 40%, except for two *Festuca* samples. These results suggest that the ratio C/(V+S+C) might be used as a proxy for distinguishing the contemporary *Erica* spp. from other vegetation types of the Bale Mountains (Fig. 4). However, the characteristic contribution of cinnamyl in *Erica* species decreases in the O-layers (C < 27%) due to degradation, whereas the two investigated O-layers under *Festuca* yield relative C contributions > 40% likely due to lignin input by roots (Abiven et al., 2011; Thevenot et al., 2010).
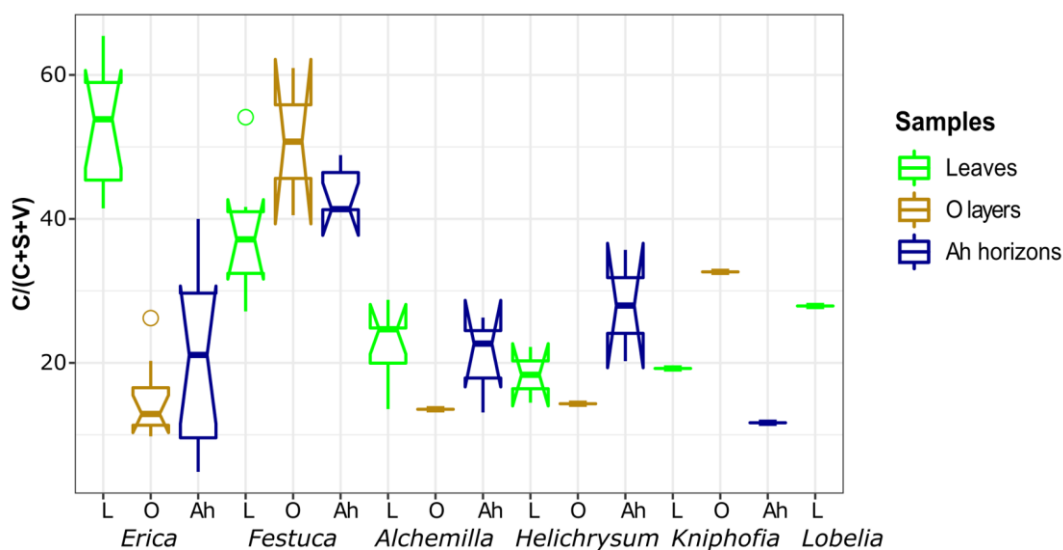
Fig. 4 Boxplot diagrams showing the relative abundance of cinnamyl phenols (expressed as C/(V+S+C) in %) in plants, O-layers, and Ah-horizons. The upper and lower bold lines indicate the 75ᵗʰ and 25ᵗʰ quartiles, respectively, and the bold middle line shows the median. The lines extending outside the box (whiskers) show variability outside the quartiles, and notches indicate the 95% confidence interval. Circles represent outliers. Note that short horizontal single lines are due to small sample sizes.

n-Alkanes distribution in leaves show a strong predominance of C_{31} in the grass, as previously observed by other authors (Schäfer et al., 2016; Zech et al., 2011b), whereas most other plant species studied here exhibited a C_{29} or C_{31} predominance. Only *Kniphofia foliosa* has a high relative abundance of C_{27} and C_{29}, while C_{31} is essentially non-existent. *Erica* litter significantly differs ($p = 0.05$) from all other plant species except *Helichrysum splendidum* by having a lower C_{31}/C_{29} ratio ($\bar{x} = 1.7$) than other plant species (Fig. 5). However, due to *n*-alkane degradation, this ratio is not feasible to chemotaxonomically distinguish between soils having developed under *Erica* versus *Alchemilla* and grass. It should be, however, noted that this interpretation is based on the assumption that the above-ground vegetation did not change for several decades.

15
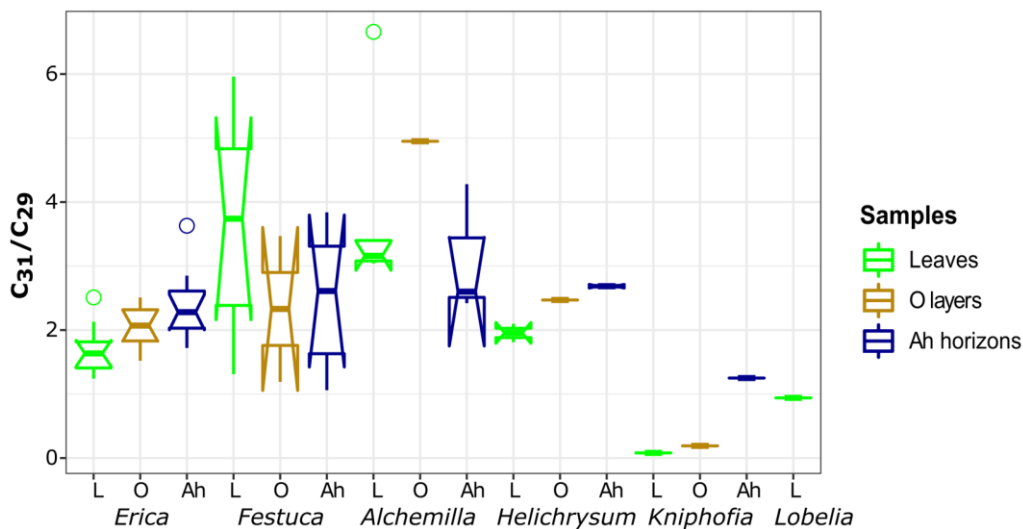
Fig. 5 *Notched boxplots for the ratio C_{31}/C_{29} in plant samples, organic layers, and Ah-horizons. The upper and lower bold lines indicate the 75th and 25th quartiles, respectively, and the bold middle line shows the median. The lines extending outside the box (whiskers) show variability outside the quartiles, and notches indicate the 95% confidence interval. Circles represent outliers. Note that short horizontal single lines are due to small sample sizes.*

5.2. Terrestrial versus aquatic source identification of sedimentary *n*-alkane and sugar biomarkers (manuscript 3)

Organic matter source identification is an important prerequisite for robust paleoenvironmental reconstructions. Therefore, the sources of the sedimentary *n*-alkane and sugar biomarkers in two sedimentary archives, Garba Guracha and B4 depression, both located in the Bale Mountains, were studied by comparing the biomarkers in sediments with the above presented modern data set. The relative abundance of long-chain *n*-alkane homologues C_{29}, $C_{31,}$ and C_{33} of Garba Guracha and B4 sediment samples are similar to modern samples (Fig. 6a). This implies that the sedimentary *n*-alkane homologues C_{29}, $C_{31,}$ and C_{33} are likely primarily of terrestrial (allochthonous) origin. By contrast, there is a difference in the relative abundance of C_{27} and mid-chain *n*-alkanes of modern and sediment samples. Most terrestrial samples are characterized by relative abundances of $C_{27} < 10\%$, whereas relative abundances of $C_{27} > 10\%$ are characteristic of the sediments of Garba Guracha and B4 (Fig. 6b). Similarly, the relative abundances of C_{25} and C_{23} are typically < 10% in terrestrial samples, whereas the relative abundances of C_{25} and C_{23} are typically >10% in the sediments of Garba Guracha and B4 (Fig. 6c). Moreover, the modern samples yielded P_{aq} values typically < 0.1, whereas the sediments samples revealed P_{aq} values typically > 0.2. These results indicate that the sedimentary *n*-alkane homologues C_{23}, $C_{25,}$ and C_{27} in Garba Guracha and B4 are mainly aquatic-derived. Moreover, the P_{aq} ratio is corroborated as a proxy for terrestrial versus aquatic organic matter input in the Bale Mountains sedimentary archives.
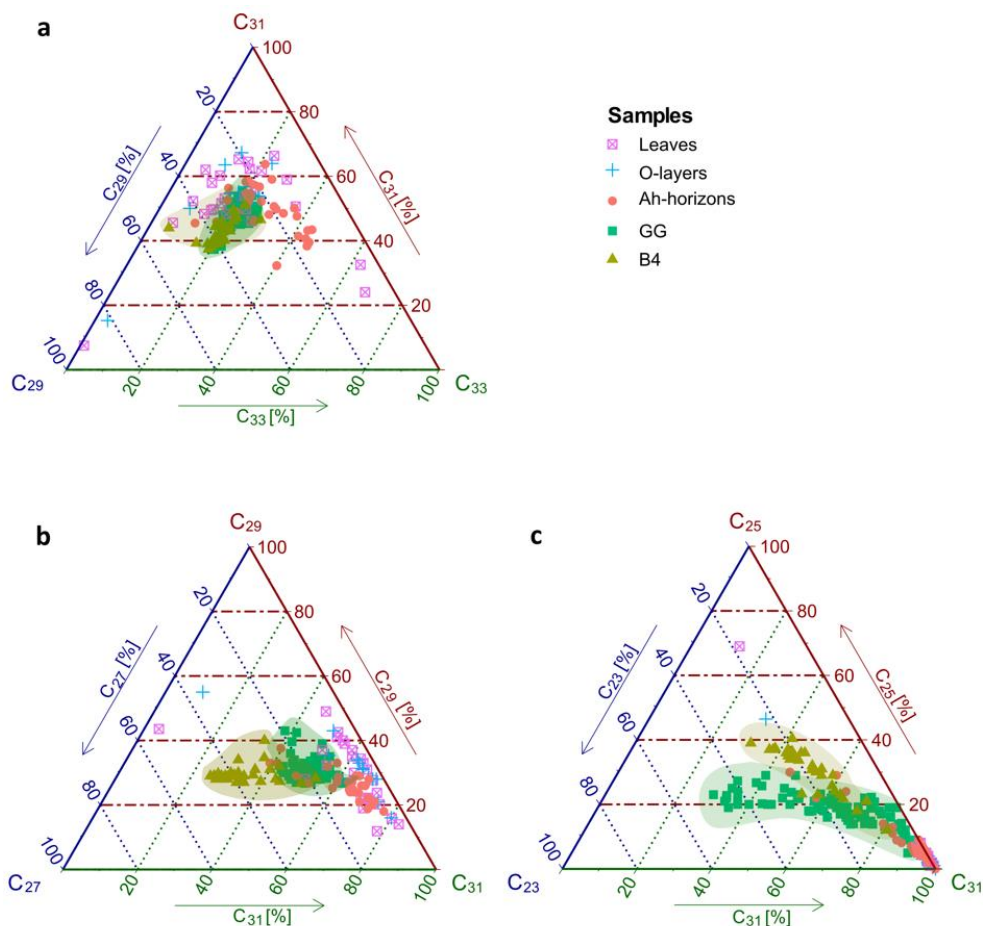
Fig. 6 *Ternary diagrams for the relative abundance of mid-chain and long chain n-alkanes in modern leaf and soil samples and sediment samples of Garba Guracha and B4 depression.*

However, caution must be taken while interpreting the source of long-chain homologues as they are also produced by the aquatic algae *Botryococcus braunii,* which is reported to be abundantly found in Garba Guracha and B4. In addition, microbial syntheses of short-, mid-, and even long-chain *n*-alkane in soils and sediments during organic matter degradation cannot be ruled out (Brittingham et al., 2017; Li et al., 2018; Nguyen Tu et al., 2011).

Sugar analyses were not carried out for B4 sediments. In the Garba Guracha sediments, galactose is the most abundant sugar biomarker, followed by xylose, fucose, arabinose, mannose, and rhamnose. Xylose and arabinose likely reflect an at least partly terrestrial input. The relatively high abundances of galactose and mannose in the Garba Guracha sediments might be attributed to contributions by both soil and aquatic microorganisms. According to Oades (1984), the ratio (G+M)/(A+X) can serve as a proxy to differentiate between plant-derived and microbial-derived sugars in soils. However, because galactose and mannose are produced by both soil and aquatic bacteria, their use for identifying terrestrial versus aquatic input is challenging.

17

The relative abundances of fucose and rhamnose are significantly higher in the Garba Guracha sediments than in modern samples. Rhamnose and fucose are reported to occur in submerged aquatic plants and are abundantly produced by algae and zooplankton, whereas xylose and arabinose strongly predominate in terrestrial plants and soils (Hepp et al., 2016; Jia et al., 2008; Marchand et al., 2005). Garba Guracha sediments are characterized by a significantly higher ratio of (fuc + rham)/ (ara + xyl) than modern samples (Fig. 7). Therefore, this ratio can be used as a proxy for terrestrial versus aquatic non-cellulose sugar source identification.
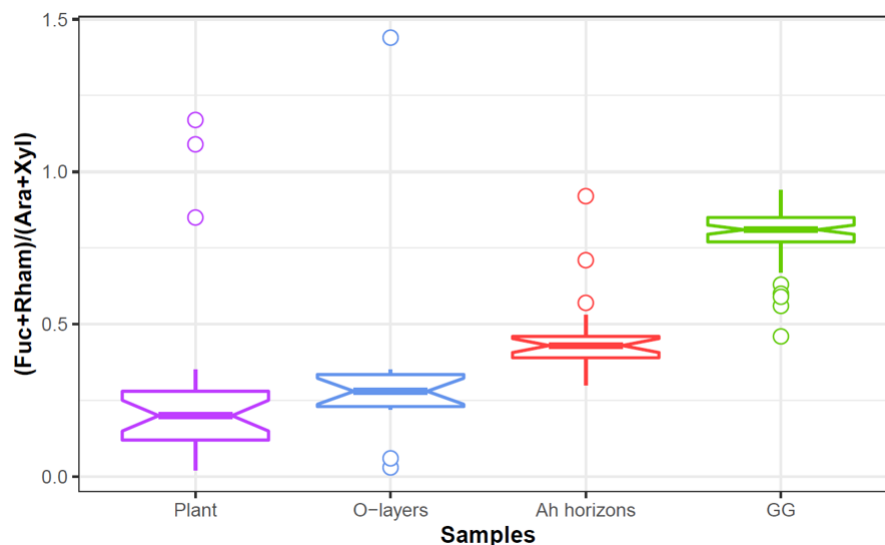
Fig. 7 The ratio of (fuc + rham)/ (ara + xyl) in plants, O-layers, Ah-horizons, and Garba Guracha sediments. The notched box plots indicate the median (solid lines between the boxes) and interquartile range (IQR) with upper (75%) and lower (25%) quartiles. The notches display the 95% confidence interval of the median. The lines extending outside the box (whiskers) show variability outside the quartiles. The circles represent outliers.

5.3. Climate, vegetation, and fire history of the Sanetti Plateau (manuscript 4)

B4 profile documents the climate, vegetation, and fire history of the Sanetti Plateau since the last 18.2 cal kyr BP. The lowermost part of the profile between 18.2 and 13.6 cal kyr BP (255-17 cm; unit 1 and 2) is characterized by high sedimentation rates (0.05 cm per year), while the upper part (upper 70 cm, unit 3) shows a low sedimentation rate (0.01 cm per year) (Fig. 8). Moreover, a hiatus is recorded between 13.6 and 10.5 cal kyr BP. Unit 3 is highly influenced by hydromorphic processes. As a result, unambiguous interpretation of proxies and paleoenvironmental reconstruction for the last 10 cal kyr BP was not possible. Therefore, this thesis presents the paleoenvironmental history of the Sanetti Plateau as documented between 18.2 and 13.6 cal kyr BP.

Deglaciation

The Age-depth model shows that the Sanetti Plateau is deglaciated at ~ 18.2 cal kyr BP (Fig. 8). The timing of the deglaciation seems reliable as the sediments are free of carbonates. Moreover, the high occurrence of *Botryoccoccus* at the bottom of the B4 profile confirms the deglaciation and the discharge of cold meltwater into the lake. However, this result is in contrast to the findings of Bittner et al. (2020) and Tiercelin et al. (2008), which reported the deglaciation of Garba Guracha at 15.9-16.7 cal kyr BP. This disparity can be explained by the fact that the ice cover in the N-exposed trough valley of Garba Guracha was thicker and lasted longer than on the Plateau around the B4 profile, which is heavily wind-exposed and has no ice-accumulating catchment.
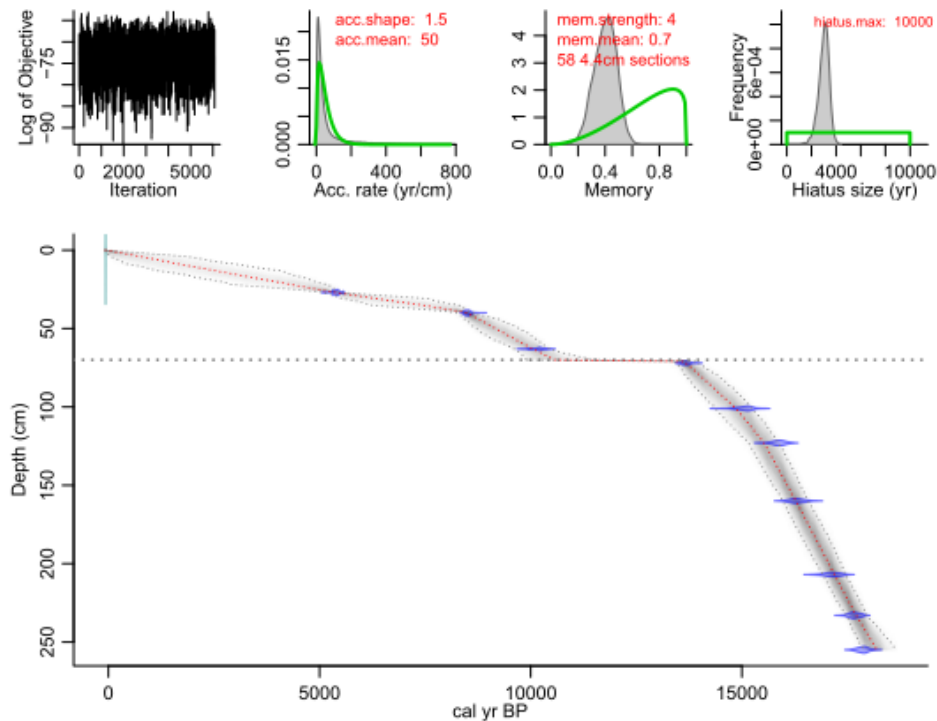
Fig. 8 *Bayesian age-depth model for profile B4 according to Blaauw and Christen (2011). Top left: The log-likelihood of the model fit for the saved iterations of the model, top middle: prior and posterior distribution of accumulation rate, and top right: prior and posterior distribution of the autocorrelation in accumulation rates (memory) and the time gap (hiatus size) at the end. The bottom panel shows the calibrated 14C dates (transparent blue), and the age-depth model (darker greys) indicate more likely calendar ages; grey stippled lines show 95% confidence intervals; the red curve shows a single 'best' model based on the mean age for each depth*

Initial phase after deglaciation

The initial phase after deglaciation was characterized by cold conditions with mainly lacustrine primary biomass production under a medium to high water level, as evidenced by low TOC and TOC/N ratios and weakly increasing Paq values documenting only minor terrestrial input (Fig. 9).
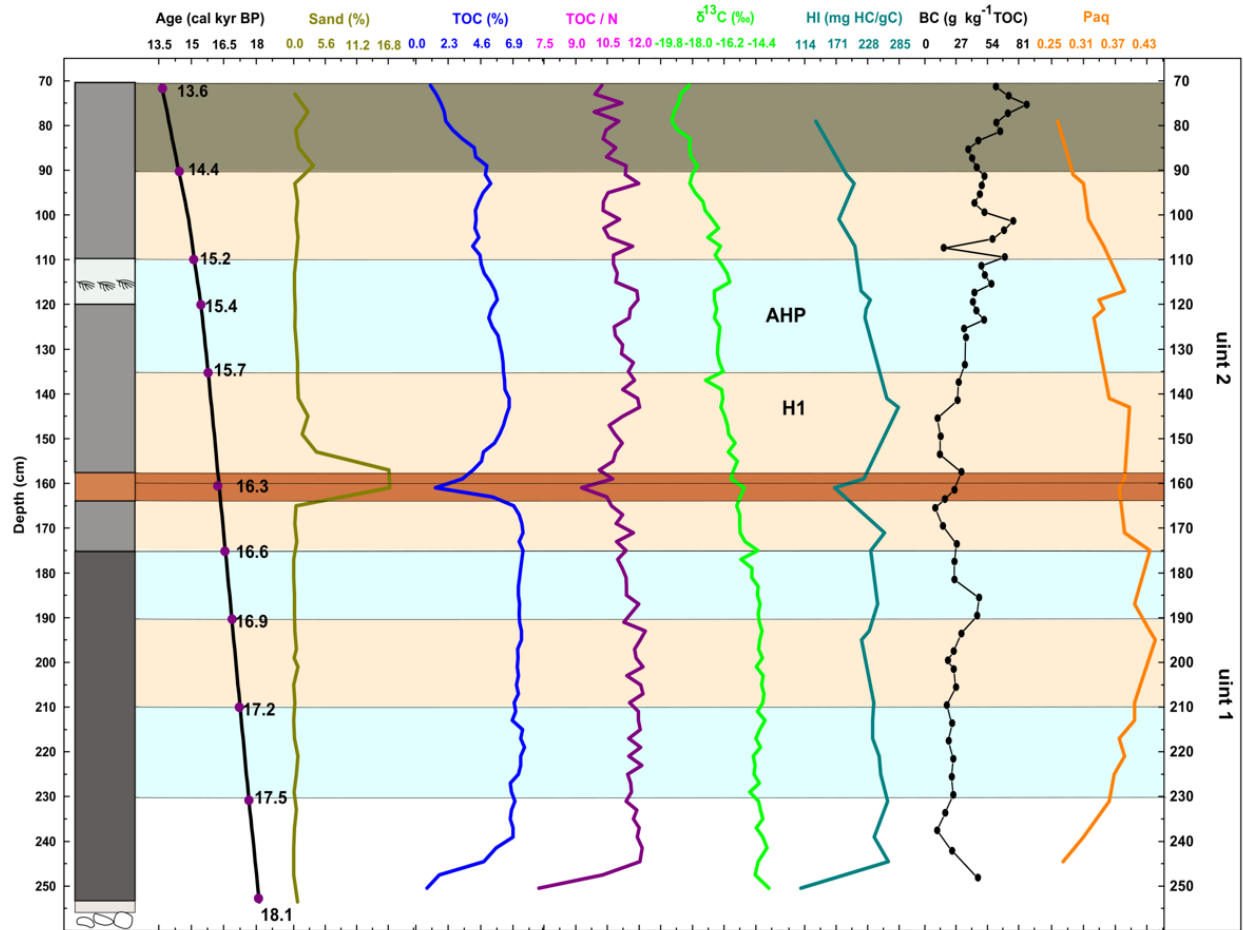
Fig. 9 Analytical properties of the B4 sediments, with depth profiles of the sand fraction (63-2000 μm), TOC, TOC/N, HI, δ¹³C values, BC, and Paq. The light orange color shows dryer events, while the orange color indicates desiccation layers developed during Hl. Blue color indicates the AHP and other humid episodes, while dark green color indicates the event characterized as humid and arid according to pollen and geochemical results, respectively

Between 18.1 and 17.2 cal kyr BP, the vegetation is characterized as herb-rich open grassland with a high number of Artemisia, Chenopodiaceae/Amaranthaceae, and Plantago (Fig. 10). Positive $\delta^{13}C$ values of bulk sediments and long-chain *n*-alkanes let assume that C4 vegetation (Ficken et al. 2002; Glaser and Zech 2005) was growing at the margin of the depression under relatively dry conditions during the Late Glacial. However, methanogenesis, assimilation of ^{13}C-enriched CO_2 and HCO_3^- by water plants due to long-lasting ice cover, especially during the early Late Glacial, and the low CO_2 concentration in the atmosphere (Monnin et al. 2001) might have contributed to such positive $\delta^{13}C$ values (Conrad et al. 2007).

Arboreal pollen *Ericaceae, Podocarpus, Myrica, Juniperus,* and *Olea* were also detected at the bottom of the profile, indicating the presence of forest down the slopes of the Bale Mountains (Fig. 10). Moreover, the weak BC maximum in the lowermost samples presumably reflects BC storage

in glacier ice during the LGM, originating from atmospheric input derived from vegetation fires elsewhere or the *Erica* belt in lower altitudes (Fig. 10).
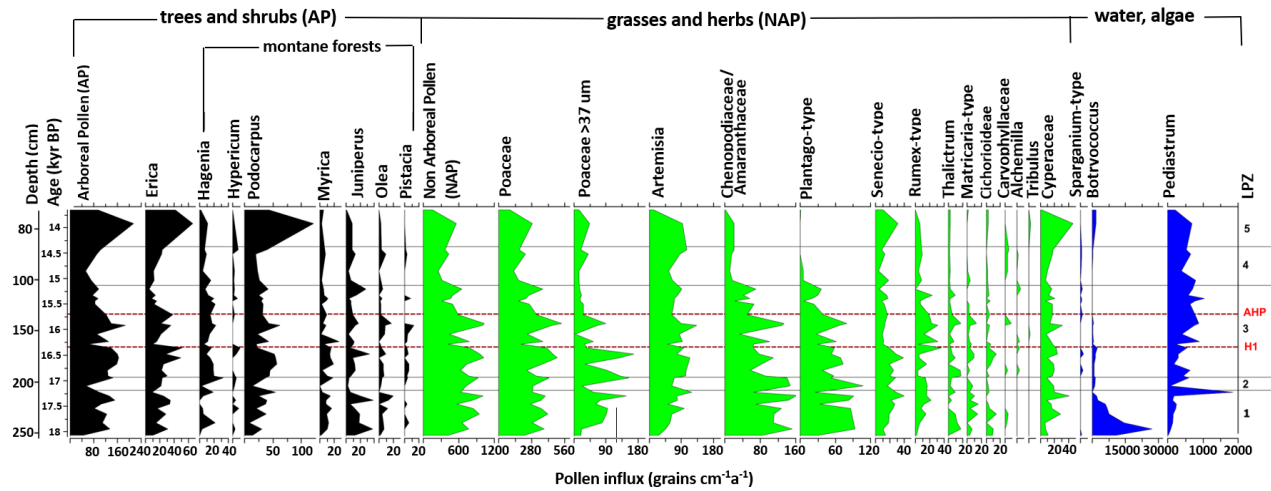
Fig. 10 Pollen influx diagram of selected taxa and algae from the B4 depression, showing pollen accumulation rate in grains cm^{-1} year^{-1}

Heinrich Event 1

In B4 depression, partly fluctuating allochthonous elements and ratios such as Zr, Hf, Zr/SiO$_2$, Zr/Rb, and Zr/TiO$_2$ document a short dry event between ~17.2 and 16.9 cal kyr BP. This ~300-year dry event likely led to a decline of the montane forest as evidenced by a decrease in *Artemisia*, *Pediastrum, Hagenia*, *Podocarpus*, *Myrica*, *Juniperus*, and *Olea* and an increase in Chenopodiaceae/Amaranthaceae and *Plantago* (Fig. 10). These findings are consistent with those of Umer et al. (2007), who found evidence of open grassland vegetation in the Garba Guracha region around16 cal kyr BP. Furthermore, this dry event possibly relates to a precursor of H1 as reported for Asia and the Mediterranean, around 17 cal kyr BP and between 17.2 and 16.9 cal kyr BP, respectively (Camuera et al., 2021; Hemming, 2004). A shift to wetter local conditions on the Sanetti Plateau slopes, as evidenced by an increase in arboreal pollen and *Pediastrum*, occurred between 16.9 and 16.6 cal kyr BP. High BC contents relative to TOC between 16.9 and 16.6 cal kyr BP record a concurrent fire occurrence, most likely caused by an increase in combustible biomass due to wetter regional conditions.
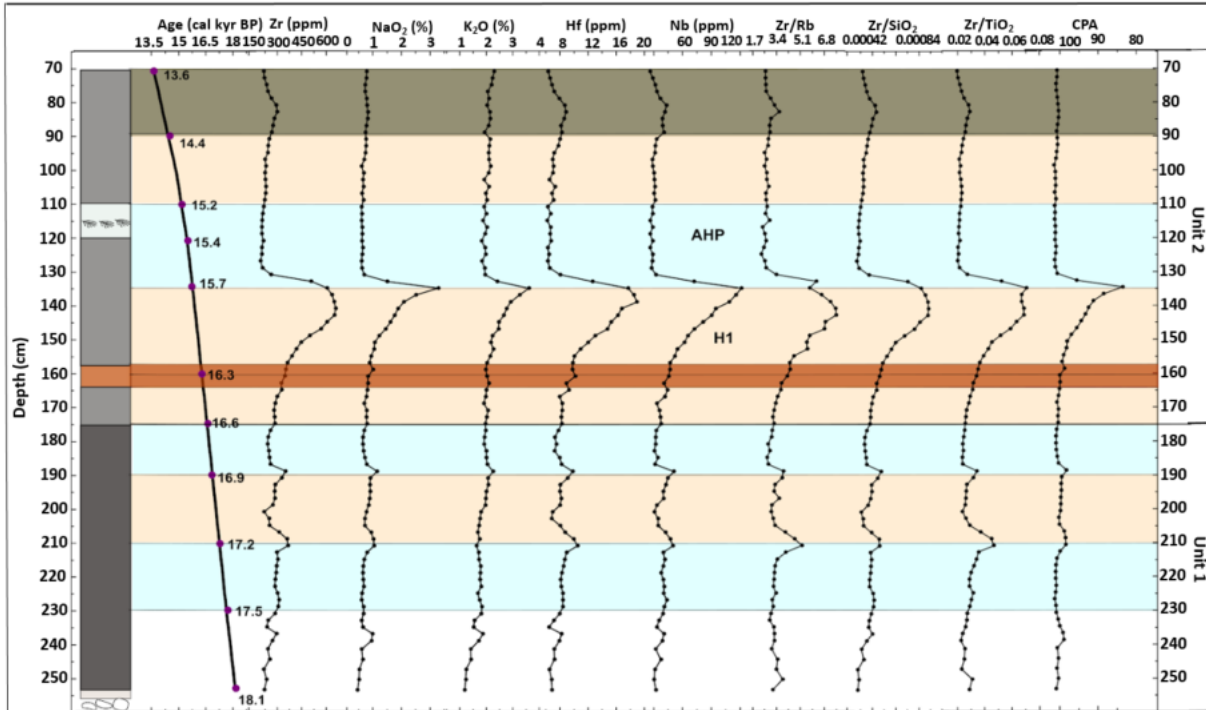
Fig. 11 *XRF results of B4 sediments. Depth profiles of Zirconium (Zr), Sodium oxide (Na₂O), Potassium oxide (K₂O), Hafnium (Hf), Niobium (Nb), Zirconium/Rubidium (Zi/Rb), Zirconium/Silica oxide (Zr/SiO₂), Zirconium/Titanium oxide (Zr/TiO₂) and the chemical proxy of alteration (CPA=Al₂O/(Al₂O₃ + Na₂O), inversed scale. The light orange color shows dryer events, while the orange color indicates desiccation layers developed during H1 and the hiatus. The blue color indicates the AHP and other humid episodes, while the dark green color indicates the event characterized as humid and arid according to pollen and geochemical results, respectively*

The B4 depression further documented a continuous increase of less weathered lithogenic elements (Fig. 11; CPA < 80, Na enriched) between 16.6 – 15.7 cal kyr BP. These less-weathered allochthonous elements are likely transported to the Sanetti Plateau by intensified dry northerly winds occurring contemporaneously with the North Hemispheric cooling during H1 (Brown et al. 2007; Marshall et al. 2011; Lamb et al. 2018). Moreover, an extremely low stand of the water table and short-term intensive desiccation is recorded in the B4 depression at 16.3 cal kyr BP, as evidenced by a substantial decrease of TOC, accompanied by sand maxima. Increased sand input from the depression margins may occur because of temporary heavy rain showers during dry phases when the sparse vegetation cover was less protecting against erosion. The desiccation surface developed around ~16.3 cal kyr BP correlates with slightly decreased contents of *Erica* pollen, *Pediastrum*, ferns, and *Botryococcus*, and elevated Chenopodiaceae/Amaranthaceae ratios, indicating a temporary phase of less favourable, drier environmental conditions. This event possibly marks the time of maximum H1 dryness. In many studies, arid conditions in tropical Africa between ~16.8 and 15.4 cal kyr BP were already described as coinciding with H1 (e.g., Bonnefille and Chalie 2000; Gasse 2000; Talbot and Lærdal 2000; Hemming 2004; Tiercelin et al. 2008; Tierney et al. 2008). Moreover, Lamb et al. (2007) also mentioned an "episode of shallow

water" in the Lake Tana basin between 16.7-15.7 cal kyr BP. Previous studies described that climatic fluctuations in eastern Africa during the Late Quaternary were related to teleconnections between North Atlantic cooling events, recorded in Greenland ice cores and in N-Atlantic sediments, and the weakening of the Indian Summer Monsoon (Lamb et al., 2018; Marshall et al., 2011; Mohtadi et al., 2014; Tierney et al., 2008).

However, unlike in other east African lowland regions, this dry event did not last long in the Bale Mountains and the environmental condition improved locally on the Sanetti Plateau as indicated by decreased sand contents and high TOC and HI values. This discrepancy between the high altitudes of the Sanetti Plateau and the vast lowlands northerly might reflect that the Bale Mountains, located close to the Indian Ocean, react more rapidly to environmental changes. In contrast, the lowland ecosystems are much more resilient due to slow negative vegetation and monsoon feedback.

African humid period

A drastic reduction of allochthonous elements input into the B4 depression is recorded at about 15.7 cal kyr BP. This likely indicates the onset of AHP, which resulted in a relatively rapid establishment of a denser vegetation cover and a drastic reduction of dust deflation from northern source areas (Fig. 11). However, pollen results of B4 (Fig. 10) do not show clear evidence for this abrupt start of the AHP. Nevertheless, Camuera et al. (2021) recorded similar timing (15.7 cal kyr BP) for the termination of HS1c and onset of AHP in the Mediterranean. Also, Lamb et al. (2007, 2018) described such an abrupt shift from Lake Tana, and Marshall et al. (2011) dated this event to 15.3 cal kyr BP. In Lake Victoria, the rapid refilling of the basin is dated to 14.5 cal kyr BP (Talbot and Lærdal, 2000). One reason for this discrepancy might be dating uncertainties. However, our data from the B4 profile let assume that locally, at the high altitudes of the Sanetti Plateau, the abrupt onset of humidity might have started almost 1000 years before the beginning of the Bølling–Allerød warming in the North-Atlantic region (Alley and Clark, 1999; Van Raden et al., 2013) and before at least some hundred years earlier than in Lake Tana region, located 630 km northward.

Within this humid period, water levels in the B4 depression did not remain permanently high but lowered already around 15.4 cal kyr BP, and a swamp developed, reflecting probably higher evaporation and less precipitation. A similar finding was reported from Lake Tana, where a papyrus swamp developed between 15.7 and 15.1 cal kyr BP due to lower lake levels and reduced rainfall (Lamb et al., 2007). Slightly rising allochthonous proxies (e.g., Zr, Nb, Hf, see (Fig. 11)) and decreasing TOC and HI values likely document progressive local drying-up after about 14.4 cal kyr BP, whereas ascending arboreals indicate regional wetter conditions (Fig. 10). A significant increase in *Erica* and *Podocarpus* pollen between 14.4 and 13.6 cal kyr BP substantiates the expansion of the Ericaceous belt and the lowland forests, together with a fundamental change in the vegetation composition on the Sanetti Plateau, likely correlating with an increase in temperature, which might be synchronous with the European Meiendorf interstadial starting at 14.4 varve years (Litt et al., 2001). BC started to increase only with the beginning of the AHP

around 15.7 cal kyr BP, correlating with warmer and more humid environmental conditions and reaching a maximum at about 15 cal kyr BP coinciding with increasing *Erica* pollen.

Despite the human settlement during 47-31 cal kyr BP, there is no evidence that hunter-gatherers lived on the Plateau and burned the *Erica* to facilitate hunting during the Late Glacial. However, we cannot rule out that fires were triggered by increased easily combustible *Erica* biomass due to improved environmental conditions. This implies that the amount of *Erica* biomass mainly controls the burning of *Erica*, being higher under warm and humid climates.

5.4. Factors influencing the present-day distribution of *Erica* on the Sanetti Plateau (manuscript 5)

To understand the major factors governing the current patchy distribution of *Erica* patches on the Sanetti Plateau, the environmental features and soil properties of sites covered by *Erica* and non-*Erica* vegetation (control) were studied. The results show that the site exposition and environmental features of *Erica* and control plots are more or less similar. However, the *Erica* plots are covered by high amounts of dark basalt boulders, while usually, there are few or no boulders on the control plots. Therefore, these boulders on the *Erica* plots may protect the *Erica* patches against the wind, provide warmth and shade, and enable the *Erica* seedlings to withstand the harsh climatic condition on the Sanetti Plateau (Wesche et al., 2008).

Regarding the soil properties, except for bulk density, TOC/N, black carbon, and δ^{13}C, other biogeochemical proxies such as soil texture, pH, and EC do not show a significant difference between *Erica* and control plots. However, slightly lower pH values are recorded below the O layers of *Erica*, which can be explained by the acidifying effects of the thick, slowly decomposing *Erica* litter (Dahlgren et al., 1997). The significantly lower soil bulk density under *Erica* could be caused by a high organic matter content and increased stone contents.

Even though statistically not significant, TOC and N contents are higher in soils of *Erica* plots than in control plots, attributed to differences in quality and quantity of the litter input (Fig. 12). Furthermore, increased insolation on control plots (Miehe and Miehe 1994) might support organic matter degradation, whereas soils under *Erica* benefit from the shade provided by large rocks and the *Erica* canopy. Moreover, the Ah3 horizons of the soil profiles of the control plots contain less TOC, N, BC, and higher B5CA/B6CA ratios than soils below *Erica*, which strongly supports that *Erica* was not a common vegetation component on these control plots in the past. This is further documented by the absence of charcoal in the control soils, whereas charcoal can be frequently found below *Erica*.

Despite lower N values of plant species growing on control plots, their O and Ah-layers show higher N values than the corresponding layers below *Erica*, likely due to fecal N input from grazing cattle (Baron et al., 2002; Johansson et al., 2012). Higher TOC/N values than *Helichrysum* and *Festuca* characterize *Erica* leaves. Similarly, TOC/N ratios are generally significantly higher in soils below *Erica* than in control plots. The low TOC/N ratios, especially of the Ah2 and Ah3

horizons of control plots, also support the interpretation that these control plots have never been fully covered by *Erica*. Besides, the higher TOC/N ratios of the mineral soils below *Erica* reflect that *Erica* litter is less decomposed by soil microorganisms (Jacob et al., 2015).

SOC and N stocks of *Erica* plots are slightly lower than those of the control plots. This is mainly due to their higher stone contents which are negatively correlated with the SOC and N stocks (R = –0.5).
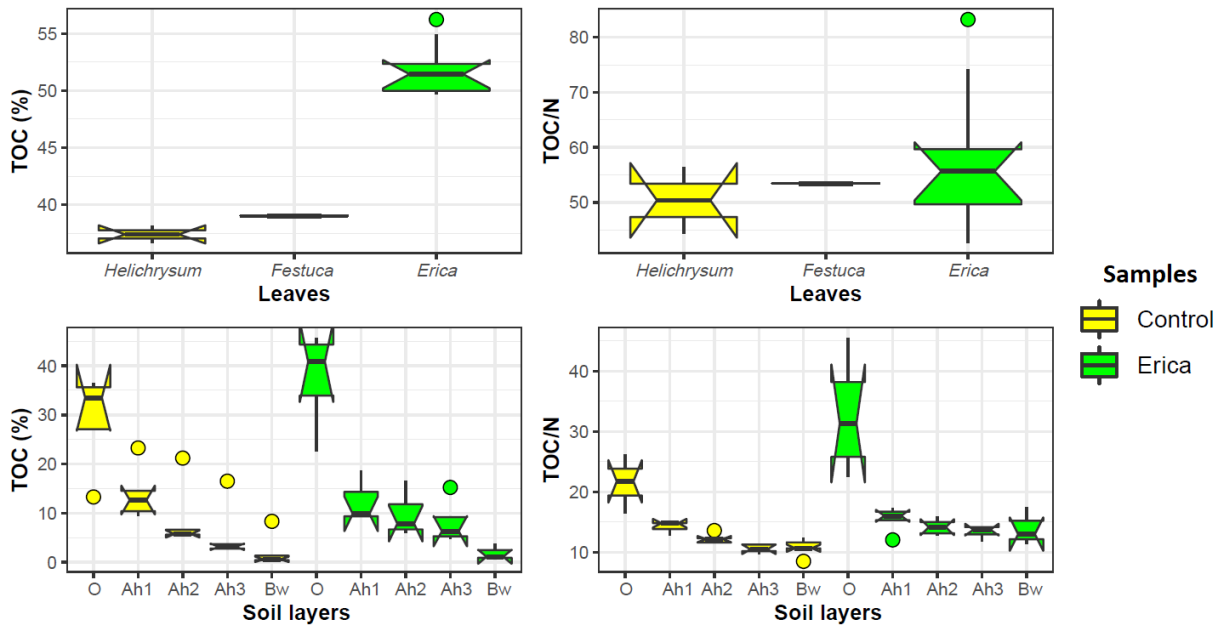
Fig. 12 *TOC and TOC/N ratio of plant leaves and soil horizons of Erica and control sites. The notched box plots indicate the median (solid lines between the boxes) and interquartile range (IQR) with upper (75%) and lower (25%) quartiles. The notches display the 95% confidence interval of the median. The lines extending outside the box (whiskers) show variability outside the quartiles. The circles represent outliers.*

The $\delta^{13}C$ values of plants from *Erica* and control sites are within the range reported for C3 plants (Marshall et al., 2007; Tiunov, 2007). Moreover, $\delta^{13}C$ values of *Erica* leaves are significantly higher than those of the other plant species. This result contrasts with the transect study finding (see sec. 4.1), where no significant difference between *Erica* and other dominant plants could be identified. This discrepancy might be due to the effect of altitude on $\delta^{13}C$ values and the different ways plants adjust their gas exchange to mitigate the decline in atmospheric CO_2 pressure along altitude (Körner et al., 1991). However, the relatively positive $\delta^{13}C$ values of *Erica* leaves from *Erica* plots on the Sanetti Plateau might suggest temporary water stress, e.g., during the dry season.

BC contents are significantly higher (related to sample: $p = 0.01$; related to TOC: $p = 0.02$) in *Erica* plots than in control plots, implying a higher amount of combustible fuel in *Erica* plots than in control plots. Furthermore, the significantly low BC contents of Ah2 and Ah3 horizons in soils below control (Fig. 12a and b) support the interpretation that *Erica* did not intensively cover these

plots previously. Otherwise, a higher accumulation of recalcitrant BC would have been preserved during the burning of former *Erica* shrubs.

Besides, the top soils of control plots have significantly higher B5CA/B6CA ratios *(p = 0.02)* (Fig. 13c) than the *Erica* profiles indicating low and high combustion temperatures in control and *Erica* plots, respectively. This is related to the high flammability of *Erica* twigs, while Afroalpine species such as *Helichrysum* are less flammable (Johansson et al., 2012).
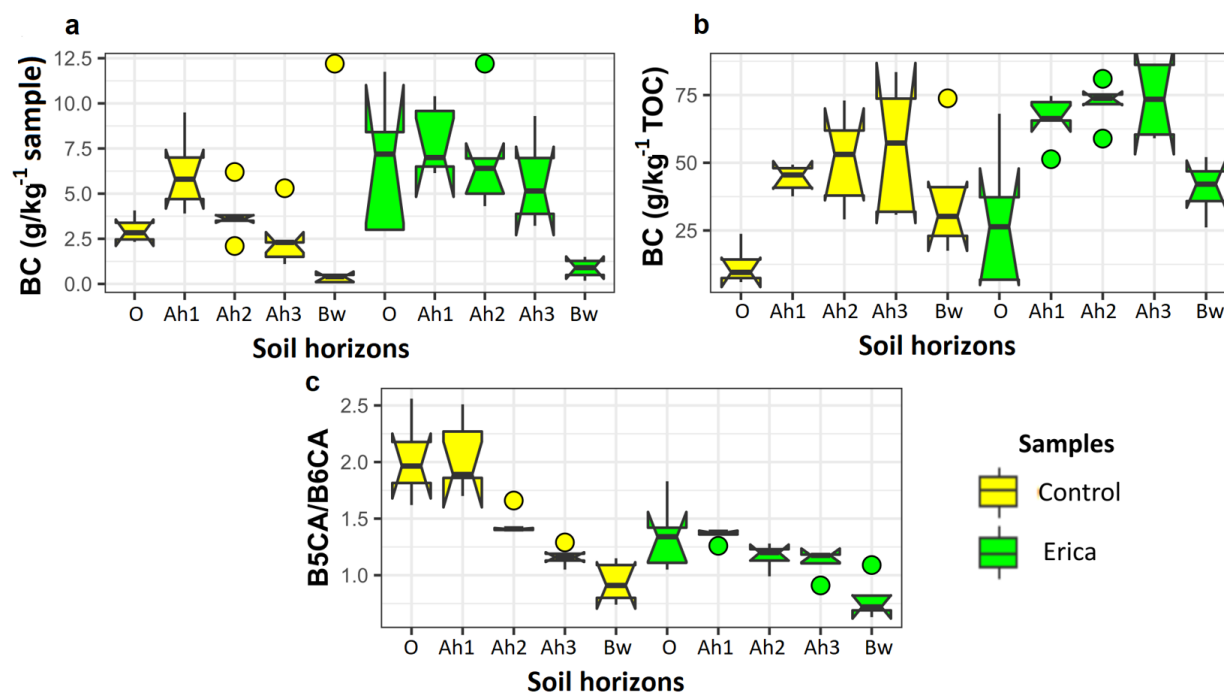
Fig. 13 *Black carbon contents (BC) (a), black carbon contribution to TOC (b), and B5CA/B6CA ratios (c) of Erica and control sites soils. The notched box sites indicate the median (solid lines between the boxes) and interquartile range (IQR) with upper (75%) and lower (25%) quartiles. The notches display the 95% confidence interval of the median. The lines extending outside the box (whiskers) show variability outside the quartiles. The circles represent outliers*

6. Conclusions

Disentangling factors responsible for ecosystem boundary shift, especially in tropical African mountain ecosystems which are highly susceptible for climate change and human impact, is vital to develop sustainable conservation strategies. In this thesis, the potential of selected biomarkers for paleoenvironmental reconstruction is evaluated, and the climate, vegetation, and fire history of the Sanetti Plateau is reconstructed using a muti-proxy approach. Moreover, potential factors for the distribution of *Erica* on the Sanetti Plateau are studied. Finally, the following conclusions are derived from the main findings of the studies.

- *Erica* cannot be chemotaxonomically differentiated from other dominant plants such as *Alchemilla, Festuca*, or *Helichrysum* based on foliar and pedogenic δ^{13}C and δ^{15}N values. Moreover, due to degradation and mineralization, both δ^{13}C and δ^{15}N become generally enriched from the leaves to the Ah-horizons. Relatively low total sugar concentrations characterize *Erica* leaves, and they can be chemotaxonomically distinguished by their higher relative amounts of galactose and mannose from the other dominant vegetation types. However, since these sugars are also produced by soil microorganisms, soils below the dominant vegetation yielded higher ratios of (G+M)/(A+X) similar to those of *Erica* leaves.

- Lignin phenols were promising and allowed the chemotaxonomic differentiation of *Erica* from non-*Erica* vegetation based on the relatively high contribution of cinnamyl ($\geq$ 40 %) phenols. However, this characteristic pattern is not reflected in the O-layers and Ah-horizons due to degradation and lignin input by roots. *Erica* is characterized by significantly lower C_{31}/C_{29} ratios. However, like lignin-derived phenol proxies, the *n*-alkane patterns are changing due to degradation from plant material over O layers to Ah horizons, thus inhibiting their application for unambiguous chemotaxonomic identification of *Erica* in soils and sediments. This suggests that these biomarkers alone do not allow the establishment of a straightforward proxy for reconstructing the former expansion of *Erica* on the Sanetti Plateau. Therefore, future work should emphasize alternative promising molecular markers, such as tannin-derived phenols and terpenoids.

- Long-chained *n*-alkanes C_{29}, C_{31}, and C_{33} in Garba Guracha and B4 sediments are mainly of terrestrial origin, while C_{23}, C_{25}, and C_{27} are primarily produced by aquatic macrophytes and microorganisms. Xylose and arabinose in sediments are at least partly derived from terrestrial origin. By contrast, the much higher relative abundances of rhamnose and fucose in the sediments compared to modern plants and soils corroborates that they are mainly produced by aquatic macrophytes and microorganisms. Therefore, the ratio (fuc + rham)/ (ara + xyl) is proposed as a sugar biomarker proxy for distinguishing aquatic versus terrestrial origin. Moreover, no unambiguous source identification is possible for sedimentary galactose and mannose as these sugars can also be produced by soil and/or aquatic microbial.

- In the environment of the B4 archive, deglaciation of the Sanetti Plateau took place around 18.2 cal kyr BP about 2000 years earlier than the N-exposed trough valley of Garba Guracha. After deglaciation, the vegetation around the B4 depression was herb-rich

grassland. However, a forest containing *Erica* was present in the lower altitudes, as indicated by the pollen results. A severe local drought related to H1 with complete desiccation of the past B4 lake was detected on the Sanetti Plateau at~ 16.3 cal kyr BP. This is in contrast to the lowland ecosystem, which documented continuous but delayed degradation between 16.6 and 15.7 cal kyr BP as documented by a high input of windblown allochthonous elements in the B4 depression. This desiccation phase is not clearly revealed in the pollen results except for a slight decrease in *Erica, Pediastrum*, fern, and *Botryococcus* pollen. An abrupt shift to humid conditions is recorded at ~ 15.7 cal kyr BP indicating the onset of AHP in the Bale Mountains some hundred years earlier than in Lake Tana region but in agreement with the termination of the HS lc phase in the Mediterranean. However, the vegetation on the Sanetti Plateau was less sensitive to increased humidity during AHP. Nevertheless, the *Erica* pollen increased in the B4 sediments at~ 14.4 cal kyr BP, correlating with a wet and warm regional climate. Fire incidences mainly coincide with an expansion of the vegetation cover and less with dry periods. Most likely, a warm and humid climate promotes biomass production of *Erica*, hence increasing the amount of fuel, which burns from time to time. This allows to conclude that biomass and, thus, fuel availability is an important factor controlling fire events in the Bale Mountains.

- Despite the boulder cover of the plots, topographic features, soil texture, soil pH, and EC did not show significant differences between *Erica* and control plots. Low TOC, TOC/N, BC contents, and missing charcoal but higher B5CA/B6CA ratios in soils of the control plots support the interpretation that *Erica* did not occupy the control plots in former times. In general, the soil conditions of most control plots would allow the growth of *Erica,* but in the absence of boulders, the microclimatic conditions above 3800–3900 m asl are too severe. Furthermore, the potential expansion of *Erica* is highly dependent on the intensity of fire and animal grazing, particularly during the seedling stage. Therefore, further investigations should focus on a detailed assessment of the temperature regime, soil moisture availability, and water potential of the *Erica* patches on the Sanetti Plateau.

7. References

Abbate, E., Bruni, P., Sagri, M., 2015. Geology of Ethiopia: A Review and Geomorphological Perspectives. In: Billi, P. (Ed.), Landscapes and Landforms of Ethiopia. Springer Netherlands, Dordrecht, pp. 33–64.

Abiven, S., Heim, A., Schmidt, M.W.I., 2011. Lignin content and chemical characteristics in maize and wheat vary between plant organs and growth stages: Consequences for assessing lignin dynamics in soil. Plant Soil 343, 369–378.

Alley, R.B., Clark, P.U., 1999. The Deglaciation of the Northern Hemisphere: A Global Perspective. Annu. Rev. Earth Planet. Sci 27, 149–82.

Amelung, W., Cheshire, M. V, Guggenberger, G., 1996. Determination of neutral and acidic sugars in soil by capillary gas liquid chromatography after trifluoroacetic acid hydrolysis. Soil Biol. Biochem. 28, 1631–1639.

Amelung, W., Martius, C., Bandeira, A.G., Garcia, M.V.B., Zech, W., 2002. Lignin characteristics and density fractions of termite nests in an Amazonian rain forest - Indicators of termite feeding guilds? Soil Biol. Biochem. 34, 367–372.

Andersson, R.A., Meyers, P., Hornibrook, E., Kuhry, P., Mörth, C.M., 2012. Elemental and isotopic carbon and nitrogen records of organic matter accumulation in a holocene permafrost peat sequence in the east European Russian arctic. J. Quat. Sci. 27, 545–552.

Baron, V.S., Mapfumo, E., Dick, A.C., Naeth, M.A., Okine, E.K., Chanasyk, D.S., 2002. Grazing intensity impacts on pasture carbon and nitrogen flow. J. Range Manag. 55, 535–541.

Batjes, N.H., 1996. Total carbon and nitrogen in the soils of the world. Eur. J. Soil Sci. 47, 151–163.

Belayneh, A., Yohannes, T., Worku, A., 2013. Recurrent and extensive forest fire incidence in the Bale Mountains National Park (BMNP), Ethiopia: Extent, Cause and Consequences. Int. J. Environ. Sci. 2, 29–39.

Beug HJ. Pollen profile from site Kolbermoor5, Rosenheim, Oberbayern, Germany, Pangaea. 2004. https://doi.org/10.1594/PANGAEA.142583.

Billi, P., 2015b. Geomorphological Landscapes of Ethiopia. In: Billi, P. (Ed.), Landscapes and Landforms of Ethiopia. Springer Netherlands, Dordrecht, pp. 3–32.

Bittner, L., Bliedtner, M., Grady, D., Gil-Romera, G., Martin-Jones, C., Lemma, B., Mekonnen, B., Lamb, H.F., Yang, H., Glaser, B., Szidat, S., Salazar, G., Rose, N.L., Opgenoorth, L., Miehe, G., Zech, W., Zech, M., 2020. Revisiting afro-alpine Lake Garba Guracha in the Bale Mountains of Ethiopia: rationale, chronology, geochemistry, and paleoenvironmental implications. J. Paleolimnol. 0123456789.

Blaauw, M., Christeny, J.A., 2011. Flexible paleoclimate age-depth models using an autoregressive gamma process. Bayesian Anal. 6, 457–474.

Bonnefille, R., 1983. Evidence for a Cooler and Drier Climate in Ethiopia 2.5 Mys. Nature 303, 487.

Bonnefille, R., Chalie, F., 2000. Pollen-inferred precipitation time-series from equatorial mountains, Africa, the last 40 kyr BP. Glob. Planet. Change 26, 25–50.

Bonnefille, R., Hamilton, C., 2015. Quaternary and Late Tertiary history of Ethiopian vegetation.

Brewer, S., Guiot, J., Barboni, D., 2013. Use of Pollen as Climate Proxies. Encycl. Quat. Sci. Second Ed. 805–815.

Brittingham, A., Hren, M.T., Hartman, G., 2017. Microbial alteration of the hydrogen and carbon isotopic composition of n-alkanes in sediments. Org. Geochem. 107, 1–8.

Brodowski, S., Rodionov, A., Haumaier, L., Glaser, B., Amelung, W., 2005. Revised black carbon assessment using benzene polycarboxylic acids. Org. Geochem. 36, 1299–1310.

Brown, E.T., Johnson, T.C., Scholz, C.A., Cohen, A.S., King, J.W., 2007. Abrupt change in tropical African climate linked to the bipolar seesaw over the past 55 , 000 years. Geophys. Res. Lett. 34, 1–5.

Camuera, J., Jiménez-Moreno, G., Ramos-Román, M.J., García-Alix, A., Jiménez-Espejo, F.J., Toney, J.L., Anderson, R.S., 2021. Chronological control and centennial-scale climatic subdivisions of the Last Glacial Termination in the western Mediterranean region. Quat. Sci. Rev. 255.

Conrad, Chan, Claus, Casper, 2007. Characterization of methanogenic Archaea and stable isotope fractionation during methane production in the profundal sediment of an oligotrophic lake (Lake Stechlin, Germany). Limniology Oceanogr. 54, 1–14.

Costa, K., Russell, J., Konecky, B., Lamb, H., 2014. Isotopic reconstruction of the African Humid Period and Congo Air Boundary migration at Lake Tana , Ethiopia. Quat. Sci. Rev. 83, 58–67.

Dahlgren, R.A., Boettinger, J.L., Huntington, G.L., Amundson, R.G., 1997. Soil development along an elevational transect in the western Sierra Nevada, California. Geoderma 78, 207–236.

Davies, S.J., Roberts, S.J., Lamb, H., 2015. Micro-XRF Core Scanning in Palaeolimnology : Recent Developments Publications Submission Cover Sheet.

Dawson, T.E., Mambelli, S., Plamboeck, A.H., Templer, P.H., Tu, K.P., 2002. Stable Isotopes in Plant Ecology. Annu. Rev. Ecol. Syst. 33, 507–559.

Eglinton, G., Hamilton, R.J., 1967. Leaf epicuticular waxes. Science (80-.). 156, 1322–1335.

Eglinton, T.I., Eglinton, G., 2008. Molecular proxies for paleoclimatology. Earth Planet. Sci. Lett. 275, 1–16.

Eshetu, Z., 2002. Historical C3-C4 vegetation pattern on forested mountain slopes: Its implication for ecological rehabilitation of degraded highlands of Ethiopia by afforestation. J. Trop. Ecol. 18, 743–758.

Eshetu, Z., Högberg, P., 2000. Reconstruction of Forest Site History in Ethiopian Highlands Based on 13C Natural Abundance of Soils. AMBIO A J. Hum. Environ. 29, 83–89.

Fagúndez, J., 2013. Heathlands confronting global change: Drivers of biodiversity loss from past to future scenarios. Ann. Bot. 111, 151–172.

Farquhar, G.D., O'Leary, M.H., Berry, J.A., 1982. On the Relationship Between Carbon Isotope Discrimination and the Intercellular Carbon Dioxide Concentration in Leaves. Aust. J. Plant Physiol. 9, 121.

Ficken, K.J., Li, B., Swain, D.L., Eglinton, G., 2000. An n-alkane proxy for the sedimentary input of submerged/floating freshwater aquatic macrophytes. Org. Geochem. 31, 745–749.

Fischer, P.M., 2011. δ 13 C as indicator of soil water availability and drought stress in Pinus radiata stands in South Africa 123.

Friis, I., 1986. Zonation Of Forest Vegetation On The South Slope Of Bale Mountains, South Ethiopia. SINET Ethiop. J. Sci 9, 29–44.

Friis, I., Demissew, S., Breugel van, P., 2010. Atlas of the Potential Vegetation of Ethiopia. 65, 321–322.

Gasse, F., 2000. Hydrological changes in the African tropics since the Last Glacial Maximum. Quat. Sci. Rev. 19, 189–211.

Gil-Romera, G., Adolf, C., Benito, B.M., Bittner, L., Johansson, M.U., Grady, D.A., Lamb, H.F., Lemma, B., Fekadu, M., Glaser, B., Mekonnen, B., Sevilla-Callejo, M., Zech, M., Zech, W., Miehe, G., 2019. Long-term fire resilience of the Ericaceous Belt, Bale Mountains, Ethiopia. Biol. Lett. 15, 20190357.

Glaser, B., Haumaier, L., Guggenberger, G., Zech, W., 1998. Black carbon in soils: The use of benzenecarboxylic acids as specific markers. Org. Geochem. 29, 811–819.

Glaser, B., Zech, W., 2005. Reconstruction of climate and landscape changes in a high mountain lake catchment in the Gorkha Himal, Nepal during the Late Glacial and Holocene as deduced from radiocarbon and compound-specific stable isotope analysis of terrestrial, aquatic and microbi. Org. Geochem. 36, 1086–1098.

Goñi, M. A. and Hedges, J. I., 1992. Lignin dimers: Structures, distribution, and potential geochemical applications. Geochimica et Cosmochimica Acta, 56(11), 4025–4043.

Gosling, W.D., Miller, C.S., Livingstone, D.A., 2013. Atlas of the tropical West African pollen flora. Rev. Palaeobot. Palynol. 199, 1–135.

Groos, A.R., Akçar, N., Yesilyurt, S., Miehe, G., 2021. Nonuniform Late Pleistocene glacier fluctuations in tropical Eastern Africa. Sci. Adv. 7.

Gunina, A., Kuzyakov, Y., 2015. Soil Biology & Biochemistry Sugars in soil and sweets for microorganisms : Review of origin , content , composition and fate. Soil Biol. Biochem. 90, 87–100.

Hailemariam, S.N., Soromessa, T., Teketay, D., 2016. Land use and land cover change in the bale mountain eco-region of Ethiopia during 1985 to 2015. Land 5.

Hedberg, O., 1951. Vegetation belts of the east african mountains, 45th ed. Sven. Bot. Tidskr, Stockholm.

Hedberg, O., 1964. Features of Afroalpine Plant Ecology, Acta Phytogeographica Suecica 49. Swedish Science Press, Uppsala, Sweden.

Hedges, J.I., Blanchette, R.A., Weliky, K., Devol, A.H., 1988. Effects of fungal degradation on the CuO oxidation products of lignin: A controlled laboratory study. Geochim. Cosmochim. Acta 52, 2717–2726.

Hedges, J.I., Cowie, G.L., Ertel, J.R., James Barbour, R., Hatcher, P.G., 1985. Degradation of carbohydrates and lignins in buried woods. Geochim. Cosmochim. Acta 49, 701–711.

Hedges, J. I. and Ertel, J. R., 1982. Characterization of lignin by gas capillary chromatography of cupric oxide oxidation products. Analytical Chemistry, 54(2), 174–178.

Hemming, S.R., 2004. Heinrich Events : Massive Late Pleistocene detritus layers of the North Atlantic and their global climate imprint.

Hepp, J., Rabus, M., Anhäuser, T., Bromm, T., Laforsch, C., Sirocko, F., Glaser, B., Zech, M., 2016. A sugar biomarker proxy for assessing terrestrial versus aquatic sedimentary input. Org. Geochem. 98, 98–104.

Herzschuh, U., 2007. Reliability of pollen ratios for environmental reconstructions on the Tibetan Plateau. J. Biogeogr. 34, 1265–1273.

Hevly, R.H., 1981. Pollen production, transport and preservation: potential and limitations in archaeological palynology 1, 39–54.

Hillman, J.C., 1986. Conservation in Bale Mountains National Park, Ethiopia. Oryx 20, 89–94.

Hillman, J.C., 1988. The Bale Mountains National Park Area , Southeast Ethiopia , and Its Management. Mt. Res. Dev. 8, 253–258.

Jacob, M., Annys, S., Frankl, A., De Ridder, M., Beeckman, H., Guyassa, E., Nyssen, J., 2015. Tree line dynamics in the tropical African highlands - identifying drivers and dynamics. J. Veg. Sci. 26, 9–20.

Jia, G., Dungait, J.A.J., Bingham, E.M., Valiranta, M., Korhola, A., Evershed, R.P., 2008. Neutral monosaccharides as biomarker proxies for bog-forming plants for application to palaeovegetation reconstruction in ombrotrophic peat deposits. Org. Geochem. 39, 1790–1799.

Johansson, M.U., Fetene, M., Malmer, A., Granström, A., 2012. Tending for cattle: Traditional fire management in ethiopian montane heathlands. Ecol. Soc. 17.

Johansson, M.U., Frisk, C.A., Nemomissa, S., Hylander, K., 2018. Disturbance from traditional fire management in subalpine heathlands increases Afro-alpine plant resilience to climate change. Glob. Chang. Biol. 24, 2952–2964.

Kidane, Y., Stahlmann, R., Beierkuhnlein, C., 2012. Vegetation dynamics, and land use and land cover change in the Bale Mountains, Ethiopia. Environ. Monit. Assess. 184, 7473–7489.

Kidane, Y.O., Hoffmann, S., Jaeschke, A., Beloiu, M., Beierkuhnlein, C., 2022. Ericaceous vegetation of the Bale Mountains of Ethiopia will prevail in the face of climate change. Sci. Rep. 12, 1–18.

Koch, K., Bhushan, B., Barthlott, W., 2009. Multifunctional surface structures of plants: An inspiration for biomimetics. Prog. Mater. Sci. 54, 137–178.

Kolattukudy, P.E., 1970. Plant Waxes, Plant Secondary Metabolism.

Körner, C., 2007. Climatic Treelines : Conventions , Global Patterns , Causes. Erdkd. Band 4, 316–324.

Körner, C., 2012. Treelines will be understood once the functional difference between a tree and a shrub is. Ambio 41, 197–206.

Körner, C., Farquhar, G.D., Wong, S.C., 1991. Carbon isotope discrimination by plants follows latitudinal and altitudinal trends. Oecologia 88, 30–40.

Kron, K.A., Judd, W.S., Stevens, P.F., Crayn, D.M., Anderberg, A.A., Gadek, P.A., Quinn, C.J., 2002. Phylogenetic classification of Ericaceae: Molecular and morphological evidence. Bot. Rev. 68, 335–423.

Kuzmicheva, E.A., Debella, H., Khasanov, B., Krylovich, O., Babenko, A., Savinetsky, A., Severova, E., Yirga, S., 2013. Holocene hyrax dung deposits in the afroalpine belt of the Bale Mountains (Ethiopia) and their palaeoclimatic implication. Environ. Archaeol. 18, 72–81.

Kuzmicheva, E.A., Khasanov, B.F., Krylovich, O.A., Savinetsky, A.B., 2014. Vegetation and climate reconstruction for the bale mountains (Ethiopia) in the Holocene according to the pollen analysis and radiocarbon dating of zoogenic deposits. Dokl. Biol. Sci. 458, 281–285.

Kuzyakov, Y., Bogomolova, I., Glaser, B., 2014. Biochar stability in soil: Decomposition during eight years and transformation as assessed by compound-specific14C analysis. Soil Biol. Biochem. 70, 229–236.

Lamb, H.F., Bates, C.R., Bryant, C.L., Davies, S.J., Huws, D.G., Marshall, M.H., Roberts, H.M., Toland, H., 2018. 150,000-year palaeoclimate record from northern Ethiopia supports early, multiple dispersals of modern humans from Africa. Nature 1–7.

Lamb, H.F., Bates, C.R., Coombes, P. V, Marshall, M.H., Umer, M., Davies, S.J., Dejen, E., 2007. Late Pleistocene desiccation of Lake Tana , source of the Blue Nile 26, 287–299.

Lemma, B., Kebede Gurmessa, S., Nemomissa, S., Otte, I., Glaser, B., Zech, M., 2020. Spatial and temporal 2H and 18O isotope variation of contemporary precipitation in the Bale Mountains, Ethiopia. Isotopes Environ. Health Stud. 56, 122–135.

Levin, N.E., Zipser, E.J., Ceding, T.E., 2009. Isotopic composition of waters from Ethiopia and Kenya: Insights into moisture sources for eastern Africa. J. Geophys. Res. Atmos. 114, 1–13.

Li, F., Sun, J., Zhao, Y., Guo, X., Zhao, W., Zhang, K., 2010. Ecological significance of common pollen ratios: A review. Front. Earth Sci. China 4, 253–258.

Li, G., Li, L., Tarozo, R., Longo, W.M., Wang, K.J., Dong, H., Huang, Y., 2018. Microbial production of long-chain n-alkanes: Implication for interpreting sedimentary leaf wax signals. Org. Geochem. 115, 24–31.

Litt, T., Brauer, A., Goslar, T., Merkt, J., Bałaga, K., Müller, H., Ralska-Jasiewiczowa, M., Stebich, M., Negendank, J.F.W., 2001. Correlation and synchronisation of Lateglacial continental sequences in northern central Europe based on annually laminated lacustrine sediments. Quat. Sci. Rev. 20, 1233–1249.

Malhi, Y., Wright, J., 2004. Spatial patterns and recent trends in the climate of tropical rainforest regions. Philos. Trans. R. Soc. B Biol. Sci. 359, 311–329.

Marchand, C., Disnar, J.R., Lallier-Vergés, E., Lottier, N., 2005. Early diagenesis of carbohydrates and lignin in mangrove sediments subject to variable redox conditions (French Guiana). Geochim. Cosmochim. Acta 69, 131–142.

Mark, B.G., Osmaston, H.A., 2008. Quaternary glaciation in Africa: Key chronologies and climatic implications. J. Quat. Sci. 23, 589–608.

Marshall, J.D., Brooks, J.R., Lajtha, K., 2007. Sources of variation in the stable isotopic composition of plants, 2nd ed. Blackwell Publishing.

Marshall, M.H., Lamb, H.F., Davies, S.J., Leng, M.J., Kubsa, Z., Umer, M., Bryant, C., 2009. Climatic change in northern Ethiopia during the past 17,000 years: A diatom and stable isotope record from Lake Ashenge. Palaeogeogr. Palaeoclimatol. Palaeoecol. 279, 114–127.

Marshall, M.H., Lamb, H.F., Huws, D., Davies, S.J., Bates, R., Bloemendal, J., Boyle, J., Leng, M.J., Umer, M., Bryant, C., 2011. Late Pleistocene and Holocene drought events at Lake Tana, the source of the Blue Nile. Glob. Planet. Change 78, 147–161.

Mcguire, A.F., Kron, K.A., 2011. Phylogenetic Relationships of European and African Ericas. Int. J. Plant Sci. 166, 311–318.

Meyers, P.A., 1994. Preservation of elemental and isotopic source identification of sedimentary organic matter. Chem. Geol. 114, 289–302.

Meyers, P.A., Ishiwatari, R., 1993. Lacustrine organic geochemistry-an overview of indicators of organic matter sources and diagenesis in lake sediments. Org. Geochem. 20, 867–900.

Miehe, G., Miehe, S., 1994. Ericaceous forests and heathlands in the Bale Mountains of South Ethiopia: ecology and man's impact. T. Warnke Verlag, Hamburg, Germany.

Mohtadi, M., Prange, M., Oppo, D.W., De Pol-Holz, R., Merkel, U., Zhang, X., Steinke, S., Lückge, A., 2014. North Atlantic forcing of tropical Indian Ocean climate. Nature 508, 76–80.

Monnin, E., Indermühle, A., Dällenbach, A., Flückiger, J., Stauffer, B., Stocker, T.F., Raynaud, D., Barnola, J.M., 2001. Atmospheric CO2 concentrations over the last glacial termination. Science (80-.). 291, 112–114.

Natelhoffer, K.J., Fry, B., 1988. Controls on Natural Nitrogen-15 and Carbon-13 Abundances in Forest Soil Organic Matter. Soil Sci. Soc. Am. J. 52, 1633–1640.

Nguyen Tu, T.T., Egasse, C., Zeller, B., Bardoux, G., Biron, P., Ponge, J.F., David, B., Derenne, S., 2011. Early degradation of plant alkanes in soils: A litterbag experiment using 13C-labelled leaves. Soil Biol. Biochem. 43, 2222–2228.

Oades, J.M., 1984. Soil organic matter and structural stability: mechanisms and implications for management. Plant Soil 76, 319–337.

Oliver, E.G.H., 1989. The Ericoideae and the southern African heathers. Bot. J. Linn. Soc. 101, 319–327.

Osmaston, H.A., Mitchell, W.A., Osmaston, J.A.N., 2005. Quaternary glaciation of the Bale Mountains, Ethiopia. J. Quat. Sci.

Ossendorf, G., Groos, A.R., Bromm, T., Tekelemariam, M.G., Glaser, B., Lesur, J., Schmidt, J., Akçar, N., Bekele, T., Beldados, A., Demissew, S., Kahsay, T.H., Nash, B.P., Nauss, T., Negash, A., Nemomissa, S., Veit, H., Vogelsang, R., Woldu, Z., Zech, W., Opgenoorth, L., Miehe, G., 2019. Middle Stone Age foragers resided in high elevations of the glaciated Bale Mountains, Ethiopia. Science (80-.). 365, 583–587.

Preston, C.M., Schmidt, M.W.I., 2006. Black (pyrogenic) carbon: A synthesis of current knowledge and uncertainties with special consideration of boreal regions. Biogeosciences 3, 397–420.

Quézel, P., 1978. Analysis of the Flora of Mediterranean and Saharan Africa. Ann Mo Bot Gard 65479–534. 65, 479–534.

R Core Team. R: a language and environment for statistical computing. R Foundation for Statistical Computing; 2013. http//www.R-project.org.

Schädel, C., Blöchl, A., Richter, A., Hoch, G., 2010. Quantification and monosaccharide composition of hemicelluloses from different plant functional types. Plant Physiol. Biochem. 48, 1–8.

Schäfer, I.K., Lanny, V., Franke, J., Eglinton, T.I., Zech, M., Vysloužilová, B., Zech, R., 2016. Leaf waxes in litter and topsoils along a European transect. Soil 2, 551–564.

Schüler, L., Hemp, A., 2016. Atlas of pollen and spores and their parent taxa of Mt Kilimanjaro and tropical East Africa. Quat. Int. 425, 301–386.

Stager, J.C., Ryves, D.B., Chase, B.M., Pausata, F.S.R., 2011. Catastrophic drought in the Afro-Asian monsoon region during Heinrich event 1. Science (80-.). 331, 1299–1302.

Talbot, M.R., Lærdal, T., 2000. The Late Pleistocene - Holocene palaeolimnology of Lake Victoria, East Africa, based upon elemental and isotopic analyses of sedimentary organic matter. J. Paleolimnol. 23, 141–164.

Talbot, M.R., Livingstone, D.A., 1989. Hydrogen index and carbon isotopes of lacustrine organic matter as lake level indicators. Palaeogeogr. Palaeoclimatol. Palaeoecol. 70, 121–137.

Tareq, S.M., Handa, N., Tanoue, E., 2006. A lignin phenol proxy record of mid Holocene paleovegetation changes at Lake DaBuSu, northeast China. J. Geochemical Explor. 88, 445–449.

Tareq, S.M., Kitagawa, H., Ohta, K., 2011. Lignin biomarker and isotopic records of paleovegetation and climate changes from Lake Erhai, southwest China, since 18.5kaBP. Quat. Int. 229, 47–56.

Tareq, S.M., Tanaka, N., Ohta, K., 2004. Biomarker signature in tropical wetland: Lignin phenol vegetation index (LPVI) and its implications for reconstructing the paleoenvironment. Sci. Total Environ. 324, 91–103.

Thevenot, M., Dignac, M.F., Rumpel, C., 2010. Fate of lignins in soils: A review. Soil Biol. Biochem. 42, 1200–1211.

Thompson, L.G., Mosley-Thompson, E., Davis, M.E., Henderson, K.A., Brecher, H.H., Zagorodnov, V.S., Mashiotta, T.A., Lin, P.N., Mikhalenko, V.N., Hardy, D.R., Beer, J., 2002. Kilimanjaro ice core records: Evidence of holocene climate change in tropical Africa. Science (80-.). 298, 589–593.

Tiercelin, J.J., Gibert, E., Umer, M., Bonnefille, R., Disnar, J.R., Lézine, A.M., Hureau-Mazaudier, D., Travi, Y., Keravis, D., Lamb, H.F., 2008. High-resolution sedimentary record of the last deglaciation from a high-altitude lake in Ethiopia. Quat. Sci. Rev. 27, 449–467.

Tierney, J.E., DeMenocal, P.B., 2013. Abrupt shifts in Horn of Africa hydroclimate since the last glacial maximum. Science (80-.). 342, 843–846.

Tierney, J.E., Lewis, S.C., Cook, B.I., Legrande, A.N., Schmidt, G.A., 2011. Model , proxy and isotopic perspectives on the East African Humid Period. Earth Planet. Sci. Lett. 307, 103–112.

Tierney, J.E., Russell, J.M., Huang, Y., Damsté, J.S.S., Ellen, C., Cohen, A.S., 2008. Northern Hemisphere Controls on Tropical Southeast African Climate During the Past 60 , 000 Years. Science (80-.). 322, 252–255.

Tierney, J.E., Smerdon, J.E., Anchukaitis, K.J., Seager, R., 2013. Multidecadal variability in East African hydroclimate controlled by the Indian Ocean. Nature 493, 389–392.

Tiunov, A. V., 2007. Stable isotopes of carbon and nitrogen in soil ecological studies. Biol. Bull. 34, 395–407.

Umer, M., Lamb, H.F., Bonnefille, R., Lézine, A.M., Tiercelin, J.J., Gibert, E., Cazet, J.P., Watrin, J., 2007. Late Pleistocene and Holocene vegetation history of the Bale Mountains, Ethiopia. Quat. Sci. Rev. 26, 2229–2246.

Van Campo, E., Gasse, F., 1993. Pollen- and diatom-inferred climatic and hydrological changes in sumxi co basin (western tibet) since 13,000 yr B.P. Quat. Res.

Van Raden, U.J., Colombaroli, D., Gilli, A., Schwander, J., Bernasconi, S.M., van Leeuwen, J., Leuenberger, M., Eicher, U., 2013. High-resolution late-glacial chronology for the Gerzensee lake record (Switzerland): δ18O correlation between a Gerzensee-stack and NGRIP. Palaeogeogr. Palaeoclimatol. Palaeoecol. 391, 13–24.

Wesche, K., Cierjacks, A., Assefa, Y., Wagner, S., Fetene, M., Hensen, I., 2008. Recruitment of trees at tropical alpine treelines: Erica in Africa versus Polylepis in South America. Plant Ecol. Divers. 1, 35–46.

Wesche, K., Miehe, G., Kaeppeli, M., 2000. The Significance of Fire for Afroalpine Ericaceous Vegetation. Mt. Res. Dev. 20, 340–347.

Wolf, M., Lehndorff, E., Wiesenberg, G.L.B., Stockhausen, M., Schwark, L., Amelung, W., 2013. Towards reconstruction of past fire regimes from geochemical analysis of charcoal. Org. Geochem. 55, 11–21.

Wu, H., Guiot, J., Brewer, S., Guo, Z., Peng, C., 2007. Dominant factors controlling glacial and interglacial variations in the treeline elevation in tropical Africa. Proc. Natl. Acad. Sci. U. S. A. 104, 9720–9724.

Yineger, H., Kelbessa, E., Bekele, T., Lulekal, E., 2008. Floristic Composition and Structure of the Dry Afromontane Forest At Bale Mountains National Park, Ethiopia. J. Sci 31, 103–120.

Zech, M., Glaser, B., 2008. Improved compound-specific d13C analysis of n-alkanes for application in palaeoenvironmental studies. RAPID Commun. MASS Spectrom. 22, 135–142.

Zech, M., Glaser, B., 2009. Compound-specific δ18O analyses of neutral sugars in soils using gas chromatography-pyrolysis-isotope ratio mass spectrometry: Problems, possible solutions and a first application. Rapid Commun. Mass Spectrom. 23, 3522–3532.

Zech, M., Leiber, K., Zech, W., Poetsch, T., Hemp, A., 2011. Late Quaternary soil genesis and vegetation history on the northern slopes of Mt. Kilimanjaro, East Africa. Quat. Int.

Zech, M., Rass, S., Buggle, B., Löscher, M., Zöller, L., 2012. Reconstruction of the late Quaternary paleoenvironments of the Nussloch loess paleosol sequence, Germany, using n-alkane biomarkers. Quat. Res. (United States).

Zech, M., Zech, R., Glaser, B., 2007. A 240,000-year stable carbon and nitrogen isotope record from a loess-like palaeosol sequence in the Tumara Valley, Northeast Siberia. Chem. Geol. 242, 307–318.

Zech, Michael, Buggle, Björn, Leiber, Katharina, Marković, S., Glaser, Bruno, Hambach, U., Huwe, Bernd, Stevens, T., Sümegi, P., Wiesenberg, G., Zöller, L., Zech, M, Buggle, B, Leiber, K, Glaser, B, Huwe, B, 2009. Reconstructing Quaternary vegetation history in the Carpathian basin, SE Europe, using *n*-alkane biomarkers as molecular fossils: Problems and possible solutions, potential and limitations. Eiszeitalter und Gegenwart – Quat. Sci. J. 58, 148–155.

Zech, W., Schad, P., Erhard, G.H., 2022. Soils of the World, Soil Science. Springer-Verlag GmbH, Berlin.

Ziegler, F., Kögel, I., Zech, W., 1986. Alteration of gymnosperm and angiosperm lignin during decomposition in forest humus layers. Zeitschrift für Pflanzenernährung und Bodenkd. 149, 323–331.

8. Authors' contribution to the included manuscripts

The presented cumulative thesis comprises five manuscripts prepared with contributions from all co-authors. In addition, a record of the specific author's contribution is given below.

Manuscript 1: Chemotaxonomic patterns of vegetation and soils along altitudinal transects of the Bale Mountains, Ethiopia, and implications for paleovegetation reconstructions – Part 1: stable isotopes and sugar biomarkers

B. Mekonnen:	field and laboratory work, data evaluation, discussion of results, manuscript preparation (45%)
W. Zech:	field work and comments to improve the manuscript (7%)
B. Glaser:	data evaluation and comments to improve the manuscript (7%)
B. Lemma:	field work and comments to improve the manuscript (5%)
T. Bromm:	laboratory support during sugar biomarker analyses, and data evaluation (6%)
S. Nemomissa:	comments to improve the manuscript (5%)
T. Bekele:	comments to improve the manuscript (5%)
M. Zech:	conceptualization, discussion of results and comments to improve the manuscript (20%)

Manuscript 2: Chemotaxonomic patterns of vegetation and soils along altitudinal transects of the Bale Mountains, Ethiopia, and implications for paleovegetation reconstructions – Part II: lignin-derived phenols and leaf-wax-derived *n*-alkanes

B. Lemma: field and laboratory work, data evaluation, discussion of results, manuscript preparation (40%)

B. Mekonnen: field work and comments to improve the manuscript (30%)

B. Glaser: data evaluation and comments to improve the manuscript (5%)

W. Zech: filed work, discussion of results and comments to improve the manuscript (5)%

S. Nemomissa: comments to improve the manuscript (3%)

T. Bekele: comments to improve the manuscript (3%)

L. Bittner: laboratory support during *n*-alkanes extraction, and data evaluation (4%)

M. Zech: conceptualization, discussion of results and comments to improve the manuscript (10%)

Manuscript 3: Terrestrial versus aquatic source identification of sedimentary *n*-alkane and sugar biomarkers – a case study from the Bale Mountains, Ethiopia

B. Mekonnen:	conceptualization, field and laboratory work, data evaluation, discussion of results, manuscript preparation (43%)
B. Glaser:	discussion of results and comments to improve the manuscript (5%)
W. Zech:	field and lab work and comments to improve the manuscript (5%)
L. Bittner:	field and lab work and comments to improve the manuscript (6%)
T. Bromm:	laboratory support and comments to improve the manuscript (5%)
B. Lemma:	field work and comments to improve the manuscript (6%)
S. Nemmomisa:	comments to improve the manuscript (4%)
T. Bekele:	comments to improve the manuscript (4%)
M. Zech:	conceptualization, discussion of results and comments to improve the manuscript (25%)

Manuscript 4: Climate, vegetation and fire history during the past 18,000 years, recorded in high altitude lacustrine sediments on the Sanetti Plateau, Bale Mountains (Ethiopia)

B. Mekonnen:	laboratory work, data evaluation, discussion of results, manuscript preparation (40%)
B. Glaser:	discussion of results and comments to improve manuscript (7%)
R. Zech:	field work, and comments to improve manuscript (3%)t
M. Zech:	discussion of results and comments to improve manuscript (5%)t
F. Schlutz:	laboratory work and data interpretation (7%)
R. Bussert:	laboratory work and comments to improve the manuscript (4%)
A. Addis:	support during laboratory work, comments to improve the manuscript (2%)
G. Gil-Romera:	comments to improve the manuscript (2%)
S. Nemomissa:	comments to improve the manuscript (2%)
T. Bekele:	comments to improve the manuscript (2%)
L. Bittner:	comments to improve the manuscript (2%)
D. Solomon:	comments to improve the manuscript (2%)
A. Manhart:	comments to improve the manuscript (2%)
W. Zech:	conceptualization, data evaluation, discussion of results and comments to improve the manuscript (20%)

Manuscript 5: Factors determining the occurrence of *Erica* patches on the Sanetti Plateau, Bale Mountains, Ethiopia

B. Mekonnen: field and laboratory work, data evaluation, discussion of results, manuscript preparation (45%)

B. Glaser: conceptualization, discussion of results and comments to improve the manuscript (10 %)

M. Zech: discussion and comments to improve manuscript (7 %)

T. Bromm: data evaluation and comments to improve manuscript (6%)

S. Nemmomisa: comments to improve manuscript (6 %)

T. Bekele: comments to improve manuscript (6 %)

W. Zech: conceptualization, field work, data evaluation, discussion of results and comments to improve the manuscript (20%)

II. Included publications and manuscripts

Manuscript 1: Chemotaxonomic patterns of vegetation and soils along altitudinal transects of the Bale Mountains, Ethiopia, and implications for paleovegetation reconstructions – Part 1: stable isotopes and sugar biomarkers

E&G Quaternary Science Journal

Chemotaxonomic patterns of vegetation and soils along altitudinal transects of the Bale Mountains, Ethiopia, and implications for paleovegetation reconstructions – Part 1: stable isotopes and sugar biomarkers

Betelhem Mekonnen[1,2], **Wolfgang Zech**[3], **Bruno Glaser**[1], **Bruk Lemma**[1,4], **Tobias Bromm**[1], **Sileshi Nemomissa**[5], **Tamrat Bekele**[5], **and Michael Zech**[1,6]

[1]Institute of Agronomy and Natural Sciences, Soil Biogeochemistry, Martin-Luther University, Halle-Wittenberg, Von-Seckendorff-Platz 3, 06120, Halle, Germany
[2]Department of Urban Agriculture, Misrak Polytechnic College, P.O. Box 785, Addis Ababa, Ethiopia
[3]Institute of Soil Science and Soil Geography, University of Bayreuth, 95440 Bayreuth, Universitätsstrasse 30, Germany
[4]Forest and Rangeland Biodiversity Directorate, Ethiopian Biodiversity Institute, P.O. Box 30726, Addis Ababa, Ethiopia
[5]Department of Plant Biology and Biodiversity Management, Addis Ababa University, P.O. Box 3434, Addis Ababa, Ethiopia
[6]Institute of Geography, Technical University of Dresden, Helmholtzstrasse 10, 01062, Dresden, Germany

Correspondence: Betelhem Mekonnen (betymekonnen19@gmail.com)

How to cite: Mekonnen, B., Zech, W., Glaser, B., Lemma, B., Bromm, T., Nemomissa, S., Bekele, T., and Zech, M.: Chemotaxonomic patterns of vegetation and soils along altitudinal transects of the Bale Mountains, Ethiopia, and implications for paleovegetation reconstructions – Part 1: stable isotopes and sugar biomarkers, E&G Quaternary Sci. J., 68, 177–188, https://doi.org/10.5194/egqsj-68-177-2019, 2019.

Abstract: Today, on the Sanetti Plateau in the Bale Mountains of Ethiopia, only fragmented patches of *Erica* species can be found at high altitudes (between 3900 and 4200 m a.s.l.). However, it is hypothesized that during the later part of the last glacial period and the early Holocene the plateau was extensively covered by *Erica* shrubs. Furthermore, it is assumed that the vegetation was later heavily destroyed by human-induced fire and/or climate change phenomena. The objective of this study is to contribute to paleovegetation reconstructions of the Sanetti Plateau by evaluating the potential of stable isotopes (δ^{13}C and δ^{15}N) and sugar biomarkers for distinguishing the dominant plant species, including *Erica*, and the soils below the plants. In a companion paper (Lemma et al., 2019a) we address the same issue by evaluating lignin-derived phenols and leaf-wax-derived *n*-alkane biomarkers.

The stable carbon (δ^{13}C) and nitrogen (δ^{15}N) isotope values of the plant samples range from -27.5 ‰ to -23.9 ‰ and -4.8 ‰ to 5.1 ‰, respectively. We found no significant δ^{13}C and δ^{15}N differences between the dominant plant species. Mineral topsoils (A$_h$ horizons) yielded more positive values than plant samples and organic layers (O layers), which reflects mineralization processes. Moreover, the δ^{15}N values became generally more negative at higher altitudes. This likely indicates that the N cycle is more closed compared to lower altitudes. δ^{15}N maxima around 4000 m a.s.l. point to fire-induced opening of the N cycle at the chosen study sites. *Erica* species yielded the lowest overall total sugar concentration (ranging from 58 to 118 mg g^{-1}), dominated by galactose (G) and mannose

(M). By contrast, *Festuca* species revealed much higher total sugar concentrations ranging from 104 to 253 mg g^{-1}, dominated by the pentose sugars arabinose (A) and xylose (X). Although a differentiation between *Erica* versus *Festuca, Alchemilla* and *Helichrysum* is possible based on $(G + M) / (A + X)$ ratios, *Erica* cannot be unambiguously distinguished from all other plant species occurring on the Sanetti Plateau. In addition, plant-characteristic $(G + M) / (A + X)$ sugar patterns change during soil organic matter formation in the A$_h$ horizons. This can be likely attributed to degradation effects and soil microbial build-up of galactose and mannose. In conclusion, soil degradation processes seem to render sugar biomarker proxies unusable for the reconstruction of the past extent of *Erica* on the Sanetti Plateau, Bale Mountains, Ethiopia. This finding is of relevance beyond our case study.

Kurzfassung: Das Sanetti Plateau in den Bale Bergen Äthiopiens ist in seinen höheren Lagen (zwischen 3900 und 4200 m ü. NN) durch das fragmentarische Vorkommen von *Erica* geprägt. Möglicherweise kam *Erica* während des Spätglazials und dem Frühholozän dagegen flächendeckend auf dem Plateau vor und wurde erst im Laufe des Holozäns durch Klimaveränderungen und menschlich verursachte Feuer zurückgedrängt. Das Ziel unserer Studie war es herauszufinden, ob sich die im Untersuchungsgebiet dominant vorkommenden Pflanzenarten einschließlich *Erica* und die sich unter der jeweiligen Vegetation entwickelten Böden anhand ihrer Stabilkohlenstoff- und Stickstoffisotopien (δ^{13}C und δ^{15}N) sowie ihrer Zucker-Biomarkermuster chemotaxonomisch unterscheiden lassen. In einem Begleitartikel (Lemma et al., 2019a) verfolgen wir dasselbe Ziel anhand von Lignin-bürtigen Phenolen und Blattwachs-bürtigen *n*-Alkan-Biomarkern.

Die δ^{13}C und δ^{15}N-Werte für die untersuchten Pflanzen reichen von $-27,5$ ‰ bis $-23,9$ ‰ bzw. von $-4,8$ ‰ bis $+5,1$ ‰ und weisen keine signifikanten Unterschiede zwischen den dominanten Pflanzenarten auf. Positivere δ^{13}C und δ^{15}N-Werte in den A$_h$ Horizonten im Vergleich zu den Pflanzenproben und O-Lagen lassen sich mit der Mineralisations-bedingten Anreicherung von ^{13}C und ^{15}N in Böden erklären. Tendenziell negativere δ^{15}N-Werte mit zunehmender Höhe spiegeln vermutlich wider, dass der N-Kreislauf klimatisch bedingt in größeren Höhen zunehmend geschlossen ist. Lokale δ^{15}N Maxima in etwa 4000 m Höhe können sehr gut mit der hier feuerbedingten Öffnung des N-Kreislaufs erklärt werden. *Erica* weist mit 58 bis 118 mg g^{-1} die niedrigsten Zucker-Konzentrationen auf; es dominieren die Zucker Galactose und Mannose (G und M). Im Gegensatz dazu variieren die Zucker-Konzentrationen im weit verbreitet vorkommenden Gras der Gattung *Festuca* zwischen 104 und 253 mg g^{-1}; hier dominieren die Zucker Arabinose und Xylose (A und X). Obwohl *Erica* anhand des $(G + M) / (A + X)$ Verhältnisses von *Festuca*, *Alchemilla* und *Helichrysum* chemotaxonomisch unterschieden werden kann, gilt dies nicht für weitere untersuchte Pflanzenarten wie *Kniphofia* und *Lobelia*. Darüber hinaus offenbaren die Datenreihen Pflanze – O-Lage – A$_h$-Horizont, dass die zum Teil pflanzencharakteristischen $(G + M) / (A + X)$ Verhältnisse systematischen Veränderungen unterliegen. Dies kann vermutlich auf Degradation und den bodenmikrobiellen Aufbau von Galactose und Mannose zurückgeführt werden und legt nahe, dass weder anhand von δ^{13}C und δ^{15}N, noch anhand von Zuckerbiomarkern eine verlässliche Rekonstruktion der Vegetation auf dem Sanetti Plateau möglich ist.

1   Introduction

The Bale Mountains in the southeast of Ethiopia constitute the largest area with afroalpine and Ericaceous vegetation on the African continent (Hedberg, 1951; Miehe and Miehe, 1994). The area is best known for its large numbers of local endemic flora such as *Lobelia rhynchopetalum*, *Lobelia scebelii* and *Senecio* species (Hillman, 1986). Similar to other tropical high-altitude mountains in East Africa such as Mount Kenya, Mount Kilimanjaro and Mount Meru, the vegetation of the Bale Mountains is characterized by altitudinal zones (or belts) with an afromontane forest belt, an Ericaceous belt and an afroalpine belt (Hedberg, 1969; Miehe and Miehe, 1994).

Vegetation reconstructions in the Bale Mountains have been done using mainly pollen records from pit cores (Hamilton, 1982) and sediments (Bonnefille, 1983; Bonnefille and Hamilton, 1986; Umer et al., 2007). Bonnefille (1983) reported, for the Gadeb basin north of the Bale Mountains, on the abundant occurrence of *Erica* pollen in sediments of a Pliocene lake between 2.5 and 2.4 myr. Pollen records from Mount Badda (north-northwest of the Bale

Mountains) and the Danka valley (Bale Mountains) suggest that the upper limit of the Ericaceous belt (3830 to 4040 m a.s.l.) developed between 8000 and 3500 years BP (Bonnefille and Hamilton, 1986; Miehe and Miehe, 1994). A pollen study from Gerba Guracha in the Bale Mountains (Umer et al., 2007) showed that the vegetation after deglaciation at about 16 cal kyr BP mainly consisted of grasses. Only with the beginning of the Holocene at 11 cal kyr BP did the Ericaceous belt rise and extend across the Sanetti Plateau, according to Miehe and Miehe, 1994. From about 4.5 cal kyr BP *Erica* shrubs and forests decreased in area and altitude and the afroalpine ecosystem with *Alchemilla* and Poaceae species expanded on the Sanetti Plateau. According to Kidane et al. (2012), Miehe and Miehe (1994), Umer et al. (2007), and Wesche et al. (2000), the most likely explanation for the decrease in *Erica* is fire caused by human invasion. Increasing aridity during the mid to late Holocene (Tiercelin et al., 2008) may have contributed to the destruction of the *Erica* woodlands on the Sanetti Plateau as well. However, the reason for the contemporary occurrence of only fragmented patches of *Erica* is still not clear.

At present, human impact is steadily increasing (Belayneh et al., 2013), despite large areas having been protected within the Bale Mountains National Park since 1970 (Hillman, 1986). During fieldwork in February 2015 and 2017, we observed people in the Bale Mountains mainly subsisting on pastoralism and illegal logging, thus increasingly placing the natural resources and wildlife under immense pressure, leading to deforestation, overgrazing and frequent fire occurrence. Wildfires have likely been a common phenomenon in the Bale Mountains for a long time. However, they seem to have become more severe in recent years (Johansson, 2013).

During the past decades the analyses of stable carbon (δ^{13}C) and nitrogen (δ^{15}N) isotopes have significantly contributed to a better understanding of (paleo-)ecological processes (Tiunov, 2007). This technique has high potential for tracing biogeochemical processes and for reconstructing past and current interactions between humans, plants and the surrounding environment (Dawson et al., 2002; Zech, 2006; Zech et al., 2011a). Furthermore, δ^{13}C analyses of soils and sediments are particularly used to reconstruct alpine vegetation changes in terms of C_3 versus C_4 photosynthetic pathway (Glaser and Zech, 2005; Zech et al., 2011b). Stable isotopes have been previously used in Ethiopia for reconstructing vegetation history (Gebru et al., 2009; Levin et al., 2011) and to infer land use and land cover change (Eshetu and Högberg, 2000; Liu et al., 2007; Solomon et al., 2002) as well as physiological processes (Krepkowski et al., 2013). Gebru et al. (2009) found that the vegetation has changed from C_3 to C_4 during the late Holocene (3300 years BP) in Tigray due to agricultural expansion. Eshetu and Högberg (2000) suggested that the vegetation shifted from grassland to forest in the Menagesha forest and Wendo Genet areas several hundred years ago.

Given that pollen preservation is often poor in soils due to oxidation (Brewer et al., 2013; Hevly, 1981; Li et al., 2007) there have been large efforts during the last decades toward developing proxies based on organic molecules that are specific to certain plant and vegetation types (chemotaxonomy) in order to contribute to the reconstruction of vegetation changes. This is mostly done with lipid biomarkers (Jansen et al., 2006a, b, 2008; see our companion paper, Lemma et al., 2019a, for further details). In addition, Kebede et al. (2007) have used amplified fragment length polymorphisms (AFLPs) to infer the phylogeographical history of the afromontane species (*Lobelia giberroa*) in the Bale Mountains. Sugar monomers build up polysaccharides such as cellulose and hemicellulose (Simoneit, 2002). While arabinose and xylose are very abundant in plants, fucose and rhamnose are important components of bacterial cell walls. Fucose and rhamnose are therefore often used as proxies for microbe-derived organic matter in soils (Sauheitl et al., 2005). Moreover, sugar biomarkers were proposed and applied as proxies for paleovegetation reconstructions (Glaser and Zech, 2005; Prietzel et al., 2013). For instance, Jia et al. (2008) could chemotaxonomically distinguish between lichens, *Sphagnum* and vascular plants based on the ratio (mannose + galactose) / (arabinose + xylose) and percentage of (rhamnose + fucose). Similarly, Hepp et al. (2016) suggested the sugar ratios fucose /(arabinose + xylose) and (fucose + xylose) / arabinose as proxies in paleolimnological studies for distinguishing between terrestrial versus aquatic sedimentary organic matter.

The objectives of this study were to evaluate (i) whether the dominant plant and vegetation types of the afroalpine region of the Bale Mountains can be distinguished chemotaxonomically based on their stable carbon and nitrogen isotopic composition and/or sugar biomarkers and (ii) whether the isotope and biomarker patterns of plants are reflected in the soils below correspond to contemporary plants. Note that in our companion paper (Lemma et al., 2019a) we address the same questions but instead focusing on other biomarkers, namely lignin-derived phenols and leaf-wax-derived *n*-alkanes. Overall the results of our two companion studies were meant to form a modern-day calibration for reconstructing the Late Quaternary vegetation history (mainly of *Erica*) on the Sanetti Plateau of the Bale Mountains.

2 Material and methods

2.1 Study site

The study was conducted in the Bale Mountains National Park, located in the Oromia Region of Ethiopia (Fig. 1) between 6°40′ and 7°10′ N and 39°30′ and 39°58′ E (Miehe and Miehe, 1994, Tiercelin et al., 2008; Umer et al., 2007). It covers an area of 2200 km^2 and an altitudinal range from 1400 to 4377 m a.s.l., including the second highest peak in the country (Tullu Dimtu). The intertropical convergence
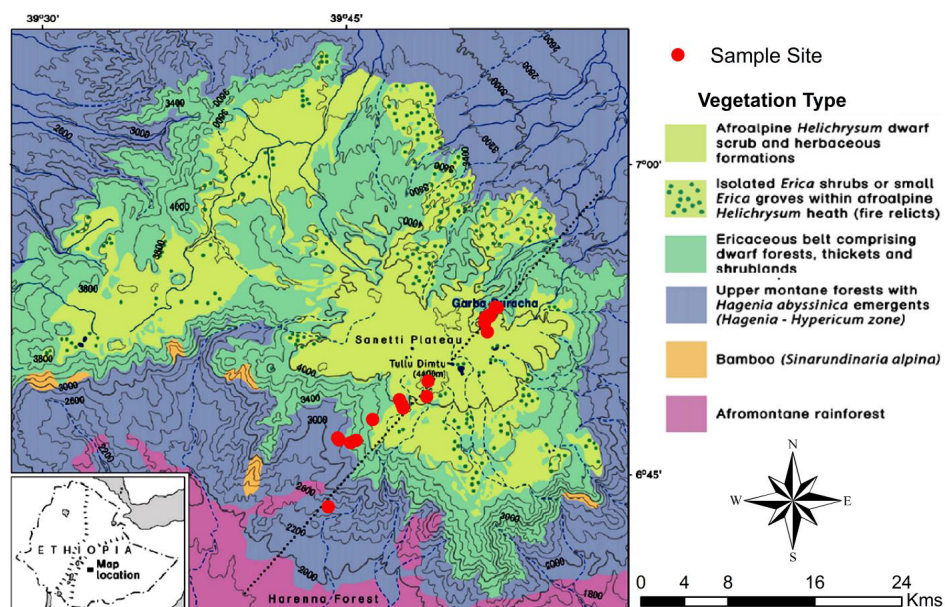
Figure 1. Map of the Bale Mountains showing the vegetation zones and study sites along the northeastern–southwestern transect (modified from Miehe and Miehe, 1994). Dominant vegetation types sampled comprise the Ericaceous and afroalpine belt.

zone (ITCZ), altitudinal and topographic features are the major factors influencing precipitation in the Bale Mountains (Miehe and Miehe, 1994; Bonnefille, 1983). Most of the year, the Bale Mountains are strongly influenced by southeasterlies originating from the Indian Ocean that provide monsoonal precipitation. A recent study done by Lemma et al. (2019b) suggested that the Bale Mountains receive precipitation from the Arabian Sea and southern Indian Ocean during the dry and wet season, respectively. The area experiences two rainy seasons: one lasting from March to June and a second heavy rainy season from July to October. In Dinsho (the Bale Mountains National Park headquarters at 3070 m a.s.l.), mean annual precipitation is 1069 mm and mean annual temperature is 11.8 °C. Monthly mean maximum and minimum temperatures are 19.9 and 3.4 °C, respectively (Ethiopian Metrological Services Agency, 2004–2015). Kidane et al. (2012) emphasized, however, that the mountains experience a highly variable climate from north to south as a result of altitudinal difference and the influence of lowland hot air masses. Extreme temperature variation between the wet and dry seasons is a common phenomenon on the Sanetti Plateau.

The afromontane forest of the Bale Mountains is divided into a southern declivity, or zonation of Harenna forest (1450 to 3200 m a.s.l. to the southwest), and northern declivity (drier montane forest 2200 to 3750 m a.s.l.). These vegetation zones are dominated by *Podocarpus falcatus, Warburgia ugandensis, Pouteria adolfi-friederici, Cro-*

ton macrostachyus, Juniperus procera, Hagenia abyssinica and *Hypericum revolutum* (Friis, 1986; Lisanework and Mesfin, 1989; Yineger et al., 2008). Regions above 3500 m a.s.l., including the tree line ecotone in eastern Africa, which is comprised of a number of taxa with small sclerophyllous leaves, are characterized as Ericaceous vegetation (Miehe and Miehe, 1994). This vegetation is commonly found on most African mountains, especially in the Atlas Range in North Africa, the Tibesti Mountains of the central Sahara, the Ethiopian Highlands and in the mountains of eastern Africa that extend southwards to Malawi (Jacob et al., 2015; Messerli and Winiger, 1992). This vegetation zone stretches from 3500 to 3800 m a.s.l. and it becomes patchy on the Sanetti Plateau above 3800 m a.s.l.. It is continuously dominated by shrubs and shrubby trees such as *Erica arborea, Erica trimera, Hypericum revolutum* and perennial shrubs or herbs such as *Alchemilla haumannii, Anthemis tigreensis, Helichrysum citrispinum, H. splendidum, H. gofense, Senecio schultzii, Thymus schimperi* and *Kniphofia foliosa* (Friis et al., 2010). Some of these species are also found in the afroalpine belt, since the upper and lower boundaries of this belt are very difficult to define. The afroalpine vegetation, which extends from 3800 to 4377 m a.s.l., is more open and richer in grass. It is mainly characterized by a combination of giant *Lobelia* (*Lobelia rhynchopetalum*), species of *Helichrysum*, shrubby species of *Alchemilla*, grasses (*Festuca richardii, Agrostis quinqueseta* and *Pentaschistis pictigluma*) and the creeping dwarf shrub *Euryops prostata*.

The soils in the Bale Mountains National Park are often shallow, rich in stones and with organic layers (O layers), mineral topsoils (A_h horizons), mineral subsoils (B horizons) and parent material (C horizons). Some soils are clearly stratified with bolder rich surface layers (O, A, B) above fine textured ash layers (2C). They are derived from volcanic materials such as lava of various kinds, basalt and agglomerates (Miehe and Miehe 1994) and can be classified as Andosols, Cambisols and Leptosols (Abbate et al., 2015; Billi, 2015; Yimer et al., 2006). In addition, Gleysols and Histosols occur frequently in depressions.

2.2 Sample collection

Leaf and soil samples were collected along a northeast (3870 to 4134 m a.s.l.) to southwest (2550 to 4377 m a.s.l.) transect (Fig. 1). Leaf samples were taken from dominant plants comprising: *Erica arborea* L. ($n = 5$), *Erica trimera* (Engl.) Beentje ($n = 5$), *Alchemilla haumannii* Rothm ($n = 5$), *Helichrysum splendidum* Thunb. L. ($n = 2$), *Lobelia rhynchopetalum* Hemsl. ($n = 1$), *Kniphofia foliosa* Hochst. ($n = 1$) and *Festuca abyssinica* Hochst. ex A. Rich. ($n = 6$) (Fig. 2). *Erica* leaves were collected from the upper part of the crown. Moreover, 23 mineral topsoils (A_h horizons) from each sampling site were collected in order to test whether these horizons represent the typical biogeochemical features of the standing vegetation. Additionally, where available, humified organic layers (O layers) excluding litter were sampled ($n = 15$).

2.3 Sample analyses

Soil samples were air dried and sieved (< 2 mm). An aliquot of plant and soil samples was ground using a ball mill and weighted into separate tin capsules. Total organic carbon (TOC), total nitrogen (TN), and the natural abundance of ^{13}C and ^{15}N of the samples were measured using an elemental analyzer coupled to an isotope ratio mass spectrometer (EA-IRMS). Samples were converted into CO_2 and NO_2 by an oxidation reactor filled with tungsten trioxide and aluminum oxide and cobalt (II, III) oxide (silvered) (1020 °C). Subsequently, NO_2 was further reduced to N_2 by a reduction reactor filled with copper wires (650 °C). Water was removed by a magnesium perchlorate trap. Helium (purity 99.9997 %) was used as carrier gas at 100 mL min^{-1}. The precision of the stable isotope analyses as determined by replication measurements of standards was 0.3 ‰ and 0.2 ‰ for δ^{13}C and δ^{15}N, respectively.

Sugar monomers in the plant and soil samples were extracted hydrolytically with 10 mL 4M trifluoroacetic acid (TFA) and 100 µg of myo-inositol (as internal standard) for 4 h at 105 °C, following the method described by Zech and Glaser (2009). This extraction procedure does not liberate considerable amounts of monosaccharides from cellulose (Amelung et al., 1996). Therefore, this fraction is sometimes called "non-cellulosic polysaccharides" (NCP) in the literature (e.g., Prietzel et al., 2013). The hydrolyzed samples were filtered through a vacuum suction system and the filtrates were collected in 100 mL conical flasks. The filtrates were then evaporated using rotary evaporators in order to remove the acid and the water that were added to the samples. In order to remove humic substances and cations, the redissolved samples were passed through XAD and Dowex resin columns, respectively, following Amelung et al. (1996), and the filtrates were collected in 50 mL conical flasks. The filtrates were dried using rotary evaporators and a freeze drier. The purified neutral sugars were transferred into Reacti-Vials. Derivatization of the freeze-dried sugars was done with N-methyl-2-pyrrolidone (NMP) at 75 °C for 30 min in a heating block. After cooling, 400 µL of BSTFA (N, O-Bis(trimethylsilyl)trifluoracetamide) were added to the vials and the samples were heated again to 75 °C for 5 min. The samples were transferred to auto-sampler vials after cooling and measured using gas chromatography (SHIMADZU GC-2010, Kyoto, Japan) equipped with a flame ionization detector (FID). Sugars were separated on a Supelco SPB-5 column (length, 30 m; inner diameter, 0.25 mm; film thickness, 0.25 µm) using helium as carrier gas. The temperature was ramped from 160 to 185 °C, held for 4 min, then ramped to 240 °C and held for 0 min, and finally ramped to 300 °C and held for 5 min. The temperature of the injector was set at 250 °C. Hierarchical cluster analysis and notch box plots for the sugar biomarkers data were done by using the R software (version 3.4.4, 15 March 2018).

3 Results and discussion

3.1 Elemental composition, δ^{13}C and δ^{15}N of dominant plants

Total organic carbon and nitrogen contents were used to calculate TOC / TN ratios in order to characterize and possibly distinguish the investigated plant types. The leaf samples yielded values covering a wide range from 14.5 (*Lobelia*) to 80.4 (*Erica*). The boxplot diagrams in Fig. 3a depict that plant leaves are characterized by significantly higher TOC / TN ratios compared to corresponding O layers and A_h horizons. Mean TOC / TN values for all investigated dominant plants are > 40, thus confirming the finding of Zech (2006) and Zech et al. (2011b) from Mt. Kilimanjaro that subalpine and alpine vegetation has typically very high TOC / TN values.

The δ^{13}C values of *Erica* are not significantly different from the other plants (Fig. 3b). Note that *Kniphofia* has a more positive value, but a statistical comparison could not be applied because only one sample is available. No significant variation in stable isotopes among the rest of dominant plant species could be detected either. Overall, the δ^{13}C values of all investigated plants range from -27.5 (*Erica*) to -23.9 ‰ (*Kniphofia*); thus, they are well within the typical
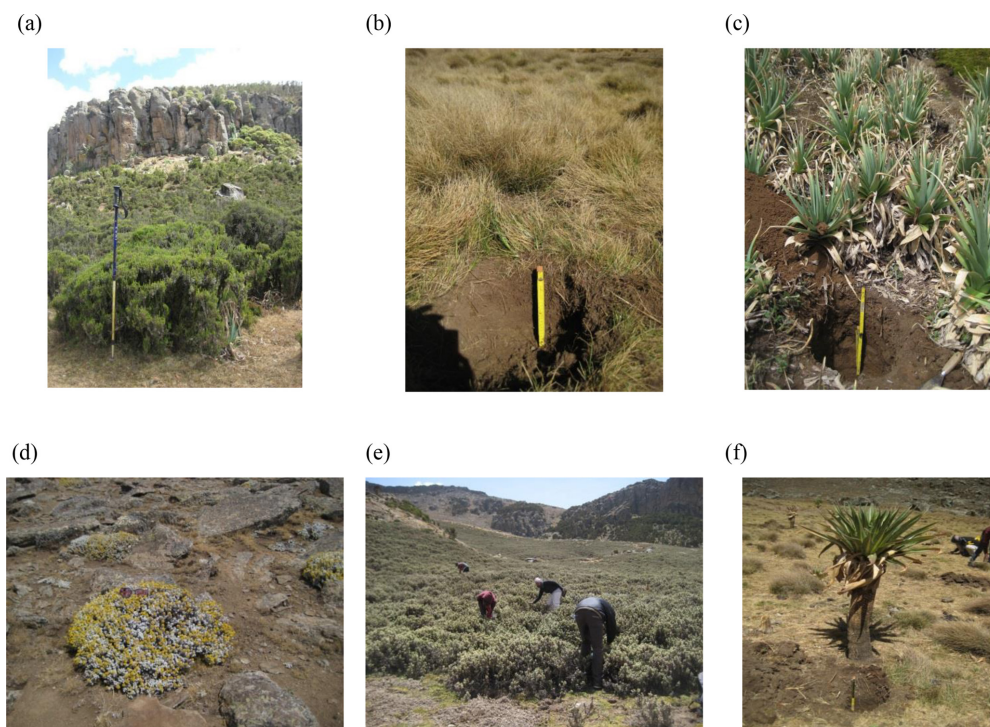
Manuscript 1

Figure 2. Photos showing plant species investigated in this study: **(a)** *Erica trimera* (3870 m a.s.l.), **(b)** *Festuca abyssinica* (3920 m a.s.l.), **(c)** *Alchemilla haumannii* (3947 m a.s.l.), **(d)** *Helichrysum splendidum* (4377 m a.s.l.), **(e)** *Kniphofia Foliosa* (3930 m a.s.l.) and **(f)** *Lobelia rhynchopetalum* (3922 m a.s.l.).

range for C_3 plants. The occurrence of (sub)alpine C_4 plants similar to those on Mt. Kenya (Street-Perrott et al., 2004; Young and Young, 1983) is hitherto not confirmed for the Bale Mountains based on the admittedly quite limited plant sample set presented here. However, the absence of C_4 would be in agreement with the findings of Zech et al. (2011b) from Mt. Kilimanjaro. Furthermore, our $\delta^{13}C$ leaf data do not reveal a dependence on altitude, as reported by Körner et al. (1991) for a global dataset. This likely reflects that local climatic conditions and other factors exert a higher control in our study area. The $\delta^{15}N$ values for leaf material range from -4.8 (*Erica*) to 5.1 ‰ (*Alchemilla*). Such a relatively large $\delta^{15}N$ variability is well described for plants and can be explained by different nitrogen sources being taken up and by different mechanisms of N uptake including mycorrhizae being present. Similar to the $\delta^{13}C$ results, $\delta^{15}N$ values of *Erica* are not significantly different from other plants (Fig. 3c).

3.2 Elemental composition, $\delta^{13}C$ and $\delta^{15}N$ in O layers and A_h horizons

Apart from revealing similarities and/or differences in TOC / TN, $\delta^{13}C$ and $\delta^{15}N$ between the dominant plants, Fig. 3a furthermore reveals that TOC / TN ratios generally

strongly decrease from leaf material over O layers to the respective A_h horizons. This reflects the preferential loss of carbon versus nitrogen during mineralization (Meyers, 1994). At the same time, this decrease implies that TOC / TN ratios of plants cannot be used as a straight-forward proxy for paleovegetation reconstructions in archives that are prone to organic matter degradation and mineralization.

According to Fig. 3b, the O layers tend to have slightly more negative $\delta^{13}C$ values compared to leaf material. By contrast, A_h horizons have generally more positive $\delta^{13}C$ values. We explain the former finding with the preferential loss of an easily degradable ^{13}C-enriched organic matter pool, like sugars during a very early stage of leaf litter degradation. The later finding is in agreement with numerous studies (Ehleringer et al., 2000; Garten et al., 2000; Natelhoffer and Fry, 1988) reporting on increasing $\delta^{13}C$ values with increasing soil depths. This ^{13}C enrichment in soils is usually explained by the preferential enzymatically controlled loss of ^{12}C during soil organic matter degradation (Farquhar et al., 1982; Friedli et al., 1986; Zech et al., 2007). It may be noteworthy that two A_h horizons of the northeastern part of the transect yielded very positive $\delta^{13}C$ values of -21.2 ‰ and -19.1 ‰, respectively, which are higher than expected for
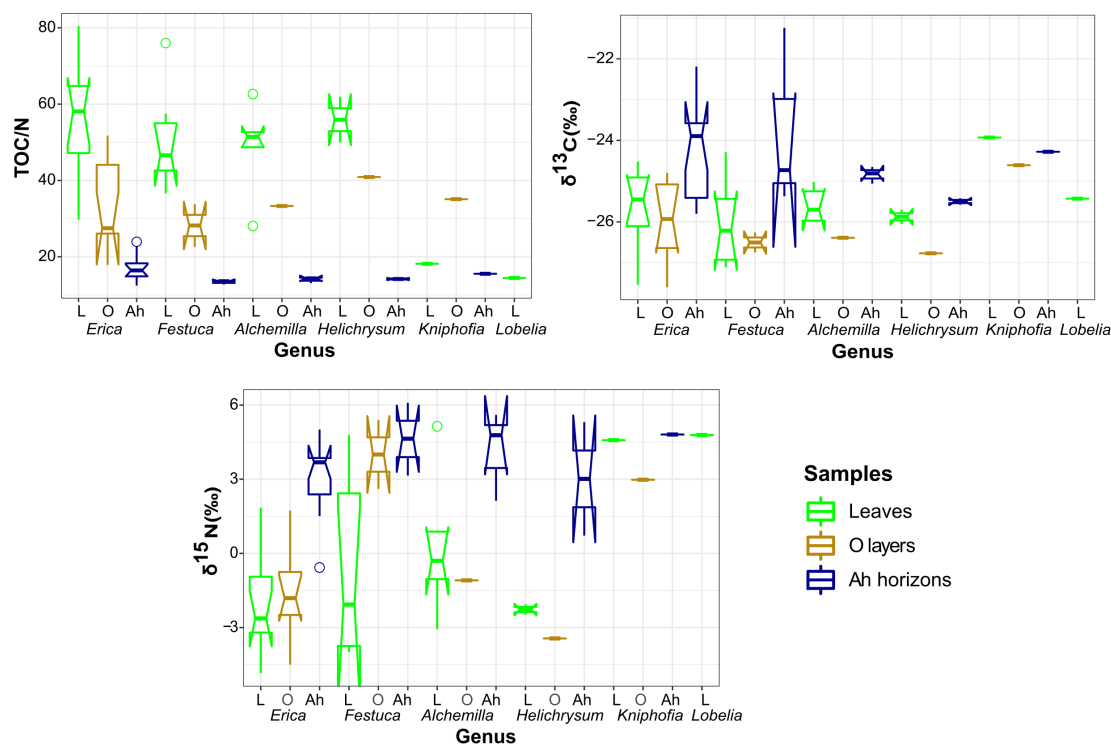
Figure 3. Boxplot diagrams showing **(a)** TOC / TN and **(b)** δ^{13}C and **(c)** δ^{15}N results for leaves (L), O layers and A_h horizons of the investigated dominant vegetation types in the Bale Mountains. The upper and lower bold lines indicate the 75th and 25th quartiles, respectively, and the middle bold line shows the median. The lines extending outside the box (whiskers) show variability outside the quartiles and notches indicate the 95 % confidence interval. White circles represent outliers. Note that short horizontal single lines are due to small sample sizes.

soils that have developed under pure C_3 vegetation. Given that our plant sample set is rather small, it cannot be excluded that those soils received litter from C_4 grasses and we encourage further studies in order to clarify whether C_4 grasses occur in the Bale Mountains like on Mt. Kenya or not (see Sect. 3.1).

Like δ^{13}C, δ^{15}N of soils is also reported to be strongly affected by soil organic matter degradation and mineralization (Natelhoffer and Fry, 1988; Zech et al., 2007). It is hence not surprising that the investigated A_h horizons are clearly ^{15}N-enriched compared to the leaf samples (Fig. 3c). Furthermore, the O layers and the A_h horizons across the altitudinal transects of the Bale Mountains reveal a general trend toward more negative values with increasing altitude (Fig. 4). Similar findings were reported for the southern and northern slopes of Mt. Kilimanjaro (Zech et al., 2011a, b) and reflect that the N cycle is open at lower altitudes as it is characterized by higher temperatures. By contrast, at higher altitudes N mineralization and N losses are reduced (closed N cycle) due to lower temperatures. As an exception from this over-

all trend, the O layers reveal a maximum between 3920 and 3950 m a.s.l. and the A_h horizons reveal two maxima around 3950 as well as around 4130 m a.s.l. Given that O layers and A_h horizons act as integrated recorders of the N cycle taken from periods of several years and hundreds of years, respectively, those maxima indicate that at the respective sampling sites the N cycle was open and significant N losses occurred during the past. Several studies emphasized already that the subalpine and alpine zones in the Bale Mountains are heavily affected by human-induced fires (Johansson, 2013; Kidane et al., 2012; Miehe and Miehe,1994; and Wesche et al., 2000). Therefore, we attribute this opening of the N cycle to the repeated burning (and thus loss) of the relatively ^{15}N-depleted vegetation cover.

3.3 Sugar concentrations and patterns of dominant plants

As shown in Fig. 5, the overall non-cellulosic sugar concentrations in leaves range from 58 to 253 mg g^{-1}. We found high contents in *Festuca* and *Alchemilla*, whereas *Erica* is
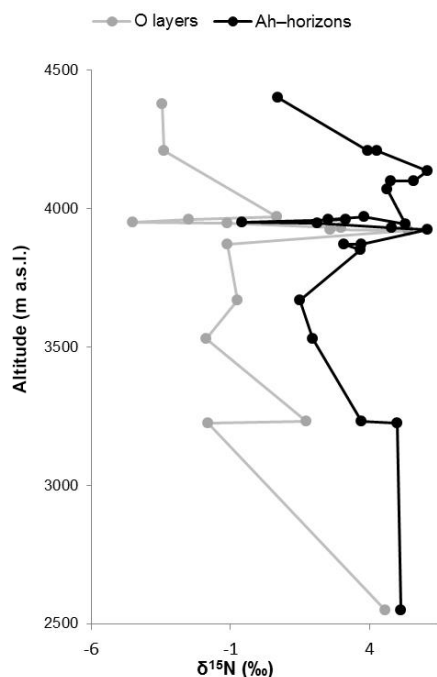
Figure 4. δ^{15}N results of O layers and A$_h$ horizons along altitudinal transects of the Bale Mountains.

Figure 5. Total sugar concentrations of the investigated plant leaves along altitudinal transects of the Bale Mountains. The upper and lower bold lines indicate 75th and 25th quartiles, respectively, and the middle bold line shows the median. The lines extending outside the box (whiskers) show variability outside the quartiles and notches indicate the 95 % confidence interval. White circles represent outliers. Note that short horizontal single lines are due to small sample sizes.

Figure 6. Cluster formation based on non-cellulosic sugar biomarker concentrations of leaf samples from the dominant vegetation types in the Bale Mountains.

characterized by relatively low non-cellulosic sugar concentrations. This has implications for paleovegetation reconstructions because plants producing lower amounts of sugars are less represented in soils and sedimentary archives. A comparable example for such an issue is leaf-wax-derived *n*-alkane biomarkers not being sensitive enough for coniferous trees due to the very low *n*-alkane concentrations of coniferous needles (Zech et al., 2012).

Nevertheless, a hierarchical cluster analysis performed for leaves on the basis of their individual sugar monomers arabinose, fucose, galactose, mannose, rhamnose, ribose, xylose, glucuronic acid and galacturonic acid resulted in three main groups, suggesting that a chemotaxonomic differentiation of the dominant vegetation types on the Bale Mountains may be possible (Fig. 6). The first group mainly represents *Kniphofia, Alchemilla* and *Helicrysum* species indicating close similarity between them. The second group predominantly contains *Erica* spp. and the third group is mainly composed of *Festuca* spp. This result allows the conclusion that the plant species under study vary in their foliar sugar composition. *Erica* and *Festuca* vary especially clearly in their sugar signatures.

Both Jia et al. (2008) and Prietzel et al. (2013) used the ratio of galactose and mannose versus arabinose and xylose ($(G + M) / (A + X)$) in particular, in order to distinguish between different vegetation types. In the Bale Mountains,

Erica leaves yielded significantly higher $(G + M) / (A + X)$ ratios compared to *Alchemilla*, *Festuca* and *Helichrysum* (Fig. 7a). Hence, one might be tempted to recommend the $(G + M) / (A + X)$ ratio as a proxy in soils and sediments for reconstructing *Erica* distribution during the past. Note that the $(G + M) / (A + X)$ ratios around 1 for *Erica, Kniphofia* and *Lobelia* are clearly higher than the ratios reported to be typical for plants according to Oades (1984). By contrast, the fucose to arabinose and xylose ratios ($F / (A + X)$) are very low, as expected for plants (cf. Hepp et al., 2016), with a mean value of 0.05 ± 0.05 ($n = 25$). *Erica* is characterized by higher ratios than *Festuca* (Fig. 7b).

3.4 Sugar patterns of O layers and A$_h$ horizons

The characteristic $(G + M) / (A + X)$ and $F / (A + X)$ ratios for the dominant vegetation types are not well reflected in

Figure 7. Boxplot diagram showing the **(a)** $(G+M)/(A+X)$ and **(b)** $F/(A+X)$ ratios of leaves (L), O layers and A_h horizons, respectively, along the altitudinal transect across the Bale Mountains. The upper and lower bold lines indicate 75th and 25th quartiles, respectively, and the middle bold line shows the median. The lines extending outside the box (whiskers) show variability outside the quartiles and notches indicate the 95 % confidence interval. White circles represent outliers. Note that short horizontal single lines are due to small sample sizes.
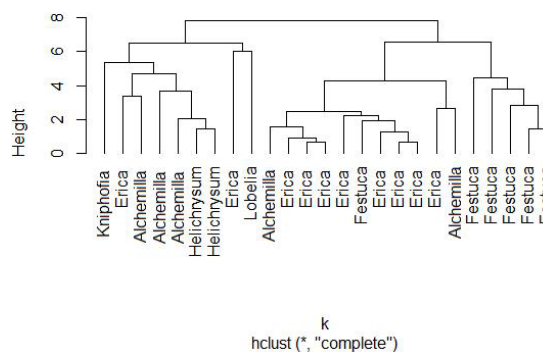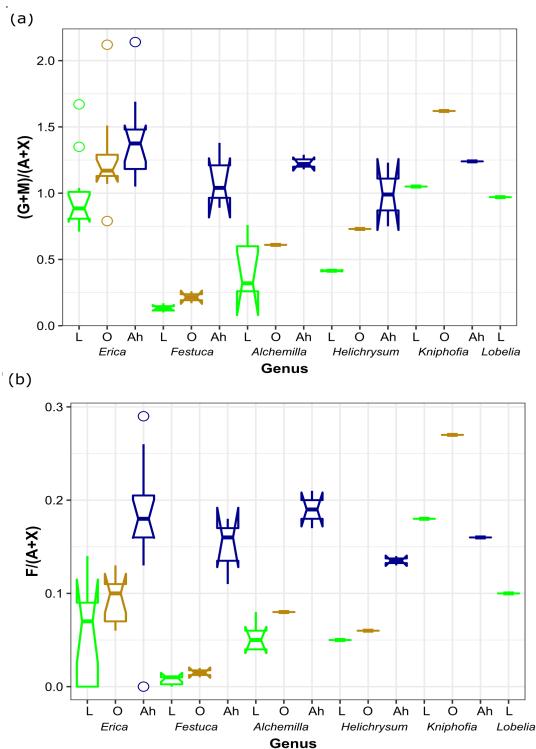
the respective O layers and A_h horizons (Fig. 7). Rather, the ratios generally increase, indicating that both arabinose and xylose are preferentially degraded or that galactose, mannose and fucose are built-up by soil microorganisms. This later interpretation is in agreement with Oades (1984), who reported that soil microorganisms are characterized by $(G+M)/(A+X)$ ratios > 2. The $F/(A+X)$ ratios of 0.18 ± 0.07 observed for A_h horizons in this study are well within the range reported for terrestrial soils by Hepp et al. (2016). Apart from soil microorganisms, a considerable contribution of root-derived sugars, including root exudates, is very likely as well (Gunina and Kuzyakov, 2015). More systematic respective biomarker studies, similar to, for instance, the one carried out by Prietzel et al. (2013) are therefore encouraged in order to address this effect more quantitatively in the future.

As a result, soils under *Alchemilla* and *Festuca* yield $(G+M)/(A+X)$ ratios similar to those of *Erica* leaves.

This has severe implications for paleovegetation reconstructions based on sugar biomarkers and resembles degradation problems reported for lignin-derived phenol and leaf-wax-derived *n*-alkane biomarkers (Lemma et al., 2019a; Zech et al., 2012). In the case of the Bale Mountains, only fresh leaves or leaf material that has undergone little degradation (as it may hold true in anoxic lacustrine sediments) allow a chemotaxonomic differentiation between *Erica* and other dominant vegetation types, such as *Alchemilla, Festuca* and *Helichrysum*. Given that by contrast good preservation of sugar biomarkers is usually not the case in soils, we consider neutral sugar biomarkers unsuitable for reconstructing former *Erica* expansion from paleosols in our study area and instead encourage studies focusing on other biomarkers.

4 Conclusions

Having investigated plant material, O layers and A_h horizons along altitudinal transects, we found no clear evidence for the modern-day occurrence of C_4 grasses in the Bale Mountains. Neither $\delta^{13}C$ nor $\delta^{15}N$ values allow a clear chemotaxonomic differentiation of *Erica* from other dominant vegetation types such as *Alchemilla, Festuca* and *Helichrysum*. TOC / TN ratios strongly decrease and both ^{13}C and ^{15}N become generally enriched from the leaves to the A_h horizons due to degradation and mineralization. $\delta^{15}N$ is furthermore generally more negative at higher altitudes, which reflects a low degree of mineralization and overall a relatively closed N cycle due to low temperatures. $\delta^{15}N$ maxima around 4000 m a.s.l. indicate the likely fire-induced opening of the N cycle at the respective study sites. *Erica* leaves are characterized by relatively low total sugar concentrations and can be chemotaxonomically distinguished from the other dominant vegetation types mainly because of their higher relative amounts of galactose and mannose. However, these sugar monomers are produced by soil microorganisms as well. Therefore, soils under *Alchemilla* and *Festuca* yielded $(G+M)/(A+X)$ ratios similar to those of *Erica* leaves, and even in soils under *Erica* this ratio significantly increased. This suggests that sugar biomarkers alone do not allow the establishment of a straight-forward proxy for reconstructing the former expansion of *Erica* on the Sanetti Plateau. Therefore, future work should emphasize alternative promising molecular markers, such as tannin-derived phenols and terpenoids. In addition, black carbon should be analyzed in order to reveal the impact of fire on the extent of the Ericaceous vegetation.

References

Abbate, E., Bruni, P., and Sagri, M.: Geology of Ethiopia: A Review and Geomorphological Perspectives, in: Landscapes and Landforms of Ethiopia, edited by: Billi, P., Springer Netherlands, Dordrecht, 33–64, 2015.

Amelung, W., Cheshire, M. V., and Guggenberger, G.: Determination of neutral and acidic sugars in soil by capillary gas liquid chromatography after trifluoroacetic acid hydrolysis, Soil Biol. Biochem., 28, 1631–1639, https://doi.org/10.1016/S0038-0717(96)00248-9, 1996.

Belayneh, A., Yohannes, T., and Worku, A.: Recurrent and extensive forest fire incidence in the Bale Mountains National Park (BMNP), Ethiopia: Extent, Cause and Consequences, Int. J. Environ. Sci., 2, 29–39, 2013.

Billi, P.: Geomorphological Landscapes of Ethiopia, in Landscapes and Landforms of Ethiopia, edited by: Billi, P., 3–32, Springer Netherlands, Dordrecht, 2015.

Bonnefille, R.: Evidence for a Cooler and Drier Climate in Ethiopia 2.5 Mys, Nature, 303, 487–491, 1983.

Bonnefille, R. and Hamilton, C.: Quaternary and Late Tertiary history of Ethiopian vegetation, Acta Uni. Upps. Symb. Bot. Upps. 26, 48–63, 1986.

Brewer, S., Guiot, J., and Barboni, D.: Use of Pollen as Climate Proxies, Encycl. Quat. Sci. Second Ed., 805–815, https://doi.org/10.1016/B978-0-444-53643-3.00180-1, 2013.

Dawson, T. E., Mambelli, S., Plamboeck, A. H., Templer, P. H., and Tu, K. P.: Stable Isotopes in Plant Ecology, Annu. Rev. Ecol. Syst., 33, 507–559, https://doi.org/10.1146/annurev.ecolsys.33.020602.095451, 2002.

Ehleringer, J. R., Buchmann, N., and Flanagan, L. B.: Carbon isotope ratios in belowground carbon cycle processes, Ecol. Appl., 10, 412–422, 2000.

Eshetu, Z. and Högberg, P.: Reconstruction of Forest Site History in Ethiopian Highlands Based on ^{13}C Natural Abundance of Soils, AMBIO A J. Hum. Environ., 29, 83–89, https://doi.org/10.1579/0044-7447-29.2.83, 2000.

Farquhar, G., O'Leary, and Berry, J.: On the relationship between carbon isotope discrimination and the intercellular carbon dioxide concentration in leaves, Aust. J. Plant Physiol., 9, 121–137, 1982.

Friedli, H., Lötscher, H., Oeschger, H., Siegenthaler, U., and Stauffer, B.: Ice core record of the ^{13}C / ^{12}C ratio of atmospheric CO$_2$ in the past two centuries, Nature, 324, 237–238, https://doi.org/10.1038/324237a0, 1986.

Friis, I.: Zonation of Forest Vegetation on the South Slope of Bale Mountains, South Ethiopia, Ethiop. J. Sci., 9, 29–44, 1986.

Friis, I., Sebsebe, D., and Breugel, P. V.: Atlas of the Potential Vegetation of Ethiopia, The Royal Danish Academy of Sciences and Letters, Addis Ababa University Press and Shama Books, Addis Ababa, Ethiopia, 307 pp., 2010.

Garten, C. T., Cooper, L. W., Post, W. M., and Hanson, P. J.: Climate Controls on Forest Soil C Isotope Ratios in the Southern Appalachian Mountains, Ecology, 81, 1108–1119, 2000.

Gebru, T., Eshetu, Z., Huang, Y., Woldemariam, T., Strong, N., Umer, M., DiBlasi, M., and Terwilliger, V. J.: Holocene palaeovegetation of the Tigray Plateau in northern Ethiopia from charcoal and stable organic carbon isotopic analyses of gully sediments, Palaeogeogr. Palaeocl., 282, 67–80, https://doi.org/10.1016/j.palaeo.2009.08.011, 2009.

Glaser, B. and Zech, W.: Reconstruction of climate and landscape changes in a high mountain lake catchment in the Gorkha Himal, Nepal during the Late Glacial and Holocene as deduced from radiocarbon and compound-specific stable isotope analysis of terrestrial, aquatic and microbial biomarkers, Org. Geochem., 36, 1086–1098, https://doi.org/10.1016/j.orggeochem.2005.01.015, 2005.

Gunina, A. and Kuzyakov, Y.: Soil Biology & Biochemistry Sugars in soil and sweets for microorganisms: Review of origin, content, composition and fate, Soil Biol. Biochem., 90, 87–100, 2015.

Hamilton, A. C.: Environmental history of East Africa, A study of the Quarternary, London, Academic Press, https://doi.org/10.2307/2259986, 328 pp., 1982.

Hedberg, O.: Vegetation belts of the east african mountains, Svenska botaniska fôreningens, Stockholm, 1951.

Hedberg, O.: Evolution and speciation in a tropical high mountain flora, Biol. J. Linn. Soc., 1, 135–148, https://doi.org/10.1111/j.1095-8312.1969.tb01816.x, 1969.

Hepp, J., Rabus, M., Anhäuser, T., Bromm, T., Laforsch, C., Sirocko, F., Glaser, B., and Zech, M.: A sugar biomarker proxy for assessing terrestrial versus aquatic sedimentary input, Org. Geochem., 98, 98–104, https://doi.org/10.1016/j.orggeochem.2016.05.012, 2016.

Hevly, R. H.: Pollen production, transport and preservation?, Potentials and limitations in archaeological palynology, 39–54, 1981.

Hillman, J. C.: Conservation in Bale Mountains National Park, Ethiopia, Oryx, 20, 89–94, https://doi.org/10.1017/S0030605300026314, 1986.

Jacob, M., Annys, S., Frankl, A., De Ridder, M., Beeckman, H., Guyassa, E. and Nyssen, J.: Tree line dynamics in the tropical African highlands – identifying drivers and dynamics, J. Veg. Sci., 26, 9–20, https://doi.org/10.1111/jvs.12215, 2015.

Jansen, B., Nierop, K. G. J., Kotte, M. C., de Voogt, P., and Verstraten, J. M.: The applicability of accelerated solvent extraction (ASE) to extract lipid biomarkers from soils, Appl. Geochem., 21, 1006–1015, https://doi.org/10.1016/j.apgeochem.2006.02.021, 2006a.

Jansen, B., Nierop, K. G. J., Hageman, J. A., Cleef, A. M., and Verstraten, J. M.: The straight-chain lipid biomarker composition of plant species responsible for the dominant biomass production along two altitudinal transects in the Ecuadorian Andes, Org. Geochem., 37, 1514–1536, https://doi.org/10.1016/j.orggeochem.2006.06.018, 2006b.

Jansen, B., Haussmann, N. S., Tonneijck, F. H., Verstraten, J. M., and de Voogt, P.: Characteristic straight-chain lipid ratios as a quick method to assess past forest-páramo transitions in the Ecuadorian Andes, Palaeogeogr. Palaeocl., 262, 129–139, https://doi.org/10.1016/j.palaeo.2008.02.007, 2008.

Jia, G., Dungait, J. A. J., Bingham, E. M., Valiranta, M., Korhola, A., and Evershed, R. P.: Neutral monosaccharides as biomarker proxies for bog-forming plants for application to palaeovegetation reconstruction in ombrotrophic peat deposits, Org. Geochem., 39, 1790–1799, https://doi.org/10.1016/j.orggeochem, 2008.

Johansson, M.: Fire and grazing in subalpine heathlands and forests of Bale Mountains, Ethiopia, Institutionen för skogens ekologi och skötsel, Sveriges lantbruksuniversitet, Umeå, 14, 1652–1668, 2013.

Kebede, M., Ehrich, D., Taberlet, P., Nemomissa, S., and Brochmann, C.: Phylogeography and conservation genetics of a giant lobelia (Lobelia giberroa) in Ethiopian and Tropical East African mountains, Mol. Ecol., 16, 1233–1243, https://doi.org/10.1111/j.1365-294X.2007.03232.x, 2007.

Kidane, Y., Stahlmann, R., and Beierkuhnlein, C.: Vegetation dynamics, and land use and land cover change in the Bale Mountains, Ethiopia, Environ. Monit. Assess., 184, 7473–7489, https://doi.org/10.1007/s10661-011-2514-8, 2012.

Körner, C., Farquhar, G. D., and Wong, S. C.: Carbon isotope discrimination by plants follows latitudinal and altitudinal trends, Oecologia, 88, 30–40, https://doi.org/10.1007/BF00328400, 1991.

Krepkowski, J., Gebrekirstos, A., Shibistova, O., and Br, A.: Stable carbon isotope labeling reveals different carry-over effects between functional types of tropical trees in an Ethiopian mountain forest, New Phytol., 199, 431–440, 2013.

Lemma, B., Mekonnen, B., Glaser, B., Zech, W., Nemomissa, S., Bekele, T., Bittner, L., and Zech, M.: Chemotaxonomic patterns of vegetation and soils along altitudinal transects of the Bale Mountains, Ethiopia, and implications for paleovegetation reconstructions – Part II: lignin-derived phenols and leaf-wax-derived n-alkanes, E&G Quaternary Sci. J., 69, 189–200, https://doi.org/10.5194/egqsj-69-189-2019, 2019a.

Lemma, B., Kebede, S., Nemomissa, S., Otte, I., Glaser, B., and Zech, M.: Spatial and temporal ^{2}H and ^{18}O isotope variation of contemporary precipitation in the Bale Mountains, Ethiopia, Isotopes in Environmental and Health Studies, submitted, 2019b.

Levin, N. E., Brown, F. H., Behrensmeyer, A. K., Bobe, R., and Cerling, T. E.: Paleosol carbonates from the omo group: Isotopic records of local and regional environmental change in East Africa, Palaeogeogr. Palaeocl., 307, 75–89, https://doi.org/10.1016/j.palaeo.2011.04.026, 2011.

Li, Y. C., Hai, Q., Corresp, X., Yang, X. L., Chen, H., Lu, X. M., Li, Y., Xu, Q., Yang, X., Chen, H. U. I., and Lu, X.: Pollen – vegetation relationship and pollen preservation on the Northeastern Qinghai – Tibetan Plateau, Grana, 44, 160–171, https://doi.org/10.1080/00173130500230608, 2005.

Lisanework, N. and Mesfin, T.: An ecological study of the vegetation of the Harenna forest, Bale, Ethiopia. Ethiop. J. Sci. 12, 63–93, 1989.

Liu, X. H., Zhao, L. J., Gasaw, M., Gao, D. Y., Qin, D. H., and Ren, J. W.: Foliar δ^{13}C and δ^{15}N values of C_3 plants in the Ethiopia Rift Valley and their environmental controls, Chinese Sci. Bull., 52, 1265–1273, https://doi.org/10.1007/s11434-007-0165-5, 2007.

Miehe, S. and Miehe, G.: Ericaceous forest and heath land in Bale Mountains of South Ethiopia, Ecology and Man's Impact, Hamburg, Stiftung Walderhaltung in Africa Hamburg, Germany, 1994.

Messerli, B. and and Winiger, M.: Climate, Environmental Change, and Resources of the African Mountains from the Mediterranean to the Equator, Mt. Res. Dev., 12, 315–336, https://doi.org/10.2307/3673683, 1992.

Meyers, P. A.: Preservation of elemental and isotopic source identification of sedimentary organic matter, Chem. Geol., 114, 289–302, https://doi.org/10.1016/0009-2541(94)90059-0, 1994.

Natelhoffer, K. J. and Fry, B.: Controls on Natural Nitrogen-15 and Carbon-13 Abundances in Forest Soil Organic Matter, Soil Sci. Soc. Am. J., 52, 1633–1640, https://doi.org/10.2136/sssaj1988.03615995005200060024x, 1988.

Oades, J. M.: Soil organic matter and structural stability: mechanisms and implications for management, Plant Soil, 76, 319–337, https://doi.org/10.1007/BF02205590, 1984.

Prietzel, J., Dechamps, N., and Spielvogel, S.: Analysis of non-cellulosic polysaccharides helps to reveal the history of thick organic surface layers on calcareous Alpine soils, Plant Soil, 365, 93–114, https://doi.org/10.1007/s11104-012-1340-2, 2013.

Sauheitl, L., Glaser, B., and Bol, R.: Short-term dynamics of slurry-derived plant and microbial sugars in a temperate grassland soil as assessed by compound-specific δ^{13}C analyses, Rapid Commun. Mass Spec., 19, 1437–1446, https://doi.org/10.1002/rcm.1965, 2005.

Simoneit, B.: Molecular Indicators (Biomarkers) of past life, The Anatomical Record, 286, 186–195, https://doi.org/10.1002/ar.10153, 2002.

Solomon, D., Fritzsche, F., Lehmann, J., Tekalign, M., and Zech, W.: Soil organic matter dynamics in the sub-humid agro-ecosystems of the Ethiopian highlands: Evidence from natural C_{13} abundance and particle-size fractionation, Soil Sci. Soc. Am. J., 66, 969–978, 2002.

56

Street-Perrott, F. A., Ficken, K. J., Huang, Y., and Eglinton, G.: Late Quaternary changes in carbon cycling on Mt. Kenya, East Africa: An overview of the δ^{13}C record in lacustrine organic matter, Quat. Sci. Rev., 23, 861–879, https://doi.org/10.1016/j.quascirev.2003.06.007, 2004.

Tiercelin, J. J., Gibert, E., Umer, M., Bonnefille, R., Disnar, J. R., Lézine, A. M., Hureau-Mazaudier, D., Travi, Y., Keravis, D., and Lamb, H. F.: High-resolution sedimentary record of the last deglaciation from a high-altitude lake in Ethiopia, Quat. Sci. Rev., 27, 449–467, https://doi.org/10.1016/j.quascirev.2007.11.002, 2008.

Tiunov, A. V.: Stable isotopes of carbon and nitrogen in soil ecological studies, Biol. Bull., 34, 395–407, https://doi.org/10.1134/S1062359007040127, 2007.

Umer, M., Lamb, H. F., Bonnefille, R., Lézine, A. M., Tiercelin, J. J., Gibert, E., Cazet, J. P., and Watrin, J.: Late Pleistocene and Holocene vegetation history of the Bale Mountains, Ethiopia, Quat. Sci. Rev., 26, 2229–2246, https://doi.org/10.1016/j.quascirev.2007.05.004, 2007.

Wesche, K., Miehe, G., and Kaeppeli, M.: The Significance of Fire for Afroalpine Ericaceous Vegetation, Mt. Res. Dev., 20, 340–347, https://doi.org/10.1659/0276-4741(2000)020[0340:TSOFFA]2.0.CO;2, 2000.

Yimer, F., Ledin, S., and Abdelkadir, A.: Soil property variations in relation to topographic aspect and vegetation community in the south-eastern highlands of Ethiopia, For. Ecol. Manage., 232, 90–99, https://doi.org/10.1016/j.foreco.2006.05.055, 2006.

Yineger, H., Kelbessa, E., Bekele, T., and Lulekal, E.: Floristic Composition and Structure of the Dry Afromontane Forest At Bale Mountains National Park, Ethiopia, J. Sci., 31, 103–120, https://doi.org/10.4314/sinet.v31i2.66551, 2008.

Young, H. J. and Young, T. P.: Local distribution of C3 and C4 grasses in sites of overlap on Mount Kenya, Oecologia, 58, 373–377, https://doi.org/10.1007/BF00385238, 1983.

Zech, M.: Evidence for Late Pleistocene climate changes from buried soils on the southern slopes of Mt. Kilimanjaro, Tanzania, Palaeogeogr. Palaeocl., 242, 303–312, https://doi.org/10.1016/j.palaeo.2006.06.008., 2006.

Zech, M. and Glaser, B.: Compound-specific δ^{18}O analyses of neutral sugars in soils using gas chromatography-pyrolysis-isotope ratio mass spectrometry: Problems, possible solutions and a first application, Rapid Commun. Mass Spec., 23, 3522–3532, https://doi.org/10.1002/rcm.4278, 2009.

Zech, M., Zech, R., and Glaser, B.: A 240,000-year stable carbon and nitrogen isotope record from a loess-like palaeosol sequence in the Tumara Valley, Northeast Siberia, Chem. Geol., 242, 307–318, https://doi.org/10.1016/j.chemgeo.2007.04.002, 2007.

Zech, M., Bimüller, C., Hemp, A., Samimi, C., Broesike, C., Hörold, C., and Zech, W.: Human and climate impact on ^{15}N natural abundance of plants and soils in high-mountain ecosystems: A short review and two examples from the Eastern Pamirs and Mt. Kilimanjaro, Isotopes Environ. Health Stud., 47, 286–296, https://doi.org/10.1080/10256016.2011.596277, 2011a.

Zech, M., Leiber, K., Zech, W., Poetsch, T., and Hemp, A.: Late Quaternary soil genesis and vegetation history on the northern slopes of Mt. Kilimanjaro, East Africa, Quat. Int., 243, 327–336, https://doi.org/10.1016/j.quaint.2011.05.020, 2011b.

Zech, M., Rass, S., Buggle, B., Löscher, M., and Zöller, L.: Reconstruction of the late Quaternary paleoenvironments of the Nussloch loess paleosol sequence, Germany, using n-alkane biomarkers, Quat. Res., 78, 326–335, https://doi.org/10.1016/j.yqres.2012.05.006, 2012.

Manuscript 2: Chemotaxonomic patterns of vegetation and soils along altitudinal transects of the Bale Mountains, Ethiopia and implications for paleovegetation reconstructions II: Lignin– derived phenols and leaf wax-derived n-alkanes

Open Access

E&G Quaternary Science Journal

Chemotaxonomic patterns of vegetation and soils along altitudinal transects of the Bale Mountains, Ethiopia, and implications for paleovegetation reconstructions – Part II: lignin-derived phenols and leaf-wax-derived *n*-alkanes

Bruk Lemma[1,2], Betelhem Mekonnen[1,3], Bruno Glaser[1], Wolfgang Zech[4], Sileshi Nemomissa[5], Tamrat Bekele[5], Lucas Bittner[1], and Michael Zech[1,6]

[1]Institute of Agronomy and Nutritional Sciences, Soil Biogeochemistry, Martin Luther University Halle-Wittenberg, Von-Seckendorff-Platz 3, 06120, Halle, Germany
[2]Forest and Rangeland Biodiversity Directorate, Ethiopian Biodiversity Institute, P.O. Box 30726, Addis Ababa, Ethiopia
[3]Department of Urban Agriculture, Misrak Polytechnic College, P.O. Box 785, Addis Ababa, Ethiopia
[4]Institute of Soil Science and Soil Geography, University of Bayreuth, Universitätsstrasse 30, 95440, Bayreuth, Germany
[5]Department of Plant Biology and Biodiversity Management, Addis Ababa University, P.O. Box 3434, Addis Ababa, Ethiopia
[6]Institute of Geography, Technical University of Dresden, Helmholtzstrasse 10, 01062, Dresden, Germany

Correspondence: Bruk Lemma (bruklemma@gmail.com)

How to cite: Lemma, B., Mekonnen, B., Glaser, B., Zech, W., Nemomissa, S., Bekele, T., Bittner, L., and Zech, M.: Chemotaxonomic patterns of vegetation and soils along altitudinal transects of the Bale Mountains, Ethiopia, and implications for paleovegetation reconstructions – Part II: lignin-derived phenols and leaf-wax-derived *n*-alkanes, E&G Quaternary Sci. J., 68, 189–200, https://doi.org/10.5194/egqsj-68-189-2019, 2019.

Abstract: *Erica* is a dominant vegetation type in many sub-afroalpine ecosystems, such as the Bale Mountains in Ethiopia. However, the past extent of *Erica* is not well known and climate versus anthropogenic influence on altitudinal shifts are difficult to assign unambiguously, especially during the Holocene. The main objective of the present study is to chemotaxonomically characterize the dominant plant species occurring in the Bale Mountains using lignin phenols and *n*-alkane biomarkers and to examine the potential of those biomarkers for reconstructing vegetation history. Fresh plant material, organic layer and mineral topsoil samples were collected along a northeastern and a southwestern altitudinal transect (4134–3870 and 4377–2550 m a.s.l., respectively). Lignin-derived vanillyl, syringyl and cinnamyl phenols were analyzed using the cupric oxide oxidation method. Leaf-wax-derived *n*-alkanes were extracted and purified using Soxhlet and aminopropyl columns. Individual lignin phenols and *n*-alkanes were separated by gas-chromatography and detected by mass spectrometry and flame ionization detection, respectively.

We found that the relative contributions of vanillyl, syringyl and cinnamyl phenols allow us to chemotaxonomically distinguish contemporary plant species of the Bale Mountains. *Erica* in particular is characterized by relatively high cinnamyl contributions of > 40 %. However, litter degradation strongly decreases the lignin phenol concentrations and completely changes the lignin phenol pat-

terns. Relative cinnamyl contributions in soils under *Erica* were $< 40\,\%$, while soils that developed under Poaceae (*Festuca abyssinica*) exhibited relative cinnamyl contributions of $> 40\,\%$.

Similarly, long-chain *n*-alkanes extracted from the leaf waxes allowed for differentiation between *Erica* versus *Festuca abyssinica* and *Alchemilla*, based on lower C_{31} / C_{29} ratios in *Erica*. However, this characteristic plant pattern was also lost due to degradation in the respective O layers and A_h horizons. In conclusion, although in modern-day plant samples a chemotaxonomic differentiation is possible, soil degradation processes seem to render the proxies unusable for the reconstruction of the past extent of *Erica* on the Sanetti Plateau, Bale Mountains, Ethiopia. This finding is of high relevance beyond our case study.

Kurzfassung: *Erica* prägt als dominante Pflanzengattung viele Subafro-alpine Ökosysteme, so auch die Bale Berge in Äthiopien. Das Ausmaß der flächenhaften Ausdehnung von *Erica* in der Vergangenheit ist jedoch unklar, genauso wie die klimatische versus menschliche Verursachung solcher Vegetationsänderungen insbesondere im Holozän. Das Ziel dieser Studie war es herauszufinden (i) ob sich die dominante Vegetation in den Bale Bergen anhand von ligninbürtigen Phenolen und blattwachsbürtigen *n*-Alkanbiomarkern chemotaxonomisch unterscheiden lässt und (ii) ob diese Biomarker das Potential haben zur Vegetationsrekonstruktion im Untersuchungsgebiet beizutragen. In einem Begleitartikel (Mekonnen et al., 2019) verfolgen wir dasselbe Ziel, jedoch anhand von Stabilkohlenstoff- und Stickstoffisotopen sowie Zuckerbiomarkern. Untersucht wurden Pflanzenproben, O-Lagen und A_h Horizonte entlang eines Nord- und eines Südwest-Höhentransektes (3870–4134 m bzw. 2550–4377 m ü. NN). Die ligninbürtigen Phenoleinheiten Vannilly, Syringyl und Cinnamyl wurden mittels der Kupferoxidationsmethode gewonnen; die *n*-Alkane wurden mittels Soxhlet extrahiert und über Aminopropylsäulen aufgereinigt. Die Quantifizierung der Ligninphenole und *n*-Alkane erfolgte mittels Gaschromatographie – Massenspektrometrie bzw. Gaschromatographie – Flammenionisationsdetektion.

Die Ergebnisse zeigen, dass sich die dominanten Pflanzenarten in den Bale Bergen anhand ihrer Vanillyl, Syringyl und Cinnamyl Einheiten chemotaxonomisch unterscheiden lassen. So weist insbesondere *Erica* charakterischerweise relativ hohe Cinnamyl-Anteile von $> 40\,\%$ auf. Vermutlich degradationsbedingt nimmt jedoch in der Reihe Pflanze – O-Lage – A_h Horizont nicht nur die Ligninkonzentration stark ab, sondern auch die Ligninmuster ändern sich völlig. Dadurch weisen Böden unter *Erica* Cinnamyl-Anteile $< 40\,\%$ auf, während Böden die sich unter der dominanten Grasart *Festuca abyssinica* entwickelt haben Cinnamyl-Anteile von $> 40\,\%$ aufweisen. Auch anhand der Alkanbiomarker ist eine chemotaxonomische Unterscheidung zumindest zwischen *Erica* versus *Festuca abyssinica* und *Alchemilla* möglich. Als Proxy dient hier das Verhältnis von C_{31} zu C_{29}. Allerdings führt auch hier Degradation in der Reihe Pflanze – O-Lage – A_h Horizont zum Verlust des charakteristischen Alkanmusters. Obwohl sich rezentes Pflanzenmaterial chemotaxonomisch unterscheiden lässt, zwingt dies zur Schlussfolgerung, dass Degradationseffekte bei der Rekonstruktion von *Erica* im Untersuchungsgebiet der Bale Berge in Äthiopien anhand von ligninbürtigen Phenolen und blattwachsbürtigen Alkanbiomarkern nicht unberücksichtigt bleiben dürfen. Dieser Befund ist über unsere Fallstudie hinaus von hoher Relevanz.

1   Introduction

The Bale Mountains are an eastern afromontane biodiversity hotspot area with 27 endemic species of flowering plants (Hillman, 1988). Like in many other afromontane ecosystems, an altitudinal zonation of the vegetation is well established, with an Ericaceous belt forming a prominent feature. Ericaceous vegetation dominates above 3300 m a.s.l., shows different stages of post-fire succession and remains continuous up to 3800 m a.s.l. However, it becomes patchy on the Sanetti Plateau (Miehe and Miehe, 1994). The Bale Moun-

tains National Park is increasingly under threat from climate change and anthropogenic impacts (Kidane et al., 2012). Ascertaining the past environmental and vegetation history of the area will support conservation efforts and may help to disentangle the influence of climate versus human impact on the present biodiversity.

Until now, the vegetation history of the Bale Mountains was studied using pollen records from lacustrine sediments and peat deposits (Bonnefille and Hamilton, 1986; Bonnefille and Mohammed, 1994; Hamilton, 1982; Umer et al., 2007). The results suggest the extension of the Ericaceous belt to-

wards higher altitudes during the early and middle Holocene. As potential drawbacks, such pollen studies depend on pollen preservation and can be biased by variable pollination rates as well as middle- and long-distance pollen transport (Hicks, 2006; Jansen et al., 2010; Ortu et al., 2006). By contrast, stable isotopes and biomarkers can also be applied to more degraded sedimentary archives and soils and are assumed to reflect the standing vegetation more (Glaser and Zech, 2005). Thus, they offer the potential to complement pollen-based vegetation reconstructions and to reconstruct vegetation at a higher temporal and spatial resolution. For instance, the stable carbon isotopic composition (δ^{13}C) of lacustrine sediments suggests an expansion of alpine C_4 grasses on Mount Kenya, especially during glacial times (Street-Perrott et al., 2004), whereas δ^{13}C results from (paleo-)soils provide no evidence for C_4 grass expansion close to Mount Kilimanjaro during late Pleistocene glacial period (Zech, 2006; Zech et al., 2011b). We focus here on lignin-derived phenols and leaf-wax-derived *n*-alkanes as biomarkers, while stable isotopes and sugar biomarkers and their chemotaxonomic potential for reconstructions of the Bale Mountains vegetation are addressed in a companion paper by Mekonnen et al. (2019).

Lignin has a polyphenolic biochemical structure produced by terrestrial vascular plants (Ertel and Hedges, 1984) providing strength and rigidity to the plants (Thevenot et al., 2010). The lignin-derived phenols vanillyl (V), syringyl (S) and cinnamyl (C) as products of cupric oxide (CuO) oxidation are used to differentiate sources of organic matter and provide information about the diagenetic state (degree of degradation) of vascular plant material in terrestrial and aquatic sediments (Castañeda et al., 2009; Hedges et al., 1988; Tareq et al., 2004, 2006; Ziegler et al., 1986). For instance, low ratios of S / V $\sim$ 0 were suggested as a proxy for the relative contribution of gymnosperms, and elevated S / V ratios were found to be indicative for the presence of angiosperms (Tareq et al., 2004). Likewise, the C / V ratio was proposed to indicate the relative contribution of woody (C / V < 0.1) and non-woody (C / V > 0.1) plants to the soil and sediment organic matter (Tareq et al., 2011). Moreover, the ratios of acid to aldehyde forms of vanillyl and syringyl units (Ac / Al)v,s were suggested as proxies for quantifying the degree of lignin degradation (Amelung et al., 2002; Hedges and Ertel, 1982; Möller et al., 2002).

n-alkanes are important constituents of plant leaf waxes (Kolattukudy, 1970), where they serve to protect plants against water loss by evaporation as well as from fungal and insect attacks (Eglinton and Hamilton, 1967; Koch et al., 2009). Due to their recalcitrant nature, they are often well preserved in sedimentary archives and used as biomarkers (also called molecular fossils) in paleoclimate and environmental studies (Eglinton and Eglinton, 2008; Glaser and Zech, 2005; Zech et al., 2011c). The potential of *n*-alkanes for chemotaxonomic studies has been suggested based on the finding that the homologues C_{27} and C_{29} are sourced pre-

dominantly from trees and shrubs, whereas the homologues C_{31} and C_{33} are sourced predominantly from grasses and herbs (Maffei, 1996; Maffei et al., 2004; Rommerskirchen et al., 2006; Schäfer et al., 2016; Zech, 2009). Potential pitfalls when applying *n*-alkane proxies in paleovegetation studies should not be overlooked. For instance, (Bush and McInerney, 2013) caution against the chemotaxonomic application of *n*-alkanes because of high *n*-alkane pattern variability within graminoids and woody plants (Schäfer et al., 2016) emphasized the need for establishing regional calibration studies and Zech et al., (2011a, 2013) point to degradation affecting *n*-alkane proxies.

While the overall aim of our research is to contribute to the reconstruction of the paleoclimate and environmental history of the Bale Mountains, this study focuses more specifically on the following questions: (i) do lignin phenols and *n*-alkane biomarkers allow a chemotaxonomic differentiation of the dominant plant types of the Bale Mountains? (ii) Are the biomarker patterns of the plants reflected by and incorporated into the respective soils? (iii) Which implications have to be drawn from those results for planned paleovegetation reconstructions in the study area, e.g., concerning the reconstruction of the former extent of *Erica*? Finally, improved knowledge of the vegetation history of the Bale Mountains may help to support the biodiversity conservation program of the park in the face of future climate change and increasing human pressure.

2 Material and methods

2.1 Study area and sample description

The Bale Mountains are located 400 km southeast of Addis Ababa, the capital of Ethiopia (Hillman, 1986). Geographically, they belong to the Bale–Arsi massif, which forms the western section of the southeastern Ethiopian Highlands (Hillman, 1988; Miehe and Miehe, 1994; Tiercelin et al., 2008). The Bale Mountains National Park (BMNP) is situated at 39°28′ to 39°57′ E and 6°29′ to 7°10′ N, (Hillman, 1988; Miehe and Miehe, 1994; Umer et al., 2007) with elevations ranging from 1400 to 4377 m a.s.l. The highest part forms the Sanetti Plateau, on which the second highest peak of the country, Mount Tullu Dimtu at 4377 m a.s.l. is also located (Hillman, 1988). The plateau is limited by the steep Harenna escarpment in the south and the southeast. The northeastern part is encompassed by high ridges and broad valleys that gradually descend towards the extensive Arsi–Bale plateaus and further into the Central Rift Valley lowlands (Hillman, 1988; Tiercelin et al., 2008). The topography of the Bale Mountains results in climatic gradients with respect to spatial and temporal distribution of rainfall as well as temperature (Tiercelin et al., 2008). Mean maximum temperature (MMT) on the mountain peaks ranges between 6 and 12 °C. At Dinsho (headquarters, 3170 m a.s.l.) the MMT is 11.8 °C. Mean mini-
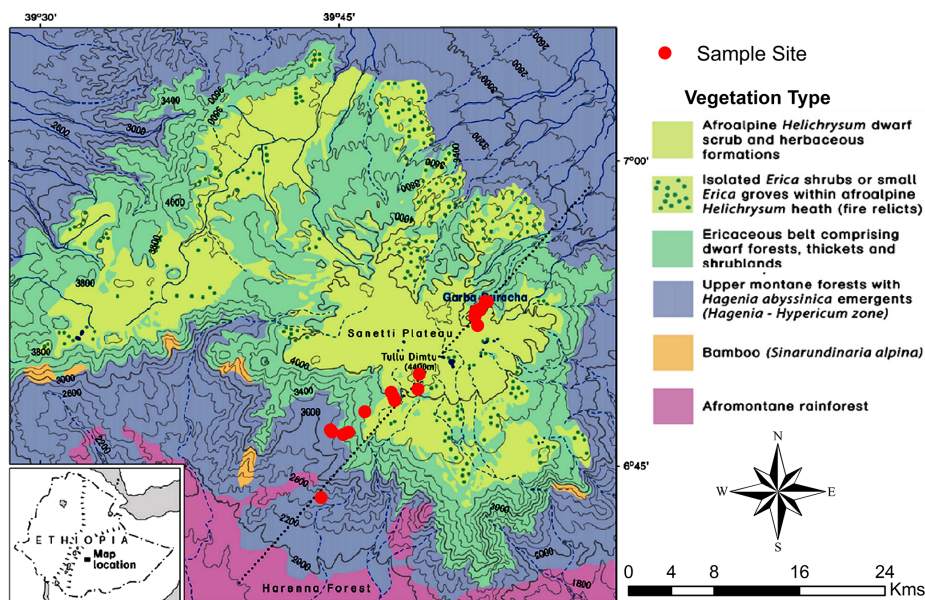
Figure 1. Map of the Bale Mountains for the vegetation zones and study sites along the northeastern and the southwestern transect (modified following Miehe and Miehe, 1994). Dominant vegetation types sampled that comprise the Ericaceous and afroalpine belt.

mum temperature ranges from 0.6 to 10 °C, with frequent frost occurring in the high peak areas during the winter season (Tiercelin et al., 2008). The highest annual rainfall and humidity occurs in the southwest part of the mountain with 1000–1500 mm yr^{-1}, and the northern part of the mountains exhibits annual rainfall ranging between 800 and 1000 mm yr^{-1} (Woldu et al., 1989). The vegetation shows an altitudinal zonation comprised of the afromontane rainforest (1450–2000 m a.s.l.), the upper montane forests dominated by *Hagenia* and *Hypericum* species (2000–3200 m a.s.l.); the Ericaceous belt (3200–3800 m a.s.l.); and the afroalpine zone (3800–4377 m a.s.l.) dominated by dwarf shrubs such as *Helichrysum, Alchemilla,* herbs, and grasses (mostly *Festuca*; Fig. 1) (Friis, 1986; Miehe and Miehe, 1994). Geologically, the Bale Mountains consist of a highly elevated volcanic plateau dominated by alkali basalt, tuffs and rhyolite rocks. During the Last Glacial Maximum (LGM), it is understood that the regions of the high peak summits were glaciated and later flattened by repeated glaciations (Kidane et al., 2012; Osmaston et al., 2005; Umer et al., 2004). The soils having developed on the basaltic and trachyte rocks can be generally characterized as silt loam, having a reddish brown to black color (Woldu et al., 1989). They are usually shallow, gravelly and are assumed to have developed since the glacial retreat (Hedberg, 1964). Andosols are the most ubiquitous soil types. Nevertheless, Cambisols and Leptosols are also prevalent soil types in some parts of the Bale Mountains. In

wetland and sedimentary basins, Gleysols and Histosols are also common (Billi, 2015; Yimer et al., 2006).

In February 2015, 25 leaf and twig samples of the dominant plant species were collected (Fig. 1) along a southwestern and a northeastern transect (ranging from 2550 to 4377 m a.s.l. and 3870 to 4134 m a.s.l., respectively). Samples comprised of *Erica trimera* (Engl.) Beentje ($n = 5$), *Erica arborea* L. ($n = 5$), *Alchemilla haumannii* Rothm. ($n = 5$), *Festuca abyssinica* Hochst. ex A. Rich. ($n = 6$), *Helichrysum splendidum* Thunb. L. ($n = 2$), *Kniphofia foliosa* Hochst. ($n = 1$) and *Lobelia rhynchopetalum* Hemsl. ($n = 1$). Additionally, 15 organic surface layers ($=$ O layers, strongly humified plant residues) and 22 mineral topsoils ($=$ A$_h$ horizons) that developed under the above listed dominant vegetation were collected from 27 sampling sites, resulting in 62 samples in total. For photos illustrating the investigated plant species and typical study sites, the reader is referred to Fig. 2 of our companion paper by Mekonnen et al. (2019). All samples were air-dried in the Soil Store Laboratory of the National Herbarium, Department of Plant Biology and Biodiversity Management, Addis Ababa University. In the laboratories of the Soil Biogeochemistry Group, Martin Luther University of Halle-Wittenberg, soil samples were sieved using a mesh size of 2 mm, finely ground, homogenized and subjected to further biogeochemical analysis.
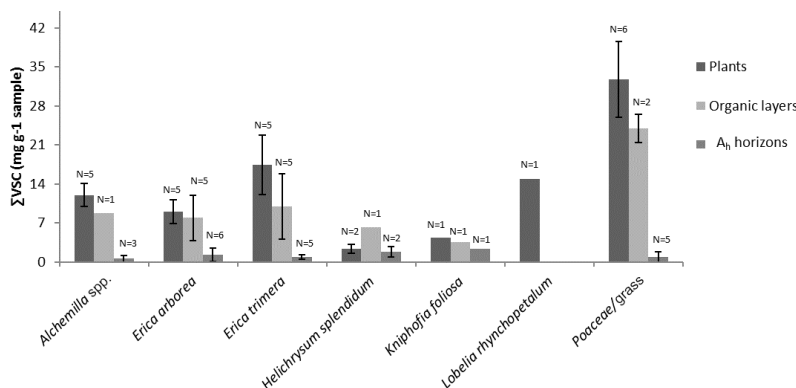
Figure 2. Sum of lignin phenol concentrations ($\sum$VSC) of contemporary plants, O layers and A_h horizons. Error bars illustrate standard deviations.

2.2 Analysis of lignin-derived phenol and leaf-wax-derived *n*-alkane biomarkers

Lignin phenols were extracted from 35, 50 and 500 mg of plant, O-layer and A_h-horizon soil samples, respectively. The analytical procedure followed the cupric oxidation (CuO) method developed by Hedges and Ertel (1982) and modified later on by Goñi and Hedges (1992). Briefly, the samples were transferred into Teflon digestion tubes together with 100 mg of $(NH_4)_2Fe(SO_4)_2 \times 6H_2O$, 500 mg of CuO, 50 mg of $C_6H_{12}O_6$, 1 mL of ethylvanillin solution (100 ppm) as internal standard 1 (IS1) and 15 mL of 2M NaOH and digested at 170 °C for 2 h under pressure. Reaction products were cooled overnight and transferred into centrifuge tubes. Then the phenolic compounds were purified by adsorption on C_{18} columns, desorbed by ethylacetate and concentrated under a stream of nitrogen gas for 30 min. Residue was dissolved in 1 mL phenylacetic acid (PAA), a working internal standard stock solution to determine the recovery of ethylvanillin before derivatization (Amelung et al., 2002; Möller et al., 2002). Finally, the samples were derivatized using 200 µL of N, O-bis(trimethylsilyl)trifluoroacetamide (BSTFA) and 100 µL of pyridine. Oxidation products of lignin phenols were quantified using a SHIMADZU QP 2010 gas chromatography (GC) instrument coupled with a mass spectrometer (MS), (GCMS–QP2010, Kyoto, Japan).

After recovery correction, the concentration of each lignin phenol (in mg g^{-1}) was calculated from two or three CuO oxidation products according to the Eqs. (1), (2) and (3), respectively.

Vanillyl (V) = vanillin + acetovanillone + vanillic acid   (1)

Syringyl (S) = syringaldehyde + acetosyringone

$\qquad$ + syringic acid   (2)

Cinnamyl (C) = *p*-coumaric acid + ferulic acid   (3)

For data evaluation, the sum of V, S, and C ($\sum$VSC); the ratios of S / V, and C / V; and the ratios of acids to aldehydes (Ac / Al) for the syringyl and vanillyl units were additionally calculated.

Leaf-wax-derived *n*-alkanes were extracted from 0.5 to 1 g of plant, O-layer and A_h-horizon soil samples using Soxhlet extraction by adding 150 mL of dichloromethane (DCM) and methanol (MeOH) as solvents (9 : 1 ratio) for 24 h following a method modified following Zech and Glaser (2008). In brief, 50 µL of 5α-androstane were added to the total lipid extracts (TLEs) as internal standard. TLEs were concentrated using rotary evaporation and transferred to aminopropyl columns. Three lipid fractions containing the *n*-alkanes, alcohols and fatty acids, respectively, were eluted successively by using 3 mL of hexane, DCM / MeOH (1 : 1), and diethyl ether and acetic acid (95 : 5) as eluent. The *n*-alkanes were separated on a gas chromatograph (GC) and detected by a flame ionization detector (FID), whereas the other two lipid fractions (alcohols and fatty acids) were archived. The GC instrument (GC–2010 SHMADZU) was equipped with a SPB–5 column (28.8 m length, 0.25 mm inner diameter, 0.25 µm film thickness). The injector and detector temperature were 300 and 330 °C, respectively. The initial oven temperature was 90 °C. It is then raised in three ramps to 250 °C at 20 °C min^{-1}, further to 300 °C at 2 °C min^{-1} and finally to 320 °C at 4 °C min^{-1}, resulting in a total oven runtime of 50 min. Helium (He) was used as carrier gas and *n*-alkane mixture (C_8–C_{40}) was used as external standard for peak identification and quantification.

The total *n*-alkane concentration (TAC), the average chain length (ACL, following Poynter et al., 1989) and the odd over even predominance (OEP, following Hoefs et al. (2002), the latter being very similar to the carbon preference index (CPI), were calculated according to the Eqs. (4), (5) and (6), respectively.
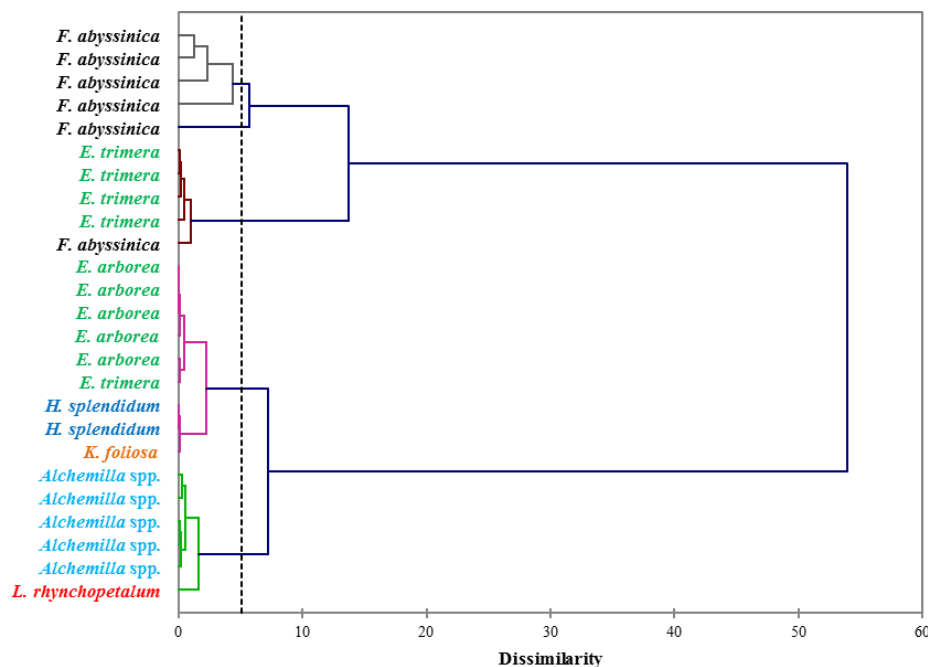
Figure 3. Dendrogram differentiating the dominant plant species of the Bale Mountains based on the concentrations of vanillyl, syringyl and cinnamyl lignin phenols (mg g^{-1} sample). The dotted vertical line represents the distance or dissimilarity between clusters.

$$\text{TAC} = \Sigma C_n, \text{ with } n \text{ ranging from 25 to 35,} \qquad (4)$$

$$\text{ACL} = \Sigma(C_n \times n)/\Sigma C_n, \qquad (5)$$

where n refers to the odd numbered n-alkanes ranging from 27 to 33

$$\text{OEP} = (C_{27} + C_{29} + C_{31} + C_{33})/(C_{26} + C_{28} + C_{30} + C_{32}). \quad (6)$$

All calibrated datasets of the analytical results were subjected to simple correlation test and agglomerative hierarchical clustering (AHC) using XLSTAT (2014) statistical software. R software version 3.4.2 was also used to demonstrate taxonomic differences and the effect of biodegradation on the sample materials via ternary diagrams and notched box plots.

3   Results and discussion

3.1   Lignin phenol concentration and patterns of contemporary vegetation

The $\sum$VSC of modern plants investigated from the two transects of the Bale Mountains ranges from 1.8 to 41.8 mg g^{-1}, the sample with *Festuca* yielding the highest average contribution to TOC with up to 33 mg g^{-1} sample (Fig. 2). This is within the range reported in the literature (Belanger et al.,

2015; Hedges et al., 1986). Note that lignin phenol concentrations of grasses are higher compared to other vegetation of the Bale Mountains, although it is known that grasses contain only low amounts of lignin when compared to trees.

The concentrations of individual lignin phenols (vanillyl, syringyl and cinnamyl) allow us to chemotaxonomically differentiate the contemporary dominant plant species of the Bale Mountains. This is illustrated in Fig. 3, based on an agglomerative hierarchical cluster analysis (AHC). The abundance of individual lignin phenols (V, S and C) was specific to individual or restricted groups of plant and/or tissues applied to cluster different taxa (Belanger et al., 2015; Castañeda et al., 2009; Goñi and Hedges, 1992; Hedges and Mann, 1979; Tareq et al., 2004, 2006).

While Fig. 3 highlights the potential for chemotaxonomic differentiation of the investigated plants, it does not yet become clear from this hierarchical cluster analyses result which lignin phenols are characteristic for which plants and which lignin proxy might have potential for paleovegetation reconstructions. Therefore, Fig. 4 shows the relative abundance of V, S and C for all investigated plant species in a ternary diagram. Accordingly, *Erica arborea* and *Erica trimera* are characterized by cinnamyl percentages of > 40 %, whereas, except for two *Festuca* samples, all other plants are characterized by cinnamyl percentages of < 40 %. Our results from fresh plant material are hence not in agree-
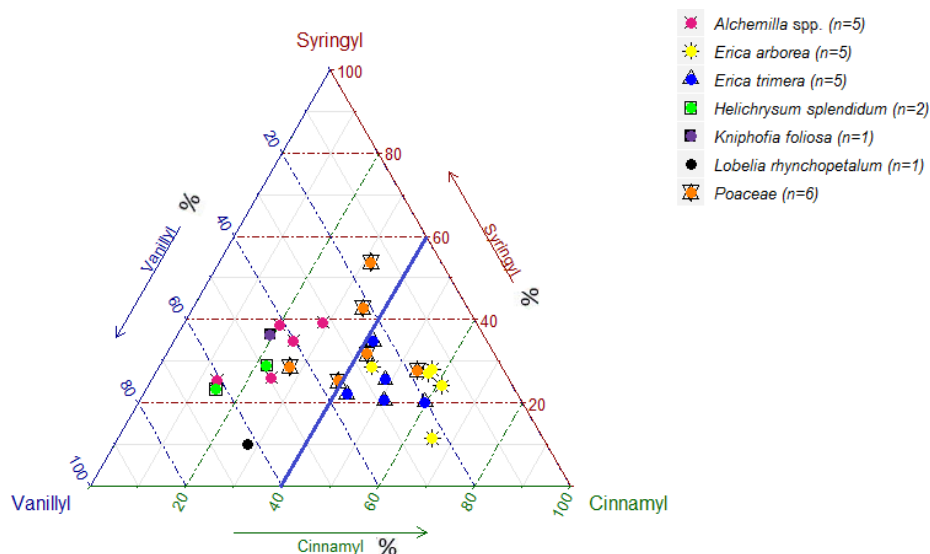
Figure 4. Ternary diagram for the relative abundances (%) of vanillyl, syringyl and cinnamyl lignin phenols of the dominant vegetation. The blue line separates samples with more (right) versus less (left) than 40 % cinnamyl.
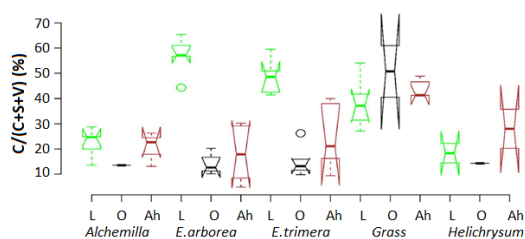

Figure 5. Box plot for the relative abundance of cinnamyl phenols (expressed as $C / (V + S + C)$ in %) in plants, O layers and A_h horizons. The box plots indicate the median (solid line between the boxes) and interquartile range (IQR), with upper (75 %) and lower (25 %) quartiles and possible outliers (white circles). The notches display the confidence interval around the median within $\pm 1.57 \times$ IQR/sqrt. Note that small sample sizes result in unidentifiable boxes (particularly *Kniphofia* and *Lobelia*).

ment with the finding of Hedges and Mann (1979) and Hedges et al. (1988) that high contributions of cinnamyl phenols are characteristic of non-woody grass and fern. Despite a relatively large scattering and a partial overlapping, our results suggest that the ratio $C / (V + S + C)$ might be used as a proxy for distinguishing *Erica* spp. from other vegetation types of the Bale Mountains, with values > 0.40 being generally characteristic for *Erica* spp.

3.2 Lignin phenol patterns of O layers and A_h horizons

$\sum$VSC strongly decreases from plants over O layers to A_h horizons, except for *Helichrysium*, which yielded the lowest $\sum$VSC values of all plants (Fig. 2). This descending trend is in agreement with the literature (Amelung et al., 1997; Belanger et al., 2015) and reflects the preferential degradation of the plant-derived lignin phenols compared to other soil organic matter constituents. At the same time, the input of root-derived lignin is very likely. As a result of both processes, i.e., degradation and lignin input by roots and the large and chemotaxonomically characteristic contribution of C in *Erica* plant material (≥ 41.5 %) is lost in the O layers (C < 27 %), whereas the two investigated O layers under *Festuca* yielded relative C contributions > 40 %. Similarly, A_h horizons under *Festuca* are characterized by C contributions > 40 %, while all A_h horizons that developed under other vegetation types are characterized by C contributions < 40 %. This finding does not ad hoc preclude the above proposed lignin phenol proxy $C / (V + S + C)$ for reconstructing vegetation history, but it definitely challenges its application. Degradation and lignin input by roots need to be considered when interpreting phenol proxies. This is relevant beyond our case study concerning *Erica* versus *Festuca* and *Helichrysium* (Fig. 5) and is likely more relevant in paleosols than in sedimentary archives.

In our study, we found no consistent increase and systematic relationship between Ac / Al ratios of V and S, which are used as degradation proxies in some studies (Amelung et al., 2002; Hedges and Ertel, 1982; Möller et al., 2002; Tareq
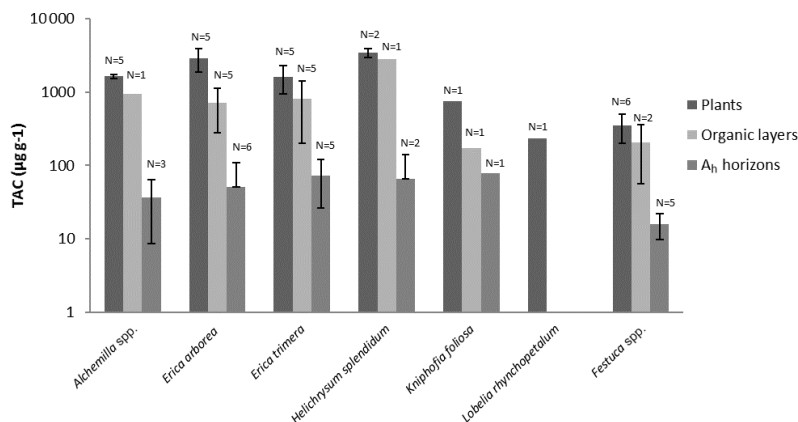
Figure 6. Total long-chain *n*-alkane concentrations (TACs) of plants, O layers and A$_h$ horizons. Error bars illustrate standard deviations.
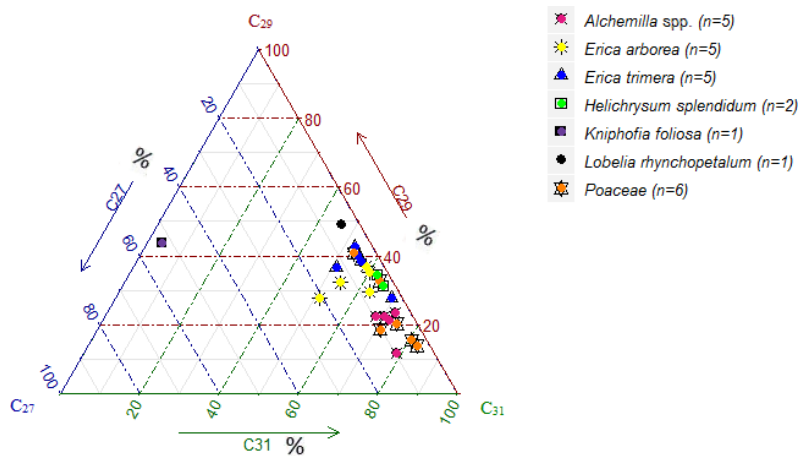
Figure 7. Ternary diagram illustrating the relative abundance (%) of the *n*-alkanes C$_{27}$, C$_{29}$ and C$_{31}$ in the investigated plant samples.

et al., 2011), and source proxy (S / V). This is in agreement with other studies (Belanger et al., 2015), and we therefore suggest that caution needs to be taken when using Ac / Al ratios as degradation proxies.

3.3 *n*-alkane concentrations and patterns of contemporary plants

To characterize the dominant plant species chemotaxonomically, *n*-alkanes with a chain length of 21–37 C atoms were considered as characteristic for epicuticular leaf waxes, typical for higher plants (Eglinton and Hamilton, 1967; Hoffmann et al., 2013). Most of the investigated plant species showed total *n*-alkane concentrations (TAC, C$_{25}$–C$_{35}$) above 800 µg g^{-1}. Only *Lobelia* and *Festuca* exhibited total *n*-alkane concentrations below 800 µg g^{-1} (Fig. 6). The TAC values of the O layers were only slightly lower when com-

pared to contemporary plants. By contrast, the TAC values of the A$_h$ horizons were significantly lower compared to contemporary plants (Fig. 6). The *n*-alkane concentrations in this study are in agreement with research findings for fresh plant materials (Bush and McInerney, 2013; Feakins et al., 2016) and soils (Schäfer et al., 2016).

Contrary to lignin phenols, hierarchical cluster analysis of individual *n*-alkanes did not allow for unambiguous differentiation between *Erica* and non-*Erica* species. Therefore, the *n*-alkane patterns do not allow for developing a proxy for identifying *Erica*, at least in the Bale Mountains. Average chain length values (ACLs) of plant and soil *n*-alkanes range between 28 to 32 and 29 to 31, respectively. The ACLs of *Erica arborea* (30.5) and *Erica trimera* (30.5) are identical, which could be explained by the monophyletic origin of the species (Guo et al., 2014). Grass sam-
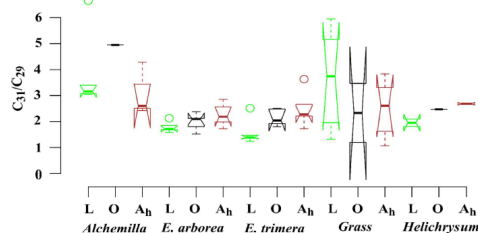
Figure 8. Box plot for the ratio C_{31}/C_{29} in plant samples, organic layers and A_h horizons. The box plots indicate the median (solid line between the boxes) and interquartile range (IQR), with upper (75 %) and lower (25 %) quartiles and possible outliers (white circles). The notches display the confidence interval around the median within $\pm 1.57 \times IQR/\sqrt{}$. Note that small sample sizes result in unidentifiable boxes (particularly *Kniphofia* and *Lobelia*).

ples (*Festuca abyssinica*) exhibited a clear predominance of C_{31} (Fig. 7), which was reported before by different authors (Schäfer et al., 2016; Zech, 2009). Most other investigated plant species revealed a predominance of either C_{29} or C_{31}. Only *Kniphofia foliosa* is characterized by high relative abundance of C_{27} and C_{29}, while C_{31} is almost absent (Fig. 7).

Apart from individual *n*-alkanes, the ratio of C_{31}/C_{29} depicts *Erica* litter as significantly distinguishable from the other species, except for *Helichrysum splendidum* (Fig. 8).

3.4 *n*-alkane concentration and pattern of O layers and A_h horizons

The TAC values decrease in the following order: plants > O layers > A_h horizon (Fig. 6). The odd over even predominance values (OEPs) of the plants, O layers and A_h horizons range from 5 to 90 ($\overline{x} = 21$), 4 to 42 ($\overline{x} = 15$) and 2 to 37 ($\overline{x} = 16$), respectively. The OEP values of the plants (which are almost identical to the CPI values) are therefore well within the range reported (Diefendorf et al., 2011) for angiosperms. Decreasing OEP values towards O layers and A_h horizons are often observed and can be explained with organic matter degradation (Schäfer et al., 2016; Zech et al., 2011b). The still relatively high OEP values ($\overline{x} = 16$) obtained for the topsoils of our study area indicate that the *n*-alkanes are not strongly degraded. Importantly, *n*-alkane degradation affects not only the OEP values but also the *n*-alkane ratios, such as the above presented ratio C_{31}/C_{29} that allows distinguishing *Erica* from non-*Erica* vegetation. As a result, this ratio in particular no longer allows for chemotaxonomically distinguishing between soils that have developed under *Erica* versus *Alchemilla* and grass (Fig. 8). Unlike with lignin phenols, a noteworthy influence from root-derived *n*-alkanes on O layers and A_h horizons can be excluded. This is based on the notion that roots contain lower *n*-alkane concentrations by several magnitudes than above-ground plant material and results from studies using

^{14}C dating of *n*-alkanes in loess–paleosol sequences (Häggi et al., 2014; Zech et al., 2017).

4 Conclusions and implications for paleovegetation reconstructions in the Bale Mountains

One of the premises within the Mountain Exile Hypothesis project (DFG-FOR 2358) is to reconstruct the dynamics of *Erica* vegetation on the Sanetti Plateau in the Bale Mountains National Park, Ethiopia. While our companion paper by Mekonnen et al. (2019) focused on stable carbon and nitrogen isotopes and hemicellulose-derived sugar biomarkers, we tested in this regional calibration study the potential of cupric oxide lignin phenols and leaf-wax-derived *n*-alkanes to serve as unambiguous proxies for differentiating between *Erica* versus non-*Erica* vegetation.

A hierarchical cluster analysis of individual lignin phenols was promising and allowed the chemotaxonomic differentiation of *Erica* from non-*Erica* vegetation based on relatively high relative contribution of cinnamyl (≥ 40 %) phenols. However, this characteristic pattern is not reflected in the O layers and A_h horizons. In all likelihood, the loss of the cinnamyl dominance is caused by preferential degradation. Unlike expected, we found no overall evidence for increasing $(Ac/Al)_{V+S}$ ratios as a proxy for degradation from plant material over O layers to A_h horizons.

Erica could not be differentiated chemotaxonomically from all other investigated plant species using *n*-alkanes in a hierarchical cluster analysis. Nevertheless, *Erica* was still characterized in our dataset by significantly lower C_{31}/C_{29} ratios compared to *Alchemilla* and grasses. However, like lignin-derived phenol proxies, the *n*-alkane patterns are changing due to degradation from plant material over O layers to A_h horizons, thus inhibiting their application for an unambiguous chemotaxonomic identification of *Erica* in soils and sediments. Therefore, future work is planned focusing on alternative molecular markers such as tannin-derived phenols and terpenoids.

References

Amelung, W., Zech, W., and Flach, K. W.: Climatic effects on soil organic matter composition in the Great Plains, Soil Sci. Soc. Am. J., 61, 115–123, 1997.

Amelung, W., Martius, C., Bandeira, A. G., Garcia, M. V., and Zech, W.: Lignin characteristics and density fractions of termite nests in an Amazonian rain forest–indicators of termite feeding guilds, Soil Biol. Biochem., 34, 367–372, 2002.

Belanger, E., Lucotte, M., Gregoire, B., Moingt, M., Paquet, S., Davidson, R., Mertens, F., Passos, C. J. S., and Romana, C.: Lignin signatures of vegetation and soils in tropical environments, Adv. Enviro. Res., 4, 247–262, 2015.

Billi, P.: Geomorphological landscapes of Ethiopia, in: Landscapes and landforms of Ethiopia, edited by: Billi, P., Springer, Dordrecht, Netherlands, 3–32, 2015.

Bonnefille, R. and Hamilton, A.: Quaternary and late Tertiary history of Ethiopian vegetation, Symb. Bot. Ups, 26, 48–63, 1986.

Bonnefille, R. and Mohammed, U.: Pollen-inferred climatic fluctuations in Ethiopia during the last 3000 years, Palaeogeogr. Palaeocl., 109, 331–343, 1994.

Bush, R. T. and McInerney, F. A.: Leaf wax n-alkane distributions in and across modern plants: implications for paleoecology and chemotaxonomy, Geochim. Cosmochim. Ac., 117, 161–179, 2013.

Castañeda, I. S., Werne, J. P., Johnson, T. C., and Filley, T. R.: Late Quaternary vegetation history of southeast Africa: the molecular isotopic record from Lake Malawi, Palaeogeogr. Palaeocl., 275, 100–112, 2009.

Diefendorf, A. F., Freeman, K. H., Wing, S. L., and Graham, H. V.: Production of n-alkyl lipids in living plants and implications for the geologic past, Geochim. Cosmochim. Ac., 75, 7472–7485, 2011.

Eglinton, G. and Hamilton, R. J.: Leaf epicuticular waxes, Science, 156, 1322–1335, 1967.

Eglinton, T. I. and Eglinton, G.: Molecular proxies for paleoclimatology, Earth Planet. Sc. Lett., 275, 1–16, 2008.

Ertel, J. R. and Hedges, J. I.: The lignin component of humic substances: distribution among soil and sedimentary humic, ful-

vic, and base-insoluble fractions, Geochim. Cosmochim. Ac., 48, 2065–2074, 1984.

Feakins, S. J., Peters, T., Wu, M. S., Shenkin, A., Salinas, N., Girardin, C. A., Bentley, L. P., Blonder, B., Enquist, B. J., and Martin, R. E.: Production of leaf wax n-alkanes across a tropical forest elevation transect, Org. Geochem., 100, 89–100, 2016.

Friis, I.: Zonation of Forest Vegetation on the South Slope of Bale Mountains, South Ethiopia, Sinet-an Ethiopian Journal of Science, 29–44, 1986.

Glaser, B. and Zech, W.: Reconstruction of climate and landscape changes in a high mountain lake catchment in the Gorkha Himal, Nepal during the Late Glacial and Holocene as deduced from radiocarbon and compound-specific stable isotope analysis of terrestrial, aquatic and microbial biomarkers, Org. Geochem., 36, 1086–1098, 2005.

Goñi, M. A. and Hedges, J. I.: Lignin dimers: Structures, distribution, and potential geochemical applications, Geochim. Cosmochim. Ac., 56, 4025–4043, 1992.

Guo, N., Gao, J., He, Y., Zhang, Z. and Guo, Y.: Variations in leaf epicuticular n-alkanes in some Broussonetia, Ficus and Humulus species, Biochem. Syst. Ecol., 54, 150–156, 2014.

Häggi, C., Zech, R., McIntyre, C., Zech, M., and Eglinton, T. I.: On the stratigraphic integrity of leaf-wax biomarkers in loess paleosols, Biogeosciences, 11, 2455–2463, https://doi.org/10.5194/bg-11-2455-2014, 2014.

Hamilton, A. C.: Environmental history of East Africa: a study of the Quaternary, Academic Press, London, UK, 328 pp., 1982.

Hedberg, O.: Features of afroalpine plant ecology, Swedish Science Press, Uppsala, Sweden, 148 pp., 1964.

Hedges, J. I. and Ertel, J. R.: Characterization of lignin by gas capillary chromatography of cupric oxide oxidation products, Anal. Chem., 54, 174–178, 1982.

Hedges, J. I. and Mann, D. C.: The characterization of plant tissues by their lignin oxidation products, Geochim. Cosmochim. Ac., 43, 1803–1807, 1979.

Hedges, J. I., Clark, W. A., Quay, P. D., Richey, J. E., Devol, A. H., and Santos, M.: Compositions and fluxes of particulate organic material in the Amazon River1, Limnol. Oceanogr., 31, 717–738, 1986.

Hedges, J. I., Blanchette, R. A., Weliky, K., and Devol, A. H.: Effects of fungal degradation on the CuO oxidation products of lignin: a controlled laboratory study, Geochim. Cosmochim. Ac., 52, 2717–2726, 1988.

Hicks, S.: When no pollen does not mean no trees, Veg. Hist. Archaeobot., 15, 253–261, 2006.

Hillman, J. C.: Conservation in Bale mountains national park, Ethiopia, Oryx, 20, 89–94, 1986.

Hillman, J. C.: The Bale Mountains National Park area, southeast Ethiopia, and its management, Mountain Research and Development, 253–258, 1988.

Hoefs, M. J., Rijpstra, W. I. C., and Damsté, J. S. S.: The influence of oxic degradation on the sedimentary biomarker record I: Evidence from Madeira Abyssal Plain turbidites, Geochim. Cosmochim. Ac., 66, 2719–2735, 2002.

Hoffmann, B., Kahmen, A., Cernusak, L. A., Arndt, S. K., and Sachse, D.: Abundance and distribution of leaf wax n-alkanes in leaves of Acacia and Eucalyptus trees along a strong humidity gradient in northern Australia, Org. Geochem., 62, 62–67, 2013.

Jansen, B., van Loon, E. E., Hooghiemstra, H., and Verstraten, J. M.: Improved reconstruction of palaeo-environments through unravelling of preserved vegetation biomarker patterns, Palaeogeogr. Palaeocl., 285, 119–130, 2010.

Kidane, Y., Stahlmann, R., and Beierkuhnlein, C.: Vegetation dynamics, and land use and land cover change in the Bale Mountains, Ethiopia, Environ. Monit. Assess., 184, 7473–7489, 2012.

Koch, K., Bhushan, B., and Barthlott, W.: Multifunctional surface structures of plants: an inspiration for biomimetics, Prog. Mater. Sci., 54, 137–178, 2009.

Kolattukudy, P. E.: Plant waxes, Lipids, 5, 259–275, 1970.

Maffei, M.: Chemotaxonomic significance of leaf wax alkanes in the Gramineae, Biochem. Syst. Ecol., 24, 53–64, 1996.

Maffei, M., Badino, S., and Bossi, S.: Chemotaxonomic significance of leaf wax *n*-alkanes in the Pinales (Coniferales), J. Biol. Res., 1, 3–19, 2004.

Mekonnen, B., Zech, W., Glaser, B., Lemma, B., Bromm, T., Nemomissa, S., Bekele, T., and Zech, M.: Chemotaxonomic patterns of vegetation and soils along altitudinal transects of the Bale Mountains, Ethiopia, and implications for paleovegetation reconstructions – Part 1: stable isotopes and sugar biomarkers, E&G Quaternary Sci. J., 69, 177–188, https://doi.org/10.5194/egqsj-69-177-2019, 2019.

Miehe, S. and Miehe, G.: Ericaceous forest and heath land in Bale Mountains of South Ethiopia, Ecology and Man's Impact, Hamburg, Stiftung Walderhaltung in Africa Hamburg, Germany, 1994.

Möller, A., Kaiser, K., and Zech, W.: Lignin, carbohydrate, and amino sugar distribution and transformation in the tropical highland soils of northern Thailand under cabbage cultivation, Pinus reforestation, secondary forest, and primary forest, Soil Res., 40, 977–998, 2002.

Ortu, E., Brewer, S., and Peyron, O.: Pollen-inferred palaeoclimate reconstructions in mountain areas: problems and perspectives, J. Quaternary Sci., 21, 615–627, 2006.

Osmaston, H. A., Mitchell, W. A., and Osmaston, J. N.: Quaternary glaciation of the Bale Mountains, Ethiopia, J. Quaternary Sci., 20, 593–606, 2005.

Poynter, J. G., Farrimond, P., Robinson, N., and Eglinton, G.: Aeolian-derived higher plant lipids in the marine sedimentary record: Links with palaeoclimate, in Paleoclimatology and paleometeorology: modern and past patterns of global atmospheric transport, Springer, 435–462, 1989.

Rommerskirchen, F., Plader, A., Eglinton, G., Chikaraishi, Y., and Rullkötter, J.: Chemotaxonomic significance of distribution and stable carbon isotopic composition of long-chain alkanes and alkan-1-ols in C$_4$ grass waxes, Org. Geochem., 37, 1303–1332, 2006.

Schäfer, I. K., Lanny, V., Franke, J., Eglinton, T. I., Zech, M., Vyslouzilová, B., and Zech, R.: Leaf waxes in litter and topsoils along a European transect, Soil, 2, 551–564, 2016.

Street-Perrott, F. A., Ficken, K. J., Huang, Y. and Eglinton, G.: Late Quaternary changes in carbon cycling on Mt. Kenya, East Africa: an overview of the δ13C record in lacustrine organic matter, Quaternary Sci. Rev., 23, 861–879, 2004.

Tareq, S. M., Tanaka, N., and Ohta, K.: Biomarker signature in tropical wetland: lignin phenol vegetation index (LPVI) and its implications for reconstructing the paleoenvironment, Sci. Tot. Environ., 324, 91–103, 2004.

Tareq, S. M., Handa, N., and Tanoue, E.: A lignin phenol proxy record of mid Holocene paleovegetation changes at Lake DaBuSu, northeast China, J. Geochem. Explor., 88, 445–449, 2006.

Tareq, S. M., Kitagawa, H., and Ohta, K.: Lignin biomarker and isotopic records of paleovegetation and climate changes from Lake Erhai, southwest China, since 18.5 ka BP, Quatern. Int., 229, 47–56, 2011.

Thevenot, M., Dignac, M.-F., and Rumpel, C.: Fate of lignins in soils: a review, Soil Biol. Biochem., 42, 1200–1211, 2010.

Tiercelin, J.-J., Gibert, E., Umer, M., Bonnefille, R., Disnar, J.-R., Lézine, A.-M., Hureau-Mazaudier, D., Travi, Y., Kéravis, D., and Lamb, H. F.: High-resolution sedimentary record of the last deglaciation from a high-altitude lake in Ethiopia, Quaternary Sci. Rev., 27, 449–467, 2008.

Umer, M., Kebede, S., and Osmaston, H.: Quaternary glacial activity on the Ethiopian Mountains, Developments in Quaternary Sciences, 2, 171–174, 2004.

Umer, M., Lamb, H. F., Bonnefille, R., Lézine, A.-M., Tiercelin, J.-J., Gibert, E., Cazet, J.-P., and Watrin, J.: Late pleistocene and holocene vegetation history of the bale mountains, Ethiopia, Quaternary Sci. Rev., 26, 2229–2246, 2007.

Woldu, Z., Feoli, E., and Nigatu, L.: Partitioning an elevation gradient of vegetation from Southeastern Ethiopia by probabilistic methods, Plateau, 81, 189–198, 1989.

Yimer, F., Ledin, S., and Abdelkadir, A.: Soil organic carbon and total nitrogen stocks as affected by topographic aspect and vegetation in the Bale Mountains, Ethiopia, Geoderma, 135, 335–344, 2006.

Zech, M.: Evidence for Late Pleistocene climate changes from buried soils on the southern slopes of Mt. Kilimanjaro, Tanzania, Palaeogeogr. Palaeocl., 242, 303–312, 2006.

Zech, M.: Reconstructing Quaternary vegetation history in the Carpathian Basin, SE Europe, using *n*-alkane biomarkers as molecular fossils: problems and possible solutions, potential and limitations, E&G Quaternary Sci. J., 58, 148–155, 2009.

Zech, M. and Glaser, B.: Improved compound-specific δ13C analysis of *n*-alkanes for application in palaeoenvironmental studies, Rapid Commun. Mass Sp., 22, 135–142, 2008.

Zech, M., Pedentchouk, N., Buggle, B., Leiber, K., Kalbitz, K., Marković, S. B., and Glaser, B.: Effect of leaf litter degradation and seasonality on D/H isotope ratios of n-alkane biomarkers, Geochim. Cosmochim. Ac., 75, 4917–4928, 2011a.

Zech, M., Leiber, K., Zech, W., Poetsch, T., and Hemp, A.: Late Quaternary soil genesis and vegetation history on the northern slopes of Mt. Kilimanjaro, East Africa, Quaternary Int., 243, 327–336, 2011b.

Zech, M., Zech, R., Buggle, B., and Zöller, L.: Novel methodological approaches in loess research – interrogating biomarkers and compound-specific stable isotopes, E&G Quaternary Sci. J., 60, 13, https://doi.org/10.3285/eg.60.1.12, 2011c.

Zech, M., Krause, T., Meszner, S., and Faust, D.: Incorrect when uncorrected: reconstructing vegetation history using *n*-alkane biomarkers in loess-paleosol sequences – a case study from the Saxonian loess region, Germany, Quaternary Int., 296, 108–116, 2013.

Zech, M., Kreutzer, S., Zech, R., Goslar, T., Meszner, S., McIntyre, C., Häggi, C., Eglinton, T., Faust, D., and Fuchs, M.: Comparative ^{14}C and OSL dating of loess-paleosol sequences to evaluate post-depositional contamination of n-alkane biomarkers, Quaternary Res., 87, 180–189, 2017.

Ziegler, F., Kögel, I. and Zech, W.: Alteration of gymnosperm and angiosperm lignin during decomposition in forest humus layers, Z. Planz. Bodenkunde, 149, 323–331, 1986.

Manuscript 3: Terrestrial versus aquatic source identification of sedimentary *n*-alkane and sugar biomarkers – a case study from the Bale Mountains, Ethiopia

ORIGINAL PAPER

Terrestrial versus aquatic source identification of sedimentary *n*-alkane and sugar biomarkers: a case study from the Bale Mountains, Ethiopia

Betelhem Mekonnen · Lucas Bittner · Tobias Bromm · Bruk Lemma · Bruno Glaser · Wolfgang Zech · Sileshi Nemomissa · Tamrat Bekele · Michael Zech

Abstract Organic matter in sedimentary archives is abundantly used to reconstruct paleoenvironmental and climate histories. Thereby, distinguishing between the terrestrial and aquatic origin of sedimentary organic matter is often a prerequisite for robust interpretations. In this case study, we use published data for modern plants and topsoils to identify the terrestrial versus aquatic source of *n*-alkane and sugar biomarkers in two afro-alpine sediment archives (Lake Garba Guracha and Depression B4) in the Bale Mountains, Ethiopia. The results of our comparative approach show that the long-chain *n*-alkanes C_{29}, C_{31}, and C_{33} in the sedimentary archives yielded patterns similar to those typical for the potential terrestrial input. By contrast, the relative abundances of the sedimentary mid-chain *n*-alkanes C_{23} and C_{25}, and at least partly C_{27}, are significantly increased compared to the plants and topsoils. This suggests that they are primarily produced by aquatic macrophytes and microorganisms. The P_{aq} ratio $(C_{23}+C_{25})/(C_{23}+C_{25}+C_{29}+C_{31})$ is validated as a suitable source identification proxy in our study area. The sugar biomarkers xylose (xyl) and arabinose (ara) are abundant in the plant and topsoil samples. By comparison, high relative abundances of fucose (fuc) and rhamnose (rham) are generally only observed in sediments. This indicates

B. Mekonnen (✉) · T. Bromm · B. Lemma · B. Glaser
Institute of Agricultural and Nutritional Sciences, Soil Biogeochemistry, Martin Luther University Halle-Wittenberg, Wittenberg, Germany
e-mail: betymekonnen19@gmail.com

T. Bromm
e-mail: tobias.bromm@landw.uni-halle.de

B. Lemma
e-mail: bruk_lemma@yahoo.com

B. Glaser
e-mail: bruno.glaser@landw.uni-halle.de

L. Bittner · M. Zech
Chair of Physical Geography with focus on paleoenvironmental research, Technische Universität Dresden, Dresden, Germany
e-mail: lucas.bittner@tu-dresden.de

M. Zech
e-mail: michael.zech@tu-dresden.de

B. Lemma
Forest and Rangeland Biodiversity Directorate, Ethiopian Biodiversity Institute, Addis Ababa, Ethiopia

W. Zech
Department of Soil Science, University of Bayreuth, Bayreuth, Germany
e-mail: w.zech@uni-bayreuth.de

S. Nemomissa · T. Bekele
Department of Plant Biology and Biodiversity Management, Addis Ababa University, Addis Ababa, Ethiopia
e-mail: sileshi.nemomissa@aau.edu.et

T. Bekele
e-mail: tambek07@gmail.com

Springer

that these sugar biomarkers are primarily produced by aquatic macrophytes or micro-organisms. Therefore, the ratio (fuc + rham)/(ara + xyl) is a suitable sugar biomarker proxy for organic matter source identification. The relative abundances of galactose and mannose are systematically decreasing and increasing, respectively, from leaves over O-layers to Ah-horizons. Furthermore, they are not significantly different from the abundances found in the sediments. This hinders terrestrial versus aquatic source identification using galactose and mannose.

Keywords Organic matter source

Introduction

Sedimentary organic matter in lake sediments is frequently used for paleoenvironmental and climate studies (Meyers and Ishiwatari 1993; Smol et al. 2002). Organic matter originates from the complex mixture of lipids, carbohydrates, proteins, and other components produced by organisms that have lived in (autochthonous) and around the lake (allochthonous) (Smol et al. 2002). As a result, organic matter source identification is an essential prerequisite for robust paleoenvironmental reconstructions (Doyle et al. 2022). During the last decades, different molecular markers and proxies were therefore suggested and developed for characterizing the organic matter and its degree of alteration in sedimentary records (Meyers and Ishiwatari 1993; Meyers 1994; Andersson et al. 2012). For instance, the total organic carbon to nitrogen ratio (TOC/TN) is used to distinguish between terrestrial and aquatic carbon sources. Organic matter derived from algae shows low TOC/TN values (between 4 and 10), whereas vascular land plants are usually characterized by high TOC/TN values (≥ 20) (Meyers 1994). Similarly, the stable carbon isotopic composition δ^{13}C is frequently used to distinguish between C3 and C4 plant-derived organic matter (Meyers and Ishiwatari 1993; Meyers and Lallier-Vergès 1999). However, TOC/TN and δ^{13}C values are affected by mineralization and degradation, resulting in more positive δ^{13}C values and a lower TOC/TN ratio (Meyers 1994). Moreover, the Hydrogen and Oxygen Indexes, which represent the amount of hydrogen and oxygen in organic matter, may be used as proxies for organic matter source identification

(Talbot and Livingstone 1989; Lüniger and Schwark 2002). Note that both indexes are affected by degradation, too.

In addition to the bulk parameters introduced above, molecular biomarkers such as *n*-alkanes (Ficken et al. 2000; Doyle et al. 2022) and hemicellulose-derived neutral sugars (Hepp et al. 2016) have been suggested for organic matter source identification. This is based on different biomarker patterns in vascular plants versus aquatic organisms. For instance, long-chain *n*-alkanes are abundant components of most vascular plant epicuticular waxes (Eglinton and Hamilton 1967; Bush and McInerney 2013), while mid- and short-chain *n*-alkanes predominate in many aquatic macrophytes and algae, respectively (Ficken et al. 2000, 2002). Similarly, the applicability of sugar biomarkers in paleoenvironmental studies is based on the notion that polysaccharides synthesized by vascular plants contain high amounts of pentose sugars (arabinose and xylose), whereas those synthesized by micro-organisms are dominated by hexose sugars (galactose, mannose, rhamnose, and fucose) (Oades 1984; Cheshire 1979).

The Bale Mountains in the southeast highland of Ethiopia comprise Africa's largest afro-alpine area, the Sanetti Plateau, above 4000 m asl (Hillman 1988; Miehe and Miehe 1994). Numerous small lakes and depressions make this area favourable for paleoenvironmental reconstructions. Even though they are few in number, paleoenvironmental and anthropological studies of the Bale Mountains (Wesche et al. 2000; Umer et al. 2007; Tiercelin et al. 2008; Kuzmicheva et al. 2014; Gil-Romera et al. 2019; Ossendorf et al. 2019; Groos et al. 2021) reveal major climatic events, vegetation changes, and anthropogenic influence. Therefore, in-depth studies of sedimentary archives can provide substantial knowledge on the past and future effects of climate change and anthropogenic activities at local and regional scales.

This study aims to identify the sources of *n*-alkane and sugar biomarkers in two sedimentary archives located at high altitudes in the Bale Mountains, namely the glacial cirque lake Garba Guracha and a depression called B4 located on the Sanetti Plateau. Bittner et al. (2020) presented the Paq ratio and sugar proxy (fuc + xyl)/ara for Garba Guracha sediments previously and Mekonnen et al. (2022) provided the Paq ratio for B4 depression sediments. However, a systematic comparison of the whole datasets with

regional reference plants and soils has not been carried out hitherto. Therefore, for this systematic comparison, we use published data from Lemma et al. (2019) and Mekonnen et al. (2019), who previously chemotaxonomically characterized modern plants and soils along the southwest and northeast transects of the Bale Mountains using *n*-alkane and sugar biomarkers, respectively.

Study site

The Bale Mountains belong to the Bale-Arsi Massif, located east of the Main Ethiopian Rift in the Oromia Regional State, southeast of Ethiopia, between 6.4833333°–7.1666667° N and 39.5°–39.9666667° E (Fig. 1). The Bale Mountains National Park covers an area of ~2200 km², including the most extensive continuous high-altitude afro-alpine plateau, the Sanetti Plateau, and the peak, Tullu Dimtu, at 4377 m asl (Kidane et al. 2012). The mountains rise from the eastern highlands beside the Ethiopian Rift Valley from 2500 m asl to the Sanetti Plateau at 3800–4000 m asl (Hillman 1988). The geology of the Bale Mountains is characterized by volcanic material

consisting of alkali basalt, trachyte, and tuffs with rhyolites formed during the Miocene and Oligocene (Billi 2015). Studies indicate that high altitudes of the mountains (> 3000 m asl) were glaciated during the Last Glacial Maximum (Osmaston et al. 2005). The soils of the Bale Mountains are generally shallow and rich in stones. They are made of silty loam that ranges from reddish brown to black. Andosols, Leptosols, and Cambisols are common types of soils in the Bale Mountains. Moreover, muddy Gleysols are found in wetlands and sedimentary basins (Yimer 2007).

Due to the differences in elevation and aspect, the climate of the Bale Mountains varies from north to south (Kidane et al. 2012). The mean annual temperature is 11.8 °C at Dinsho (the Bale Mountains National Park headquarters at 3170 m asl), while the mean minimum temperature is around 0.6 °C in mountainous areas (Hillman 1988; Miehe and Miehe 1994). The precipitation of the Bale Mountains is governed by the movement of the Intertropical Convergence Zone and Congo Air Boundary, resulting in longer rainy (March–October) and shorter dry (November–February) seasons. The rainy season is bimodal, with a maximum from July to October and a second peak from
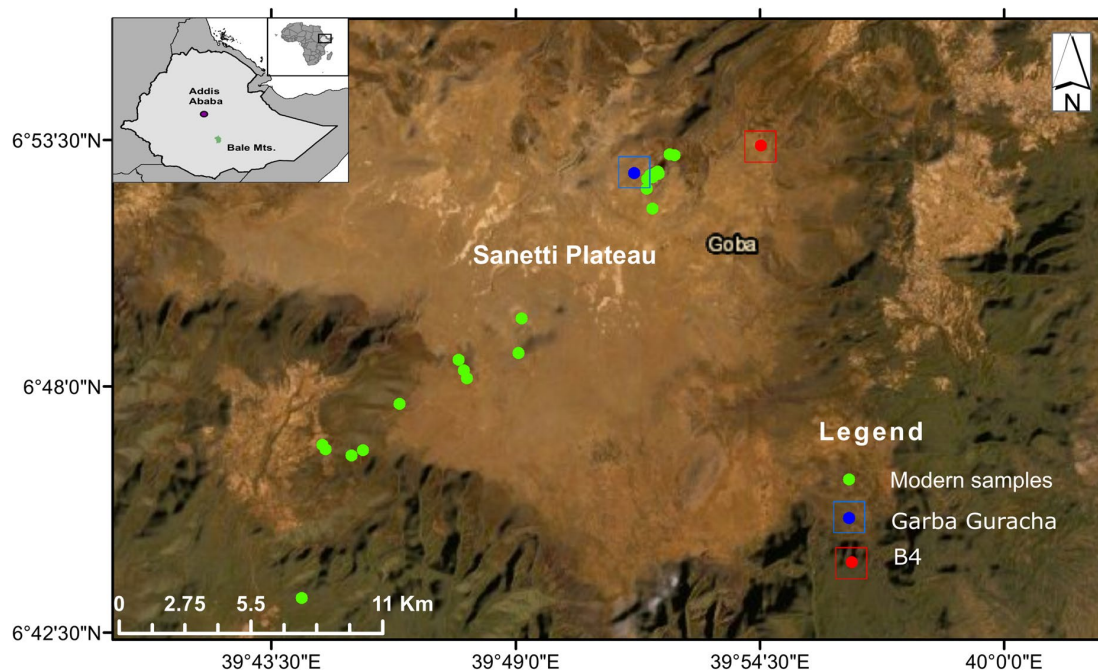

Fig. 1 Map showing the geographical location of the study area and sampling sites

March to June. While the northeasterly winds from the Arabian Peninsula dominate during the dry season, the southwesterly monsoon transports moisture from the Indian Ocean and the Atlantic Ocean via the Congo Basin during the rainy seasons (Tierney et al. 2013; Lemma et al. 2020). The southwestern part of the Bale Mountains experiences the highest precipitation and humidity, with 1000–1500 mm/yr, and the northern part receives annual rainfall ranging between 800 and 1000 mm/yr (Woldu et al. 1989). The Sanetti Plateau is characterized by strong diurnal temperature fluctuations and night frost (Hillman 1988).

Following the climate variability along altitude, the vegetation of the Bale Mountains is divided into three main zones: the afromontane, the Ericaceous, and the afro-alpine belt (Hedberg 1951; Friis 1986). The afromontane forest, which is further divided into dry and moist afromontane forests, covers an altitude of 1450–3750 m asl. The dry afromontane forest in the north is dominated by *Juniperus procera, Hagenia abyssinica*, and *Hypericum revolutum* (Yineger et al. 2008), while the southern afromontane forest is dominated by *Warburgia ugandensis, Croton macrostachyus, Podocarpus falcatus*. The Ericaceous belt spans between 3200 and 3800 m asl and is characterized by *Erica arborea* and *Erica trimera* in the form of shrubland in most parts and moist forest on the southern slopes (Harenna forest). Finally, the afro-alpine vegetation is characterized by *Helichrysum splendidum-Alchemilla haumannii* dwarf-scrubs, *Kniphofia foliosa* Giant *Lobelia* (*L. rhynchopetalum*) and grasses (Hedberg 1964), accompanied by patches of *Erica* growing beside big boulders above 3800 m asl. The wetlands of the Bale Mountains at higher altitudes are mainly characterized by wetland plant species such as *Carex monostachya, Haplocarpha rueppellii, Ranunculus* sp. and *Eriocaulon schimperi* (Dullo et al. 2015; Chignell et al. 2019). Water plants such as *Potamogeton thunbergii* and *Ranunculus trichophyllus* and *Pediastrum* algae are common on the shallow lakes nearby the B4 depression (Mekonnen et al. 2022).

Materials and methods

Sample collection

Modern reference samples (leaves as well as surface soil samples from O-layers and Ah-horizons) were collected from the northeastern and southwestern transects (3870 to 4134 m asl and 2550 to 4377 m asl,

respectively) of the Bale Mountains, including the surrounding area of Garba Guracha (Fig. 1). Twenty-five leaf samples from *Erica* spp. and afro-alpine plants such as *Alchemilla haumannii*, *Helichrysum splendidum*, *Lobelia rhynchopetalum*, *Kniphofia foliosa*, and *Festuca abyssinica*, and 38 surface soil samples (15 humified organic O-layers and 23 Ah-horizon soil samples) were collected (cf. Lemma et al. 2019 and Mekonnen et al. 2019).

Late Glacial and Holocene sediment samples were collected from the glacial lake Garba Guracha and a periodically dry depression referred to as "B4" (cf. Bittner et al. 2020 and Mekonnen et al. 2022, respectively). In brief, Garba Guracha is a NEE-oriented glacial cirque located at 3950 m asl (6.875781° N, 39.878075° E) between the Ericaceous and afro-alpine belts. It is about 500 m long and 300 m wide, has a maximum water depth of 6 m, and has a watershed of 0.15 km^2. Previous studies by Umer et al. (2007) and Tiercelin et al. (2008) provided a detailed description of the lake's geochemistry. In 2017, Bittner et al. (2020) retrieved a 15 m long core using a Livingstone piston corer operated from a raft anchored at 4.8 m of water depth. Sediments were sub-sampled in the laboratory from the core depth between 75 and 948 cm at 10 cm intervals for *n*-alkanes (n = 88) and sugar biomarker (n = 69) analyses. Further details on the core retrieval, stratigraphy, and chronology of this 16.7 kyr BP paleolimnological archive are presented in Bittner et al. (2020).

The B4 depression is located above the upper limit of the Ericaceous belt at 3970 m asl (6.88905° N; 39.90869° E). A pit profile with humic-rich lacustrine sediments was dug down to a depth of 2.55 m, and samples were taken every 2-cm, from 69 to 255 cm, and every 5 cm above 69 cm. In brief, the B4 profile is composed of three stratigraphic units covering the Late Glacial and Holocene according to Mekonnen et al. (2022). Unit 1 (255–175 cm) is dark-grey, laminated silty-clay above a thin grayish sandy silt layer and basalt boulders. Unit 2, from 175 to 70 cm depth, is gray partly laminated silty clay, deposited between 16.6 and 13.6 cal kyr BP. Unit 3 is about 70 cm thick and consists of light brown, weakly clayey sandy silt with red mottles and bleached aggregate surfaces, indicating waterlogging during the rainy season. Given that Unit 3 is strongly affected by degradation; only the 34 *n*-alkane data from Unit 1 and 2 were

further evaluated within this study here. The basal sediments of this profile are dated to 18 cal kyr BP.

Laboratory analyses

n-Alkane and sugar biomarker analyses

The analyses for all here reviewed *n*-alkane datasets (Lemma et al. 2019; Bittner et al. 2020; Mekonnen et al. 2022) were carried out using the Soxhlet lipid extraction method by adding dichloromethane (DCM) and methanol (MeOH) as solvents (9:1 ratio) for 24 h, following the method described by Zech and Glaser (2008). After obtaining the total lipid extracts (TLEs), 5α-androstane was added as an internal standard to the TLEs. The samples were concentrated using rotary evaporation and transferred to amino-propyl columns. The *n*-alkanes were eluted from the TLEs using 3 mL of hexane as solvent. Subsequently, the *n*-alkanes were quantified using a GC-2010 series gas chromatograph coupled with a flame ionization detector (GC-FID; Shimadzu, Kyoto, Japan). The GC instrument was equipped with an SPB-5 column (28.8 m length, 0.25 mm inner diameter, and 0.25 µm film thickness). An *n*-alkane mixture (C_8–C_{40}) was used as an external standard for linear calibration, and helium was used as a carrier gas.

The analyses for the reviewed sugar dataset from modern reference samples and the newly generated sugar dataset from Garba Guracha (B4 sediments were not studied using sugars) were carried out following the method described by Mekonnen et al. (2019). Samples were hydrolyzed at 105 °C for four hours after adding 10 ml of 4 M trifluoroacetic acid (TFA) and 100 µg of the internal recovery standard (myo-inositol). The hydrolyzed samples were filtrated over glass fiber filters, and TFA was removed using a rotary evaporator. The samples were further purified over XAD-7 and DOWEX 50WX8 columns. Thereafter, the sugars were freeze-dried and derivatized. Unlike Bittner et al. (2020), who applied methylboronic acid (MBA) derivatization, we used N-methyl-2-pyrrolidone (NMP) and N, O-Bis(trimethylsilyl) trifluoroacetamide (BSTFA) for derivatization following the procedure described by Mekonnen et al. (2019). This has the advantage that in addition to arabinose, fucose, and xylose, also fructose, galactose, glucose, mannose, rhamnose, and ribose can be quantified using subsequent gas chromatograph-flame

ionization detection (GC-FID, Shimadzu, Kyoto, Japan). Still, glucose was not further considered during data evaluation because the partial contribution of cellulose structures could not be excluded. Similarly, fructose and ribose were not further evaluated because of their very low concentrations.

Results

n-Alkane contents and patterns of modern plants, top soils, and sediment samples

The average total *n*-alkane contents are 1764, 859, and 58 µg g^{-1} for leaves, O-layers, and Ah-horizons, respectively, according to the dataset published by Lemma et al. (2019) (Fig. 2). In the Garba Guracha and B4 sediments, the average total *n*-alkane contents are 64 and 177 µg g^{-1}, respectively, according to the datasets published by Bittner et al. (2020) and Mekonnen et al. (2022). All *n*-alkane patterns reveal a strong odd-over-even predominance (OEP). The long-chain *n*-alkanes C_{29}, C_{31}, and C_{33} are dominant in modern samples. While C_{31} is the predominant *n*-alkane also in the Garba Guracha sediments, C_{27} is predominant in the B4 sediments. In contrast to the modern samples, the mid-chain *n*-alkanes C_{23} and C_{25} are abundantly present in the sediment of B4 and Garba Guracha (Figs. 2 and 4).

The relative abundances of mid- and long-chain *n*-alkanes for all samples are presented in the form of ternary diagrams in Fig. 3. Accordingly, regarding the homologues C_{29}, $C_{31,}$ and C_{33} (Fig. 3a), the modern samples show a larger variability than the sediments of Garba Guracha and B4. Still, the mean relative abundances of these long-chain homologues are quite congruent. However, when the *n*-alkane homologue series $\leq C_{27}$ are included in the ternary diagrams, the congruency of the modern samples with the sedimentary samples disappears. For instance, with regard to the homologues C_{27}, $C_{29,}$ and C_{31}, most terrestrial samples are characterized by relative abundances of $C_{27} < 10\%$, whereas relative abundances of $C_{27} > 10\%$ are characteristic for the sediments of Garba Guracha and B4 (Fig. 3b). Similarly, including mid-chain homologues in the ternary diagrams reveals that the relative abundances of C_{25} and C_{23} are typically $< 10\%$ in most terrestrial samples. By contrast, the relative abundances of C_{25} and C_{23} are typically $> 10\%$ in the

Fig. 2 Average *n*-alkane contents and patterns of leaves, O-layers, and Ah-horizons (Lemma et al. 2019), as well as of the Garba Guracha and B4 sediments
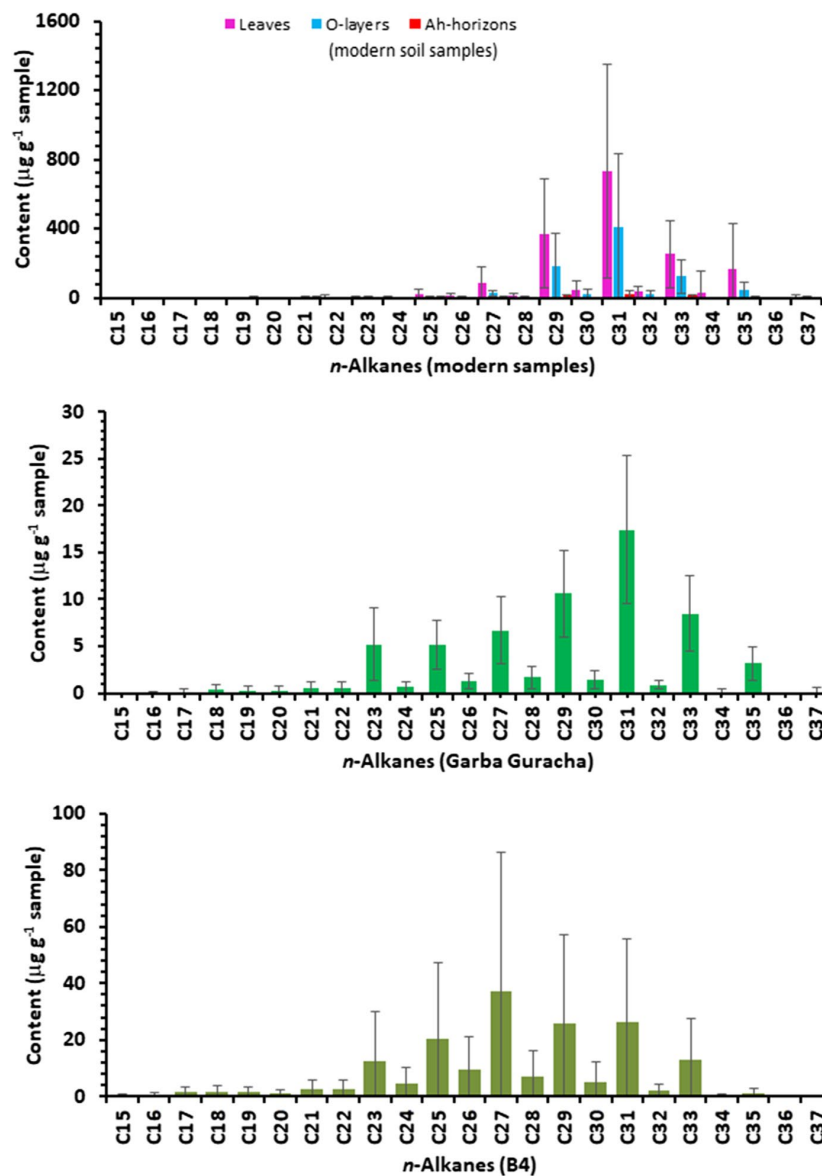
sediments of Garba Guracha and B4 (Fig. 3c). Figure 4 depicts that modern samples (leaves, O-layers, and Ah-horizons) yielded P_{aq} values typically < 0.1, whereas the Garba Guracha and B4 sediments yielded P_{aq} values typically > 0.2.

Sugar contents and patterns of modern plants, top soils, and sediment samples.

The average sugar contents in the modern samples range between 0.8 (fucose in topsoils) and 40.7 mg

g^{-1} (xylose in leaves), according to the dataset published by Mekonnen et al. (2019), whereas for the Garba Guracha sediment samples, they range between 2.3 (rhamnose) and 4.4 mg g^{-1} (galactose) (Fig. 5). No sugar analyses were carried out for the B4 sediments. The modern samples are characterized by a pronounced predominance of xylose, arabinose, and galactose, and all sugar biomarkers significantly decrease from the leaves to the Ah-horizons.
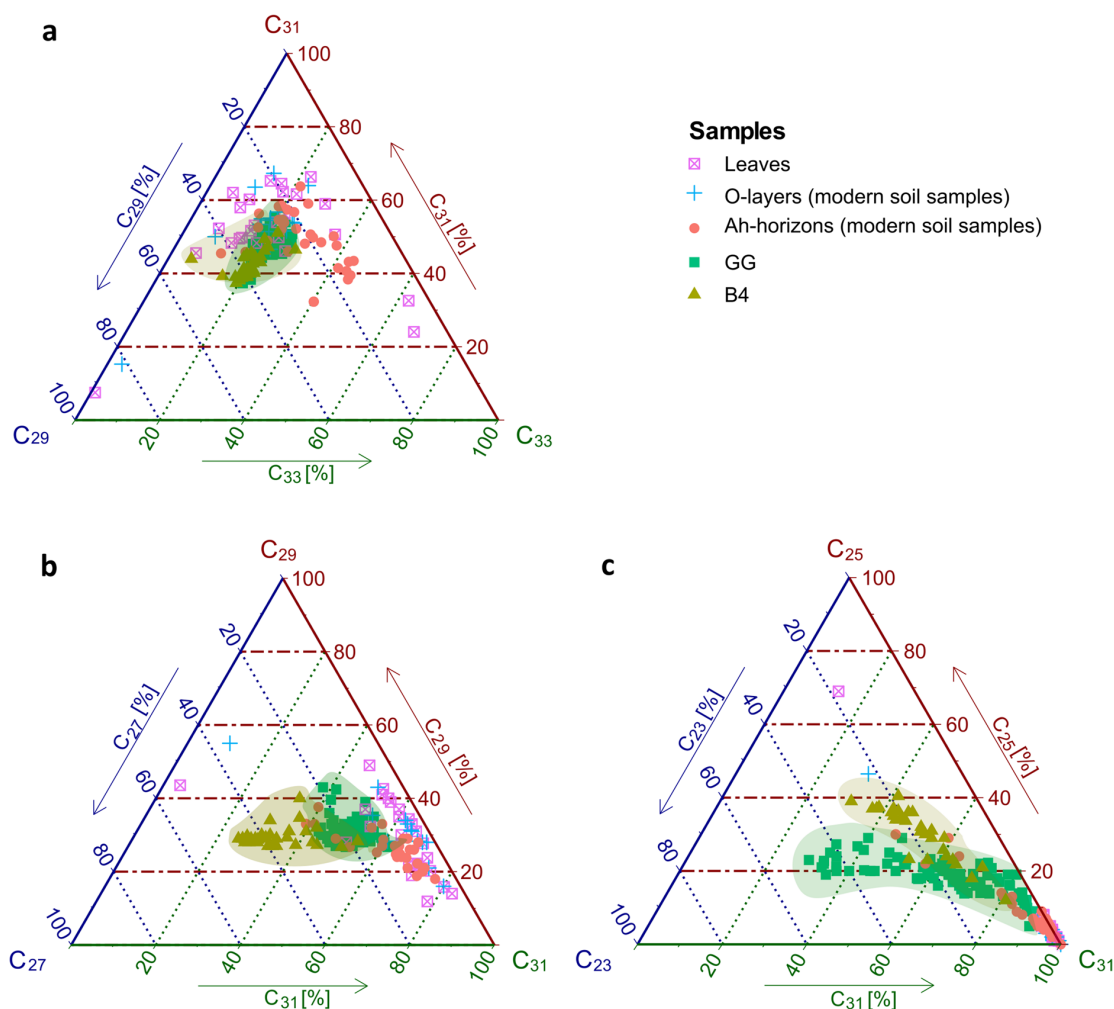
Fig. 3 Ternary diagrams for the relative abundances (%) of long- and mid-chain *n*-alkanes in modern leaf and soil samples (Lemma et al. 2019) versus in Garba Guracha and B4 sediment samples

By contrast, the predominance of xylose, arabinose, and galactose is by far less pronounced for the Garba Guracha sediments (Fig. 5).

Figure 6 depicts the relative abundances of the individual sugar biomarkers. Accordingly, xylose and galactose are the most abundant hemicellulose-derived sugar in leaves, followed by arabinose. The relative abundances of xylose, arabinose, and galactose significantly decrease from leaves over O-layers to the Ah-horizons (Fig. 6). By contrast, the relative abundance of mannose substantially increases. The relative abundances of rhamnose and fucose are very

low in leaves and do not show significant increases from leaves to the Ah-horizons (Fig. 6).

Galactose is the predominant sugar biomarker in the Garba Guracha sediments, followed by xylose, fucose, arabinose, mannose, and rhamnose. The relative abundances of fucose and rhamnose are significantly higher in the Garba Guracha sediments than in the modern samples (Fig. 6). Therefore, we calculated the ratio (fuc + rham)/(ara + xyl) as a proxy for organic matter source identification. Our comparison reveals significantly higher values for the Garba Guracha sediments than for the modern samples

�publishing Springer

Fig. 4 Comparison of the P_{aq} ratios yielded for leaves (n = 25), O-layers (n = 15), Ah-horizons (n = 23) versus sediments from B4 (n = 34) (Mekonnen et al. 2022) and Garba Guracha (n = 88) (Bittner et al. 2020). The notched box plots indicate the median (solid lines between the boxes) and interquartile range (IQR) with upper (75%) and lower (25%) quartiles. The notches display the 95% confidence interval of the median. The lines extending outside the box (whiskers) show variability outside the quartiles. The circles represent outliers
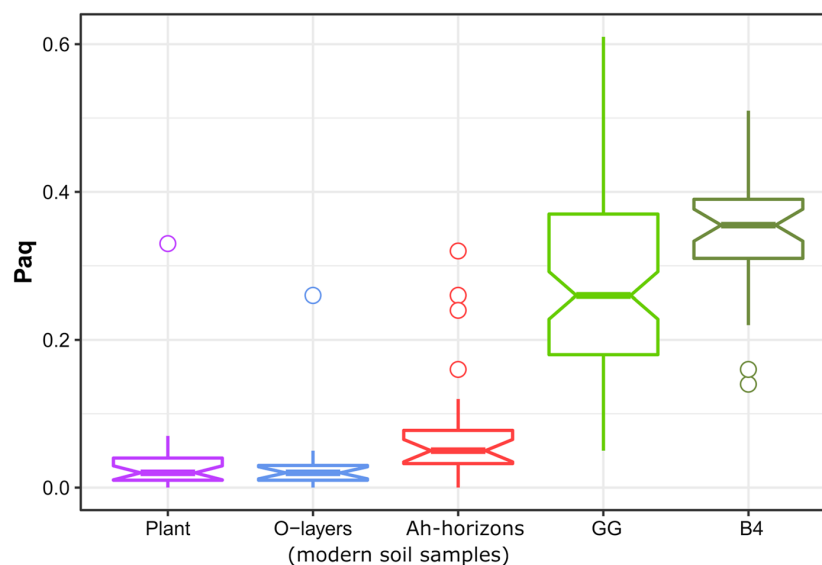
(Fig. 7). The sediments are typically characterized by (fuc + rham)/(ara + xyl) ratios > 0.75, whereas the modern leaf and soil samples are typically characterized by ratios < 0.75.

Discussion

Terrestrial versus aquatic source identification of the sedimentary *n*-alkanes

The dominance of long-chain *n*-alkanes in modern samples from the Sanetti Plateau is consistent with several studies reporting the dominance of long-chain *n*-alkanes in leaves and modern soils (Eglinton and Hamilton 1967; Bush and McInerney 2013). The low *n*-alkane contents in modern soils can be explained by dilution with minerogenic soil components as well as by degradation (Zech et al. 2011; Schäfer et al. 2016). The average total *n*-alkane content is higher in B4 than in Garba Guracha, likely due to high *n*-alkane preservation in the lower section of the profile.

As shown in Fig. 3a using a ternary diagram, the relative contributions of the sedimentary *n*-alkane homologues C_{29}, C_{31}, and C_{33} are well concordant with the modern leaves, O-layer, and Ah-topsoil samples. Albeit this is no prove, it indicates that these sedimentary long-chain *n*-alkanes are likely primarily of terrestrial (allochthonous) origin. By contrast,

the concordance in the ternary diagrams of Fig. 3 is lost when including the *n*-alkane homologues C_{23}, C_{25}, and C_{27}. This suggests that these sedimentary *n*-alkanes are not of pure terrestrial origin but at least partly originate from a different source. Indeed, Ficken et al. (2000) reported on aquatic macrophytes producing such homologues and proposed the P_{aq} ratio $(C_{23} + C_{25})/(C_{23} + C_{25} + C_{29} + C_{31})$ as a proxy to identify the sedimentary input of submerged or floating aquatic macrophytes. According to Ficken et al. (2000), P_{aq} values < 0.1 are characteristic for terrestrial plants, whereas values between 0.1 and 1 are characteristic for emergent and submerged macrophytes. This boundary is also well suited for distinguishing our modern reference (terrestrial) and sediment samples (Fig. 4) and, at the same time, strongly suggests that the sedimentary *n*-alkane homologues C_{23} and C_{25} in Garba Guracha and B4 are mainly aquatic-derived.

While Bittner et al. (2020) stated that an unambiguous terrestrial versus aquatic source identification of the *n*-alkane record of Garba Guracha seems challenging at the current state of research, the results and the interpretation of our comparative approach are well in agreement with other studies reporting on short- and mid-chain *n*-alkane production by submerged and floating plants, algae, and bacteria (e.g. Aichner et al. 2010; Cranwell et al. 1987; Liu and Liu 2016).

Fig. 5 Average contents of the sugar biomarkers xylose, arabinose, rhamnose, fucose, mannose, and galactose in leaves, O-layers, Ah-horizons (Mekonnen et al. 2019) and the Garba Guracha sediments
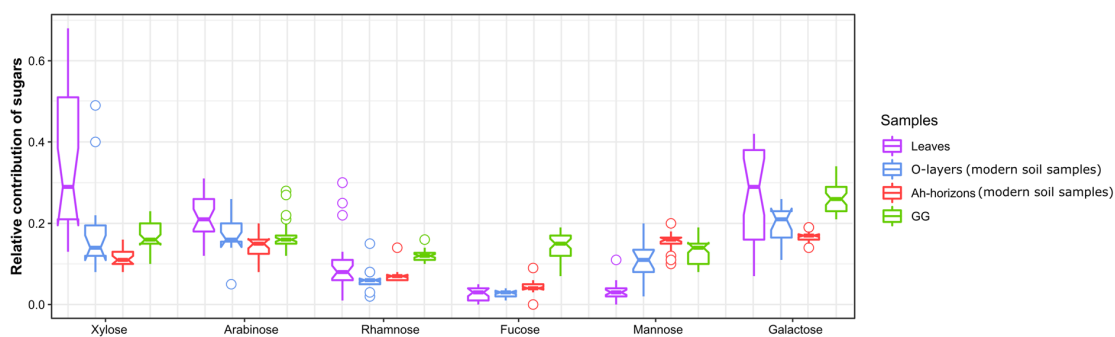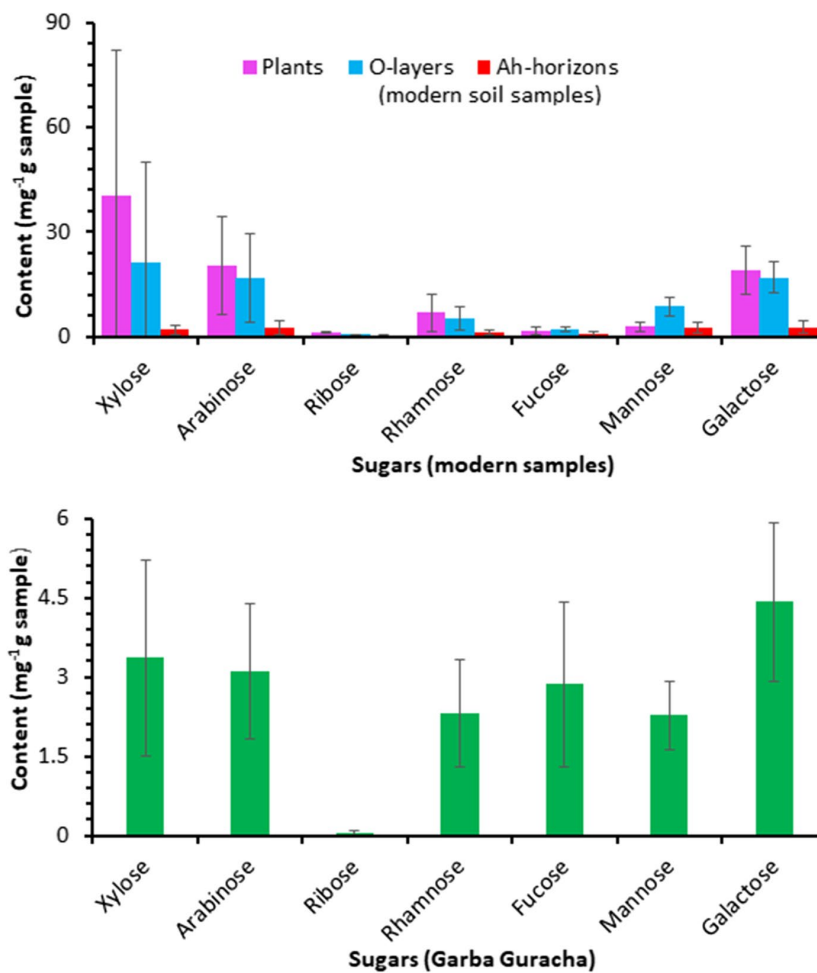
Fig. 6 Relative abundances of sugar biomarkers in leaves (n=25), O-layers (n=15), Ah-horizons (n=23) and the Garba Guracha sediments (n=69). The notched box plots indicate the median (solid lines between the boxes) and interquartile range (IQR) with upper (75%) and lower (25%) quartiles. The notches display the 95% confidence interval of the median. The lines extending outside the box (whiskers) show variability outside the quartiles. The circles represent outliers

Fig. 7 The ratio (fuc + rham)/(ara + xyl) in leaves (n = 25), O-layers (n = 15), Ah-horizons (n = 23), and the Garba Guracha sediments (n = 69). The notched box plots indicate the median (solid lines between the boxes) and interquartile range (IQR) with upper (75%) and lower (25%) quartiles. The notches display the 95% confidence interval of the median. The lines extending outside the box (whiskers) show variability outside the quartiles. The circles represent outliers
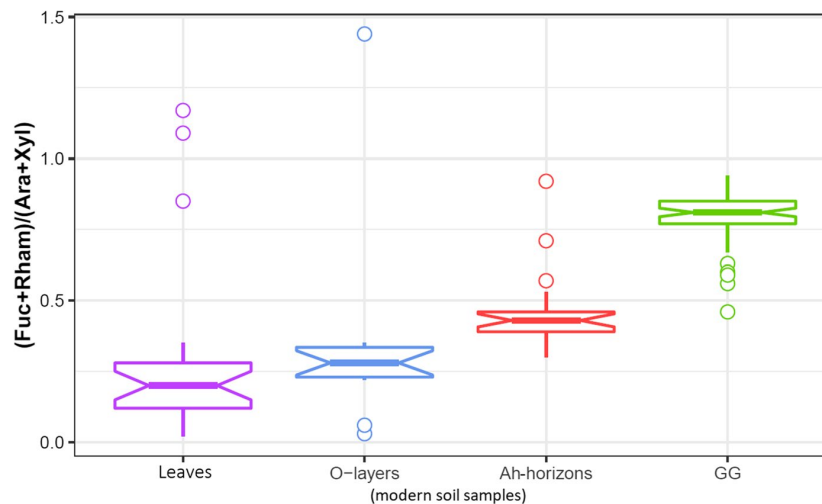
Still, it is noteworthy that the interpretation of the sedimentary long-chain homologues in terms of primarily terrestrial input is not completely unambiguous. According to Lichtfouse et al. (1994), Dennis and Kolattukudy (1991), Metzger and Largeau (2005) and He et al. (2018), *Botryococcus braunii*, a green algae commonly found in tropical freshwater lakes (Jankovská and Komárek 2000), is characterized by an abundant production of the long-chain *n*-alkadienes C_{27}, C_{29}, and C_{31}. A diagenetic reduction is suggested as an important source of sedimentary *n*-alkanes. Indeed, Umer et al. (2007) found abundant *Botryococcus* pollen in the Garba Guracha sediments. Similarly, pollen results from the B4 sediments show high amounts of *Botryococcus*, especially at the bottom of the profile (Mekonnen et al. 2022). Therefore, *Botryococcus* may not be excluded from having also contributed to the long-chain *n*-alkanes of the sedimentary archives of the Bale Mountains. According to published data, the ambiguity in the interpretation of sedimentary long-chain n-alkanes can be alleviated by compound specific δ13C values of the n-alkanes and through the application of isotopic mixing models (Aichner et al., 2010; Gao et al., 2011; Liu et al., 2015; Andrae et al., 2020; Yang and Bowen, 2022). Andrae et al. (2020) for instance have shown that in their case study from Australia aquatic macrophyte input significantly influenced the δ13C isotopic composition of the long-chain n-alkanes C27 and C29. This finding together with our own results shown in Figs. 2 and 3b suggests that the C27 n-alkane

homologue in the Garba Guracha and B4 sediments are the results of mixing terrestrial and aquatic sources. While bulk δ13C values for Garba Guracha (ranging between -22.7 and -13.9 ‰) and B4 (average ~ 14 ‰) clearly indicate that bulk sedimentary organic matter is strongly influenced by aquatic input, compound-specific δ13C analyses were only realized on two selected samples from B4 for the most abundant long-chain n-alkanes C27, C29 and C31 (Mekonnen et al., 2022). The obtained δ13Cn-alkane values range from -22.1 to -29.8‰ and hence reflect an isotopic mixing of aquatic and terrestrial sources for these long-chain n-alkanes.

Last but not least, apart from "terrestrial" versus "aquatic" input, a "microbial" input should not be completely overlooked. Several studies have highlighted that soil micro-organisms (as well as likely sedimentary micro-organisms) do not only degrade organic matter, including *n*-alkanes, but are also able to contribute to the built-up of a microbial short-, mid-, and even long-chain *n*-alkane pool in soils and sediments (Jones 1969; Nguyen Tu et al. 2011; Zech et al. 2011; Brittingham et al. 2017; Li et al. 2018).

Terrestrial versus aquatic source identification of the sedimentary sugar biomarkers

As presented above, the leaf samples from the Sanetti Plateau are characterized by high abundances of xylose and arabinose. This is in agreement with literature reporting on the high production of these

sugar biomarkers by vascular plants (Oades 1984; Jia et al. 2008; Hepp et al. 2016). Similarly, the high abundance of galactose in the terrestrial reference dataset of Mekonnen et al. (2019) is well explicable with dominant vegetation such as *Erica*, *Alchemilla*, and *Lobelia* (Schädel et al. 2010; Gunina and Kuzyakov 2015). The significant decrease of most sugars from leaves to soils can be attributed to dilution with minerogenic soil components as well as to degradation (Hedges et al. 1985; Jia et al. 2008). For instance, Jia et al. (2008) and Hernes et al. (1996) reported on the labile nature of arabinose and glucose, whereas fucose, rhamnose, xylose, and mannose were described as more refractory. In the terrestrial reference dataset of Mekonnen et al. (2019), mannose is the only sugar substantially increasing with regard to its relative contribution in soils. This likely reflects the soil microbial build-up of this sugar biomarker. Indeed, Oades (1984) and Murayama (1984) reported on the substantial synthesis of mannose by soil microbial populations. The dataset of Mekonnen et al. (2019) does not show a significant increase in the relative abundances of rhamnose and fucose from the leaf to the soil samples. This contrasts with studies showing such an increase during soil degradation (Murayama 1984; Oades 1984).

Given the high terrestrial production of xylose and arabinose (Fig. 5), we suggest that their predominance in the Garba Guracha sediments reflects an at least partly terrestrial input. The relatively high abundances of galactose and mannose in the Garba Guracha sediments might be attributed to contributions by both soil and aquatic micro-organisms. According to Oades (1984), the ratio $(G+M)/(A+X)$ can serve as a proxy to differentiate between plant-derived and microbial-derived sugars in soils. However, because galactose and mannose are produced by both soil and aquatic bacteria, their use for identifying terrestrial versus aquatic input is challenging. The results of our comparative approach show that the relative contributions of rhamnose and fucose are significantly higher in sediments compared to the terrestrial reference samples of Mekonnen et al. (2019) (Fig. 6). Rhamnose and fucose are reported to occur in submerged aquatic plants (Jia et al. 2008). Furthermore, organic matter decomposition in sediments can lead to the in situ microbial synthesis of fucose and rhamnose (Marchand et al. 2005). Last but not least, also Hepp et al. (2016) reported that fucose is abundantly

produced by algae and zooplankton, whereas xylose and arabinose strongly predominate in terrestrial plants and soils. This different behavior of the here discussed specific sugar biomarkers results in the ratio of $(fuc+rham)/(ara+xyl)$ clearly allowing to distinguish between modern terrestrial reference samples of Mekonnen et al. (2019) and Garba Guracha sediments (Fig. 7). This finding suggests that the ratio $(fuc+rham)/(ara+xyl)$ is a promising proxy for terrestrial versus aquatic source identification, also beyond our case study.

Conclusions

In this study, we aimed to identify the terrestrial versus aquatic sources of partly published *n*-alkane and sugar biomarker datasets from two afro-alpine sedimentary archives in the Bale Mountains of Ethiopia. We compared the Late Glacial and Holocene sedimentary biomarker patterns with those of published modern plants and soils serving as terrestrial reference samples. Our comparative approach shows that long-chain *n*-alkanes predominate in both the modern and sediment samples. Ternary diagrams reveal that there is a high concordance of the sedimentary C_{29}, C_{31}, and C_{33} patterns with those of the terrestrial samples, whereas C_{23}, C_{25}, and C_{27} occur at strikingly higher relative abundances in the sediments. This strongly indicates that the latter are produced by aquatic macrophytes and micro-organisms. The P_{aq} ratio $(C_{23}+C_{25})/(C_{23}+C_{25}+C_{29}+C_{31})$ reveals a significant difference between modern plant and soil samples and the sediments. Regarding the sugar biomarkers, unambiguous terrestrial versus aquatic source identification of arabinose and xylose in the sediments is challenging. By contrast, the much higher relative abundances of rhamnose and fucose in the sediments compared to modern plants and soils corroborate that they are mainly produced by aquatic macrophytes and micro-organisms. Therefore, we propose that the ratio $(fuc+rham)/(ara+xyl)$ is a valuable sugar biomarker proxy for distinguishing aquatic versus terrestrial origin. The last conclusion that can be drawn from our comparative approach is that no unambiguous source identification is possible for sedimentary galactose and mannose.

Declarations

Conflict of interest The authors declare no competing interests.

References

Aichner B, Herzschuh U, Wilkes H (2010) Influence of aquatic macrophytes on the stable carbon isotopic signatures of sedimentary organic matter in lakes on the Tibetan Plateau. Org Geochem 41:706–718. https://doi.org/10.1016/j.orggeochem.2010.02.002

Andersson RA, Meyers P, Hornibrook E et al (2012) Elemental and isotopic carbon and nitrogen records of organic matter accumulation in a holocene permafrost peat sequence in the east european russian arctic. J Quat Sci 27:545–552. https://doi.org/10.1002/jqs.2541

Andrae JW, McInerney FA, Sniderman JMK (2020) Carbon isotope systematics of leaf wax n-alkanes in a temperate lacustrine depositional environment. Org Geochem 150:104121. https://doi.org/10.1016/j.orggeochem.2020.104121

Billi P (2015) Geomorphological Landscapes of Ethiopia. In: Billi P (ed) Landscapes and landforms of Ethiopia. Springer Netherlands, Dordrecht, pp 3–32

Bittner L, Bliedtner M, Grady D et al (2020) Revisiting afro-alpine Lake Garba Guracha in the Bale Mountains of Ethiopia: rationale, chronology, geochemistry, and paleoenvironmental implications. J Paleolimnol. https://doi.org/10.1007/s10933-020-00138-w

Brittingham A, Hren MT, Hartman G (2017) Microbial alteration of the hydrogen and carbon isotopic composition of n-alkanes in sediments. Org Geochem 107:1–8. https://doi.org/10.1016/j.orggeochem.2017.01.010

Bush RT, McInerney FA (2013) Leaf wax n-alkane distributions in and across modern plants: implications for paleoecology and chemotaxonomy. Geochim Cosmochim Acta 117:161–179. https://doi.org/10.1016/j.gca.2013.04.016

Cheshire MV (1979) Nature and origin of carbohydrates in soil. Academic Press, London, p 216

Chignell SM, Laituri MJ, Young NE, Evangelista PH (2019) Afroalpine wetlands of the Bale Mountains, Ethiopia: distribution, dynamics, and conceptual flow model. Annals American Assoc Geog 109:791–811

Cranwell PA, Eglinton G, Robinson N (1987) Lipids of aquatic organisms as potential contributors to lacustrine sediments-II. Org Geochem 11:513–527. https://doi.org/10.1016/0146-6380(87)90007-6

Dennis MW, Kolattukudy PE (1991) Alkane biosynthesis by decarbonylation of aldehyde catalyzed by a microsomal preparation from Botryococcus braunii. Arch Biochem Biophys 287:268–275. https://doi.org/10.1016/0003-9861(91)90478-2

Doyle RM, Longstaffe FJ, Moser KA (2022) An isotope, elemental, and n-alkane baseline for organic matter sources in sediments of high-altitude lakes in the Uinta Mountains, Utah, USA. J Paleolimnol 69:123–139. https://doi.org/10.1007/s10933-022-00265-6

Dullo BW, Grootjans AP, Roelofs JGM et al (2015) Fen mires with cushion plants in Bale Mountains, Ethiopia. Mires Peat 15:1–10

Eglinton G, Hamilton RJ (1967) Leaf epicuticular waxes. Sci (80-) 156:1322–1335. https://doi.org/10.1126/science.156.3780.1322

Ficken KJ, Li B, Swain DL, Eglinton G (2000) An n-alkane proxy for the sedimentary input of submerged/floating freshwater aquatic macrophytes. Org Geochem 31:745–749. https://doi.org/10.1038/nmat4240

Ficken KJ, Wooller MJ, Swain DL et al (2002) Reconstruction of a subalpine grass-dominated ecosystem, Lake Rutundu, Mount Kenya: a novel multi-proxy approach. Palaeogeogr Palaeoclimatol Palaeoecol 177:137–149. https://doi.org/10.1016/S0031-0182(01)00356-X

Friis I (1986) Zonation of forest vegetation on the South Slope of Bale Mountains, South Ethiopia. SINET Ethiop J Sci 9:29–44

Gao L, Hou J, Toney J, MacDonald D, Huang Y (2011) Mathematical modeling of the aquatic macrophyte inputs of mid-chain n-alkyl lipids to lake sediments: Implications for interpreting compound specific hydrogen isotopic records. Geochimica et Cosmochimica Acta 75(13):3781–3791

Gil-Romera G, Adolf C, Benito BM et al (2019) Long-term fire resilience of the Ericaceous Belt, Bale Mountains, Ethiopia. Biol Lett 15:20190357. https://doi.org/10.1098/rsbl.2019.0357

Groos AR, Akçar N, Yesilyurt S, Miehe G (2021) Nonuniform late pleistocene glacier fluctuations in tropical Eastern Africa. Sci Adv. https://doi.org/10.1126/sciadv.abb6826

Gunina A, Kuzyakov Y (2015) Soil biology & biochemistry sugars in soil and sweets for microorganisms: review of origin, content, composition and fate. Soil Biol Biochem 90:87–100

He D, Simoneit BRT, Jaffé R (2018) Environmental factors controlling the distributions of Botryococcus braunii (A, B and L) biomarkers in a subtropical freshwater wetland. Sci Rep 8:1–9. https://doi.org/10.1038/s41598-018-26900-9

Hedberg O (1951) Vegetation belts of the east african mountains, 45th edn. Sven. Bot. Tidskr, Stockholm

Hedberg O (1964) Features of afroalpine plant ecology. Swedish Science Press, Uppsala, Sweden

Hedges JI, Cowie GL, Ertel JR et al (1985) Degradation of carbohydrates and lignins in buried woods. Geochim Cosmochim Acta 49:701–711. https://doi.org/10.1016/0016-7037(85)90165-6

Hepp J, Rabus M, Anhäuser T et al (2016) A sugar biomarker proxy for assessing terrestrial versus aquatic sedimentary input. Org Geochem 98:98–104. https://doi.org/10.1016/j.orggeochem.2016.05.012

Hernes PJ, Hedges JI, Peterson ML et al (1996) Neutral carbohydrate geochemistry of particulate material in the central equatorial Pacific. Deep Res Part II Top Stud Oceanogr 43:1181–1204. https://doi.org/10.1016/0967-0645(96)00012-4

Hillman JC (1988) The Bale Mountains National Park Area, Southeast Ethiopia, and its management. Mt Res Dev 8:253–258

Jankovská V, Komárek J (2000) Indicative value of Pediastrum and other coccal green algae in palaeoecology. Folia Geobot 35:59–82. https://doi.org/10.1007/BF02803087

Jia G, Dungait JAJ, Bingham EM et al (2008) Neutral monosaccharides as biomarker proxies for bog-forming plants for application to palaeovegetation reconstruction in ombrotrophic peat deposits. Org Geochem 39:1790–1799. https://doi.org/10.1016/j.orggeochem.2008.07.002

Jones JG (1969) Studies on lipids of soil micro-organisms with particular reference to hydrocarbons. J Gen Microbiol 59:145–152. https://doi.org/10.1099/00221287-59-2-145

Kidane Y, Stahlmann R, Beierkuhnlein C (2012) Vegetation dynamics, and land use and land cover change in the Bale Mountains, Ethiopia. Environ Monit Assess 184:7473–7489. https://doi.org/10.1007/s10661-011-2514-8

Kuzmicheva EA, Khasanov BF, Krylovich OA, Savinetsky AB (2014) Vegetation and climate reconstruction for the bale mountains (Ethiopia) in the Holocene according to the pollen analysis and radiocarbon dating of zoogenic deposits. Dokl Biol Sci 458:281–285. https://doi.org/10.1134/S0012496614050019

Lemma B, Mekonnen B, Glaser B et al (2019) Chemotaxonomic patterns of vegetation and soils along altitudinal transects of the Bale Mountains, Ethiopia, and implications for paleovegetation reconstructions–part II: lignin-derived phenols and leaf-wax-derived n-alkanes. E&G Quat Sci J 68:189–200. https://doi.org/10.5194/egqsj-68-189-2019

Lemma B, Kebede Gurmessa S, Nemomissa S et al (2020) Spatial and temporal 2H and 18O isotope variation of contemporary precipitation in the Bale Mountains, Ethiopia. Isot Environ Health Stud 56:122–135. https://doi.org/10.1080/10256016.2020.1717487

Li G, Li L, Tarozo R et al (2018) Microbial production of long-chain n-alkanes: implication for interpreting sedimentary leaf wax signals. Org Geochem 115:24–31. https://doi.org/10.1016/j.orggeochem.2017.10.005

Lichtfouse É, Derenne S, Mariotti A, Largeau C (1994) Possible algal origin of long chain odd n-alkanes in immature sediments as revealed by distributions and carbon isotope ratios. Org Geochem 22:1023–1027. https://doi.org/10.1016/0146-6380(94)90035-3

Liu H, Liu W (2016) n-Alkane distributions and concentrations in algae, submerged plants and terrestrial plants from the Qinghai-Tibetan Plateau. Org Geochem 99:10–22. https://doi.org/10.1016/j.orggeochem.2016.06.003

Liu W, Yang H, Wang H, An, Z, Wang Z, Leng Q (2015) Carbon isotope composition of long chain leaf wax n-alkanes in lake sediments: A dual indicator of paleoenvironment in the Qinghai-Tibet Plateau. Org Geochem 83–84:190–201. https://doi.org/10.1016/j.orggeochem.2015.03.017

Lüniger G, Schwark L (2002) Characterisation of sedimentary organic matter by bulk and molecular geochemical proxies: an example from oligocene maar-type Lake Enspel, Germany. Sediment Geol 148:275–288. https://doi.org/10.1016/S0037-0738(01)00222-6

Marchand C, Disnar JR, Lallier-Vergés E, Lottier N (2005) Early diagenesis of carbohydrates and lignin in mangrove sediments subject to variable redox conditions (french Guiana). Geochim Cosmochim Acta 69:131–142. https://doi.org/10.1016/j.gca.2004.06.016

Mekonnen B, Zech W, Glaser B et al (2019) Chemotaxonomic patterns of vegetation and soils along altitudinal transects of the Bale Mountains, Ethiopia, and implications for paleovegetation reconstructions–part I: stable isotopes and sugar biomarkers. E&G Quat Sci J 68:177–188. https://doi.org/10.5194/egqsj-68-177-2019

Mekonnen B, Glaser B, Zech R et al (2022) Climate, vegetation and fire history during the past 18,000 years, recorded in high altitude lacustrine sediments on the Sanetti Plateau, Bale Mountains (Ethiopia). Prog Earth Planet Sci. https://doi.org/10.1186/s40645-022-00472-9

Metzger P, Largeau C (2005) Botryococcus braunii: a rich source for hydrocarbons and related ether lipids. Appl Microbiol Biotechnol 66:486–496. https://doi.org/10.1007/s00253-004-1779-z

Meyers PA (1994) Preservation of elemental and isotopic source identification of sedimentary organic matter.

Chem Geol 114:289–302. https://doi.org/10.1016/0009-2541(94)90059-0

Meyers PA, Ishiwatari R (1993) Lacustrine organic geochemistry-an overview of indicators of organic matter sources and diagenesis in lake sediments. Org Geochem 20:867–900. https://doi.org/10.1016/0146-6380(93)90100-P

Meyers PA, Lallier-Vergès E (1999) Lacustrine sedimentary organic matter records of late quaternary paleoclimates. J Paleolimnol 21:345–372. https://doi.org/10.1023/A:1008073732192

Miehe G, Miehe S (1994) Ericaceous forests and heathlands in the Bale Mountains of South Ethiopia: ecology and man's impact. T. Warnke Verlag, Hamburg, Germany

Murayama S (1984) Changes in the monosaccharide composition during the decomposition of straws under field conditions. Soil Sci Plant Nutr 30:367–381. https://doi.org/10.1080/00380768.1984.10434702

Nguyen Tu TT, Egasse C, Zeller B et al (2011) Early degradation of plant alkanes in soils: a litterbag experiment using 13 C-labelled leaves. Soil Biol Biochem 43:2222–2228. https://doi.org/10.1016/j.soilbio.2011.07.009

Oades JM (1984) Soil organic matter and structural stability: mechanisms and implications for management. Plant Soil 76:319–337. https://doi.org/10.1007/BF02205590

Osmaston HA, Mitchell WA, Osmaston JAN (2005) Quaternary glaciation of the Bale Mountains, Ethiopia. J Quat Sci. https://doi.org/10.1002/jqs.931

Ossendorf G, Groos AR, Bromm T et al (2019) Middle Stone Age foragers resided in high elevations of the glaciated Bale Mountains, Ethiopia. Sci (80-) 365:583–587. https://doi.org/10.1126/science.aaw8942

Schädel C, Blöchl A, Richter A, Hoch G (2010) Quantification and monosaccharide composition of hemicelluloses from different plant functional types. Plant Physiol Biochem 48:1–8. https://doi.org/10.1016/j.plaphy.2009.09.008

Schäfer IK, Lanny V, Franke J et al (2016) Leaf waxes in litter and topsoils along a european transect. Soil 2:551–564. https://doi.org/10.5194/soil-2-551-2016

Smol JP, Birks HJB, Last WM (eds) (2002) Tracking Environmental Change using Lake sediments. Volume 3: Terrestrial, Algal, and Siliceous indicators. Kluwer Academic Publisher

Talbot MR, Livingstone DA (1989) Hydrogen index and carbon isotopes of lacustrine organic matter as lake level indicators. Palaeogeogr Palaeoclimatol Palaeoecol 70:121–137

Tiercelin JJ, Gibert E, Umer M et al (2008) High-resolution sedimentary record of the last deglaciation from a high-altitude lake in Ethiopia. Quat Sci Rev 27:449–467. https://doi.org/10.1016/j.quascirev.2007.11.002

Tierney JE, Smerdon JE, Anchukaitis KJ, Seager R (2013) Multidecadal variability in east african hydroclimate controlled by the Indian Ocean. Nature 493:389–392. https://doi.org/10.1038/nature11785

Umer M, Lamb HF, Bonnefille R et al (2007) Late pleistocene and holocene vegetation history of the Bale Mountains, Ethiopia. Quat Sci Rev 26:2229–2246. https://doi.org/10.1016/j.quascirev.2007.05.004

Wesche K, Miehe G, Kaeppeli M (2000) The significance of fire for Afroalpine Ericaceous Vegetation. Mt Res Dev 20:340–347. https://doi.org/10.1659/0276-4741(2000)020[0340:TSOFFA]2.0.CO;2

Woldu Z, Feoli E, Nigatu L (1989) Partitioning an elevation gradient of vegetation from southeastern Ethiopia by probabilistic methods. Vegetatio 81:189–198. https://doi.org/10.1007/BF00045524

Yang D, Bowen GJ (2022) Integrating plant wax abundance and isotopes for paleo-vegetation and paleoclimate reconstructions: a multi-source mixing model using a bayesian framework. Clim Past 18:2181–2210. https://doi.org/10.5194/cp-18-2181-2022

Yimer F (2007) Soil Properties in Relation to Topographic aspects. Vegetation Communities and Land Use in the South-eastern Highlands of Ethiopia

Yineger H, Kelbessa E, Bekele T, Lulekal E (2008) Floristic composition and structure of the Dry Afromontane Forest at Bale Mountains National Park, Ethiopia. J Sci 31:103–120. https://doi.org/10.4314/sinet.v31i2.66551

Zech M, Glaser B (2008) Improved compound-specific d13C analysis of n-alkanes for application in palaeoenvironmental studies. RAPID Commun MASS Spectrom 22:135–142. https://doi.org/10.1002/rcm.3342

Zech M, Pedentchouk N, Buggle B et al (2011) Effect of leaf litter degradation and seasonality on D/H isotope ratios of n-alkane biomarkers. Geochim Cosmochim Acta 75:4917–4928. https://doi.org/10.1016/j.gca.2011.06.006

Manuscript 4: Climate, vegetation and fire history during the past 18,000 years, recorded in high altitude lacustrine sediments on the Sanetti Plateau, Bale Mountains (Ethiopia)

RESEARCH ARTICLE   **Open Access**

Climate, vegetation and fire history during the past 18,000 years, recorded in high altitude lacustrine sediments on the Sanetti Plateau, Bale Mountains (Ethiopia)

Betelhem Mekonnen[1,2*] , Bruno Glaser[1], Roland Zech[3], Michael Zech[1,4], Frank Schlütz[5,6], Robert Bussert[7], Agerie Addis[8], Graciela Gil-Romera[9], Sileshi Nemomissa[10], Tamrat Bekele[10], Lucas Bittner[1,4], Dawit Solomon[11], Andreas Manhart[12] and Wolfgang Zech[12]

Abstract

Low-altitude lakes in eastern Africa have long been investigated and have provided valuable information about the Late Quaternary paleohydrological evolution, such as the African Humid Period. However, records often suffer from poor age control, resolution, and/or ambiguous proxy interpretation, and only little focus has been put on high-altitude regions despite their sensitivity to global, regional, and local climate change phenomena. Here we report on Last Glacial environmental fluctuations at about 4000 m asl on the Sanetti Plateau in the Bale Mountains (SE Ethiopia), based on biogeochemical and palynological analyses of laminated lacustrine sediments. After deglaciation at about 18 cal kyr BP, a steppe-like herb-rich grassland with maximum Chenopodiaceae/Amaranthaceae and Plantago existed. Between 16.6 and 15.7 cal kyr BP, conditions were dry with a desiccation layer at ~ 16.3 cal kyr BP, documenting a temporary phase of maximum aridity on the plateau. While that local event lasted for only a few decades, concentrations of various elements (e.g. Zr, HF, Nb, Nd, and Na) started to increase and reached a maximum at ~ 15.8–15.7 cal kyr BP. We interpret those elements to reflect allochthonous, aeolian dust input via dry northerly winds and increasingly arid conditions in the lowlands. We suggest an abrupt versus delayed response at high and low altitudes, respectively, in response to Northern Hemispheric cooling events (the Heinrich Event 1). The delayed response at low altitudes might be caused by slow negative vegetation and monsoon feedbacks that make the ecosystem somewhat resilient. At ~ 15.7 cal kyr BP, our record shows an abrupt onset of the African Humid Period, almost 1000 years before the onset of the Bølling–Allerød warming in the North-Atlantic region, and about 300 years earlier than in the Lake Tana region. *Erica* pollen increased significantly between 14.4 and 13.6 cal kyr BP in agreement with periodically wet and regionally warm conditions. Similarly, intense fire events, documented by increased black carbon, correlate with wet and warm environmental conditions that promote the growth of *Erica* shrubs. This allows to conclude that biomass and thus fuel availability is one important factor controlling fire events in the Bale Mountains.

Keywords: Bale Mountains, High-altitude lacustrine sediments, Heinrich event 1, African humid period, Fire, *Erica*

1 Introduction

East African lakes have attracted scientific interest for decades. This is because global atmospheric circulation systems strongly influence this region and its hydrological dynamics (e.g. Thompson et al. 2002; Costa et al. 2014; Lamb et al. 2018). For instance, during the Last

*Correspondence: betymekonnen19@gmail.com
[1] Institute of Agricultural and Nutritional Sciences, Soil Biogeochemistry, Martin Luther University Halle-Wittenberg, Halle, Germany
Full list of author information is available at the end of the article

Glacial Maximum (LGM; 23–18 kyr BP) the decrease of tropical sea surface temperatures resulted in glaciation on East African Mountains (Mount Kenya, Kilimanjaro, Ruwenzori, and Ethiopian highlands) (Osmaston et al. 2005; Mark and Osmaston 2008). In addition, the southward shift of the Intertropical convergence zone (ITCZ) during ice rafting episodes throughout Heinrich event 1 (H1) are considered as a major cause for the dry event in northern and southeastern Africa around 16–17 cal kyr BP (Tierney et al. 2008; Marshall et al. 2007; Stager et al. 2011; Mohtadi et al. 2014). During the African humid period (AHP) maximum northern Hemisphere summer insolation shifted the rain belt associated with the ITCZ to the north (Bastian et al. 2021), generating increased rainfall across Northern Africa which turned the Saharan desert into green savanna (Gasse 2000). Palaeoclimatic studies suggest the southward extension of the AHP to eastern Africa (Tierney et al. 2008; Tierney and DeMenocal 2013; Costa et al. 2014).

Besides, lacustrine sediments (Tiercelin et al. 2008; Bittner et al. 2020; and many others), tropical glaciers (Gasse 2000; Thompson et al. 2002), peat bogs (Bonnefille and Mohammed 1994; Brown et al. 2007) and marine sediments (Camuera et al. 2021; Tierney and deMenocal 2013) have been serving as potential archives for the reconstruction of paleoenvironmental fluctuations in eastern Africa. However, the regional, topographic, and climate complexities, together with dating inaccuracy and lack of unambiguous proxies, lead to differences in the reconstructed timing of the onset and termination of major climatic events such as H1 and AHP across sites (Lamb et al. 2007; Tierney et al. 2011; Costa et al. 2014; Bastian et al. 2021). Moreover, the impact of these drastic climatic events on the migration of humans and on vegetation dynamics is yet not fully understood.

The highlands of the Bale Mountains in southeastern Ethiopia are promising sites for studying paleoenvironmental fluctuations. Their unique exposition to main atmospheric circulation systems (SW monsoon, SE monsoon, NE trades, and NW disturbances) (Miehe and Miehe 1994; Hillman 1986; Camberlin 2018) contribute to their climate sensitivity. In addition, the special geomorphological features, characterized by high altitudes up to 4377 m above sea level (asl), by moraines and small glacial depressions, support the reconstruction of the landscape evolution (Nicholson 2000). During MIS 3, the Bale Mountains were one of the most extensively glaciated mountains in Ethiopia (Messerli 1980; Osmaston et al. 2005; Groos et al. 2021). Groos et al. (2021) suggest that about 265 km² of the Bale Mountains were ice-covered between 42 to 28 kyr BP, well before the onset of the global LGM. This caused a temperature decrease and a downward shift of Afroalpine vegetation. Umer

et al. (2007) and Ossendorf et al. (2019) suggested that the glaciers retreated from the Bale Mountains at ~ 15.9–16.7 cal kyr BP. Geochemical and pollen results from Lake Garba Guracha, in a north-exposed, deeply incised trough valley at 3950 m asl, and from peat deposits on the Sanetti Plateau, inform about Late Pleistocene-Holocene climate fluctuations (Tiercelin et al. 2008; Bittner et al. 2020) and respective vegetation changes (Umer et al. 2007; Kuzmicheva et al. 2013, 2014; Gil-Romera et al. 2019). These studies suggest that the warm and humid conditions during the early Holocene led to the expansion of *Erica* vegetation on the Sanetti Plateau, and dry climate and natural and/or human-induced fires might be major causes for the current patches of *Erica* on the Plateau. A study by Ossendorf et al., (2019), revealed human settlements in high elevation (3469 m asl) already during 47–31 cal kyr BP. Gil-Romera et al. (2019) reported that fire played a major role in determining the ecological dynamics of the *Erica* vegetation on the Bale Mountains. However, the influence of humans on the vegetation remains unclear. Open questions are: (1) Did the high altitudes of the Sanetti Plateau experience similar climatic fluctuations in intensity and timing as the lower regions in northern and eastern Africa during the Late Glacial? (2) Did the highlands of the Sanetti Plateau deglaciate at the same time as the north exposed trough valleys? (3) When and to what degree did *Erica* occupy the high altitudes of the Sanetti Plateau, where at present only patches can be found? (4) Are these patches of *Erica* relics documenting climate deterioration or human-induced fire?

In order to address these questions, and to better understand the paleoecological evolution of these high altitudes above the upper timberline, we analysed laminated lake sediments in high resolution, deposited in a glacial depression on the Plateau in about 4000 m asl using a multi-proxy approach. The depression has no noteworthy outflow and its catchment is not densely vegetated, thus being highly sensitive to local and regional environmental fluctuations.

2 Site information and methods/experimental
2.1 Study area
The Bale Mountains covering an area of 2200 km² include the Sanetti Plateau, which is the largest alpine ecosystem in Africa (Fig. 1). The area is widely perceived as natural (Miehe and Miehe 1994; Kidane et al. 2012). The Plateau (Fig. 1) extends between ca. 3800 to 4100 m asl, surrounded by the peaks of Tullu Konteh (4050 m asl) and Tullu Dimtu (4377 m asl), the second-highest peak of the country (Hillman 1988; Messerli and Winiger 1992). Erratic boulders, moraines, small lakes present on the plateau and in trough valleys are clear indicators

Fig. 1 Location map of the study area. **A** Location of Ethiopia in Africa and regional location of the Bale Mountains National Park (BMNP) and Lake Tana. **B** Location of B4 depression on the Sanetti Plateau and location of Lake Garba Guracha. **C** Photo of B4 depression
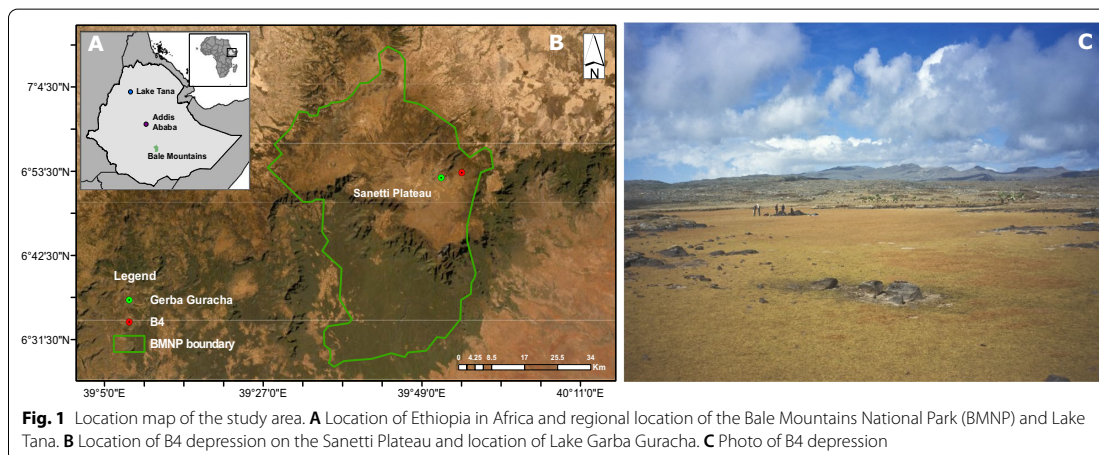
of former glaciations (Osmaston et al. 2005). The parent rocks comprise Oligo-Miocene basalts and Quaternary rhyolites with trachytes, which weather to brown or brownish-black silty loams (Billi 2015). Muddy Gleysols are developed in depressions (Yimer et al. 2006).

Due to the annual migration of the ITCZ between 10° North and South, the climate of the Bale Mountains is characterized by a pronounced rainfall seasonality with a short dry (November to February) and a long rainy season (March to October) (Levin et al. 2009; Costa et al. 2014). The rainfall pattern is bimodal, with a peak from July to October, followed by a second peak from March to June (Kidane et al. 2012). The rain-bearing air masses derive from the Indian Ocean and the Atlantic Ocean via the Congo Basin (Gasse 2000; Tierney et al. 2011; Costa et al. 2014; Lemma et al. 2020), whereas northerly winds dominate during the dry season. In Dinsho (3170 m asl), the mean maximum temperature is 11.8 °C while the mean minimum temperature ranges from 0.6 to 10 °C, with frequent frost occurring in the high mountain areas during winter season (November to January) (Hillman 1986; Tiercelin et al. 2008). The highest precipitation and humidity occurs in the southern part of the mountains with 1000–1500 mm/a, while the northern part exhibits annual rainfall ranging between 800 and 1000 mm/a (Miehe and Miehe 1994; Umer et al. 2007).

The south to north rainfall gradient and the altitudinal temperature gradient stratify the vegetation into the Afromontane forest, the Ericaceous belt, and Afroalpine zone (Hedberg 1951; Friis 1986). The Afromontane forest spans from ~ 1450 to 3200 m asl in southern exposition, and from ~ 2800 to 3300 m asl along northern slopes. The southern declivity comprises *Podocarpus gracilior* associated with *Syzygium guineense* and *Aningeria*

adolfi-friederici, whereas the northern slopes are mainly dominated by *Juniperus procera*, *Hagenia abyssinica,* and *Hypericum revolutum* (Friis 1986; Bussmann 1997). The Ericaceous belt covers ~ 90,000 ha between ca. 3200 and 3800 m asl and is dominated by *Erica arborea* L. and *Erica trimera* (Engl.) (Hailemariam et al. 2016). While the lower boundary of the Ericaceous belt (3300–3500 m asl) is covered with *Erica*-dominated *Hagenia-Hypericum* forests, the central part comprises monotonous *Erica trimera* stands, which continues to the upper limit (ca. 3800 m asl) of the boundary. The Afroalpine vegetation above 3800 m asl is open and rich in Tussock grasses and mainly dominated by *Helichrysum splendidum-Alchemilla haumannii* dwarf-scrubs and Giant *Lobelia* (*L. rhynchopetalum*) (Yineger et al. 2008), accompanied by patches of *Erica,* growing between big boulders along steep slopes (Miehe and Miehe 1994).

2.2 Sampling
We investigated a depression, located in an extended plain on the Sanetti Plateau, above the upper limit of the *Erica* belt at 3970 m asl (Fig. 1; 6° 53.3433′ S and 39° 54.5217′ E). A pit was dug down to the glacial boulders in a depth of 255 cm to prepare a profile named "B4" (Fig. 2). Subsequently, sediments were described (color, texture, structure, ect.) and sampled every 2 cm from 55 to 255 cm, representing humic-rich lacustrine, partly laminated material, and every 5 to 10 cm from the brownish upper part, rich in reddish mottles. Samples were air-dried and stored in plastic bags. In addition, 10 sediment samples were collected from the pit for radiocarbon dating. The air-dried samples were analyzed for elemental and mineral compositions, electrical conductivity (EC), pH (H_2O), stable C isotopes, alkanes, pollen,

Fig. 2 Stratigraphy and photo of the studied profile. **A** Photo of the B4 profile; the red pocketknife (10 cm) serves as scale. **B** Stratigraphy of the sediments in profile B4, divided in units 1–3, based on morphological features and calibrated radiocarbon ages (see Fig. 3; Table 1; YD = Younger Dryas, H1 = Heinrich Event 1)
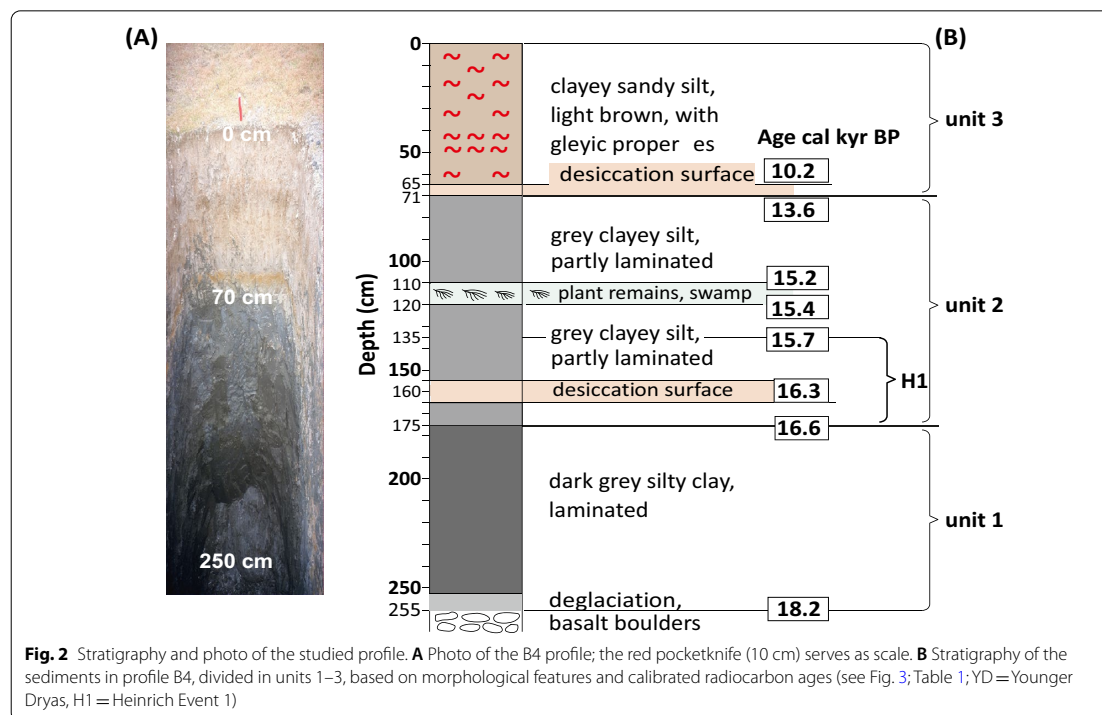
and black carbon (BC). Plant leaves (*Alchemilla* sp., *Helichrysum* sp., *Pennisetum* sp., *Potamogeton thunbergii*, and *Ranunculus trichophyllus*) and algae (*Pediastrum* sp.) were collected from the surrounding area to compare the stable isotopes composition of the sediment organic matter with its potential parent material.

2.3 Radiocarbon analysis

For the establishment of a reliable chronology, radiocarbon dates were obtained by dating alkali-soluble organic matter extracted from carbonate-free bulk samples using accelerated mass spectrometry (AMS) in the Radiocarbon Laboratory of the University Erlangen, Germany (Table 1). We established a Bayesian age-depth model using the IntCal13 calibration curve implemented in the package Bacon (Blaauw and Christen 2011) in R software (R Core Team 2013).

2.4 Sediment analyses
2.4.1 Physical properties

Texture analyses were performed quantitatively in the laboratory on 52 air-dried and 2 mm sieved samples. Clay (< 6.3 μm) and silt (6.3–63 μm) fractions were quantified with a Mastersizer S (Malvern Instruments) after treating the samples with H_2O_2 and HCl. The sand fraction

(63–2000 μm) was determined by wet sieving. We are aware that the fraction < 6.3 μm used in this study does not quantitatively correspond to the clay fraction defined by the pipette method as the fraction < 2 μm is underestimated by the Mastersizer (Antoine et al. 2009).

2.4.2 Inorganic geochemistry

For X-Ray Fluorescence (XRF) analyses, ground aliquots of 103 samples were dried at 105 °C. Major and minor elemental composition was determined using a Philips 2404 X-Ray Fluorescence Spectrometer. Given that the samples were carbonate-free, results were corrected for soil organic matter and water contents according to Eq. (1)

$$\%X_{\text{corrected}} = \%X_{\text{measured}} \times \left[\frac{100}{100 - \%GV_{1000} - \%H_2O} \right]$$
(1)

X is the content of an element in percent and $\%GV_{1000}$ is the mass loss upon ignition at 1000 °C.

In order to evaluate the intensity of chemical weathering, the chemical proxy of alteration (CPA) was calculated according to Buggle et al. (2011) (Eq. 2).

Table 1 Radiocarbon ages using Accelerated Mass Spectrometry of alkali soluble organic matter; calibrated according to Blaauw and Christen (2011)

Lab number	Sample depth (cm)	Dated material	¹⁴C age (uncalibrated a BP)	Cal. (INTCAL13, 2 Sigma ranges)	¹⁴C age (calibrated, median cal year BP)
Erl-5563	27	Bulk sediment	4650 ± 55	5078–5532	5396
Erl-5564	40	Bulk sediment	7718 ± 72	8225–8678	8481
Erl-5173	63	Bulk sediment	9047 ± 108	9603–10,472	10,052
Erl-5092	72	Bulk sediment	$11,856 \pm 86$	13,436–13,969	13,667
Erl-5175	101	Bulk sediment	$12,696 \pm 96$	14,372–15,241	14,876
Erl-5173	123	Bulk sediment	$13,214 \pm 95$	15,155–15,867	15,518
Erl-5093	160	Bulk sediment	$13,525 \pm 106$	15,979–16,568	16,276
Erl-5172	207	Bulk sediment	$14,094 \pm 119$	16,916–17,458	17,193
Erl-5565	233	Bulk sediment	$14,485 \pm 81$	17,472–17,958	17,701
Erl-5568	255	Bulk sediment	$14,681 \pm 92$	17,879–18,653	18,173

$$CPA = \left[\frac{Al_2O_3}{Al_2O_3 + Na_2O} \right] \times 100 \qquad (2)$$

Qualitative mineral identification was carried out on bulk samples ($n = 100$) using X-ray diffraction. The powdered samples were packed into aluminum sample holders and scanned in a Philips PW 1710 diffractometer from 3 to $80°2^\theta$ with Cu Kα radiation generated at 50 kV and 30 mA, at $0.02°2\theta$ step size and 2.5 s step time. Phases identified in the samples are quartz, feldspar, pyroxene (probably mainly augite), clay minerals, hematite, pyrite, gypsum, and amorphous silica. No special clay mineral analysis was performed, yet characteristic peaks of clay minerals between ~ 6–12.5 and ~ 60–$62°2^\theta$ show a wide range of clay minerals, including smectite, chlorite, illite, kaolinite and mixed-layer minerals.

2.4.3 Organic geochemistry

Total organic carbon (TOC) and total nitrogen (*N*) of homogenized samples ($n = 103$) were quantified by dry combustion on a Vario EL elemental analyser (Elementar, Langenselbold, Germany). In order to complement the organic matter source identification and preservation status, *n*-alkanes and hydrogen index (HI) were analysed in 34 samples (Talbot and Livingstone 1989). *n*-Alkanes were extracted by soxhlet extraction using dichloromethane (DCM) and methanol (1:1) as solvents for 24 h (Zech and Glaser 2008). After adding 50 μl of 5α androstane as an internal standard, the excess solvent was removed by rotary evaporation and transferred to aminopropyl columns. Subsequently, *n*-alkanes were eluted with 3 ml of hexane DCM/MeOH (1:1). Finally, *n*-alkanes were quantified using gas chromatography (SHIMADZU, GC-2010, Kyoto Japan) equipped with an SPB-5 columns of 30 m length, 0.25 mm ID, 0.25 μm film thickness, and detected using a flame ionization detector (FID). Here, we used the *n*-alkane ratio Paq ($C_{23} + C_{25}$)/ ($C_{23} + C_{25} + C_{29} + C_{31}$) to identify the source of organic matter. HI was analysed by pyrolysis of dried (40 ℃) and fine powdered bulk sediments (Talbot and Livingstone 1989).

We measured the natural abundance of $\delta^{13}C$ ($n = 101$) by dry combustion of a 40 mg homogenized aliquot with a Fision 1108 elemental analyser coupled to a Delta S gas isotope ratio mass spectrometer (EL-IRMS) with a Conflow III interface (Thermo Finnigan MAT, Bremen, Germany). Sucrose (ANU, IAEA, Vienna, Austria) and $CaCO_3$ (NBS 19, TS limestone) were used as calibration standards for $\delta^{13}C$. The precision of $\delta^{13}C$ measurement was 0.2‰. In addition to bulk stable isotopes, we measured compound-specific carbon isotopes ($\delta^{13}C$) of long chain terrestrial *n*-alkanes C_{27}, C_{29} and C_{31} to complement on the paleovegetation reconstruction (C3 vs C4). Compound-specific $\delta^{13}C$ analyses of long chain *n*-alkanes (C_{27}, C_{29} and C_{31}) were carried out and measured as described above.

Black carbon (BC) refers to polycondensed aromatic moieties formed during thermochemical combustion. While charcoal is usually detected visually using a microscope, BC is usually detected through chemical extraction, which enables to quantify the complex signature of pyrogenic carbon more precisely, especially when charcoal is not visible anymore. Thus, BC allows the reconstruction of fire events even if soot or char are not visible. Moreover, its polycyclic aromatic structure resists chemical and biological degradation in soil (Glaser et al. 1998; Wang and Li 2007; Wiedemeier et al. 2015) and persists for a long period of time in soil and sediments (Kuzyakov et al. 2014). We analysed BC ($n = 72$) using benzene polycarboxylic acids (BPCAs) as molecular markers following Glaser et al. (1998) and modified according to Brodowski et al. (2005). Five hundred mg of each sample was hydrolyzed with 10 ml 4 M TFA for 4 h at 105 ℃.

91

The hydrolyzed samples were filtrated on glass fiber filters and rinsed several times with de-ionized water to remove polyvalent cations. Subsequently, the samples were digested with 65% nitric acid for 8 h at 170 °C in a high-pressure digestion apparatus. The solution was passed through Dowex 50 W resin columns (200 to 400 meshes) to remove polyvalent cations. After derivatization, BPCAs were separated using GC and detected using FID with an injection temperature of 300 °C.

2.4.4 Palynomorph analysis

For palynological analyses, samples of 1 ml were prepared using standard procedures, including *Lycopodium* spores as exotic markers, acetolysis, HF treatment, and ultrasonic sieving (5 μm), and storage in glycerol (Stockmarr 1971). Microscopic analyses took place under $400 \times$ magnifications, backed by oil immersion ($1250 \times$). For pollen identification, we used an existing reference collection of ~5000 slides (in Goettingen) and relevant literature (Gosling et al. 2013; Schüler and Hemp 2016). The nomenclature of the common types follows Beug (2004). Detailed analyses were carried out on 38 samples from the lower part of the profile (251–69 cm) with pollen counting sums of about 250 to 300 per sample. Pollen influx (grains $cm^{-1}\, a^{-1}$) was calculated using exotic *Lycopodium* spore markers. To estimate humidity conditions, we calculated the A/C (*Artemisia*/Chenopodiaceae) ratio (Van Campo and Gasse 1993; Herzschuh 2007; Li et al. 2010) by dividing the number of Artemisia by that of Chenopodiaceae/Amaranthaceae. Poaceae pollen were size differentiated between small (<37 μm) and large (>37 μm) diameter grains. Counts of the larger grains allow an approximate estimate of C4 grasses, which produce larger pollen grains than C3 Poaceae (Jan et al. 2015). Diagrams were plotted with the software C2 (Juggins 2007).

3 Results

3.1 Age-depth model and sedimentation rates

B4 profile records sedimentation during the last 18.2 cal kyr BP. Our age-depth model (Fig. 3) illustrates that the sedimentation rate was 0.05 and 0.01 cm per year between 18.2 and 13.6 cal kyr BP and from 10.5 cal kyr BP to present, respectively. Between 13.6 and 10.5 cal kyr BP, a sedimentation hiatus is indicated.

3.2 Lithostratigraphy and interpretation of the depositional environment

The B4 sediments can be stratified into three units (Fig. 2). The lowermost unit 1 from 255 to 175 cm (18.2–16.6 cal kyr BP) is a dark-grey, laminated, silty clay with low sand content. It was deposited above a thin greyish sandy silt layer and basalt boulders. Unit 2, from 175 to

71 cm depth, is a grey, partly laminated silty clay, deposited between 16.6–13.6 cal kyr BP. A stiff sandy-silty light layer, preserved between 167 and 160 cm, likely documents intensive desiccation of the B4 depression at about 16.3 cal kyr BP. From 120 to110 cm (~15.4–15.2 cal kyr BP) plant root relics occur displaying swampy, shallow-water conditions. The upper lithostratigraphic unit 3 is about 70 cm thick, deposited during the last 10 cal kyr BP. It comprises light brown, weakly clayey, sandy silt with red mottles and bleached aggregate surfaces, showing water-logging during the rainy season. Unit 3 is strongly influenced by gleysation, which makes paleoenvironmental interpretations and regional comparisons ambiguous. Therefore, in the following, we present geochemical and palynological results only from units 1 and 2 in detail.

3.3 Grain size and geochemical results

3.3.1 Unit 1: 255–175 cm (18.2–16.6 cal kyr BP)

According to Fig. 4 and Additional file 1, clay and silt contents are high (partly up to 60% and 40%, respectively) and weakly fluctuating, whereas the sand contents are very low. TOC values, being low at the bottom of the core, constantly increase from ~0.7 to ~7% in 239 cm; then high values (~7%) persist until the top of unit 1. Low TOC/N values at the bottom of the profile increase to an average value <12 (Fig. 4). HI values range between 107 and 266, with low values at the bottom of the profile.

Our results show an average δ^{13}C value of -14.3‰ with a slight decrease from the bottom to the top of unit 1. Analyses of water plants (*Potamogeton thunbergii*, *Ranunculus trichophyllus*) and algae (*Pediastrum*), sampled from nearby shallow lakes, resulted in δ^{13}C values of -18.6, -15.5, and -17.3‰, respectively. Modern terrestrial plants growing around the B4 depression are characterized by δ^{13}C values between -30.1‰ (*Helichrysum argyaranthum*) and -26.9‰ (*Alchemilla fischeri*). Compound-specific analysis of long chain *n*-alkanes C_{27}, C_{29}, and C_{31} revealed δ^{13}C values of -27, -25.6, and -25.1‰, respectively. Paq values increase from 0.27 at 244.5 cm to 0.44 at 175 cm. Despite high value at the bottom of the profile, BC values were very low in this unit (around 10 g kg^{-1} TOC) increasing between 195 and 175 cm (~16.9–16.6 cal kyr BP) to around 30 g kg^{-1} TOC.

Lithogenic elements such as Zr, Hf, Nb, and Na_2O show minimum values except for a slight increase at 210 cm and ~190 cm (~17.2 and ~17.0 cal kyr BP) (Fig. 5). Besides primary minerals such as quartz, feldspar, and pyroxene, unit 1 sediments contain traces of pyrite and gypsum. CPA values do not show fluctuation except a slight decrease at 17.2 and ~16.9 cal kyr BP.

Fig. 3 Bayesian age-depth model for profile B4 according to Blaauw and Christen (2011). Top left: The log-likelihood of the model fit for the saved iterations of the model, top middle: prior and posterior distribution of accumulation rate, and top right: prior and posterior distribution of the autocorrelation in accumulation rates (memory) and the time gap (hiatus size) at the end. Bottom panel shows the calibrated ^{14}C dates (transparent blue) and the age-depth model (darker greys) indicate more likely calendar ages; grey stippled lines show 95% confidence intervals; red curve shows single 'best' model based on the mean age for each depth

3.3.2 Unit 2: 175–71 cm (16.6–13.6 cal kyr BP)

Unit 2 starts at 175 cm depth with slightly increasing values of the lithogenic proxies (Fig. 5). Most striking is a pronounced sand maximum and a TOC minimum in ~160 cm, corresponding to ~16.3 cal kyr BP (Fig. 4). Strongly increasing values of the lithogenic compounds such as Zr, Na_2O, K_2O, Hf, Nd, and Nb and minimum CPA values are recorded between 160 and 135 cm (Fig. 5). Noteworthy is that these elements do not show the drastic excursion of TOC and sand in ~160 cm depth. Moreover, strong positive correlations ($R = ~0.8–0.9$; Additional file 2) are recorded between Na_2O, K_2O, Zr, Hf, Nb, and Nd in this unit. This constellation changed abruptly at ~15.7 cal kyr BP, documented by the abrupt decrease of most lithogenic elements and their ratios. However, some proxies such as sand content, TOC, HI, and $\delta^{13}C$ do not show such an abrupt change except Paq values, which decrease between 140 and 120 cm (Fig. 4).

BC which was partly very low in unit 1, increased between 15.7 and 15.2 cal kyr BP (Fig. 4). The uppermost part of unit 2, (deposited between ~14.4 and 13.6 cal kyr BP (90–71 cm) is characterized by a distinct decrease in

TOC, HI, varying sand contents, absence of pyrite, and higher contents of terrestrial *n*-alkanes and BC (Fig. 4).

3.4 Palynological results

The pollen record is divided into five local pollen zones (LPZ 1–5; Figs. 6, 7) based on changes in the pollen spectra. No pollen was detected in unit 3 due to pedogenetic processes that disturbed pollen preservation. About 75 pollen taxa have been identified in the record. The green algae *Botryococcus* and *Pediastrum* attributed to the intermittent presence of a water body in the B4 depression, thus their palynological record reflects local conditions.

Poaceae < 37 μm dominate the pollen spectra with values around 35%. Other relatively common non-arboreal taxa are *Artemisia*, Chenopodiaceae/Amaranthaceae, Poaceae > 37 μm, and *Plantago*. The sum of arboreal pollen (AP) makes up around 15% in LPZ 1–4 (from 250.5 to 90 cm; 18.1–14.4 cal kyr BP) and increased to 38% during LPZ 5 (from 90 to 70 cm; 14.3–13.6 cal kyr BP). The green algae *Botryococcus* is most common in the lowest part of the record. *Pediastrum* increases with parallel decreases

Fig. 4 Analytical properties of the B4 sediments, with depth profiles of the sand fraction (63–2000 μm), total organic carbon (TOC), organic carbon-to-nitrogen ratio (TOC/N), Hydrogen Index (HI), δ¹³C values, Black Carbon (BC) and Paq. The light orange color shows dryer events while orange color indicates desiccation layers developed during Heinrich Event 1(H1). Blue color indicates the African Humid Period (AHP) and other humid episodes while dark green color indicates the event characterized as humid and arid according to pollen and geochemical results, respectively

of *Botryococcus*. Pollen of modern water plants, *Potamogeton thunbergii* and *Ranunculus trichophyllus* are not present in the fossil pollen record.

LPZ 1 (250.5–204 cm; 18.1–17.2 cal kyr BP) is characterized by *Botryococcus* maxima, which abruptly decreases at 17.3 cal kyr BP and is replaced by high amounts of *Pediastrum* pollen (Fig. 7). Moreover, high percentages of Poaceae, herbs (non-arboreal pollen, NAP), *Artemisia,* and Chenopodiaceae/Amaranthaceae are recorded in LPZ1. Plantain (*Plantago*) has been very common. Arboreal pollen of Ericaceae, *Podocarpus, Myrica, Juniperus,* and *Olea* are found from the beginning of the archive.

LPZ 2 (204–194 cm; 17.2–16.9 BP) records an increase in Chenopodiaceae/Amaranthaceae and *Plantago* and

strongly reduced occurrence of *Artemisia* and *Pediastrum.* Similarly, pollen percentage and pollen influx of *Hagenia, Podocarpus, Myrica, Juniperus,* and *Olea* show low values between 17.2 and 16.9 cal kyr BP.

LPZ 3 (194–110 cm, 16.9–15.2 cal kyr BP) starts with a subsequent increase of *Podocarpus, Juniperus,* and *Olea* from 194 to 177 cm (16.9–16.6 cal kyr BP) and a higher presence of *Pediastrum*. The afroalpine element, *Alchemilla*, which is highly underrepresented in the pollen record, is sporadically present from now on. The influx of *Erica, Pediastrum, Hagenia,* and *Botryococcus* pollen decrease between 165 and 155 cm (16.3 and 16.1 cal kyr BP), while Chenopodiaceae/Amaranthaceae pollen increase. Subsequently, higher *Pediastrum* values, more frequent fern spores,

Fig. 5 XRF results of B4 sediments. Depth profiles of Zirconium (Zr), Sodium oxide (Na_2O), Potassium oxide (K_2O), Hafnium (Hf), Niobium (Nb), Zirconium/Rubidium (Zi/Rb), Zirconium/Silica oxide (Zr/SiO_2), Zirconium/Titanium oxide (Zr/TiO_2) and of the chemical proxy of alteration (CPA = $Al_2O_3/(Al_2O_3 + Na_2O)$, inversed scale. The light orange color shows dryer events while orange color indicate desiccation layers developed during Heinrich Event 1(H1) and the hiatus. Blue color indicates the African Humid Period (AHP) and other humid episodes while dark green color indicates the event characterized as humid and arid according to pollen and geochemical results, respectively

and *Sparganium*-type are recorded between 155 and 135 cm (16.1 and 15.7 cal kyr BP). A lower occurrence of *Erica* pollen and the montane forest tree *Hagenia* recorded from 15.4 to 15.2 kyr BP, while absolute values of montane forest taxa like *Podocarpus* and *Juniperus* increase. By contrast, *Pediastrum*, *Plantago*-type, and *Grass* pollen influx show high values.

LPZ 4 (110–90 cm, 15.2–14.4 cal kyr BP) records the most abundant Ericaceae and *Podocarpus*. Similarly, the sum of all arboreal pollen (AP) increases but does not exceed their former values. The same holds true for Artemisia. In contrast, the ratio of Chenopodiaceae/Amaranthaceae falls as low as never before. In consequence, the A/C ratio increases strongly.

LPZ 5 (90–71 cm, 14.4–13.6 cal kyr BP) is marked by a strong expansion of *Erica* and *Podocarpus*. The previously significant elements Chenopodiaceae/Amaranthaceae and *Plantago* disappeared nearly completely, and *Artemisia* reduced strongly. Besides Poaceae, a wide range of *Asteraceae* (*Senecio*, *Matricaria*-type, Cichorioideae), which was present since the beginning

of the record, became the most important vegetation constituents.

4 Discussion

4.1 Radiocarbon dating
Our radiocarbon ages show that depression B4 became ice-free at ~18 cal kyr BP and thus records the climate, vegetation, and fire history from the end of the LGM to the Late Holocene. The timing of deglaciation (18.2 cal kyr BP) seems reliable, as the sediments are free of carbonates.

4.2 Organic geochemistry
Low TOC contents at the bottom of the profile (Fig. 4) mark cold conditions with low biomass production in, and around, the lake. TOC/N ratios are used to distinguish between terrestrial and aquatic carbon sources. Organic matter derived from algae usually shows TOC/N values between 4 and 10, while vascular land plants and terrestrial soil organic matter may have TOC/N ratios > 20 (Meyers 1994) and ~15, respectively

Fig. 6 Percentage diagram of selected pollen taxa referring to the counting sum of pollen grains of a sample and fivefold exaggeration

Fig. 7 Pollen influx diagram of selected taxa and algae from B4 depression, showing pollen accumulation rate in grains cm^{-1} year^{-1}
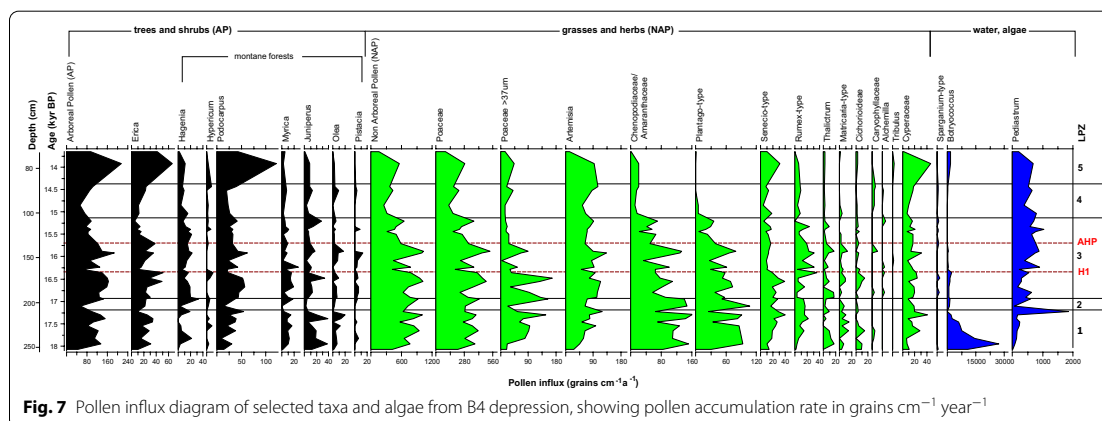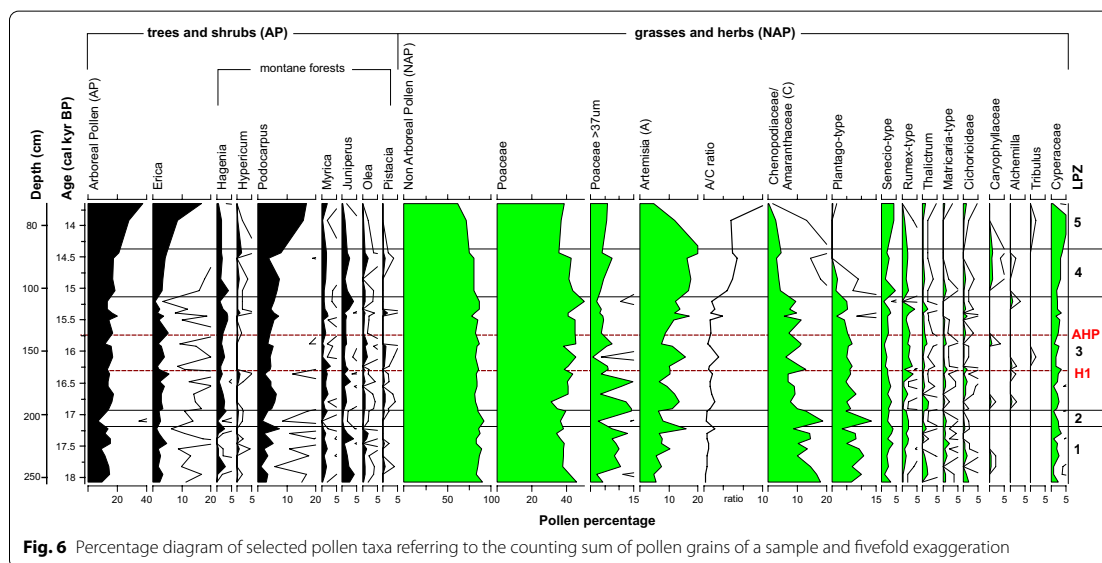
(Mekonnen et al. 2019). However, the use of TOC/N ratios as organic matter source indicators is highly constrained by degradation and mineralization, which results in low TOC/N values. TOC/N values of the B4 depression range between 3.5 and 12.3, suggesting mainly primary lacustrine biomass production. According to Ficken et al. (2000), Paq values, between 0.4 and 1 characterize submerged and floating aquatic plants, while terrestrial plants yield values lower than 0.1. Indeed, average HI values of ~250, together with elevated Paq values support the interpretation that mainly lacustrine primary biomass was produced under medium to high water levels,

generating anoxic conditions in B4 depression. TOC values substantially decrease at 160 cm (16.3 cal kyr BP) accompanied by sand maxima. This likely documents an extremely low stand of the water table and the development of a desiccation surface. Increased sand input from the depression margins may take place because of temporary heavy rains during dry phases when the sparse vegetation cover protected less against erosion. Decreasing Paq values between 140 and 120 cm shows higher terrestrial input, likely due to higher rainfall intensities and accelerated erosion at the margins of the depression. Nevertheless, water levels dropped again already

at ~ 15.4 cal kyr BP as evidenced by the formation of a swamp around 15.4–15.2 cal kyr BP (120–110 cm; Fig. 4). Decreasing TOC and HI values and absence of pyrite in sediments deposited between 14.4 and 13.6 cal kyr BP indicate accelerated local desiccation, likely correlated with periodic sediment input. Varying sand contents suggest that humid and dry phases alternated, leading to deflation of small particles and organic matter, leaving behind sand in the depression. Intensive deflation and complete desiccation are likely responsible for the hiatus at 70 cm depth (13.6–10.2 kyr BP), coinciding with the transition from Late Glacial to Holocene.

Stable C isotopes are frequently used in paleovegetation reconstructions due to their potential in discerning between C3 and C4 plants (Eshetu 2002; Glaser and Zech 2005). Our bulk $\delta^{13}C$ values and those of long-chain *n*-alkanes show average values of −14.3‰ and −25.9‰, respectively. This might show C4 vegetation (Ficken et al. 2002; Glaser and Zech 2005) growing at the margin of the depression under relatively dry conditions during the Late Glacial. However, methanogenesis, assimilation of ^{13}C-enriched CO_2 and HCO_3^- by water plants due to long-lasting ice cover, especially during the early Late Glacial, and the low CO_2 concentration in the atmosphere (Monnin et al. 2001) might have contributed to such positive $\delta^{13}C$ values (Conrad et al. 2007). In contrast, modern plants from the surroundings of the lake show values indicating C3 vegetation. This result agrees with a study of Mekonnen et al. (2019), reporting that the modern vegetation in high altitudes of the Bale Mountains comprises only C3 plants.

BC produced by incomplete combustion of plant biomass is ubiquitous in lake sediments and glaciers (Glaser 1998). The weak BC maximum in the lowermost samples (~ 250 cm) presumably reflects BC storage in glacier ice during the LGM, originating from atmospheric input. In contrast, high BC between 16.9 and 16.6 cal kyr BP and between 15.7 and 14.4 cal kyr BP provides evidence for frequent fire events, likely due to increased amounts of combustible biomass under regionally wetter than under dry conditions.

4.3 Inorganic geochemistry

After deglaciation, the period between 18.1 and 16.6 cal kyr BP started with the accumulation of electrolyte-poor melting water in depression B4 (see EC in Additional file 1). The presence of pyrite at the bottom of the B4 profile implies a sedimentary environment with mainly anoxic conditions and sufficient organic matter that acts as a reductant and energy source for pyrite formation (Berner 1984). Due to their geochemical stability, lithogenic elements such as Zr, Hf, Nb, and Ti are often used in paleoenvironmental studies as indicators

of detrital and allochthonous input (Davies et al. 2015). For instance, Zr and Zr based ratios (Zr/Ti, Zr/Rb, Zr/Al) are often used as proxies for aeolian input of Saharan dust (Jimenez-Espejo et al. 2014; Scheuvens et al. 2013; Moreno et al. 2006, and Hemming 2007), while Si ratios (Ti/Si, Zr/Si) are used as indicators of biogenic silica production during favorable seasons (Lamb et al. 2018; Davies et al. 2015; Brown et al. 2007). Furthermore, also K is used as an effective moisture fluctuation indicator (Foerster et al. 2012). In our B4 profile, lithogenic elements and ratios such as Zr, Hf, Zr/SiO_2, Zr/Rb, and Zr/TiO_2 show minimum values after deglaciation; they slightly increased around 210 and 190 cm (~ 17.2 and 16.9 cal kyr BP), while a continuous increase of these elements and ratios is recorded from 175 to 135 cm (~ 16.6–15.7 cal kyr BP) (Fig. 5). In contrast, CPA values show a weak minimum at ~ 210 and 190 cm and further decrease to < 80 between 175 and 135 cm. These results likely reflect intensified dry northerly winds (Brown et al. 2007; Marshall et al. 2011; Lamb et al. 2018; Jimenez-Espejo et al. 2014), which transported less weathered (low CPA, Na enriched, Fig. 5), allochthonous material in the Sanetti Plateau. The occurrence of gypsum-bearing layers in ~ 210 cm (~ 17.2 cal kyr BP) and between 166 and 152 cm (16.4–16.1 cal kyr BP) show lower water tables and provide evidence for dry events. The latter is further confirmed by increasing values of K_2O (Fig. 5), which agrees with results from Chew Bahir (Foerster et al. 2012). Moreover, increased values of K_2O and Na_2O (Fig. 5) coincide with the high abundance of Feldspar in ~ 135 cm (Additional file 3), highlighting Feldspar containing allochthonous input. The abrupt decrease of most allochthonous elements and ratios (Fig. 5) at about 15.7 cal kyr BP indicates a drastic atmospheric reorganization with an abrupt decrease of dust inputs related to the beginning of the AHP, attributed to the northward migration of the rain belt and the ITCZ (Bastian et al. 2021).

4.4 Palynology

The green algae *Botryococcus* is generally found in tropical freshwater lakes under very cold environmental conditions (Jankovská and Komárek 2000). Therefore, the high occurrence of *Botryoccoccus* at the bottom of the B4 profile indicates deglaciation and discharge of cold meltwater into the lake. The abundant presence of *Botryoccocus,* which is usually characterized by high TOC/N values of 18–36 (Last and Smol 2002; Bittner et al. 2020) and high $\delta^{13}C$ values (Grice et al. 2001), may have contributed to the TOC/N increase recorded between 250 and 240 cm depth and positive $\delta^{13}C$ values at the bottom of the profile (Fig. 4). This supports the interpretation of predominant lacustrine TOC production after

deglaciation. The decrease of *Botryococcus* and a parallel increase of *Pediastrum* also show a relatively stable water body in the investigated depression.

The high percentages of *Poaceae* and herbs (non-arboreal pollen, NAP) between 18.1 and 17.2 cal kyr BP documents open grass-land vegetation around the Sanetti Plateau. The high number of *Artemisia* and Chenopodiaceae/Amaranthaceae pollen indicate that the vegetation may have been steppe-like. The abundant presence of *Plantago* suggests a sparse vegetation cover with less competition shortly after deglaciation. However, the presence of arboreal pollen points to forests down the slopes of the Bale Mountains during the LGM. An increase in Chenopodiaceae/Amaranthaceae and *Plantago* and a decrease in *Artemisia*, *Pediastrum*, *Hagenia*, *Podocarpus*, *Myrica*, *Juniperus*, and *Olea* between ~17.2 and 16.9 cal kyr BP reflect a reduction of the montane forests due to a ~300-year interval with dry and/or cold climate. This interpretation further agrees with the mineralogical results which recorded a dry event between 17.2 and 16.9 cal kyr BP. The increase of arboreal pollen and *Pediastrum* between about 16.9–16.6 cal kyr BP marks a recovery of the montane forest and wetter local setting at the slopes of the Sanetti Plateau. At around 16.5 cal kyr BP, low values of *Pediastrum*, *Erica*, *Hagenia,* and *Botryococcus* indicate dry environmental conditions. The decrease in the influx of *Erica* pollen and subsequent increase of Chenopodeacea/Amaranthaceae around 16.3 cal kyr BP related to the desiccation phase of the B4 depression recorded by low TOC and high sand input. After this desiccation phase, a trend to locally more humid conditions is indicated by higher *Pediastrum* values, more frequent fern spores, and *Sparganium*-type between 155 and 135 cm (16.1 and 15.8 cal kyr BP). This is in agreement with increasing TOC values and it documents that on the SP the H1 stadial is characterized by a short-term desiccation, in contrast to the lowland archives (Fig. 8). Dry environmental conditions are also evidenced from 15.4 to 15.2 cal kyr BP by the decrease in *Erica* and *Hagenia* pollen, while tolerant montane taxa such as *Podocarpus* and *Juniperus* survived. Nevertheless, as indicated by constant high *Pediastrum* influx and high Paq values, the B4 depression was partly or periodically flooded. Changes in seasonality and longer dry seasons may have given way to swamp formation. However, pollen types, including typical swamp and water plants (Cyperaceae, *Sparganium*-type), show no increase. The increasing *Plantago*-type includes the amphibious species *Littorella uniflora*, but this swamp species is not known from Africa today (Hoggard et al. 2003). Possibly, the increased Poaceae influx marks the spreading of swamp grasses at the site. A temporary decrease in the influx of arboreal pollen may be related to a short cold event that also decreased the flourishing of grasses and herbs (NAP). The long-time trend in NAP influx reduction

can relate to a change in the vegetation from wind-pollinated plant groups (Poaceae, Chenopodiaceae/Amaranthaceae, *Plantago*-type, *Rumex*-type) to insect-pollinated taxa (*Senecio*-type, *Caryophyllaceae*), leading to an overall reduced NAP pollen input. By contrast, the decrease in Chenopodiaceae/Amaranthaceae and consequent increase of A/C between 15.2 and 14.4 cal kyr BP indicate the most humid conditions regionally, whereas locally the B4 depression started to dry out due to increased silting up. A significant increase in *Erica* and *Podocarpus* pollen between 14.4 and 13.6 cal kyr BP substantiates the expansion of the Ericaceous belt and the lowland forests, together with a fundamental change in vegetation composition on the Sanetti Plateau. This is in contrast to the sedimentological results which document progressive local drying out. This discrepancy might be due to the potential of pollen assemblage to provide regional environmental signals, while biogeochemical proxies (Fig. 4), mainly reflect the local conditions of the B4 record.

5 Environmental implications and comparison with other records
5.1 Deglaciation and climate fluctuations
[14]C ages from the lower sediment of depression B4 suggest that the Sanetti Plateau became at least locally, ice-free already at ~18.2 cal kyr BP. Surface exposure dating of erratic boulders in *N*-exposed valleys and on the Sanetti Plateau suggest the onset of deglaciation at 15.2 ± 1.2 cal kyr BP (Groos et al. 2021; Ossendorf et al. 2019). The basal ^{14}C-age of Garba Guracha sediments (15.9–16.7 cal kyr BP) is almost in agreement with the age of deglaciation estimated from cosmogonic ages (Umer et al. 2007; Tiercelin et al. 2008; Bittner et al. 2020). This discrepancy might be due to the ice cover in the *N*-exposed trough valley of Lake Garba Guracha that might have been thicker and thus longer lasting than on the Plateau around the B4 profile, which is strongly wind-exposed and has no ice accumulating catchment (Fig. 1). Besides, methodological uncertainties (exposure dating versus radiocarbon analysis) cannot be ruled out. Nevertheless, the deglaciation age of B4 depression seems reliable.

Our palynological and biogeochemical results record climate fluctuations on the Sanetti Plateau since the end of the LGM. Disregarding the initial phase around 18 cal kyr BP, the environmental conditions during unit 1 can be characterized as predominantly lacustrine, correlating with results from Lake Tanganyika, Challa, and Chew Bahir, which also show predominantly humid conditions (Fig. 8). However, between ~17.2 and 16.9 cal kyr BP partly fluctuating allochthonous elements (Fig. 5), correlating with increased deflation in the northerly dust source areas, and an increase in Chenopodiaceae/Amaranthaceae and reduction in montane forest indicate

a short dry event during this time. Possibly, this event relates to a short weakening of the East-Asian monsoon system as reported by Wang et al. (2001) for Asia around 17 cal kyr BP as a precursor of Heinrich Event 1 (Hemming 2004). Also, Camuera et al. (2021) described such an early H1 phase (refers to HS1b) between 17.2–16.9 cal kyr BP in the Mediterranean. The ~ 300 years of climate deterioration are also weakly documented in sediments of Chew Bahir (Fig. 8) and might be part of the mega-drought postulated for the Afro-Asian monsoon system between 17–16 cal kyr BP (Stager et al. 2011).

We interpret increasing input of allochthonous elements between 16.6 and ca.15.9 cal kyr BP (Fig. 5) as an indicator of the dominance of northerly wind, correlated with progressive ecosystem degradation in the lowlands, and occurring contemporaneously with the North Hemispheric cooling during H1. Interestingly, on the Sanetti Plateau TOC-minima and sand-maxima indicate only short-term intensive desiccation at 16.3 cal kyr BP, and already between ~ 16.1 and 15.7 cal kyr BP TOC and HI increased again, whereas sand contents rapidly decreased (Fig. 4), reflecting that the environmental conditions locally, on the Sanetti Plateau improved, in agreement with the palynological results. This discrepancy between the high altitudes of the Sanetti Plateau and the vast lowlands northerly might reflect that the Bale Mountains, located close to the Indian Ocean, react more rapidly to environmental changes, whereas the lowland ecosystems are much more resilient, due to slow negative vegetation and monsoon feedbacks.

In many studies, arid conditions in tropical Africa between ~ 16.8 and 15.4 cal kyr BP were already described, coinciding with H1 (e.g. Bonnefille and Chalie 2000; Gasse 2000; Talbot and Lærdal 2000; Hemming 2004; Tiercelin et al. 2008; Tierney et al. 2008). Lamb et al. (2007) also mentioned an "episode of shallow water" in the Lake Tana basin between 16.7 and 15.7 cal kyr BP. Based on δD values of higher plant leaf waxes from Lake Challa (Fig. 8), Tierney et al. (2011) concluded that these arid conditions in eastern Africa were due to reduced moisture input from the Indian Ocean. Previous studies described that climatic fluctuations in eastern Africa during the Late Quaternary were related to teleconnections between North Atlantic cooling events, recorded in Greenland ice cores and *N*-Atlantic sediments, and

the weakening of the Indian Summer Monsoon (Tierney et al. 2008; Marshall et al. 2011; Mohtadi et al. 2014; Lamb et al. 2018). It is suggested that during these cooling events, caused by massive iceberg surges and cold meltwater entering the North Atlantic, the ITCZ and the Northern Hemisphere westerlies shifted abruptly southwards and abruptly northward at the end of the cooling, thus controlling deflation of lithogenic elements out of the northern source areas and their input in the surrounding areas (Tierney et al. 2008; Marshall et al. 2009; Lamb et al. 2018). This might explain the high input of allochthonous lithogenic elements (Fig. 5). A similar finding is presented by Brown et al. (2007), reporting elevated inputs of e.g. Zr to Lake Malawi due to intensified northerly winds.

The allochthonous elements decreased abruptly at about 15.7 cal kyr BP, likely correlating with the onset of the AHP, and evoked by rapid northward migration of the rain belt and the ITCZ in relation to precession-driven insolation changes (Bastian et al. 2021). We assume that this resulted in a relatively rapid establishment of a denser vegetation cover and a drastic reduction of dust deflation from northern source areas (Figs. 5 and 8). The timing of this event agrees with the results of Camuera et al. (2021). They concluded that the AHP started in the Mediterranean at 15.7 cal kyr BP after the termination of HS1c. Also, Lamb et al. (2007, 2018), described such an abrupt shift from Lake Tana, and Marshall et al. (2011) dated this event to 15.3 cal kyr BP. In Lake Victoria, the rapid refilling of the basin is dated to 14.5 cal kyr BP (Talbot and Lærdal 2000). One reason for this discrepancy might be dating uncertainties. However, our data from the B4 profile let assume that locally, at the high altitudes of the Sanetti Plateau, the abrupt onset of humidity might have started almost 1000 years before the onset of the Bølling–Allerød warming in the North-Atlantic region (Alley and Clark 1999; Van Raden et al. 2013) and before at least some hundred years earlier than in Lake Tana region, located 630 km northward. In contrast to the sedimentological and geochemical results, our pollen results (Figs. 6 and 7) do not show clear evidence for this abrupt start of the AHP. Within this humid period, water levels in the B4 record did not remain high but lowered already around 15.4 cal kyr BP, and a swamp developed, reflecting probably higher evaporation and less precipitation.

(See figure on next page.)

Fig. 8 A summary figure comparing palynological and biogeochemical results from unit 1 and unit 2 of the B4 sediments with relevant proxies from Lake Tanganyika (Tierney et al. 2008), Lake Challa (Tierney et al. 2011) and Lake Chew Bahir (Foerster et al. 2012) sediments. Light orange color indicate dryer events, orange color indicates a desiccation layer developed during Heinrich Event 1 (H1). Blue color characterizes the African Humid Period (AHP) and other humid episodes while dark green color indicates the event characterized as humid and arid according to pollen and geochemical results, respectively. δD and K values are in inversed scale
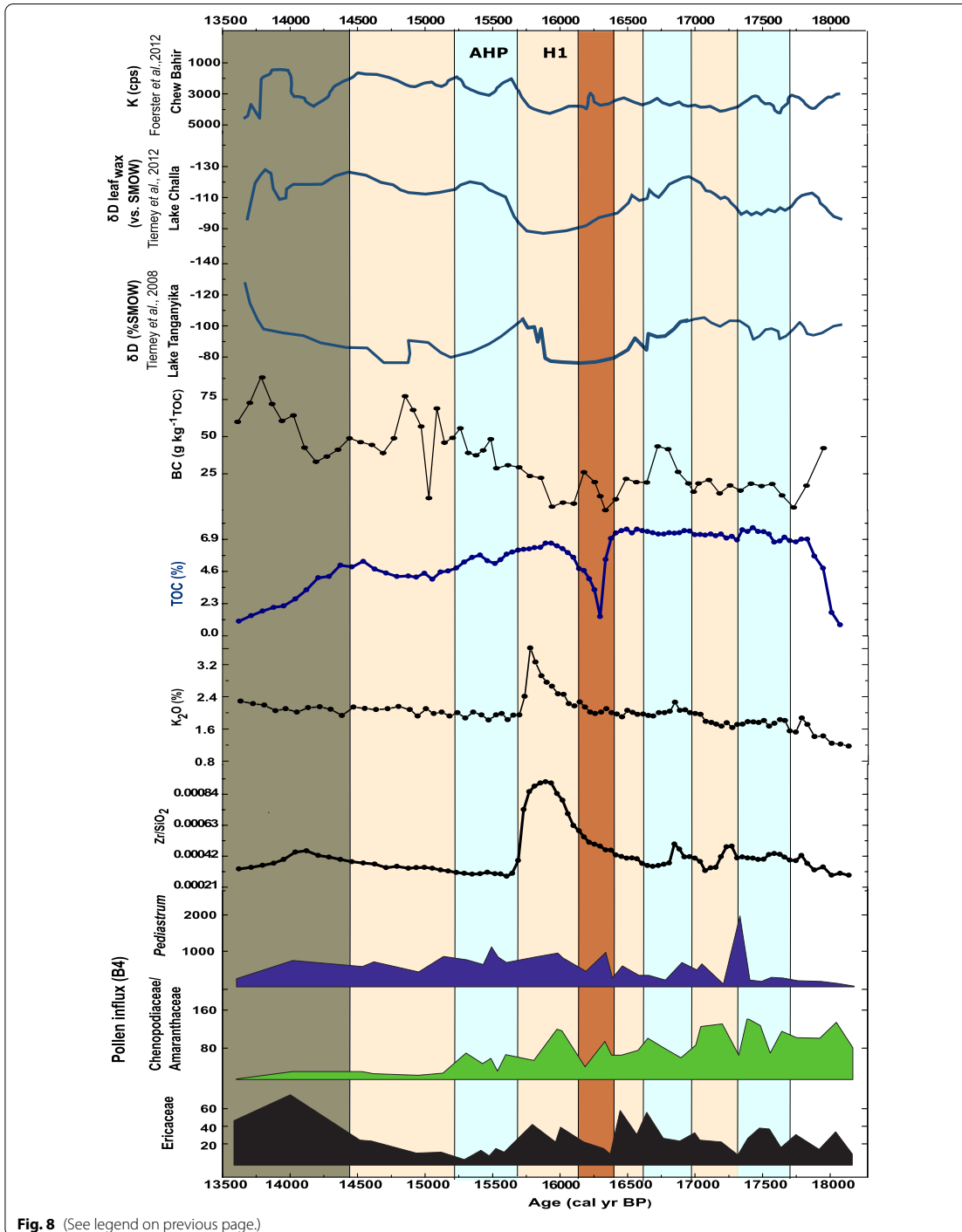
Fig. 8 (See legend on previous page.)

A similar finding was reported from Lake Tana, where a papyrus swamp developed between 15.7 and 15.1 cal kyr BP, due to lower lake levels and reduced rainfall (Lamb et al. 2007). Slightly rising allochthonous proxies (e.g. Zr, Nb, Hf, see Fig. 5) likely document progressive local drying-up after about 14.4 cal kyr BP, whereas ascending arboreals indicate regional wetter conditions (Fig. 7). The uppermost part of the unit 2 sediments, deposited between ~ 14.4–13.6 cal kyr BP, is enriched in arboreal pollen, reflecting regional wetting; but fluctuating sand contents and higher input of terrestrial alkanes let assume that drying-up of the B4 depression by advanced periodic sediment input continued. These processes do not allow a reliable correlation of the environmental dynamics affecting the Sanetti Plateau with those documented in sediments of Lake Tanganyika, Challa, and Chew Bahir (Fig. 8); also an unambiguous relationship with climatic phenomena known from the North Atlantic region (e.g. Allerød) cannot be identified in the upper part of unit 2.

5.2 Vegetation
The B4 pollen record allows the reconstruction of vegetation changes from 18.1 to 13.6 cal kyr BP. Between 18.1 and 16.8 cal kyr BP, the vegetation is characterized as herb-rich grassland with Chenopodiaceae/Amaranthaceae. Plantago maxima between 17.2–16.9 cal kyr BP are related to dry and/or cold environmental conditions (see Section 4.4). These results are roughly in agreement with Umer et al. (2007), reporting open grassland vegetation at 16 cal kyr BP around Lake Garba Guracha. Our pollen record further shows high Arboreals such as *Podocarpus, Hygenia, Erica,* and *Juniperus* at 16.9 cal kyr BP, indicating more favorable conditions, in agreement with the sedimentological data. Increased aridity between 16.6 and 15.7 cal kyr BP, well documented by most biogeochemical proxies and interpreted to correlate with H1, is not clearly revealed in the palynological data. The desiccation surface developed around ~ 16.3 cal kyr BP correlates with decreased contents of *Erica* pollen, *Pediastrum*, ferns, and *Botryococcus*, and elevated Chenopodiaceae/Amaranthaceae ratios, indicating a temporary phase of less favorable, drier environmental conditions. This possibly marks the time of maximum H1 dryness. Similarly, the AHP, recorded by biogeochemical proxies, is not obvious in the pollen results. Our data show that Ericaceae pollen content considerably increased on the Sanetti Plateau from 14.4 to 13.6 cal kyr BP, likely correlating with an increase in temperature, which might be synchronous with the European Meiendorf interstadial starting at 14.4 varve years (Litt et al. 2001). According to pollen results from Lake Garba Guracha and peat

deposits, Umer et al. (2007) and Kuzmicheva et al. (2014) assume that *Erica* vegetation expanded on the Sanetti Plateau above the actual upper limit of the *Erica* belt, only during the early Holocene beginning at 11.2 cal kyr BP. The dry climate during mid to Late Holocene and natural and/or human-induced fires (Miehe and Miehe 1994) are suggested as major causes for the decline of *Erica* which at present exists above the upper line of the *Erica* belt only in form of isolated fragments, mainly restricted to slopes rich in basalt boulders. Furthermore, Miehe and Miehe (1994) assumed that these *Erica* patches are relics that document an intensive extension of *Erica* species on the Sanetti Plateau after deglaciation, which were later on destroyed because of the invasion of hunter-gatherers and pastoralists. However, since the upper timberline is temperature-controlled (Körner 2008), we hypothesize these *Erica* patches on the plateau survive due to better microclimate, generated by dark basalt boulders.

5.3 Fire dynamics on the Sanetti Plateau
Our black carbon results (Fig. 4) show that fire was a common phenomenon in the Bale Mountains even during the early Late Glacial. However, pollen data indicate that at this time *Erica* was not growing around the B4 depression (Fig. 8). Therefore, BC in the lower part of the B4 profile likely originates from other vegetation fires or the *Erica* belt in lower altitudes. This interpretation is supported by the fact that BC, even in the dry mode H1 sediments, is not clearly increased. Only with the beginning of the AHP around 15.7 cal kyr BP, BC started to increase, correlating with warmer and more humid environmental conditions, and reaching a maximum at about 15 cal kyr BP coinciding with increasing *Erica* pollen. In the uppermost part of unit 2 (70–80 cm) *Erica* pollen further increased, again correlating with maximum BC at about 13.6 cal kyr BP.

Up to now, despite the human invasion during 47–31 cal kyr BP, there is no evidence that during the Late Glacial hunter-gatherers were living on the plateau and burned the *Erica* to facilitate hunting. However, we cannot rule out that fires were triggered by the increase of easily combustible *Erica* biomass due to improved environmental conditions. For a different time period, but in connection with the fuel-controlled fire process, the charcoal record from Garba Guracha supports a strong correlation between fire occurrence and heathland expansion during the Holocene (Gil-Romera et al. 2019). Elevated BC in the early humid Holocene deposits of the B4 record (not shown here) supports our interpretation that the burning of *Erica* is mainly controlled by the amount of *Erica* biomass, being higher under warm and humid climates.

6 Conclusions

Our high altitude sedimentary archive provides a new older deglaciation age of 18.2 cal kyr BP for the Sanetti Plateau. Biogeochemical results show that the Plateau was sensitive to local, regional and global climate changes. We detected a severe local drought event on the Sanetti Plateau at ∼16.3 cal kyr BP with complete desiccation of the past B4 lake for some decades, related to H1. Between ∼16.6 and 15.7 cal kyr BP allochthonous elements like Zr, Hf, Nd, Nb, Na, presumably windblown by dry northerly winds during H1, accumulated increasingly in the B4 record, indicating continuous but delayed degradation of the wind source areas in lower altitudes but without documenting maximum dryness at 16.3 cal kyr BP. This is in contrast to our high altitude B4 archive and reflects the resilience of the lowland ecosystems. The Abrupt change to humid conditions at ∼15.7 cal kyr BP indicates the onset of AHP in the Bale Mountains some hundred years earlier than in the Lake Tana region but in agreement with the termination of the HS1c phase in the Mediterranean.

The vegetation on the Sanetti Plateau was less sensitive to increased aridity during H1 and also to increased humidity during AHP. Nevertheless, the *Erica* pollen increased in the B4 sediments at ∼14.4 cal kyr BP, correlating with a wet and warm regional climate. Despite this increase, it remains open whether the Ericaceous belt expanded to the plateau during that time or during the early Holocene, except for the currently existing isolated patches on boulder-rich steep slopes. Our results indicate that fire incidences mainly coincide with an expansion of the vegetation cover and less with dry periods. Most likely, a warm and humid climate promotes biomass production of *Erica*, hence increasing the amount of fuel, which burns from time to time. This allows to conclude that biomass and thus fuel availability is important factor controlling fire events in the Bale Mountains.

Abbreviations

AHP: African humid period; A/C: Artemisia/Chenopodiaceae; AP: Arboreal pollen; BC: Black carbon; BPCAs: Benzene polycarboxylic acids; CPA: Chemical proxy of alteration; DCM: Dichloromethane; FID: Flame ionization detector; GC: Gas chromatography; H1: Heinrich event 1; HI: Hydrogen index; LGM: Last Glacial Maximum; NPA: Non-arboreal pollen; XRF: X-ray fluorescence; YD: Younger Dryas.

Supplementary Information

The online version contains supplementary material available at https://doi.org/10.1186/s40645-022-00472-9.

Additional file 1. Grain size distribution (clay < 6.3 μm, silt 6.3–63 μm and sand 63-2000 μm), electrical conductivity (EC), pH, and depth profiles of SiO$_2$ of the B4 sediments. Light orange color indicates drier event while orange color indicates desiccation during H1 and the hiatus. Blue colors characterize the AHP and other humid episodes while dark green color

indicate the event characterized as humid and arid according to pollen and geochemical results, respectively.

Additional file 2. PCA biplot results based on geochemical compounds of the B4 sediments in unit 1 and unit 2. In this figure 63.5% of variance is explained (component 1 = 45.5% and component 2 = 18%). The two ellipses show the cluster of our samples based on the stratigraphic units. The arrows indicate each proxy and the distance between each arrow exhibits the strength of the correlation between elements and compounds. While SiO$_2$, MnO, P$_2$O$_5$ and Ba contents are high in unit 1, unit 2 is characterized by high Zr, Hf, Sm, Nd, Ce, Y and Na$_2$O values. However, MgO, Al$_2$O$_3$, TiO$_2$, Cu, Cr, Rb, Sr, Sc etc. are very low in both units.

Additional file 3. A table showing mineralogical results of selected samples from the B4 profile.

Declarations

Competing interests
The authors declare that they have no competing interest.

Author details
[1]Institute of Agricultural and Nutritional Sciences, Soil Biogeochemistry, Martin Luther University Halle-Wittenberg, Halle, Germany. [2]Department of Urban Agriculture, Misrak Polytechnic College, Addis Ababa, Ethiopia. [3]Institute of Geography, Friedrich-Schiller-University Jena, Jena, Germany. [4]Institute of Geography, Technische Universität Dresden, Dresden, Germany. [5]Lower Saxony Institute for Historical Coastal Research, Wilhelmshaven, Germany. [6]Department of Palynology and Climate Dynamics, Albrecht-Von-Haller Institute for Plant Sciences, Gottingen University, Göttingen, Germany. [7]Institute of Applied Geosciences, TU Berlin, Berlin, Germany. [8]Department of Natural Resource Management, Jigjiga University, Jigjiga, Ethiopia. [9]Department of Geo-Environmental Processes and Global Change, Pyrenean Institute of Ecology, CSIC, Zaragoza, Spain. [10]Department of Plant Biology and Biodiversity Management, Addis Ababa University, Addis Ababa, Ethiopia. [11]International Livestock Research Institute, Addis Ababa, Ethiopia. [12]Department of Soil Science, University of Bayreuth, Bayreuth, Germany.

References

Alley RB, Clark PU (1999) The deglaciation of the northern hemisphere: a global perspective. Annu Rev Earth Planet Sci 27:149–182

Antoine P, Rousseau D-D, Moine O, Kunesch S, Hatte C, Lang A, Tissoux H, Zoller L (2009) Rapid and cyclic aeolian deposition during the Last Glacial in European loess: a high-resolution record from Nussloch, Germany. Quat Sci Rev 28:2955–2973. https://doi.org/10.1016/j.quascirev.2009.08.001

Bastian L, Mologni C, Vigier N, Bayon G, Lamb H, Bosch D, Kerros ME, Colin C, Revel M (2021) Co-variations of climate and silicate weathering in the Nile Basin during the Late Pleistocene. Quat Sci Rev 264:107012. https://doi.org/10.1016/j.quascirev.2021.107012

Berner RA (1984) Sedimentary pyrite formation: an update. Geochim Cosmochim Acta 48(4):605–615. https://doi.org/10.1016/0016-7037(84)90089-9

Beug HJ. Pollen profile from site Kolbermoor5, Rosenheim, Oberbayern, Germany, Pangaea. 2004. https://doi.org/10.1594/PANGAEA.142583.

Billi P (2015) Geomorphological landscapes of Ethiopia. In: Billi P (ed) Landscapes and landforms of Ethiopia. Springer, pp 3–32. https://doi.org/10.1007/978-94-017-8026-1_1

Bittner L, Bliedtner M, Grady D, Gil-Romera G, Martin-Jones C, Lemma B, Mekonnen B, Lamb HF, Yang H, Glaser B, Szidat S, Salazar G, Rose NL, Opgenoorth L, Miehe G, Zech W, Zech M (2020) Revisiting afro-alpine Lake Garba Guracha in the Bale Mountains of Ethiopia: rationale, chronology, geochemistry, and paleoenvironmental implications. J Paleolimnol. https://doi.org/10.1007/s10933-020-00138-w

Blaauw M, Christen JA (2011) Flexible paleoclimate age-depth models using an autoregressive gamma process. Bayesian Anal 6(3):457–474. https://doi.org/10.1214/11-BA618

Bonnefille R, Chalie F (2000) Pollen-inferred precipitation time-series from equatorial mountains, Africa, the last 40 kyr BP. Glob Planet Change 26(1–3):25–50. https://doi.org/10.1016/S0921-8181(00)00032-1

Bonnefille R, Mohammed U (1994) Pollen-inferred climatic fluctuations in Ethiopia during the last 3000 years. Palaeogeogr Palaeoclimatol Palaeoecol 109(2–4):331–343. https://doi.org/10.1016/0031-0182(94)90183-X

Brodowski S, Rodionov A, Haumaier L, Glaser B, Amelung W (2005) Revised black carbon assessment using benzene polycarboxylic acids. Org Geochem 36(9):1299–1310. https://doi.org/10.1016/j.orggeochem.2005.03.011

Brown ET, Johnson TC, Scholz CA, Cohen AS, King JW (2007) Abrupt change in tropical African climate linked to the bipolar seesaw over the past 55,000 years. Geophys Res Lett 34:1–5. https://doi.org/10.1029/2007GL031240

Buggle B, Glaser B, Hambach U, Gerasimenko N, Marković S (2011) An evaluation of geochemical weathering indices in loess-paleosol studies. Quat Int 240(1–2):12–21. https://doi.org/10.1016/j.quaint.2010.07.019

Bussmann RW (1997) The forest vegetation of Harenna escarpment (Bale Province, Ethiopia)—syntxomomy and phytogeographical affinities. Phytocoenologia 1(27):1–23

Camberlin P (2018) Climate of Eastern Africa. Oxford research Encyclopedia of climate science. Oxford University Press

Camuera J, Jiménez-Moreno G, Ramos-Román MJ, García-Alix A, Jiménez-Espejo FJ, Toney JL, Anderson RS (2021) Chronological control and centennial-scale climatic subdivisions of the Last Glacial Termination in the western Mediterranean region. Quat Sci Rev 255(March):106814. https://doi.org/10.1016/j.quascirev.2021.106814

Conrad R, Chan OC, Claus P, Casper P (2007) Characterization of methanogenic Archaea and stable isotope fractionation during methane production in the profundal sediment of an oligotrophic lake (Lake Stechlin, Germany). Limniology Oceanogr 54(2):1–14

Costa K, Russell J, Konecky B, Lamb H (2014) Isotopic reconstruction of the African Humid Period and Congo Air Boundary migration at Lake Tana, Ethiopia. Quat Sci Rev 83:58–67. https://doi.org/10.1016/j.quascirev.2013.10.031

Davies SJ, Lamb HF, Roberts SJ (2015) Micro-XRF core scanning in palaeolimnology: recent developments, micro-XRF. Springer

Eshetu Z (2002) Historical C3–C4 vegetation pattern on forested mountain slopes: its implication for ecological rehabilitation of degraded highlands of Ethiopia by afforestation. J Trop Ecol 18(5):743–758. https://doi.org/10.1017/S0266467402002481

Ficken KJ, Li B, Swain DL, Eglinton G (2000) An n-alkane proxy for the sedimentary input of submerged/floating freshwater aquatic macrophytes. Org Geochem 31:745–749. https://doi.org/10.1038/nmat4240

Ficken KJ, Wooller MJ, Swain DL, Street-Perrott FA, Eglinton G (2002) Reconstruction of a subalpine grass-dominated ecosystem, Lake Rutundu, Mount Kenya: a novel multi-proxy approach. Palaeogeogr Palaeoclimatol Palaeoecol 177(1–2):137–149. https://doi.org/10.1016/S0031-0182(01)00356-X

Foerster V, Foerster V, Junginger A, Langkamp O, Gebru T, Asrat A (2012) Climatic change recorded in the sediments of the Chew Bahir basin, Southern Ethiopia, during the last 45,000 years Climatic change recorded in the sediments of the Chew Bahir basin, southern Ethiopia, during the last 45,000 years. Quat Int 274:25–37. https://doi.org/10.1016/j.quaint.2012.06.028

Friis I (1986) Zonation of forest vegetation on the south slope of Bale Mountains, South Ethiopia. Ethiop J Sci 9(12):29–44

Gasse F (2000) Hydrological changes in the African tropics since the Last Glacial Maximum. Quat Sci Rev 19:189–211

Gil-Romera G, Adolf C, Benito BM, Bittner L, Johansson MU, Grady DA, Lamb HF, Lemma B, Fekadu M, Glaser B, Mekonnen B, Sevilla-Callejo M, Zech M, Zech W, Miehe G (2019) Long-term fire resilience of the Ericaceous Belt, Bale Mountains, Ethiopia. Biol Lett 15(7):20190357. https://doi.org/10.1098/rsbl.2019.0357

Glaser B, Zech W (2005) Reconstruction of climate and landscape changes in a high mountain lake catchment in the Gorkha Himal, Nepal during the Late Glacial and Holocene as deduced from radiocarbon and compound-specific stable isotope analysis of terrestrial, aquatic and microbi. Org Geochem 36:1086–1098. https://doi.org/10.1016/j.orggeochem.2005.01.015

Glaser B, Haumaier L, Guggenberger G, Zech W (1998) Black carbon in soils: the use of benzenecarboxylic acids as specific markers. Org Geochem 29(4):811–819. https://doi.org/10.1016/S0146-6380(98)00194-6

Gosling WD, Miller CS, Livingstone DA (2013) Atlas of the tropical West African pollen flora. Rev Palaeobot Palynol 199:1–135. https://doi.org/10.1016/j.revpalbo.2013.01.003

Grice K, Audino M, Boreham CJ, Alexander R, Kagi Rl (2001) Distributions and stable carbon isotopic compositions of biomarkers in torbanites from different palaeogeographical locations. Org Geochem 32(10):1195–1210. https://doi.org/10.1016/S0146-6380(01)00087-0

Groos AR, Akçar N, Yesilyurt S, Miehe G (2021) Nonuniform Late Pleistocene glacier fluctuations in tropical Eastern Africa. Sci Adv. https://doi.org/10.1126/sciadv.abb6826

Hailemariam SN, Soromessa T, Teketay D (2016) Land use and land cover change in the bale mountain eco-region of Ethiopia during 1985 to 2015. Land 5(4):41. https://doi.org/10.3390/land5040041

Hedberg O (1951) Vegetation belts of the East African Mountains. Results of the Swedish East African expedition. Sven Bot Tidskr 45:1–144

Hemming SR (2004) Heinrich events: massive late pleistocene detritus layers of the North Atlantic and their global climate imprint. Rev Geophys. https://doi.org/10.1029/2003RG000128.1

Hemming SR (2007) Terrigenous sediments. In: Elias SA (ed) Encyclopedia of quaternary science, vol 3. Elsevier, pp 1776–1785

Herzschuh U (2007) Reliability of pollen ratios for environmental reconstructions on the Tibetan Plateau. J Biogeogr 34(7):1265–1273. https://doi.org/10.1111/j.1365-2699.2006.01680.x

Hillman JC (1986) Conservation in Bale Mountains National Park, Ethiopia. Oryx 20(2):89–94. https://doi.org/10.1017/S0030605300026314

Hillman JC (1988) The Bale Mountains National Park Area, Southeast Ethiopia, and its management. Mt Res Dev 8(2):253–258

Hoggard RK, Kores PJ, Molvray M, Hoggard GD, Broughton DA (2003) Molecular systematics and biogeography of the amphibious genus Littorella (Plantaginaceae). Am J Bot 90(3):429–435. https://doi.org/10.3732/ajb.90.3.429

Jan F, Schüler L, Behling H (2015) Trends of pollen grain size variation in C3 and C4 Poaceae species using pollen morphology for future assessment of grassland ecosystem dynamics. Grana 54(2):129–145. https://doi.org/10.1080/00173134.2014.966754

Jankovská V, Komárek J (2000) Indicative value of Pediastrum and other coccal green algae in palaeoecology. Folia Geobot 35(1):59–82. https://doi.org/10.1007/BF02803087

Jimenez-Espejo FJ et al (2014) Saharan aeolian input and effective humidity variations over western Europe during the Holocene from a high altitude record. Chem Geol 374–375:1–12

Mekonnen *et al. Progress in Earth and Planetary Science*   (2022) 9:14

Page 18 of 19

Juggins S (2007) C2 user guide. Software for ecological and palaeoecological data analysis and visualisation. University of Newcastle

Kidane Y, Stahlmann R et al (2012) Vegetation dynamics, and land use and land cover change in the Bale Mountains, Ethiopia. Environ Monit Assess 184(12):7473–7489. https://doi.org/10.1007/s10661-011-2514-8

Körner C (2008) Winter crop growth at low temperature may hold the answer for alpine tree line formation. Plant Ecol Divers 1(1):3–11. https://doi.org/10.1080/17550870802273411

Kuzmicheva EA, Debella H, Khasanov B, Krylovich O, Babenko A, Savinetsky A, Severova E, Yirga S (2013) Holocene hyrax dung deposits in the afroalpine belt of the Bale Mountains (Ethiopia) and their palaeoclimatic implication. Environ Archaeol 18(1):72–81. https://doi.org/10.1179/1461410313Z.00000000018

Kuzmicheva EA, Khasanov BF, Krylovich OA, Savinetsky AB (2014) Vegetation and climate reconstruction for the bale mountains (Ethiopia) in the Holocene according to the pollen analysis and radiocarbon dating of zoogenic deposits. Dokl Biol Sci 458(1):281–285. https://doi.org/10.1134/S0012496614050019

Kuzyakov Y, Bogomolova I, Glaser B (2014) Biochar stability in soil: decomposition during eight years and transformation as assessed by compound-specific ^{14}C analysis. Soil Biol Biochem 70:229–236. https://doi.org/10.1016/j.soilbio.2013.12.021

Lamb HF, Bates CR, Coombes PV, Marshall MH, Umer M, Davies SJ, Dejen E (2007) Late Pleistocene desiccation of Lake Tana, source of the Blue Nile. Quat Sci Rev 26:287–299. https://doi.org/10.1016/j.quascirev.2006.11.020

Lamb HF, Bates CR, Bryant CL, Davies SJ, Huws DG, Marshall MH, Roberts HM, Toland H (2018) 150,000-year palaeoclimate record from northern Ethiopia supports early, multiple dispersals of modern humans from Africa. Nature. https://doi.org/10.1038/s41598-018-19601-w

Last MW, Smol PJ (2002) Tracking environmental change using lake sediments. Physical and geochemical methods, 2nd edn. Kluwer Acadamic Publishers

Lemma B, Kebede Gurmessa S, Nemomissa S, Otte I, Glaser B, Zech M (2020) Spatial and temporal ^{2}H and ^{18}O isotope variation of contemporary precipitation in the Bale Mountains, Ethiopia. Isotopes Environ Health Stud 56(2):122–135. https://doi.org/10.1080/10256016.2020.1717487

Levin NE, Zipser EJ, Ceding TE (2009) Isotopic composition of waters from Ethiopia and Kenya: insights into moisture sources for eastern Africa. J Geophys Res Atmos 114(23):1–13. https://doi.org/10.1029/2009JD012166

Li F, Sun J, Zhao Y, Guo X, Zhao W, Zhang K (2010) Ecological significance of common pollen ratios: a review. Front Earth Sci China 4(3):253–258. https://doi.org/10.1007/s11707-010-0112-7

Litt T, Brauer A, Goslar T, Merkt J, Bałaga K, Müller H, Ralska-Jasiewiczowa M, Stebich M, Negendank JFW (2001) Correlation and synchronisation of Lateglacial continental sequences in northern central Europe based on annually laminated lacustrine sediments. Quat Sci Rev 20(11):1233–1249. https://doi.org/10.1016/S0277-3791(00)00149-9

Mark BG, Osmaston HA (2008) Quaternary glaciation in Africa: key chronologies and climatic implications. J Quat Sci 23(6–7):589–608. https://doi.org/10.1002/jqs.1222

Marshall JD, Brooks JR, Lajtha K (2007) Sources of variation in the stable isotopic composition of plants, 2nd edn. Blackwell Publishing

Marshall MH, Lamb HF, Huws D, Davies SJ, Bates R, Bloemendal J, Boyle J, Leng MJ, Umer M, Bryant C (2011) Late Pleistocene and Holocene drought events at Lake Tana, the source of the Blue Nile. Glob Planet Change 78(3–4):147–161. https://doi.org/10.1016/J.GLOPLACHA.2011.06.004

Mekonnen B, Zech W, Glaser B, Lemma B, Bromm T, Nemomissa S, Bekele T, Zech M (2019) Chemotaxonomic patterns of vegetation and soils along altitudinal transects of the Bale Mountains, Ethiopia, and implications for paleovegetation reconstructions—part I: stable isotopes and sugar biomarkers. E&G Quat Sci J 68(2):177–188. https://doi.org/10.5194/egqsj-68-189-2019

Messerli B (1980) Mountain glaciers in the Mediterranean area and in Africa. World Glacier Invent Work Publ 126:197–211

Messerli B, Winiger M (1992) Climate, environmental change, and resources of the African mountains from the Mediterranean to the equator. Mt Res Dev 12(4):315. https://doi.org/10.2307/3673683

Meyers PA (1994) Preservation of elemental and isotopic source identification of sedimentary organic matter. Chem Geol 114(3–4):289–302. https://doi.org/10.1016/0009-2541(94)90059-0

Miehe G, Miehe S (1994) Ericaceous forests and heathlands in the Bale Mountains of South Ethiopia: ecology and man's impact. Warnke

Mohtadi M, Prange M, Oppo DW, De Pol-Holz R, Merkel U, Zhang X, Steinke S, Lückge A (2014) North Atlantic forcing of tropical Indian Ocean climate. Nature 508(7498):76–80. https://doi.org/10.1038/nature13196

Monnin E, Indermühle A, Dällenbach A, Flückiger J, Stauffer B, Stocker TF, Raynaud D, Barnola JM (2001) Atmospheric CO_2 concentrations over the last glacial termination. Science 291(5501):112–114. https://doi.org/10.1126/science.291.5501.112

Moreno T, Querol X, Castillo S, Alastuey A, Cuevas E, Herrmann L, Mounkaila M, Elvira J, Gibbons W (2006) Geochemical variations in aeolian mineral particlesfrom the Sahara-Sahel Dust Corridor. Chemosphere 65:261–270

Nicholson SE (2000) The nature of rainfall variability over Africa on time scales of decades to millenia. Glob Planet Change 26(1–3):137–158. https://doi.org/10.1016/S0921-8181(00)00040-0

Osmaston HA, Mitchell WA, Osmaston JAN (2005) Quaternary glaciation of the Bale Mountains. J Quat Sci, Ethiopia. https://doi.org/10.1002/jqs.931

Ossendorf G, Groos AR, Bromm T, Tekelemariam MG, Glaser B, Lesur J, Schmidt J, Akçar N, Bekele T, Beldados A, Demissew S, Kahsay TH, Nash BP, Nauss T, Negash A, Nemomissa S, Veit H, Vogelsang R, Woldu Z, Zech W, Opgenoorth L, Miehe G (2019) Middle stone age foragers resided in high elevations of the glaciated Bale Mountains, Ethiopia. Science 365(6453):583–587. https://doi.org/10.1126/science.aaw8942

R Core Team. R: a language and environment for statistical computing. R Foundation for Statistical Computing; 2013. http://www.R-project.org.

Scheuvens D, Schütz L, Kandler K, Ebert M, Weinbruch S (2013) Bulk composition of northern African dust and its source sediments—a compilation. Earth Sci Rev 116:170–194. https://doi.org/10.1016/j.earscirev.2012.08.005

Schüler L, Hemp A (2016) Atlas of pollen and spores and their parent taxa of Mt Kilimanjaro and tropical East Africa. Quat Int 425:301–386. https://doi.org/10.1016/j.quaint.2016.07.038

Stager JC, Ryves DB, Chase BM, Pausata FSR (2011) Catastrophic drought in the Afro-Asian monsoon region during Heinrich event 1. Science 331(6022):1299–1302. https://doi.org/10.1126/science.1198322

Stockmarr J. Tablets with spores used in absolute pollen analysis. Pollen et Spores XIII: 615–621; 1971.

Talbot MR, Lærdal T (2000) The Late Pleistocene–Holocene palaeolimnology of Lake Victoria, East Africa, based upon elemental and isotopic analyses of sedimentary organic matter. J Paleolimnol 23(2):141–164. https://doi.org/10.1023/A:1008029400463

Talbot MR, Livingstone DA (1989) Hydrogen index and carbon isotopes of lacustrine organic matter as lake level indicators. Palaeogeogr Palaeoclimatol Palaeoecol 70:121–137

Thompson LG, Mosley-Thompson E, Davis ME, Henderson KA, Brecher HH, Zagorodnov VS, Mashiotta TA, Lin PN, Mikhalenko VN, Hardy DR, Beer J (2002) Kilimanjaro ice core records: evidence of holocene climate change in tropical Africa. Science 298(5593):589–593. https://doi.org/10.1126/science.1073198

Tiercelin JJ, Gibert E, Umer M, Bonnefille R, Disnar JR, Lézine AM, Hureau-Mazaudier D, Travi Y, Keravis D, Lamb HF (2008) High-resolution sedimentary record of the last deglaciation from a high-altitude lake in Ethiopia. Quat Sci Rev 27(5–6):449–467. https://doi.org/10.1016/j.quascirev.2007.11.002

Tierney JE, DeMenocal PB (2013) Abrupt shifts in Horn of Africa hydroclimate since the last glacial maximum. Science 342(6160):843–846. https://doi.org/10.1126/science.1240411

Tierney JE, Russell JM, Huang Y, Damsté JSS, Ellen C, Cohen AS (2008) Northern hemisphere controls on tropical southeast African climate during the past 60,000 years. Science 322:252–255. https://doi.org/10.1016/j.epsl.2011.04.038,2011

Tierney JE, Lewis SC, Cook BI, Legrande AN, Schmidt GA (2011) Model, proxy and isotopic perspectives on the East African Humid Period. Earth Planet Sci Lett 307(1–2):103–112. https://doi.org/10.1016/j.epsl.2011.04.038

Umer M, Lamb HF, Bonnefille R, Lézine AM, Tiercelin JJ, Gibert E, Cazet JP, Watrin J (2007) Late Pleistocene and Holocene vegetation history of the Bale Mountains, Ethiopia. Quat Sci Rev 26(17–18):2229–2246. https://doi.org/10.1016/j.quascirev.2007.05.004

Van Campo E, Gasse F (1993) Pollen- and diatom-inferred climatic and hydrological changes in sumxi co basin (western tibet) since 13,000 yr B.P. Quat Res 39:300–313

Van Raden UJJ, Colombaroli D, Gilli A, Schwander J, Bernasconi SM, van Leeuwen J, Leuenberger M, Eicher U (2013) High-resolution late-glacial chronology for the Gerzensee lake record (Switzerland): δ^{18}O correlation between a Gerzensee-stack and NGRIP. Palaeogeogr Palaeoclimatol Palaeoecol 391:13–24. https://doi.org/10.1016/j.palaeo.2012.05.017

Wang X, Li A (2007) Preservation of black carbon in the shelf sediments of the East China Sea. Chin Sci Bull 52(22):3155–3161. https://doi.org/10.1007/s11434-007-0452-1

Wang YJ, Cheng H, Edwards RL, An ZS, Wu JY, Shen CC, Dorale JA (2001) A high-resolution absolute-dated late pleistocene monsoon record from Hulu Cave, China. Science 294(5550):2345–2348. https://doi.org/10.1126/science.1064618

Wiedemeier DB, Abiven S, Hockaday WC, Keiluweit M, Kleber M, Masiello CA, McBeath AV, Nico PS, Pyle LA, Schneider MPW, Smernik RJ, Wiesenberg GLB, Schmidt MWI (2015) Aromaticity and degree of aromatic condensation of char. Org Geochem 78:135–143. https://doi.org/10.1016/j.orggeochem.2014.10.002

Yimer F, Ledin S, Abdelkadir A (2006) Soil property variations in relation to topographic aspect and vegetation community in the south-eastern highlands of Ethiopia. For Ecol Manag 232(1–3):90–99. https://doi.org/10.1016/j.foreco.2006.05.055

Yineger H, Kelbessa E, Bekele T, Lulekal E (2008) Floristic composition and structure of the dry afromontane forest at Bale Mountains National Park, Ethiopia. J Sci 31(2):103–120. https://doi.org/10.4314/sinet.v31i2.66551

Zech M, Glaser B (2008) Improved compound-specific δ^{13}C analysis of n-alkanes for application in palaeoenvironmental studies. RAPID Commun Mass Spectrom 22:135–142. https://doi.org/10.1002/rcm.3342

Publisher's Note

Springer Nature remains neutral with regard to jurisdictional claims in published maps and institutional affiliations.

Manuscript 5: Factors determining the distribution of *Erica* patches on the Sanetti Plateau, Bale Mountains, Ethiopia

ORIGINAL ARTICLE

Factors determining the distribution of *Erica* patches on the Sanetti Plateau, Bale Mountains, Ethiopia

Betelhem Mekonnen[1,2] · Bruno Glaser[1] · Michael Zech[3] · Tobias Bromm[1] · Sileshi Nemmomisa[4] · Tamrat Bekele[4] · Wolfgang Zech[2]

Abstract

In the Bale Mountains, the ericaceous belt ranges between 3200 and 3800 m asl. Studies indicate an expansion on the Sanetti Plateau at the end of the Late Glacial and during the early Holocene. Currently, only patches of *Erica* growing between boulders are found on the Plateau, while most of the landscape above 3800 m asl is covered by afro-alpine plants. Driving factors for *Erica* patches above the upper ericaceous ecotone is a matter of debate. This study evaluates site variables and biogeochemical properties of soils under *Erica* patches and nearby *Erica*-free control to understand the environmental conditions responsible for the patchy occurrence of *Erica* on the Sanetti Plateau. Except for the boulder richness, *Erica* and control plots have comparable topography, soil texture, and electrical conductivity. However, soils below *Erica* patches have higher total organic carbon, nitrogen, carbon-to-nitrogen ratios, and black carbon contents than the control plots indicating fresh organic matter input and availability of combustible fuel. This implies that *Erica* did not fully cover the control plots in former times. Carbon and nitrogen stocks were slightly higher in control plots due to the lower stone contents of the profiles. In addition, soils of the *Erica* plots showed more positive δ^{13}C values than the control soils, possibly attributed to water stress. In general, the relief and soil conditions of control plots may support the growth of *Erica*. However, *Erica* growing between boulders seems to benefit from the favorable microclimate and physical protection against grazing and fire.

Keywords *Erica* patches · Environmental factors · Fire · Boulders · Sanetti Plateau · Ethiopia · Bale Mountains

Introduction

Defining the tree line ecotone of high-elevation vegetation is often problematic and debatable as it is difficult to unambiguously identify and quantify the factor that plays the most significant role (Körner 2007; Jacob et al. 2015). Such difficulties have been observed in the East African Mountains, which are vulnerable to climate change and

✉ Betelhem Mekonnen
  betymekonnen19@gmail.com

1 Institute of Agricultural and Nutritional Sciences, Soil Biogeochemistry, Martin Luther University Halle-Wittenberg, Halle, Germany

2 Department of Soil Science, University of Bayreuth, Bayreuth, Germany

3 Institute of Geography, Technical University of Dresden, Dresden, Germany

4 Department of Plant Biology and Biodiversity Management, Addis Ababa University, Addis Ababa, Ethiopia

anthropogenic impacts (Wesche et al. 2000; Jacob et al. 2015). *Erica*, also known as heathers or heath, is one of the most widely distributed plant genera in the Ericaceae family (Oliver 1989; Kron et al. 2002). Its geographical distribution covers Europe, the Middle East, South America, and Africa (Mcguire and Kron 2011). *Erica* species (*Erica trimera* and *Erica arborea*) dominate and characterize most high-elevation mountains in eastern Africa, forming the upper tree line forest (Hedberg 1951; Wesche et al. 2000; Fetene et al. 2006). Ericaceous vegetation is widespread in northern (Siemen Mountains) and southern Ethiopia (Bale Mountains, Mt. Chillalo, Mt. Kaka, Galama Mountains, and Arsi highlands) (Hedberg 1951; Miehe and Miehe 1994). In the Bale Mountains, the ericaceous belt covers an area of 90,000 ha and spans between 3200 and 3800 m asl (Miehe and Miehe 1994). According to Fetene et al. (2006), the ericaceous vegetation is grouped into three elevational subzones. The lower subzone is characterized by the *Erica*-dominated *Hagenia-Hypericum* forest, which spans between 3000 and 3400 m asl. The central part covers the elevation

between 3400 and 3600 m asl; dominated by *Erica trimera*, *Hypericum revolutum,* and *Alchemilla abyssinica*. In the upper subzone between 3600 and 4200 m asl, the Erica-ceous vegetation has a patchy appearance, especially at the Sanetti Plateau between 3800 and 4200 m asl. Such patchy appearance of *Erica* vegetation is also reported from other high-elevation African mountains such as Mt. Kilimanjaro, Mt. Elgon, Mt. Kenya, and the Rwenzori Mountains (Hedberg 1951; Beck et al. 1983; Wesche et al. 2000) and the Andes in South America (Kessler 2000). The presence of these *Erica* patches, mainly growing between big boulders, makes the demarcation of the upper limit of *Erica* difficult (Friis 1986; Miehe and Miehe 1994). The Sanetti Plateau is one of the largest afro-alpine areas in Africa (Hillman 1988; Groos et al. 2021). The area is mainly covered by afro-alpine plant species such as *Helichrysum*, *Alchemilla*, *Lobelia*, and grasses (Friis 1986; Miehe and Miehe 1994). However, big boulders, frequently present on slopes of the Plateau, serve as "refugee camps" for *Erica* above the upper ericaceous ecotone at ca. 3800 m (Miehe and Miehe 1994).

Climatic stress, fire, and overgrazing are postulated as potential drivers for tree line changes in the ericaceous vegetation of the Bale Mountains (Miehe and Miehe 1994; Wesche et al. 2000; Fagúndez 2013; Jacob et al. 2015; Johansson et al. 2018; Kidane et al. 2022). Similarly, the presence of *Erica* patches in the highest elevation east African mountains is explained by the impact of human-induced fire and climate change (Kessler 2000; Hemp and Beck 2001; Hemp 2005). For instance, Chala et al. (2017) suggested the downward shift of the tree line by 1000 m and the corresponding expansion of the afro-alpine habitat during the Last Glacial Maximum (LGM) in eastern Africa. Furthermore, paleoenvironmental studies in the Bale Mountains revealed the effect of climate fluctuation on vegetation (Umer et al. 2007; Gil-Romera et al. 2019; Groos et al. 2021; Mekonnen et al. 2022). Umer et al. (2007) reported that the ericaceous vegetation extended to the Sanetti Plateau during the beginning of the Holocene in response to the warm and humid climate, and they suggested that the vegetation expansion started to decrease during the mid-Holocene due to increasing aridity. Kidane et al. (2022) and Chala et al. (2016) assumed that the current climate warming might alter the spatial arrangement of the ericaceous vegetation in the Bale Mountains by supporting its expansion to the Plateau and simultaneously the extinction of afro-alpine vegetation.

At present, the growth of *Erica* on the Sanetti Plateau is mainly restricted to boulder-rich sites. In contrast, areas nearby without boulders are generally free of *Erica* and mainly covered by afro-alpine species such as *Alchemilla haumannii*, *Helichrysum splendidum* and *Festuca abyssinica*. These *Erica* patches are assumed to be relics of the ericaceous vegetation expansion during the humid Early Holocene (Miehe and Miehe 1994; Umer et al. 2007). Fire

has been prominent in the Bale Mountains for hundreds to thousands of years (Gil-Romera et al. 2019; Mekonnen et al. 2022). This is because the pastoralists in the Bale Mountains believe that fire stimulates the growth of new grass for cattle grazing, thus improving fodder quality, controlling insect pests, and protecting their cattle from predators (Miehe and Miehe 1994; Fetene et al. 2006; Belayneh et al. 2013). As a result, the spatial extent of different vegetation groups in the Bale Mountains, including the isolated patches of *Erica,* has drastically changed over time (Kidane et al. 2012). Grazing is also considered to play a significant role in controlling the expansion of *Erica*. According to Johansson et al. (2010), cattle, goats, and sheep are the main grazing domestic animals in the ericaceous vegetation. Furthermore, according to Gebremedhin et al. (2016), *Erica arborea* is a highly preferred diet by domestic goats in the Semien Mountains. In particular, goats and sheep intensively graze the *Erica* seedlings sprouting after fire, thus putting immense pressure on their regeneration. However, in addition to these biotic factors, temperature, precipitation, soil quality, and wind speed have determinant effects on the growth of trees (Jacob et al. 2015). Miehe and Miehe (1994) hypothesized that temperature and moisture availability could be factors limiting the growth of *Erica* on the Sanetti Plateau. Moreover, Groos et al (2022) have presented ground temperature data sets for the Bale Mountains high-elevation sites. However, up to now, except for observational descriptions, there has been no quantified evidence that can explain the patchy occurrence of *Erica* on boulder-rich slopes of the Sanetti Plateau above ca. 3800 m asl.δ^{13}C analyses of leaves and soils are used to determine historical alterations in the boundary between C3 woodland and C4 grasslands (Eshetu 2002). This is mainly due to the differences in the photosynthetic pathways between C3 and C4 plants. While C3 plants are characterized by δ^{13}C values of -22 to $-35‰$, C4 plants show δ^{13}C values of -11 to $-17‰$ (Marshall et al. 2007; Tiunov 2007). In addition, δ^{13}C is a prominent proxy for determining plant water status. It decreases the δ^{13}C value in dry tissue due to stomatal constraints on gas diffusion during periods of biomass production (Körner 2012a). Black carbon (BC) is a highly condensed carbonaceous product of organic matter combustion (Glaser et al. 1998; Brodowski et al. 2005). Due to its highly stable polycyclic hydrocarbons, black carbon is widely used as a proxy for fire history reconstruction (Kuzyakov et al. 2014). Applying this proxy in this study is promising because fire is a common incidence in the ericaceous vegetation of the Bale Mountains. In addition, the patchy distribution of *Erica* on the Sanetti Plateau is assumed to document fire disturbance (Miehe and Miehe 1994; Wesche et al. 2000; Gil-Romera et al. 2019).

In this study, we aim to contribute to a better understanding of the distribution of *Erica* on the Sanetti Plateau by comparing *Erica* and non-*Erica* plots (control plots) based

on different environmental and biogeochemical proxies such as topography and selected soil properties. Specifically, our research questions are: (i) Is topography (elevation, exposition, inclination) a limiting factor, and is stone cover a favoring factor for the growth of *Erica*? (ii) Do *Erica* sites have different soil properties than control plots (e.g., pH, TOC, N contents and stocks, stable isotopes, and BC contents)? Finally, (iii) Is there any evidence that *Erica* has previously occupied the control plots?

Materials and methods

Study area

Geology, vegetation, and climate

The Bale Mountains National Park is located in the Oromia National Regional State, south-east Ethiopia (6°29′–7°10′N and 39°28′–39°57′E; Fig. 1), covering an area of ~2200 km² (Hillman 1988). The park was established in 1970 to conserve its endemic fauna and flora. The Bale Mountains were formed by volcanic eruptions during the Miocene and Oligocene, releasing large amounts of basalt, rhyolite, and ignimbrite (Mohr 1983). They rise from the eastern highlands (2500 m asl) alongside the Ethiopian rift valley to the Sanetti Plateau (3800–4000 m asl) and Tullu Dimtu (4377 m asl) (Miehe and Miehe 1994). Besides, the Bale Mountains were one of the most glaciated mountains in Ethiopia during the Late Pleistocene (Osmaston et al. 2005; Mark and Osmaston 2008; Groos et al. 2021).

Fig. 1 Map showing the geographical location of the Bale Mountains in Ethiopia and the study sites; five covered by *Erica* patches (E1–E5) and five located nearby without *Erica* (Control sites C1–C5), covered by grass and *Helichrysum* and temperature loggers installed by Groos et al. (2022) at the site 1 (TM09m and TM08) and site 2 (TM07 and TM10)

Spatial and temporal variability prevailed in the different vegetation compositions of the Bale Mountains along elevation. The northern and southern declivities between 1450 and 3200 m asl are characterized as dry and moist Afromontane forests, respectively. One of the dominant vegetation types in the Bale Mountains is the Ericaceous belt mediating between Afromontane and afro-alpine vegetation (Miehe and Miehe 1994). It spans between about 3200 and 3800 m asl, dominated by *Erica arborea L.* and *Erica trimera* (Engl.) Beentje (Hedberg 1951) in the form of shrubland and moist forest along the northern and southern slopes, respectively. The afro-alpine vegetation dominates above 3800 m asl up to 4377 m asl, punctuated by patches of *Erica* (Miehe and Miehe 1994). The dominant plant species in each elevational zone are covered in depth elsewhere (Hedberg 1951; Friis 1986; Miehe and Miehe 1994).

The climatic conditions of the Bale Mountains are defined by topography and the movement of the Intertropical Convergence Zone and the Congo air basin (Levin et al. 2009; Costa et al. 2014). As a result, the climate is characterized by a dry and bimodal rainy season. The dry season spans from November to February, and two rainy seasons prevail from March to June and from July to October, respectively. In Dinsho (the Bale Mountains National Park headquarters at 3070 m asl), the mean annual precipitation is 1069 mm, and the mean annual temperature is 11.8 °C. The southwestern part of the mountains experiences higher precipitation, with 1000–1500 mm per year, than the northern part, which exhibits annual rainfall ranging between 800 and 1000 mm per year (Hillman 1986; Tiercelin et al. 2008). The watershed of the Plateau is characterized by flat, swampy areas and many small, shallow lakes crucial for stream and river flow regulation (Belayneh et al. 2013). While the northern winds from the Arabian Peninsula dominate during the dry season, the southeasterly monsoon transports moisture from the Indian Ocean during the rainy seasons (Lemma et al. 2020). During the rainy season, snow can fall on the Plateau and highest peaks but usually does not persist for longer than a few hours or some days (Miehe and Miehe 1994).

Sample collection

Five sites were identified along a NE-SW transect over the Sanetti Plateau (Fig. 1). For each site two plots were identified; one covered by dense *Erica* patches (*Erica* plot) and the second one only by grass spp., *Helichrysum*, and a few *Alchemilla* plants (Figs. 1, 2) but without *Erica* (control plot). After testing the soil homogeneity using a soil auger, a total of ten representative soil profiles (five under *Erica* patches and five in adjacent control plots) were dug until the bedrock was reached, and the main topographic variables (elevation, aspect, and slope) and soil depth were recorded. Soil profiles were described (e.g., color, texture,
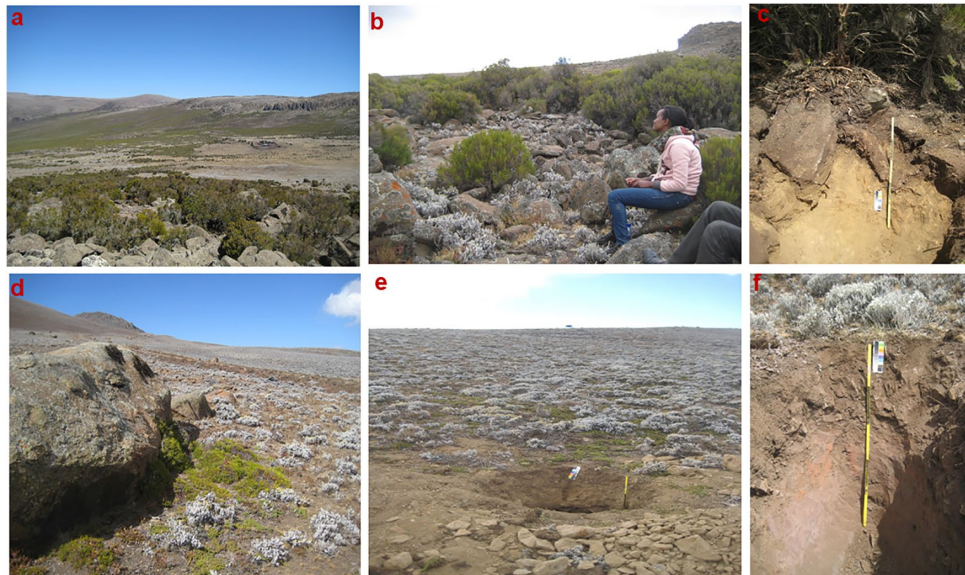
Fig. 2 Pictures showing sampling sites. **a** Site of *Erica* patch (E4) at 3970 m asl in north exposition **b** *Erica* patch E2 with *Erica* shrubs growing between stones and boulders. **c** Soil profile below *Erica* shrubs (E2). **d** *Erica* seedlings growing beside a single big boulder on a control plot. **e** Control plot (C1) covered by *Helichrysum* sp at 4150 m asl. **f** Soil profile below control plot (C3)

stone contents in vol.%, and root content, see Table S1 and Bodenkundliche Kartieranleitung (Ad-hoc-Arbeitsgruppe Boden 2005)), and samples were taken from each soil horizon, air dried, and stored in plastic bags. In addition to soil samples, leaves of *Erica*, grass (*Festuca*), and *Helichrysum,* the dominant afro-alpine species, were collected randomly from the study plots.

Laboratory analyses and statistical evaluation

pH and electrical conductivity were measured using 10 g of O-layer and 20 g of mineral soil samples. After placing the samples in containers, 25 ml of distilled water was added. The suspensions were shaken for 30 min and allowed to settle. Subsequently, electrical conductivity and pH were measured with a glass electrode. Soil texture analyses were done using PARIO Soil Particle Analyzer (METER Group, Munich, Germany). Before measurement, samples were treated using 50 ml of 30% H_2O_2 and 40 g/L solution of $Na_4P_2O_7$. Total organic carbon (TOC), total nitrogen (N), and the natural abundance of $\delta^{13}C$ and $\delta^{15}N$ were measured using an elemental analyzer coupled to an isotope ratio mass spectrometer (EL-IRMS). While sucrose (ANU, IAEA, Vienna, Austria) and $CaCO_3$ (NBS 19, TS limestone) were used as calibration standards for $\delta^{13}C$, IAEA 305A, IAEA N_2, IAEA NO_3, and USGS 41 were used for $\delta^{15}N$.

The precision of $\delta^{13}C$ and $\delta^{15}N$ measurements was 0.2‰ and 0.3‰, respectively.

Soil organic C and N stocks of each mineral soil horizon and the whole soil profile were calculated according to Batjes (Batjes 1996).

$$\text{SOC}_{\text{stock}} = \sum_{i=1}^{k} SOC \times BD \times t \times \left(1 - \left(\frac{S}{100}\right)\right), \quad (1)$$

where $\text{SOC}_{\text{stock}}$ is the total amount of organic carbon (in kg m^{-2}), SOC is the proportion of organic carbon (kg Mg^{-1}) in layer i, BD is the bulk density (Mg m^{-3}) of layer i, t is the thickness of this layer (m), and S is the volume of the fraction of fragments > 2 mm.

The carbon stock of the O-layers was calculated differently from that of the mineral soils:

$$\text{C} - \text{stockO} - \text{layer} = \left(\left(\frac{weight}{40}\right) \times SOC\right)/100, \quad (2)$$

The organic material has been sampled using a 20 cm × 20 cm metal frame. This procedure provides the weight of all the organic material sampled per unit area, independently of its depth.

BC was analyzed using benzene polycarboxylic acids (BPCAs) as molecular markers, following Glaser et al. (1998) with modifications by Brodowski et al. (2005). Five

hundred mg of each sample were hydrolyzed with 10 ml 4 M TFA for 4 h at 105 °C. The hydrolyzed samples were filtrated on glass fiber filters and rinsed several times with de-ionized water to remove polyvalent cations. Subsequently, the samples were digested with 65% nitric acid for 8 h at 170 °C in a high-pressure digestion apparatus. The solution was passed through Dowex 50 W resin columns (200 to 400 meshes) to remove polyvalent cations. After derivatization, the BPCAs were separated using gas chromatography (SHIMADZU, GC-2010, Kyoto, Japan) and detected using a flame ionization detector (FID) with an injection temperature of 300 °C. All statistical analyses were done using R software.

Results

Environmental features and soil properties

Erica and control plots of a given site generally have comparable topographic features; they are located in southern (sites 1, 2, and 3) and north-eastern (sites 4 and 5) expositions between 3850 and 4150 m asl (Table 1).

Except for E4, usually, the inclination is weak. *Erica* plots are generally covered by big boulders (average 60%), with *Erica* shrubs (~1.5 m tall) growing between the boulders (Fig. 2a, b). In contrast, control plots are completely covered by grass and afro-alpine plant species with no visible big stones/boulders on the surface (Fig. 2e, f).

The soils under study are characterized by thick Ah horizons (up to 75 cm), which were further subdivided into Ah1, Ah2, and Ah3. Additionally, B, C, and transitional horizons could be identified based on morphological properties such as color, stone content, roots, etc. (Fig. 2c, f; Table S1). Due to the very high stone contents of the C horizons, the comparison between *Erica* plots and the corresponding control plots was restricted to O, Ah, and Bw horizons; only the

SOC stocks were calculated for the whole soil profile. Since the percentage of stones is a very influential factor for root penetration, water storage capacity, carbon, and nutrient accumulation, stoniness was determined per horizon. The results showed that, even though not statistically significant, stone contents are often higher below *Erica* than in soils of control plots (Fig. 3). For instance, the Ah1 horizons of control and *Erica* plots have an average stone content of 36 and 45, respectively. In the Bw horizons of *Erica* and control plots, stone contents increased to ca. 90 (Fig. 3). Bulk density of control soils was significantly higher than that below *Erica* (Fig. S1, $p = 0.002$).

Soil texture fractions are highly variable along the soil depth of *Erica* and control profiles (Fig. S2). However, no significant difference is obtained between *Erica* and the
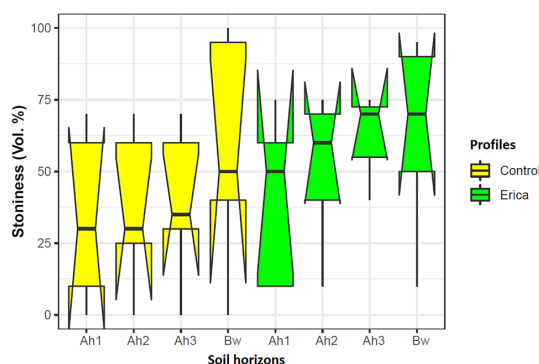

Fig. 3 Stone content in soil horizons of all *Erica* and control sites, estimated according to Bodenkundliche Kartieranleitung (2005). The notched box plots indicate the median (solid lines between the boxes) and interquartile range (IQR) with upper (75%) and lower (25%) quartiles. The notches display the 95% confidence interval of the median. The lines extending outside the box (whiskers) show variability outside the quartiles

Table 1 Topographic features and estimated surface stone cover of (**a**) the *Erica* plots (E1–E5) on the Sanetti Plateau, and (**b**) *Erica*-free control plots (C1–C5) on the Sanetti Plateau

Sites	Latitude	Longitude	Elevation m asl	Exposition	Inclination	Stone cover of surface (vol. %)
(a) (E1–E5) on the Sanetti Plateau						
E1	6.8133	39.81968	4140	SE	5°	80
E2	6.79183	39.81035	3900	S	3°	80
E3	6.78887	39.77353	3850	S	3°	25
E4	6.802583	39.78088	3940	NNE	30°	50
E5	6.8956	39.90972	3975	N	2°	60
(b) (C1–C5) on the Sanetti Plateau						
C1	6.8193	39.81148	4150	SE	5°	0
C2	6.826067	39.8049	3920	S	3°	0
C3	6.78827	39.77207	3850	S	2°	0
C4	6.80228	39.78257	3900	N	3°	0
C5	6.89313	39.9092	3990	E	1°	0

control plots. pH values range between 5.6 and 6.8 in *Erica* and control soils (Fig. 4). However, the pH values do not vary significantly between *Erica* and control plots, except for the O layers below *Erica*, which show a slight decrease in pH values ($\bar{x} = 5.6$). EC values vary between 45 and 198 µS cm^{-1} below *Erica* and between 31 and 488 µS cm^{-1} in control soils (Fig. 4). Moreover, EC values decrease with increasing soil depth in both *Erica* and control soil profiles.

Soil organic carbon and nitrogen contents

TOC values of *Erica* plants show significantly higher values than *Helichrysum* and *Festuca* ($p = 0.009$) (Fig. 5). However, there is no significant difference between the TOC contents in the soils of *Erica* and control plots. Nevertheless, the mineral soil horizons of the *Erica* plots tend to have higher TOC contents than the control profiles. TOC values of organic
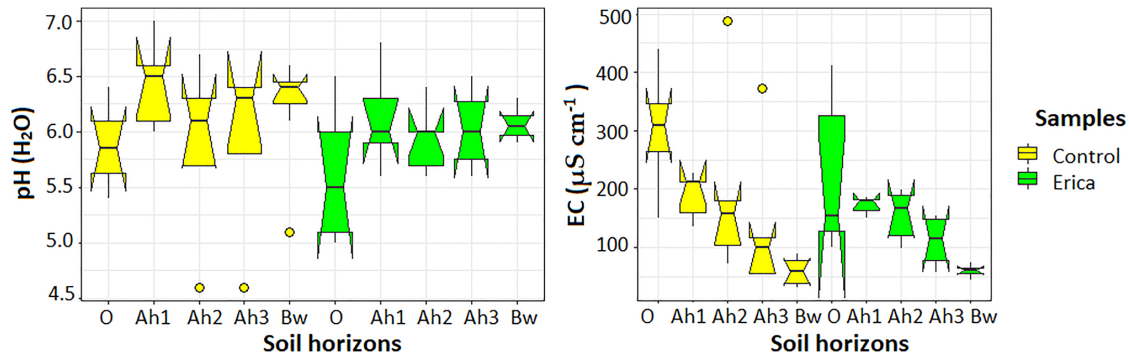
Fig. 4 Electrical conductivity (EC) and pH in soil horizons of *Erica* and control sites. The notched box plots indicate the median (solid lines between the boxes) and interquartile range (IQR) with upper (75%) and lower (25%) quartiles. The notches display the 95% confidence interval of the median. The lines extending outside the box (whiskers) show variability outside the quartiles. The circles represent outliers
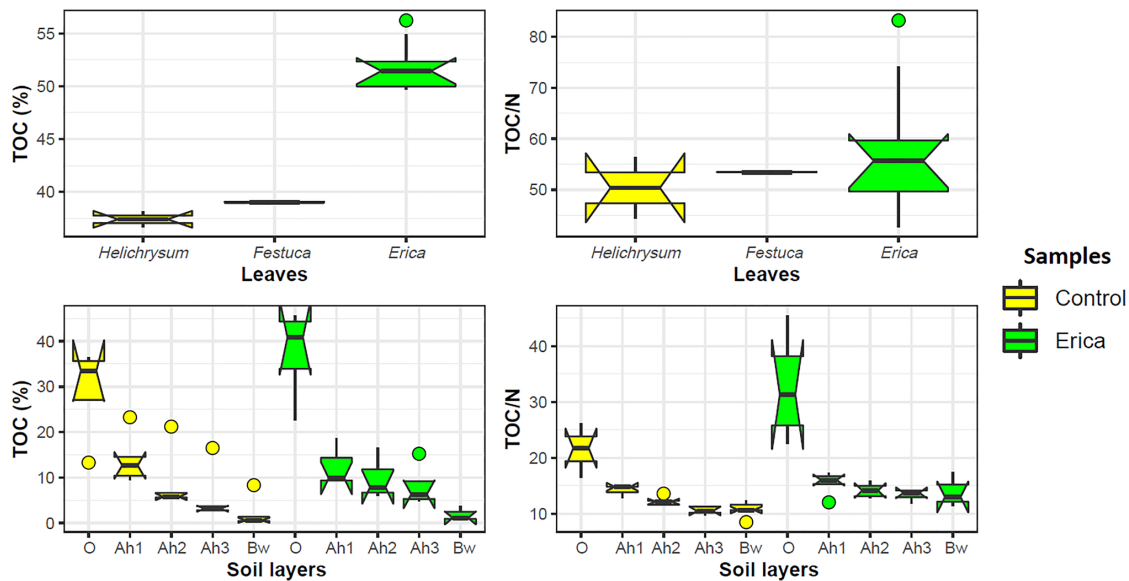

Fig. 5 Total organic carbon (TOC) and TOC/N ratio of plant leaves and soil horizons of *Erica* and control sites. The notched box plots indicate the median (solid lines between the boxes) and interquartile range (IQR) with upper (75%) and lower (25%) quartiles. The notches display the 95% confidence interval of the median. The lines extending outside the box (whiskers) show variability outside the quartiles. The circles represent outliers

layers vary between 13 and 33% in control plots and range from 23 to 46% in *Erica* plots. Moreover, the TOC values of the Ah3 layers below *Erica* are higher ($\bar{x} = 8.2$%) than those of the control plots ($\bar{x} = 5.7$%). Similar to TOC, the N contents of *Erica* leaves are higher than those of *Festuca* and *Helichrysum* (Fig. S3). In the organic and Ah1 horizons of control plots, N contents are slightly higher than below *Erica*, while N in the other horizons is somewhat enriched below *Erica*. N values, like TOC values, decline with increasing depth in all soil profiles.

In soils, TOC/N ratios range from 10 to 45 below *Erica* and 9–26 in control plots (Table S2). They are, in general, significantly higher in *Erica* plots than in control plots ($p = 0.006$). While TOC/N ratios in control soils drastically decrease with increasing soil depth (from Ah1 to Ah3), they remain significantly high in Ah2 ($p = 0.03$) and Ah3 ($p = 0.01$) soil horizons under *Erica* (Fig. 5).

Soil organic carbon and nitrogen stocks

Figure 6 depicts soil organic carbon stocks restricted to soil depths of 0–30 cm, 0–50 cm, and the whole profile that considers the profile's maximum depth in each plot. The results show that, even if not statistically significant, SOC stocks are slightly higher in control plots than in *Erica* plots (Fig. 6).

Black carbon

Our results demonstrate significantly higher BC contents (related to sample: $p = 0.01$ and related to TOC: $p = 0.02$) in *Erica* soils than in control soils (Fig. 7a, b). Moreover, the BPCA pattern shows a higher contribution of B4CA, B5CA, and B6CA and a lower percentage of B3CA in both
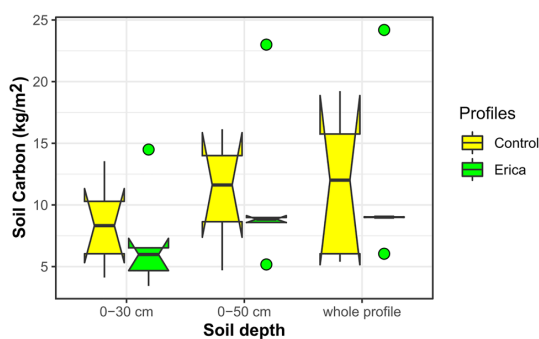

Fig. 6 Soil organic carbon (SOC) in soil profiles under *Erica* and control sites. The notched box plots indicate the median (solid lines between the boxes), and interquartile range (IQR) with upper (75%) and lower (25%) quartiles. The notches display the 95% confidence interval of the median. The lines extending outside the box (whiskers) show variability outside the quartiles. The circles represent outliers

Erica and control plots (Fig. S4). The B5CA/B6CA ratios range from 0.63 to 1.39 below *Erica* and from 0.74 to 2.51 in the control plots (Fig. 7c). Topsoils of control plots have significantly higher B5CA/B6CA ratios ($p = 0.02$) than the *Erica* profiles. The Bw horizons of the control soils always have lower BC and B6CA contents than those below *Erica*.

Stable isotopes

δ^{13}C values of leaves sampled from the *Erica* and control plots range between – 28.6 and – 23.8‰. *Erica* leaves have significantly higher values than *Festuca* and *Helichrysum* ($p = 0.03$) (Fig. 8). δ^{13}C values vary between – 24.7 and – 22.3 in soils of *Erica* plots and from – 27 to – 22‰ in control plot soils, with the highest values recorded in Bw horizons (Fig. 8). In general, δ^{13}C values are significantly higher in soils under *Erica* ($p = 0.02$) than in control profiles, and they increase with increasing soil depth in both *Erica* and control plots. δ^{15}N values vary between – 6.5 and 0.1 in leaves (Fig. 8). *Helichrysum* and *Festuca* show higher δ^{15}N values than *Erica* leaves. Similarly, soils under *Erica* shrubs reveal δ^{15}N values ranging from – 3.4 to 7.0‰, with the highest values recorded in Bw horizons. Control plot soil exhibits δ^{15}N values between – 2.7 and 9.0‰, with the highest value recorded in Ah3 horizons (Fig. 8).

Discussion

Our results illustrate similarity in site exposition and environmental features of *Erica* and control plots established per site. The most striking difference is the high amount of boulders covering the *Erica* plots. The Sanetti Plateau is characterized by harsh climatic conditions with strong winds, extreme solar radiation, heating, desiccation, and frequent frost at night (Miehe and Miehe 1994; Wesche 2003; Groos et al. 2022). Alpine plants adapt to such extreme conditions, whereas woody plants face difficulties regulating the ambient temperature (Wesche 2003; Wesche et al. 2008; Körner 2012b). According to Körner (2012a, b), the upper tree line is globally seen as controlled by the mean temperature during the growing season. Therefore, we assume that the big boulders positioned above the upper timber line of the *Erica* belt protect the *Erica* patches against wind and provide warmth and shade, particularly for the *Erica* seedlings (Wesche et al. 2008). On the other hand, afro-alpine plants are rather shade-intolerant due to their high photosynthetic light-compensation points (Billings and Mooney 1968; Johansson et al. 2018). Therefore, *Erica* seedlings growing beside boulders may outcompete the afro-alpine plants and mature into shrubs. This interpretation is supported by Fig. 2d, which depicts *Erica* seedlings growing in the south exposition alongside a single big boulder on a control plot.
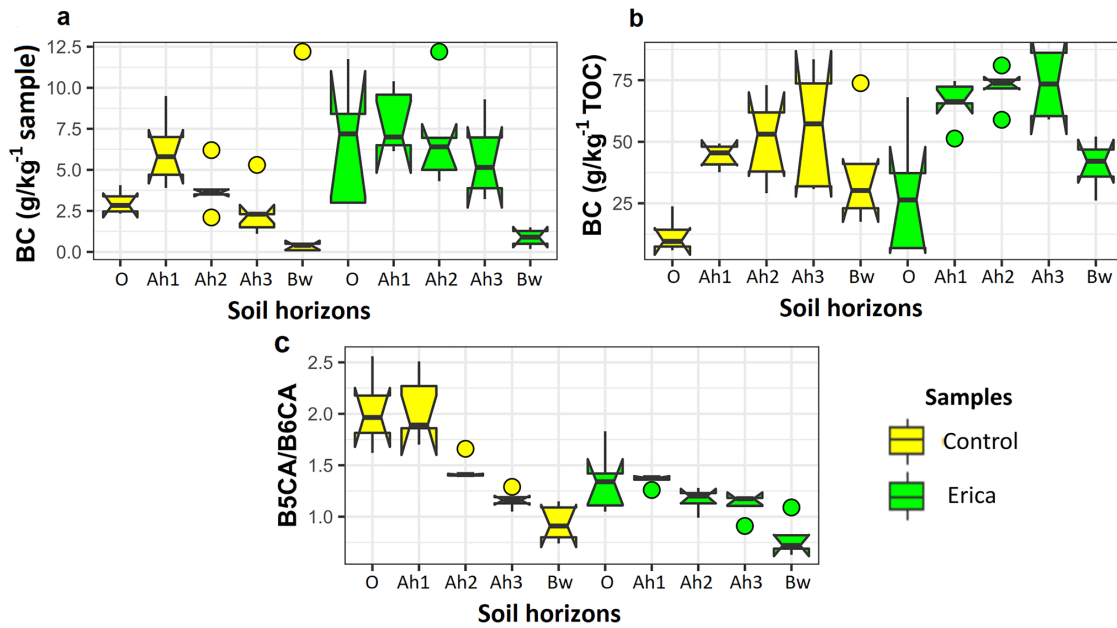
Fig. 7 Black carbon contents (BC) (**a**), black carbon contribution to TOC (**b**), and B5CA/B6CA ratios **c** of *Erica* and control sites soils. The notched box sites indicate the median (solid lines between the boxes), and interquartile range (IQR) with upper (75%) and lower (25%) quartiles. The notches display the 95% confidence interval of the median. The lines extending outside the box (whiskers) show variability outside the quartiles. The circles represent outliers
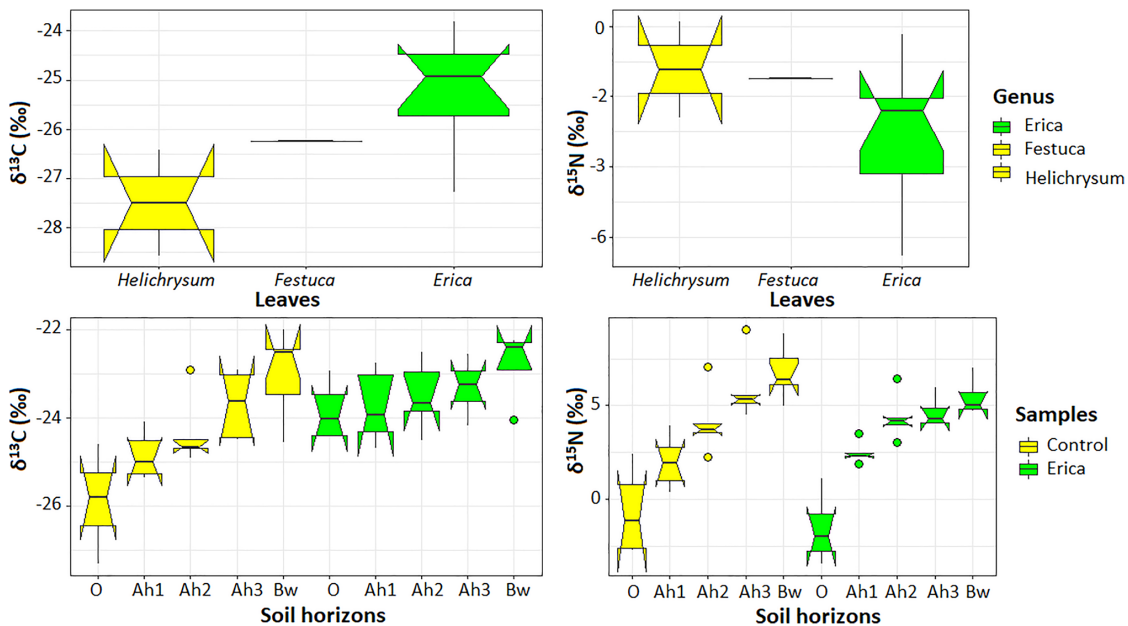
Fig. 8 $\delta^{13}C$ and $\delta^{15}N$ values of leaves and soil layers of *Erica* and control plots. The notched box plots indicate the median (solid lines between the boxes) and interquartile range (IQR) with upper (75%) and lower (25%) quartiles. The notches display the 95% confidence interval of the median. The lines extending outside the box (whiskers) show variability outside the quartiles. The circles represent outliers

However, the *Erica* plants were confined to short stature due to intensive grazing.

Groos et al. (2022) installed temperature data loggers at the elevation range from 3493 to 4377 m asl. From these temperature data loggers, four were installed at 10 cm depth at our *Erica* (E1 and E2, TM09m and TM10m) and control (C1 and C2, TM08m and TM07m) plots (see Fig. 1). The results show no difference in the temperature pattern between *Erica* and control plots (Fig. S5). At site 1, a high temperature was recorded during the dry season, decreasing during the rainy season at both *Erica* and control plots. In contrast, at site 2, the temperature decreased during the dry season and increased during the rainy season at both the control and *Erica* plots. According to Groos et al. (2022), the temperature difference between the sites can be attributed to a difference in exposition. Nevertheless, since the number of data loggers installed at our study sites was very low, further studies are required to check whether there is a difference in microclimate between *Erica* and the control plots.

Except for bulk density, TOC, TOC/N and BC, other biogeochemical proxies do not show a significant difference between *Erica* and control plots. The significantly lower soil bulk density under *Erica* could be caused by a high organic matter content and increased stone contents (Fig. 3). Even though statistically not significant, the lower pH values recorded in soils of *Erica* plots (Fig. 4) can be explained by the acidifying effects of the thick, slowly decomposing *Erica* litter (Dahlgren et al. 1997). Nevertheless, pH values recorded in our *Erica* profiles are slightly higher than those reported by Johansson (2013) from the *Erica* belt in the Bale Mountains. These high pH values might be caused by increased alkaline dust inputs from the surroundings on the Sanetti Plateau. Moreover, the decrease of EC values along soil depth in both *Erica* and control soil profiles might be due to the ascendance of water and ions during the dry period.

Higher soil TOC and N contents of *Erica* plots compared to the control plots can be attributed to differences in quality and quantity of the litter input (see Fig. 5 and S3, high TOC and N values of *Erica* leaves) (Andrén and Kätterer 1997). Furthermore, increased insolation on control plots (Miehe and Miehe 1994) might support organic matter degradation, whereas soils under *Erica* benefit from the shade provided by large rocks and the *Erica* canopy. Moreover, the Ah3 and Bw horizons at the bottom of the soil profiles of the control plots contain less TOC and N than the control soils, which may indicate that *Erica* was not a common vegetation component on these plots in the past. Despite lower N values of plant species growing on control plots, their O and Ah layers show higher N values (Fig. S3), likely due to fecal N input from grazing cattle (Baron et al. 2002; Johansson et al. 2012). High TOC/N values recorded in our *Erica* plots agree with Mekonnen et al. (2019) and Zech (2006), reporting

that such high values characterize the *Erica* vegetation and its soils at high elevations in other African Mountains. The low TOC/N ratios, especially of the Ah3 and Bw horizons of control plots, also support the interpretation that the control plots have never been fully covered by *Erica*. Besides, the higher TOC/N ratios of the mineral soils below *Erica* reflect that *Erica* litter is less decomposed by soil microorganisms (Jacob et al. 2015).

SOC and N stocks of *Erica* plots are partly lower than those of control plots (Fig. 6; Fig. S3). This is mainly due to their higher stone contents which are negatively correlated with the SOC and N stocks ($R = -0.5$). Furthermore, the PCA results demonstrate the impact of stone contents on the carbon and nitrogen stock accumulation (Fig. S6). Similarly, Gebrehiwot et al. (2018) found higher SOC stocks in the afro-alpine grassland soils of the Abune Yosef Mountain in Northern Ethiopia compared to soils below the ericaceous forest. In a study about soils under different vegetation in the Bale Mountains, Yimer et al. (2006) noted higher carbon stocks in 0.3–1 m soil depth below *Erica*. However, this difference can be explained by the variability of climatic conditions and environmental factors between the lower elevation of the *Erica* belt and our high-elevation sites on the Sanetti Plateau.

Our results further show that soils under *Erica* are enriched in BC compared to soils of the control plots (Fig. 7a, b). This indicates a higher amount of combustible fuel on *Erica* plots than on control plots. Furthermore, the significantly increased BC contents, especially of Ah2 and Ah3 horizons in soils below *Erica* (Fig. 7a, b), support our interpretation that *Erica* did not intensively cover these plots previously. Otherwise, a higher accumulation of recalcitrant BC would have been preserved during the burning of former *Erica* shrubs.

In addition to BC contents, the relative contribution of benzene polycarboxylic acids (BPCA) provides information on fire temperature and fuel source (Schneider et al. 2010; Wolf et al. 2013). For instance, benzene rings with four and five carboxylic groups (B4CA and B5CA) are primarily produced at low temperatures (~ 300 °C), whereas benzene rings with six carboxylic groups (B6CA) are mainly produced at high temperatures (600 °C). Moreover, the B5CA/B6CA ratio is supposed to indicate the type of vegetation burned in the area. According to Wolf et al. (2013), forest ground and grass fires have B5CA/B6CA ratios of 1.5–2.0, whereas shrub fires have B5CA/B6CA ratios of 0.8–1.7. Our result correlates with the range suggested by Wolf et al. (2013) for shrubs and grassland fires. Moreover, significantly high B5CA/B6CA values in control plots indicate low temperature, while low B5CA/B6CA values in *Erica* plots indicate high combustion temperature. The latter is attributed to the high flammability of *Erica* twigs due to low moisture content and high concentrations of oils, waxes,

and terpenes, which are readily volatile and contribute to the energy released by burning. In contrast, *Helichrysum*, the main vegetation constituent of the control sites, is naturally less flammable (Johansson et al. 2012).

The δ^{13}C values of plants from our *Erica* and control plots are within the range reported for C3 plants (Marshall et al. 2007; Tiunov 2007) (Fig. 8). This is consistent with results of our previous transect study in the Bale Mountains reporting that the dominant plants including grasses, growing between 2550 and 4377 m asl are characterized as C3 plants (Mekonnen et al. 2019). However, the significantly high δ^{13}C values of *Erica* plants (Fig. 8) seem to contrast with the finding of the transect study (Mekonnen et al. 2019), where no significant difference between *Erica* and other dominant plants could be identified. This discrepancy might be due to the effect of elevation on δ^{13}C values and the different ways plants adjust their gas exchange to mitigate the decline in atmospheric CO_2 pressure along elevation (Körner et al. 1991). To prove this, we ran a correlation analysis between elevation and δ^{13}C values of dominant plants from the transect study. The results showed that elevation correlates positively with δ^{13}C of *Erica* leaves ($R = 0.5$) but negatively with *Festuca* ($R = -0.7$), whereas δ^{13}C of *Alchemilla* leaves did not change with elevation. The isotope pattern found for *Erica* in this study is in agreement with the elevation effect (Körner et al. 1991), whereas the isotope pattern of *Festuca* does not. A similar statistical test was not possible for *Helichrysum* due to limited data. Moreover, the relatively positive δ^{13}C values of *Erica* leaves from our *Erica* plots on the Sanetti Plateau might suggest temporary water stress, e.g., during the dry season. In contrast, *Festuca* does not respond similarly, most likely due to distinct physiological conditions that enable it to mitigate water scarcity (Hedberg 1964). Moreover, the high stone content of the soil profiles under *Erica* patches reduces the plant-available water storage capacity. δ^{13}C values of the O, Ah1, and Ah2 horizons under *Erica* correspond to the values of the *Erica* leaves. The more negative δ^{13}C values of these horizons from control soils correlate with the negative δ^{13}C values of *Helichrysum* and *Festuca*. The increase from O to Bw shows progressing organic matter mineralization with increasing soil depth in both plots. This interpretation is supported by the negative correlation between δ^{13}C and carbon stocks (Fig. S6). Generally, higher δ^{15}N values in control profiles correlate with high δ^{15}N values of *Helichrysum* and *Festuca*. The continual increase of δ^{15}N along soil depth is attributed to the loss of δ^{14}N during microbial decomposition of organic matter (Natelhoffer and Fry 1988; Eshetu 2004; Andersson et al. 2012). Besides, the frequent vegetation fires at the high elevations of the Bale Mountains could also be responsible for increased δ^{15}N values, recorded in both *Erica* and control plot soils (Zech et al. 2011; Johansson 2013). Generally, higher δ^{15}N values in control profiles

likely correlate with the high δ^{15}N values of *Helichrysum* and *Festuca*, implying that control plots were previously dominated by afro-alpine vegetation.

Conclusions

In this study, we examined potential factors responsible for the patchy occurrence of *Erica* above the upper ericaceous ecotone on the Sanetti Plateau, Bale Mountains. Apart from the boulder cover, topographic features, soil texture, and EC did not show significant differences between *Erica* and control plots. High TOC and TOC/N values were recorded below *Erica* and can be attributed to increased fresh organic matter input. Still, slightly higher SOC stocks were calculated for the control plots due to their lower stone contents. *Erica* leaves on the Sanetti Plateau were characterized by more positive δ^{13}C values compared to leaves of *Helichrysum* and grass growing on the control plots. This difference is also reflected in the soils, probably influenced by water stress on the *Erica* plots. In addition, *Erica* sites are characterized by high BC contents indicating a high amount of combustible fuel at *Erica* plots. Low TOC, TOC/N ratio, and BC contents but high B5CA/B6CA ratios in the control plots indicate that *Erica* did not occupy the control plots in former times. However, *Erica* shrubs growing between the surface boulders appear to benefit from the improved microclimate created by the big dark basal rocks and from physical protection against grazing and fire. We conclude that, in general, the soil conditions of most control plots would allow the growth of *Erica*, but in the absence of boulders, the microclimatic conditions above 3800 m asl are too severe. Therefore, further investigations should focus on a detailed assessment of the microclimate conditions, soil moisture availability, and water potential of the *Erica* patches on the Sanetti Plateau.

BG, MZ, SN, TB, TB reviewed and edited the manuscript. All authors read and approved the final manuscript.

Data availability All data generated or analysed during this study are included in the supplementary information files.

Declarations

Conflict of interest The authors declare no conflict of interest.

References

Andersson RA, Meyers P, Hornibrook E et al (2012) Elemental and isotopic carbon and nitrogen records of organic matter accumulation in a holocene permafrost peat sequence in the east European Russian arctic. J Quat Sci 27:545–552. https://doi.org/10.1002/jqs.2541

Andrén O, Kätterer T (1997) ICBM: the introductory carbon balance model for exploration of soil carbon balances. Ecol Appl 7:1226–1236. https://doi.org/10.1890/1051-0761(1997)007[1226:ITICBM]2.0.CO;2

Baron VS, Mapfumo E, Dick AC et al (2002) Grazing intensity impacts on pasture carbon and nitrogen flow. J Range Manag 55:535–541. https://doi.org/10.2307/4003996

Batjes NH (1996) Total carbon and nitrogen in the soils of the world. Eur J Soil Sci 47:151–163. https://doi.org/10.1111/j.1365-2389.1996.tb01386.x

Beck E, Scheibe R, Senser M (1983) The vegetation of the Shira Plateau and the western slopes of Kibo (Mt. Kilimanjaro, Tanzania). Phytocoenologia 11:1–30. https://doi.org/10.1127/phyto/11/1983/1

Belayneh A, Yohannes T, Worku A (2013) Recurrent and extensive forest fire incidence in the Bale Mountains National Park (BMNP), Ethiopia: extent, cause and consequences. Int J Environ Sci 2:29–39

Billings WD, Mooney HA (1968) The ecology of Arctic and Alpine plants. Biol Rev 43:481–529. https://doi.org/10.1111/J.1469-185X.1968.TB00968.X

Boden AhA (2005) Bodenkundliche Kartieranleitung, Hrsg, 5th edn. Bundesanstalt für Geowissenschaften und Rohstoffe in Zusammenarbeit mit den Staatliche Geologische Dienste, Hannover

Brodowski S, Rodionov A, Haumaier L et al (2005) Revised black carbon assessment using benzene polycarboxylic acids. Org Geochem 36:1299–1310. https://doi.org/10.1016/j.orggeochem.2005.03.011

Chala D, Brochmann C, Psomas A et al (2016) Good-bye to tropical alpine plant giants under warmer climates? Loss of range and genetic diversity in Lobelia rhynchopetalum. Ecol Evol 6:8931–8941. https://doi.org/10.1002/ece3.2603

Chala D, Zimmermann NE, Brochmann C, Bakkestuen V (2017) Migration corridors for alpine plants among the 'sky islands' of eastern Africa: do they, or did they exist? Alp Bot 127:133–144. https://doi.org/10.1007/s00035-017-0184-z

Costa K, Russell J, Konecky B, Lamb H (2014) Isotopic reconstruction of the African humid period and congo air boundary migration at Lake Tana, Ethiopia. Quat Sci Rev 83:58–67. https://doi.org/10.1016/j.quascirev.2013.10.031

Dahlgren RA, Boettinger JL, Huntington GL, Amundson RG (1997) Soil development along an elevational transect in the western Sierra Nevada, California. Geoderma 78:207–236. https://doi.org/10.1016/S0016-7061(97)00034-7

Eshetu Z (2002) Historical C3–C4 vegetation pattern on forested mountain slopes: its implication for ecological rehabilitation of degraded highlands of Ethiopia by afforestation. J Trop Ecol 18:743–758. https://doi.org/10.1017/S0266467402002481

Eshetu Z (2004) Natural15N abundance in soils under young-growth forests in Ethiopia. For Ecol Manag 187:139–147. https://doi.org/10.1016/S0378-1127(03)00315-3

Fagúndez J (2013) Heathlands confronting global change: drivers of biodiversity loss from past to future scenarios. Ann Bot 111:151–172. https://doi.org/10.1093/aob/mcs257

Fetene M, Assefa Y, Gashaw M, Woldu Z, Beck E (2006) Diversity of afroalpine vegetation and ecology of treeline species in the Bale Mountains, Ethiopia, and the influence of fire. In: Spehn EM, Liberman M, Korner C (eds) Land use change and mountain biodiversity. CRC Press, New York, pp 25–38

Friis I (1986) Zonation of forest vegetation on the south slope of Bale Mountains, South Ethiopia. SINET Ethiop J Sci 9:29–44

Gebrehiwot K, Desalegn T, Woldu Z et al (2018) Soil organic carbon stock in Abune Yosef afroalpine and sub-afroalpine vegetation, northern Ethiopia. Ecol Process 7:1–9. https://doi.org/10.1186/s13717-018-0117-9

Gebremedhin B, Flagstad O, Bekele A et al (2016) DNA metabarcoding reveals diet overlap between the endangered walia ibex and domestic goats-Implications for conservation. PLoS One. https://doi.org/10.1371/journal.pone.0159133

Gil-Romera G, Adolf C, Benito BM et al (2019) Long-term fire resilience of the Ericaceous Belt, Bale Mountains, Ethiopia. Biol Lett 15:20190357. https://doi.org/10.1098/rsbl.2019.0357

Glaser B, Haumaier L, Guggenberger G, Zech W (1998) Black carbon in soils: the use of benzenecarboxylic acids as specific markers. Org Geochem 29:811–819. https://doi.org/10.1016/S0146-6380(98)00194-6

Groos AR, Akçar N, Yesilyurt S et al (2021) Nonuniform Late Pleistocene glacier fluctuations in tropical Eastern Africa. Sci Adv. https://doi.org/10.1126/sciadv.abb6826

Groos AR, Niederhauser J, Lemma B et al (2022) An hourly ground temperature dataset for 16 high-elevation sites (3493–4377mgma.s.l.) in the Bale Mountains, Ethiopia (2017–2020). Earth Syst Sci Data 14:1043–1062. https://doi.org/10.5194/essd-14-1043-2022

Hedberg O (1951) Vegetation belts of the east african mountains, 45th edn. Sven. Bot. Tidskr, Stockholm

Hedberg O (1964) Features of Afroalpine plant ecology. Swedish Science Press, Uppsala

Hemp A (2005) Climate change-driven forest fires marginalize the impact of ice cap wasting on Kilimanjaro. Glob Chang Biol 11:1013–1023. https://doi.org/10.1111/j.1365-2486.2005.00968.x

Springer

Hemp A, Beck E (2001) Erica excelsa as a fire-tolerating component of Mt. Kilimanjaro's forests. Phytocoenologia 31:449–475. https://doi.org/10.1127/phyto/31/2001/449

Hillman JC (1986) Conservation in Bale Mountains National Park, Ethiopia. Oryx 20:89–94. https://doi.org/10.1017/S0030605300026314

Hillman JC (1988) The Bale Mountains National Park Area, Southeast Ethiopia, and its Management. Mt Res Dev 8:253–258

Jacob M, Annys S, Frankl A et al (2015) Tree line dynamics in the tropical African highlands—Identifying drivers and dynamics. J Veg Sci 26:9–20. https://doi.org/10.1111/jvs.12215

Johansson M (2013) Fire and grazing in subalpine heathlands and forests of Bale Fire ecology and traditional use of fire. Swedish University of Agricultural Sciences

Johansson M, Rooke T, Fetene M, Granström A (2010) Browser selectivity alters post-fire competition between Erica arborea and E. trimera in the sub-alpine heathlands of Ethiopia. Plant Ecol 207:149–160. https://doi.org/10.1007/s11258-009-9661-9

Johansson MU, Fetene M, Malmer A, Granström A (2012) Tending for cattle: traditional fire management in ethiopian montane heathlands. Ecol Soc. https://doi.org/10.5751/ES-04881-170319

Johansson MU, Frisk CA, Nemomissa S, Hylander K (2018) Disturbance from traditional fire management in subalpine heathlands increases Afro-alpine plant resilience to climate change. Glob Chang Biol 24:2952–2964. https://doi.org/10.1111/gcb.14121

Kessler M (2000) Observations on a human-induced fire event at a humid timberline in the Bolivian Andes. Ecotropica 6:89–93

Kidane Y, Stahlmann R, Beierkuhnlein C (2012) Vegetation dynamics, and land use and land cover change in the Bale Mountains, Ethiopia. Environ Monit Assess 184:7473–7489. https://doi.org/10.1007/s10661-011-2514-8

Kidane YO, Hoffmann S, Jaeschke A et al (2022) Ericaceous vegetation of the Bale Mountains of Ethiopia will prevail in the face of climate change. Sci Rep 12:1–18. https://doi.org/10.1038/s41598-022-05846-z

Körner C (2007) Climatic treelines: conventions, global patterns, causes. Erdkd 4:316–324. https://doi.org/10.3112/erdkunde.2007.04.02

Körner C (2012a) Alpine treelines: functional ecology of the global high elevation tree limits. Springer, Basel

Körner C (2012b) Treelines will be understood once the functional difference between a tree and a shrub is. Ambio 41:197–206. https://doi.org/10.1007/s13280-012-0313-2

Körner C, Farquhar GD, Wong SC (1991) Carbon isotope discrimination by plants follows latitudinal and altitudinal trends. Oecologia 88:30–40. https://doi.org/10.1007/BF00328400

Kron KA, Judd WS, Stevens PF et al (2002) Phylogenetic classification of Ericaceae: molecular and morphological evidence. Bot Rev 68:335–423. https://doi.org/10.1663/0006-8101(2002)068[0335:pcoema]2.0.co;2

Kuzyakov Y, Bogomolova I, Glaser B (2014) Biochar stability in soil: decomposition during eight years and transformation as assessed by compound-specific ^{14}C analysis. Soil Biol Biochem 70:229–236. https://doi.org/10.1016/j.soilbio.2013.12.021

Lemma B, Kebede Gurmessa S, Nemomissa S et al (2020) Spatial and temporal 2H and 18O isotope variation of contemporary precipitation in the Bale Mountains, Ethiopia. Isot Environ Health Stud 56:122–135. https://doi.org/10.1080/10256016.2020.1717487

Levin NE, Zipser EJ, Ceding TE (2009) Isotopic composition of waters from Ethiopia and Kenya: insights into moisture sources for eastern Africa. J Geophys Res Atmos 114:1–13. https://doi.org/10.1029/2009JD012166

Mark BG, Osmaston HA (2008) Quaternary glaciation in Africa: key chronologies and climatic implications. J Quat Sci 23:589–608. https://doi.org/10.1002/jqs.1222

Marshall JD, Brooks JR, Lajtha K (2007) Sources of variation in the stable isotopic composition of plants, 2nd edn. Blackwell Publishing, Hoboken

Mcguire AF, Kron KA (2011) Phylogenetic relationships of European and African Ericas. Int J Plant Sci 166:311–318

Mekonnen B, Zech W, Glaser B et al (2019) Chemotaxonomic patterns of vegetation and soils along altitudinal transects of the Bale Mountains, Ethiopia, and implications for paleovegetation reconstructions—Part I: stable isotopes and sugar biomarkers. E G Quat Sci J 68:177–188. https://doi.org/10.5194/egqsj-68-189-2019

Mekonnen B, Glaser B, Zech R et al (2022) Climate, vegetation and fire history during the past 18,000 years, recorded in high altitude lacustrine sediments on the Sanetti Plateau, Bale Mountains (Ethiopia). Prog Earth Planet Sci. https://doi.org/10.1186/s40645-022-00472-9

Miehe G, Miehe S (1994) Ericaceous forests and heathlands in the Bale Mountains of South Ethiopia: ecology and man's impact. T. Warnke Verlag, Hamburg

Mohr P (1983) Volcanotectonic aspects of Ethiopian Rift evolution. In: Popoff, M., Tiercelin, J.-J. (Eds) Ancient Rifts and Troughs, Symposium of the French National Centre of Scientific Research (CNRS), Marseilles, pp. 175–189. Bull Volcanol 46–1:320

Natelhoffer KJ, Fry B (1988) Controls on natural nitrogen-15 and carbon-13 abundances in forest soil organic matter. Soil Sci Soc Am J 52:1633–1640. https://doi.org/10.2136/sssaj1988.03615995005200060024x

Oliver EGH (1989) The Ericoideae and the Southern African heathers. Bot J Linn Soc 101:319–327. https://doi.org/10.1111/j.1095-8339.1989.tb00167.x

Osmaston HA, Mitchell WA, Osmaston JAN (2005) Quaternary glaciation of the Bale Mountains Ethiopia. J Quat Sci. https://doi.org/10.1002/jqs.931

Schneider MPW, Hilf M, Vogt UF, Schmidt MWI (2010) Organic geochemistry the benzene polycarboxylic acid (BPCA) pattern of wood pyrolyzed between 200 °C and 1000 °C. Org Geochem 41:1082–1088. https://doi.org/10.1016/j.orggeochem.2010.07.001

Tiercelin JJ, Gibert E, Umer M et al (2008) High-resolution sedimentary record of the last deglaciation from a high-altitude lake in Ethiopia. Quat Sci Rev 27:449–467. https://doi.org/10.1016/j.quascirev.2007.11.002

Tiunov AV (2007) Stable isotopes of carbon and nitrogen in soil ecological studies. Biol Bull 34:395–407. https://doi.org/10.1134/S1062359007040127

Umer M, Lamb HF, Bonnefille R et al (2007) Late Pleistocene and Holocene vegetation history of the Bale Mountains, Ethiopia. Quat Sci Rev 26:2229–2246. https://doi.org/10.1016/j.quascirev.2007.05.004

Wesche K (2003) The importance of occasional droughts for Afroalpine landscape ecology. J Trop Ecol 19:197–207. https://doi.org/10.1017/S0266467403003225

Wesche K, Miehe G, Kaeppeli M (2000) The significance of fire for Afroalpine Ericaceous vegetation. Mt Res Dev 20:340–347. https://doi.org/10.1659/0276-4741(2000)020[0340:TSOFFA]2.0.CO;2

Wesche K, Cierjacks A, Assefa Y et al (2008) Recruitment of trees at tropical alpine treelines: Erica in Africa versus Polylepis in South America. Plant Ecol Divers 1:35–46. https://doi.org/10.1080/17550870802262166

Wolf M, Lehndorff E, Wiesenberg GLB et al (2013) Towards reconstruction of past fire regimes from geochemical analysis of charcoal. Org Geochem 55:11–21. https://doi.org/10.1016/j.orggeochem.2012.11.002

Yimer F, Ledin S, Abdelkadir A (2006) Soil organic carbon and total nitrogen stocks as affected by topographic aspect and vegetation in the Bale Mountains, Ethiopia. Geoderma 135:335–344. https://doi.org/10.1016/j.geoderma.2006.01.005

Zech M (2006) Evidence for Late Pleistocene climate changes from buried soils on the southern slopes of Mt. Kilimanjaro Tanzania.

Palaeogeogr Palaeoclimatol Palaeoecol 242(3–4):303–312. https://doi.org/10.1016/j.palaeo.2006.06.008

Zech M, Bimüller C, Hemp A et al (2011) Human and climate impact on 15N natural abundance of plants and soils in high-mountain ecosystems: a short review and two examples from the Eastern Pamirs and Mt. Kilimanjaro. Isot Environ Health Stud 47:286–296. https://doi.org/10.1080/10256016.2011.596277

⚛ Springer

Additional publications

A list of additional publications not included in the cumulative PhD thesis are given below.

Bittner, L., Bliedtner, M., Grady, D., Gil-Romera, G., Martin-Jones, C., Lemma, B., **Mekonnen, B.**, Lamb, HF., Yang, H., Glaser, B., Szidat, S., Salazar, G., Rose, NL., Opgenoorth, L., Miehe, G., Zech, W., Zech, M. (2020) Revisiting afro-alpine Lake Garba Guracha in the Bale Mountains of Ethiopia: rationale, chronology, geochemistry, and paleoenvironmental implications. J Paleolimnol. https://doi.org/10.1007/s10933-020-00138-w

Gil-Romera, G., Adolf, C., Benito, B.M., Bittner, L., Johansson, M. U., Grady, D. A., Lamb, H. F., Lemma, B., Fekadu, M., Glaser, B., **Mekonnen, B.,** Callejo, M. S., Zech, M., Zech, W., Miehe, G. (2019) Long-term fire resilience of the Ericaceous Belt, Bale Mountains, Ethiopia. Biology Letters, 15 (7).

Lemma, B.; Grehl, C.; Zech, M.; **Mekonnen, B.**; Zech, W.; Nemomissa, S.; Bekele, T.; Glaser, B. (2019) Phenolic Compounds as Unambiguous Chemical Markers for the Identification of Keystone Plant Species in the Bale Mountains, Ethiopia. Plants, 8, 228. https://doi.org/10.3390/plants8070228

Curriculum Vitae/Lebenslauf

PERSONAL INFORMATION

Sex: Female

Nationality: Ethiopian

Job Related Skills

Field research skills

▪ Soil profile preparation
▪ Soil and plant leaves sampling
▪ Lake and depression sediment coring and sampling
▪ Mountain Ecology
▪ Forest Ecology
▪ Alpine Ecology

Laboratory research skill

▪ Stable isotope analysis (^{13}C, ^{15}N)
▪ Biomarker analysis (Sugar, Black carbon, Lignin and *n*-alkane)

Experience with measuring machine

▪ GC-MS
▪ GC-IRMS
▪ GC-FID

Skills in evaluating chromatography results using Isodat and GC softwares

PROFESSIONAL BACKGROUND

Ph.D. fellow

Martin-Luther-University Halle-Wittenberg
Soil Biogeochemistry
Since June 2017

Project: Human impact on fire history and destruction of *Erica* vegetation at the Sanetti Plateau, Bale Mountains as assessed by biogeochemical proxies
Aim: Contributing to a semi-quantitative reconstruction of the Late Quaternary paleoenvironmental history of the Bale Mountains in Ethiopia.

Responsibility
− Field research work (leaf and soil sampling etc…)
− Identifying suitable biomarkers for planned paleovegetation and paleoclimate studies
− Analyzes of isotopes (^{13}C and ^{15}N), sugar biomarkers and black carbon
− Reconstructing the climate, vegetation and fire history of the Bale Mountains using a multi-proxy approach
− Preparing four publications for peer review journals

M.Sc. Fellow (College trainer)
Addis Ababa University
Plant Biology and Biodiversity Management
Addis Ababa, Ethiopia
From October 2014 to June 2016

Project: Paleoecology
Aim: Identifying suitable biomarker for the identification of the paleo-extent of *Erica* shrubs in the Bale Mountains, Ethiopia.

Responsibility
− Complete 120 ECTS course works
− Field research work (sampling plants, organic and mineral soil)
− Stable isotopes and sugar biomarker analyses
− Preparing M.Sc. Thesis

Digital Skills

I have experience in the following software programs and packages:

- ✓ Microsoft office suite
- ✓ R
- ✓ SPSS
- ✓ Origin
- ✓ Grapher
- ✓ Inkscape

Communication Skills

I have excellent interpersonal communication skills with many individuals worldwide.

I develop this skill through my experience as a teacher and researcher.

Also, I use social media networks like
- ✓ **Research Gate (Betelhem Mekonnen)**
- ✓ **Linkedin (Betelhem Mekonnen)**

to share my scientific views with the wider public. So, such activities helped me to strengthen my innate communication skill.

Leadership Skills

- ✓ Plant Science section head
- ✓ Technology department leader

Other Skills

- ✓ Driving (Class B)
- ✓ Hiking and Climbing high mountains

PROFESSIONAL BACKGROUND

Technology transfer coordinator
Industry extension and technology transfer office
Misrak Polytechnic College
Addis Ababa, Ethiopia
From September 2016 to March 2016
− Evaluation of technologies
− Assisting trainers during the assembly of the technologies
− Coordinating the annual technology symposia
− Processing transfer of selected technologies to the small-scale institutes
− Leading the Technology coordination team
Trainer (Lecturer)
Misrak Polytechnic College
Urban Agriculture Department, Plant Science section
Addis Ababa, Ethiopia
From September 2012 to August 2014

Responsibility
− Teaching vegetable and mushroom production for Level 1 college trainees
− Giving short-term training for entrepreneurs on mushroom and vegetable production
− Giving curriculum development training for new trainers
− Preparing teaching syllabus
− Advising and technical supporting small-scale urban agriculture institutes
− Student Supervision
− Plant science section supervision
− Evaluating the annual performance of trainers

PERSONALITY

Teamwork

Self-collaboration

Communication with colleagues

Social/Cultural outlooks

Computer skill

Microsoft Office

Grapher

Statistical software

Language Skills

Amharic

English

German

Hobbies

Reading
Participating in social activities

EDUCATIONAL BACKGROUND

Ph.D. student
   Martin-Luther-University Halle-Wittenberg
   Soil Biogeochemistry
   Halle (Saale), Germany
   Since October 2016
   Working title: Reconstructing the paleoenvironmental history of the Bale Mountains, Ethiopia

M.Sc. in Plant Biology and Biodiversity Management
   Addis Ababa University
   Plant Biology and Biodiversity Management
   Addis Ababa, Ethiopia
   From October 2014 to July 2016
   M.Sc. Thesis title: Variation of carbon and nitrogen stable isotopes (^{13}C and ^{15}N) and sugar biomarkers in plants and soils along altitudinal transects in the Bale Mountains (Ethiopia)
   Final Grade: 4.0 with honor
   Thesis Grade: Excellent

   B.Sc. in Dryland Crop and Horticultural Sciences (Agronomy)
   Jigjiga University
   Jigjiga, Ethiopia
   From March 2010 to June 2012
   Final Grade: 3.80, Very Great distinct with honor

OTHER RELEVANT TRAININGS

Certificate in Statistics
Kassel University
Department of Environmental Chemistry
Witzenhausen,
Germany
From 28 March 2019 to 2 April 2019

Eidesstattliche Erklärung / Declaration under Oath

Ich erkläre an Eides statt, dass ich die Arbeit selbstständig und ohne fremde Hilfe verfasst, keine anderen als die von mir angegebenen Quellen und Hilfsmittel benutzt und die den benutzten Werken wörtlich oder inhaltlich entnommenen Stellen als solche kenntlich gemacht habe.

I declare under penalty of perjury that this thesis is my own work entirely and has been written without any help from other people. I used only the sources mentioned and included all the citations correctly both in word or content.

Datum	Betelhem Mekonnen Muluneh

Erklärung über bestehende Vorstrafen und anhängige Ermittlungsverfahren / Declaration concerning Criminal Record and Pending Investigations

Hiermit erkläre ich, dass ich weder vorbestraft bin noch dass gegen mich Ermittlungsverfahren anhängig sind.

I hereby declare that I have no criminal record, and there are no preliminary criminal proceedings pending against me.

_____   _____

Datum   Betelhem Mekonnen Muluneh